DiverLog

Effects of Offshore Wind Farms on the Behaviour, Energetics and Habitat Use of Red-throated Divers

Final report

Version 2.0

Claudia Burger, Stephen Salazar, Jannis Liedtke,
Stefan Heinänen, Jorg Welcker, Georg Nehls

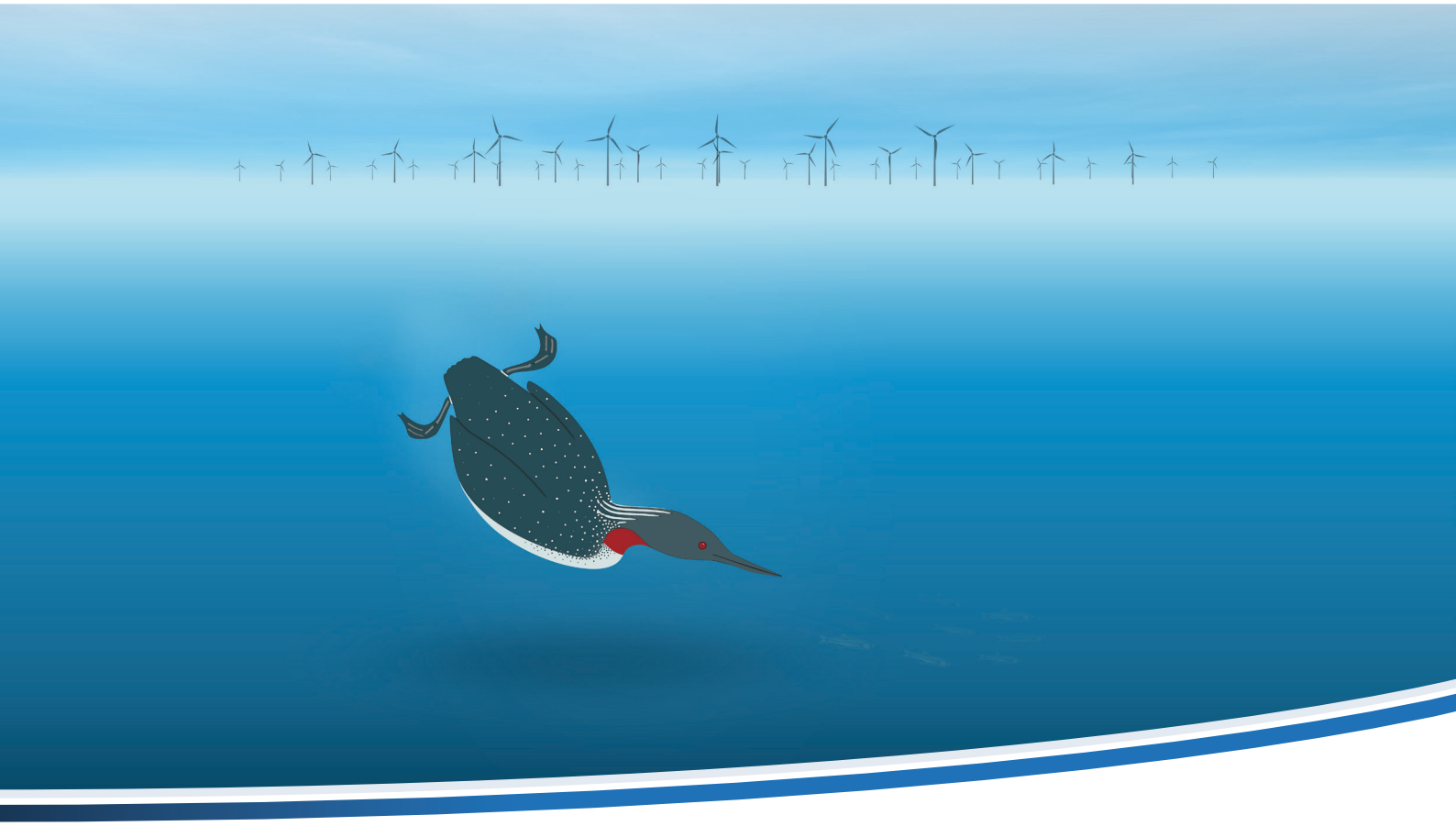

Husum, June 2026

Funded by

Bundesamt für Seeschifffahrt und Hydrographie (BSH)
Bernhard-Nocht-Straße 78, 20359 Hamburg

BioConsult SH GmbH & Co. KG
Schobüller Str. 36
25813 Husum

info@bioconsult-sh.de
www.bioconsult-sh.de

Project name	**DiverLog**	
Project number	**21_1185**	
Contractor	BioConsult SH GmbH & Co. KG Schobüller Straße 36 25813 Husum www.bioconsult-sh.de	
Project lead	Claudia Burger, Jorg Welcker	+49 (0)4841 77937-44 c.burger@bioconsult-sh.de
Substitute of the project lead	Stephen Salazar	+49 (0)4841 77937-096 s.salazar@bioconsult-sh.de
Report preparation	Claudia Burger, Stephen Salazar, Jannis Liedtke, Stefan Heinänen, Miriam Brandt, Vladislav Kosarev	
QA / Approval	Date 01.06.2026 Jorg Welcker	Version: 2.0 j.welcker@bioconsult-sh.de
Project partner	Justus Liebig Universität Gießen Prof. Dr. Petra Quillfeldt	Novia University of Applied Sciences Dr. Stefan Heinänen
		Ornitela Dr. Ramunas Zydelis
Cover Image	Stephen Salazar	
Suggested citation	Burger, C. and Salazar, S. and Liedtke, J. and Heinänen, S. and Welcker, J. and Nehls, G. (2026): DiverLog - Effects of Offshore Wind Farms on the Behaviour, Energetics and Habitat Use of Red-throated Divers. Final report. BioConsult SH, Husum.	
Funding	Bundesrepublik Deutschland, vertreten durch das Bundesministerium für Verkehr, vertreten durch das Bundesamt für Seeschifffahrt und Hydrographie, Bernhard-Nocht-Straße 78, 20359 Hamburg	

CONTENTS

List of figures

List of tables

1 ENGLISH SUMMARY

Red-throated divers (*Gavia stellata*) are among the species most susceptible to anthropogenic disturbance from shipping traffic and offshore wind farms (OWFs). The species' preferred wintering and staging areas are relatively shallow coastal waters where such activities are widespread. Divers maintain large avoidance distances from OWFs, resulting in substantial habitat loss and conflicts under species protection legislation.

Although existing data from the eastern German Bight do not indicate a recent decline in the local population of red-throated divers, they do suggest a shift in the species' main distribution area. However, the long-term consequences of this habitat loss and spatial displacement remain unclear so far.

To enable the continued expansion of offshore wind energy in line with the objectives of the German government, it is essential to improve our understanding of how red-throated divers respond to OWFs and associated maintenance vessel traffic. This includes assessing potential population-level effects and developing strategies to avoid or mitigate negative impacts while simultaneously optimizing maintenance logistics.

The current study assesses whether the displacement of divers from areas surrounding OWFs in the German and Danish North Sea has led to changes in foraging behaviour, activity budgets, and energy expenditure. Such behavioural changes may entail fitness costs and could have long-term effects on local populations. The aim of this project was to extend investigations of individual behavioural patterns and to record them with much higher precision using modern GPS loggers. This approach allows for a comprehensive assessment of the impacts of OWFs on red-throated divers, ranging from individual behavioural responses to potential population-level effects. In addition, the study goes beyond quantifying direct habitat loss by focusing on the species' most important activity— foraging—through detailed analyses of diving behaviour.

Results on habitat quality, daily movements, activity budgets and energy expenditure lay the foundation for individual-based modelling, which can be used to estimate the effects on fitness and potential population level effects. The aim was to compare the current situation in the North Sea (Eastern German Bight) with several operational OWFs to a hypothetical scenario where no OWFs are present and to estimate the consequences on body condition. This can help to better understand the impacts of OWFs on the individual and population level.

In this study, during three years (2022-2024), 68 red-throated divers were equipped with GPS-transmitters (external or implanted). External transmitters also recorded diving activity. All birds were captured and tagged during spring within their main concentration area in the Eastern German Bight of the North Sea. High-resolution GPS and dive data were analysed for a focal area in the North Sea, while also (long-distance) migration movements to breeding grounds were investigated for birds with implanted transmitters.

In the current study, breeding locations as well as migration routes of divers were very similar to the previous DIVER project. 70% of birds migrated to northern Russia, while the remaining birds migrated to potential breeding grounds in Norway, Sweden, Greenland and Svalbard. Only two birds, one migrating to Sweden and one to southern Norway, could be regarded as short-distance migrants. These results confirm that our sample size was representative of showing the full range of breeding locations of birds staging in the focal area. Little direct overlap with existing or planned

OWFs during the non-breeding season was found, however the potentially large disturbance effects from installations and associated vessel traffic have to be taken into account.

A habitat model for the focal area showed that the distribution of divers was affected by water depth, salinity, distance to OWF and ship traffic. The results were similar to previous work, although the OWF effect appeared to be weaker than in previous analyses and was mainly limited to the OWF footprint. The model also showed a significant amount of variance that could not be explained by the model covariates, suggesting that also other factors play an important role for the distribution of birds, such as prey availability or site fidelity, which could not be measured directly.

This study also provided the first fine-scale assessment of the foraging behaviour of red-throated divers in an important non-breeding offshore habitat. Foraging activity was found to be strictly diurnal, lasting only on average 2.3 h per day. Most dives were short in duration (mostly <30 seconds) and shallow in depth within the water column (depths <10 m). We found no evidence of divers changing their foraging patterns in the presence of OWFs.

An analysis of time-activity budgets showed that divers spend most of their time resting at the water surface and engaging in low-energy activities, a pattern that is essential for interpreting results, because it highlights how even small behavioural shifts towards more energetically costly activities (such as flight) can influence overall daily energy expenditure. Flight activity was only recorded during 1.3% of the time. Step-length was significantly longer during daylight hours, suggesting that most locomotion—both active swimming and flight—occurs mainly during the day. As divers approach OWFs, they exhibit a slight but significant increase in flying behaviour, driving modest increases in daily energy expenditure.

The above described analyses provided important estimates for the habitat use, dive behaviour, time-activity budgets as well as energy expenditure of these birds in the focal area, and in a next step these data were integrated into an individual-based model (IBM) in order to determine the energetic consequences of the presence of OWFs on individual body condition.

The IBM was parametrized such that the activity and energy budgets of simulated divers resembled those from our dataset of real divers during the simulation period of four weeks of spring staging phase. The results of the IBM indicate that the presence of OWFs has a slight negative effect on the mean body mass of divers. A lower negative-density dependent effect led to improved foraging efficiency, alleviating the costs of OWF presence on body mass. Because the extent of both negative density dependence and food constraints in overwintering diver populations in nature is currently unknown, it remains speculative to what degree the modest negative effect observed in the IBM translates into long-term consequences for population viability (i.e. over multiple years). Nevertheless, the results suggest that any future potential reduction in foraging efficiency within the focal area (e.g., due to climate-change) is likely to amplify the negative effects of OWFs. Developing methods to study foraging efficiency (e.g., by use of body mounted video loggers or stomach temperature logger) in these birds, particularly in the non-breeding phase is challenging but could provide us with much-needed data on this topic.

Given the observed impacts of OWFs on red-throated divers, the most important measure to avoid such impacts is maritime spatial planning such as choosing development sites away from key areas of these species. In cases when (complete) avoidance of sensitive areas is not an option or when

OWFs were built before knowledge of their large-scale effects emerged, direct mitigation measures might be required. Based on the results of this study as well as a review of previous work, the only mitigation measure proven to successfully reduce negative effects of OWFs on red-throated divers is the regulation of OWF related shipping traffic. Other promising measures (e.g. reducing night-lighting of OWFs) will need to be investigated further, and long-term aerial-survey monitoring can help to track any changes in bird behaviour towards OWFs over time.

2 DEUTSCHE ZUSAMMENFASSUNG

Sterntaucher (*Gavia stellata*) reagieren sehr sensibel auf Offshore Windparks (OWPs) und Schiffsverkehr, und zählen damit zu den am stärksten von anthropogenen Aktivitäten im marinen Bereich betroffen Arten. Die Hauptüberwinterungsgebiete in relativ flachen Küstengewässern weisen eine hohe Überschneidung mit diesen anthropogenen Aktivitäten auf, und mehrere Studien wiesen eine starke mehrere Kilometer weit reichende Meidung von OWPs durch Sterntaucher nach. Dies führt zu stärkeren Lebensraumverlusten als ursprünglich erwartet wurde sowie zu artenschutzrechtlichen Konflikten.

Die vorhandenen Daten aus der östlichen Deutschen Bucht lassen zwar keinen Rückgang der lokalen Population der Sterntaucher erkennen, deuten jedoch auf eine Verlagerung des Hauptverbreitungsgebiets dieser Art hin. Die langfristigen Folgen dieses Lebensraumverlusts und der räumlichen Verlagerung sind bislang jedoch noch unklar.

Um den weiteren Ausbau der Offshore-Windenergie im Einklang mit den Zielen der Bundesregierung zu ermöglichen, ist eine genauere Untersuchung der Reaktionen von Sterntauchern auf OWPs und auf die mit den Wartungsarbeiten verbundene Zunahme des Schiffsverkehrs notwendig. Dies umfasst auch die Untersuchung potenzieller Auswirkungen auf Populationsebene und die Entwicklung von Strategien zur Vermeidung oder Minderung negativer Folgen bei gleichzeitiger Optimierung der Wartungslogistik.

Die aktuelle Studie diente daher dazu, um zu beurteilen, ob die Verdrängung von Sterntauchern aus Gebieten mit OWPs in der Nordsee zu Veränderungen im Nahrungssuchverhalten, im Aktivitätsbudget und im Energieverbrauch führen. Solche Verhaltensänderungen können mit Fitnesseinbußen verbunden sein und langfristige Auswirkungen auf die lokalen Populationen haben. Ziel des Projekts war es, die Untersuchungen individueller Verhaltensmuster auszuweiten und diese mithilfe moderner GPS-Logger deutlich präziser zu erfassen. Dieser Ansatz ermöglicht eine umfassende Bewertung der Auswirkungen von OWPs auf Sterntaucher, von individuellen Verhaltensreaktionen bis hin zu potenziellen Auswirkungen auf Populationsebene. Des Weiteren geht die Studie über die Quantifizierung des direkten Habitatverlusts hinaus, indem sie die Auswirkungen auf das Tauchverhalten der Sterntaucher, und damit deren Nahrungssuche untersucht.

Die Ergebnisse zu Habitatqualität, täglichen Bewegungsmustern, Aktivitätsbudgets und Energieverbrauch bildeten die Grundlage für eine individuenbasierte Modellierung (IBM), mit der sich die Auswirkungen auf die Fitness und mögliche Auswirkungen auf Populationsebene abschätzen lassen. Ziel war es, die aktuelle Situation in der Nordsee (Ostdeutsche Bucht) mit mehreren in Betrieb befindlichen Offshore-Windparks mit einem hypothetischen Szenario ohne Offshore-Windparks zu vergleichen und die Auswirkungen auf die Kondition der Sterntaucher abzuschätzen. Dies kann zu einem besseren Verständnis der Auswirkungen von Offshore-Windparks auf individueller und populationsbezogener Ebene beitragen.

In dieser Studie wurden über einen Zeitraum von drei Jahren (2022–2024) 68 Sterntaucher mit GPS-Sendern (extern oder implantiert) ausgestattet, wobei die externen Sender auch die Tauchaktivitäten der Sterntaucher erfassten. Alle Vögel wurden im Frühjahr in ihrem Hauptkonzentrationsgebiet in der östlichen Deutschen Bucht der Nordsee gefangen und markiert. Die hochauflösenden GPS- und Tauchdaten wurden für ein ausgewähltes Untersuchungsgebiet in der Nordsee analysiert,

während bei Vögeln mit implantierten Sendern auch das Zugverhalten in die Brutgebiete und zurück in die Überwinterungsgebiete untersucht wurde.

Die während der vorliegenden Studie festgestellten Brutgebiete und Zugwege der Sterntaucher waren sehr ähnlich wie im vorherigen DIVER-Projekt: 70 % der Vögel zogen nach Nordrussland, während die übrigen Vögel zu potenziellen Brutgebieten in Norwegen, Schweden, Grönland und Spitzbergen zogen. Nur zwei Vögel konnten als Kurzstreckenzieher klassifiziert werden, wovon einer nach Schweden und einer nach Südnorwegen zog. Diese Ergebnisse bestätigen, dass unsere Stichprobengröße repräsentativ war, um das gesamte Spektrum der Brutplätze von Sterntauchern aus dem Untersuchungsgebiet abzubilden. Es wurde nur eine geringe direkte Überschneidung der von überwinternden Sterntauchern genutzten Gebiete mit bestehenden oder geplanten OWPs festgestellt, jedoch müssen die potenziell großen Störungseffekte durch die Windkraftanlagen und durch den damit verbundenen Schiffsverkehr berücksichtigt werden.

Ein Habitatmodell für das untersuchte Schwerpunktgebiet zeigte, dass die Verteilung der Sterntaucher von Wassertiefe, Salinität, Distanz zu OWPs und Schiffsverkehr abhängig war. Die Ergebnisse ähnelten denen früherer Studien, obwohl der OWP-Effekt schwächer zu sein schien und sich hauptsächlich auf den Bereich der OWPs selbst beschränkte und anders als in vorhergehenden Studien, nicht weit über diesen hinaus reichte. Weiterhin konnte ein bedeutender Anteil der Varianz im Habitatmodell nicht durch die im Modell verwendeten Parameter erklärt werden konnte. Dies weist darauf hin, dass auch andere, nicht betrachtete Faktoren eine wichtige Rolle für die Verteilung der Vögel spielen. Dies könnten z. B. nicht direkt messbare Parameter, wie die tatsächliche Nahrungsverfügbarkeit oder die Standorttreue der Sterntaucher, sein.

Die vorliegende Studie lieferte weiterhin die erste detaillierte Untersuchung des Nahrungssuchverhaltens von Sterntauchern in einem Offshorehabitat außerhalb der Brutzeit. Es wurde festgestellt, dass die Nahrungssuche ausschließlich tagsüber stattfand und die Vögel durchschnittlich nur 2,3 Stunden pro Tag mit Nahrungssuche verbrachten. Die meisten Tauchgänge waren von kurzer Dauer (meist <30 Sekunden) und fanden in geringer Tiefe innerhalb der Wassersäule statt (Tiefen <10 m). Es wurden keine Hinweise auf eine Veränderung des Nahrungssuchverhaltens der untersuchten Sterntaucher in der Nähe von OWPs gefunden.

Eine Analyse der Zeit-Aktivitäts-Budgets ergab, dass Sterntaucher die meiste Zeit mit Rasten an der Wasseroberfläche und weiteren wenig energieaufwendigen Aktivitäten verbrachten. Dieses Muster ist für die Interpretation der Ergebnisse von entscheidender Bedeutung, da es verdeutlicht, wie selbst kleine Verhaltensänderungen hin zu energieaufwändigeren Aktivitäten (wie z. B. Fliegen) den gesamten täglichen Energieverbrauch beeinträchtigen können. Flugaktivität wurde nur während 1,3 % der Zeit aufgezeichnet. Die von Seetauchern zurückgelegte Distanz („step length“) war während der Tagesstunden deutlich länger, was darauf hindeutet, dass die meiste Fortbewegung – sowohl aktives Schwimmen als auch Fliegen – hauptsächlich tagsüber stattfand. Wenn Seetaucher sich OWPs annäherten, zeigten sie eine leichte, aber signifikante, Zunahme des Flugverhaltens, was zu einem moderaten Anstieg des täglichen Energieverbrauchs führte.

Die oben beschriebenen Analysen lieferten wichtige Informationen zur Habitatnutzung, zum Tauchverhalten, zum Zeit-Aktivitäts-Budget sowie zum Energieverbrauch der Sterntaucher im Untersuchungsgebiet. In einem nächsten Schritt wurden diese Daten in ein individuenbasiertes Modell

(IBM) integriert, um die energetischen Auswirkungen der Präsenz von OWPs auf die Kondition der Sterntaucher zu untersuchen.

Das IBM wurde so parametrisiert, dass Zeit- und Energiehaushalt der Sterntaucher dem entsprachen, was in der Natur beobachtet wurde, und es wurde über einen Zeitraum von vier Wochen während des Frühjahrs simuliert. Die Ergebnisse des IBM ergaben einen leicht negativen Effekt von OWPs auf das durchschnittliche Körpergewicht der Sterntaucher. Eine geringere negative Dichteabhängigkeit führte zu einer effizienteren Nahrungssuche und schwächte dadurch den negativen Effekt der OWPs auf das Körpergewicht ab. Da das Ausmaß sowohl der negativen Dichteabhängigkeit als auch der Nahrungslimitierung bei Sterntauchern im Überwinterungsgebiet nicht bekannt ist, bleibt es ebenfalls spekulativ, inwieweit der im IBM beobachtete moderate negative Effekt von OWPs auf die Kondition und das Überleben von Individuen zu längerfristigen negativen Effekten auf Populationsebene führt. Dennoch deuten die Ergebnisse darauf hin, dass jede zukünftige potentielle Verringerung der Nahrungssucheffizienz (z.B. bedingt durch den Klimawandel) innerhalb des untersuchten Gebietes die negativen Auswirkungen von OWPs verstärken kann. Die Entwicklung von Methoden zur Untersuchung der Nahrungssucheffizienz von Sterntauchern, wie z.B. an Vögel befestigte Videokameras oder Temperaturlogger im Magen der Tiere, stellt eine Herausforderung dar, könnte in Zukunft jedoch dringend benötigte Daten zu diesem Thema liefern.

Angesichts der beobachteten Auswirkungen von OWPs auf Sterntaucher ist die wichtigste Maßnahme zur Vermeidung solcher Auswirkungen die marine Raumordnung, beispielsweise die Auswahl von Standorten fernab der für Seetaucher wichtigen Habitate. In Fällen, in denen eine (vollständige) Vermeidung sensibler Gebiete nicht möglich ist oder in denen Offshore-Windparks gebaut wurden, bevor ihre großräumigen Auswirkungen bekannt wurden, könnten direkte Minderungsmaßnahmen erforderlich sein. Basierend auf den Ergebnissen dieser Studie sowie einer Auswertung früherer Arbeiten ist die einzige Minderungsmaßnahme, die nachweislich die negativen Auswirkungen von OWPs auf Sterntaucher erfolgreich reduziert, die Regulierung des mit OWPs assoziierten Schiffsverkehrs. Andere vielversprechende Maßnahmen (z.B. die Reduktion der nächtlichen OWP-Beleuchtung) müssen noch weiter untersucht werden. Ein langfristiges, luftbild-basiertes, Monitoring der Seetaucher erscheint sinnvoll, um potenzielle zukünftige Veränderungen im Verhalten der Vögel gegenüber OWPs zu untersuchen und zu dokumentieren.

3 INTRODUCTION TO THE PROJECT

3.1 Background

The expansion of offshore wind energy use in the North Sea and Baltic Sea is an important component of the energy transition and, in accordance with the German government's objectives, should be carried out in an environmentally friendly manner. Unavoidable impacts on the marine environment arise, among other things, from the physical presence of wind turbines, night-time lighting and shipping traffic associated with the operation of offshore wind farms (OWFs). These impacts of offshore wind energy are examined and assessed during the planning phase as part of environmental impact studies. As knowledge about the impact on the various protected assets is still limited at the start of development, the expansion of wind energy use in the German North Sea and Baltic Sea is accompanied by monitoring during construction and operation, as well as by research projects.

Red-throated divers and black-throated divers occur in the North Sea and Baltic Sea outside the breeding season, with red-throated divers accounting for over 90% of the diver population in the North Sea (MENDEL ET AL. 2008; GARTHE ET AL. 2015). Despite their widespread occurrence, red-throated divers and black-throated divers are still among the least studied waterbird species in northern European marine areas due to the difficulties to obtain crucial individual-level data during the non-breeding season which requires catching and tagging birds with transmitters or data loggers. At the same time, red-throated divers are one of the species most susceptible to anthropogenic influences such as shipping traffic and OWFs (FLIESSBACH ET AL. 2019; MENDEL ET AL. 2019; HEINÄNEN ET AL. 2020; VILELA ET AL. 2020; GARTHE ET AL. 2023).

A previous research project, DIVER, which was completed in 2018, showed that red-throated divers in the German Bight exhibit a significantly greater avoidance response to OWFs than previously assumed. With the help of telemetry data and large-scale aerial counts west of Schleswig-Holstein, the resulting habitat losses could be classified in relation to individual foraging areas and in relation to the population in the main resting area. An avoidance response could be detected up to a distance of 10–15 km, with almost complete displacement occurring within 5 km of the OWFs (HEINÄNEN ET AL. 2020). Similar displacement distances have also been confirmed by other studies in this area (MENDEL ET AL. 2019; VILELA ET AL. 2022; GARTHE ET AL. 2023). Furthermore, the results from DIVER showed a significant disruptive effect of ship traffic in the area (BURGER ET AL. 2019). However, this could only be described with limited accuracy, as the transmitter technology used in the DIVER project (Argos satellite transmitters) allowed only for a low temporal resolution and location errors were larger than from GPS-data.

The findings from the DIVER project and other publications do not indicate a decline in the population of red-throated divers (VILELA ET AL. 2021), but rather a shift in the main concentrations. As a consequence of this shift, there is concern that divers are displaced from preferred foraging areas with possible fitness consequences. Especially reductions in body condition just before the start of migration to breeding grounds might reduce fecundity of these birds and could lead to population declines on the long term (GARTHE ET AL. 2025).

Further insights are needed into whether the displacement of divers from areas around OWFs can have such long-term effects on the local population, or whether they can relocate to other suitable areas within the German North Sea without incurring fitness costs.

The results of DIVER, as well as the accompanying post-construction monitoring studies conducted in accordance with StUK4 on existing OWFs in the German Bight, also raise important implications and questions for both the expansion of offshore wind energy and the protection of divers. These must be taken into account in future planning with regard to the approvability of new OWFs, but also from the point of view of optimizing construction and logistics processes. In addition, maintenance traffic passing through important diver areas can have further significant impacts and must be taken into account when reviewing the areas. In order to further expand the use of offshore wind energy in line with the German government's objectives, it is therefore important to increase knowledge about the reaction of divers to OWFs and the associated maintenance-vessel traffic, to investigate possible effects on the population, and, based on this, to develop strategies that avoid or mitigate the effects on divers while at the same time optimizing maintenance logistics.

3.2 Project objectives

The DIVER project has already yielded important new insights into the reaction of red-throated divers to OWFs and the associated shipping traffic. However, that project was still based on traditional satellite transmitters, which have relatively low positional accuracy and are also unable to record the birds' daily activities in detail.

The aim of the current project was to expand the investigation of movement patterns and record them much more accurately using modern GPS loggers, in order to determine the impact of OWFs on red-throated divers, from individual reactions to possible effects on their body condition. Furthermore, the investigations go beyond measuring direct habitat loss to include the most important activity of red-throated divers, namely foraging, by determining their diving activity.

Foraging is a key activity for birds outside the breeding season and may require a high proportion of the day especially during winter. The energy expenditure required for birds to catch and consume sufficient food can have direct consequences for their fitness (DAUNT ET AL. 2014). Red-throated divers feed mainly on fish and catch their prey by diving, which is a very energy-intensive activity for warm-blooded animals, especially in the winter months. Information on foraging behaviour (e.g. diving frequency) therefore allows accurate conclusions to be drawn about daily energy expenditure. Especially the amount of time that birds need to spend on this activity to maintain their body condition is a crucial factor that will potentially affect how flexible these birds can respond to (anthropogenic) disturbances. Studies on the diving behaviour of red-throated divers in marine areas (outside breeding areas) are currently scarce (but see DUCKWORTH ET AL. 2021) and no investigation of the responses close to OWFs have been done so far. The goal of this study was to fill these knowledge gaps.

Environmental gradients such as water depth influence the occurrence of prey animals on which red-throated divers feed (mainly fish) and can limit the possibility of avoiding disturbing influences. When there is high variation in habitat quality, red-throated divers are likely strongly tied to certain areas (including those with OWF), while when habitat quality is good across a large area, they can

more easily avoid disturbed areas. More specifically, if red-throated divers are displaced from areas rich in food to areas poorer in food, this can lead to reduced food intake and thus poorer physiological condition of the animals, which might consequently reduce individual fitness and may have an impact on populations. Using a habitat model which included a range of environmental parameters as well as possible disturbing factors such as OWF and ship traffic, the aim was to identify areas of high quality that appear suitable as foraging habitat.

Results on habitat quality, daily movements, activity budgets and energy expenditure lay the foundation for individual-based modelling, which can be used to estimate the effects on fitness and possible population effects. The aim is to compare the current situation in the North Sea (Eastern German Bight) with several operational OWF to a hypothetical scenario where no OWF are present and to estimate the consequences on individual fitness. This can help to better understand the impacts of OWF on the individual and population level.

At the beginning of the project, the aim was to similarly analyse tracking data from the Baltic Sea and compare results to data from the North Sea with regard to diving behaviour and habitat preferences. However, the tagged birds provided too little suitable data from that area, especially diving data, which did not allow for an in-depth analysis. In Chapter 9, an overview of all tracked birds is given, showing also the usage of the Baltic Sea as staging and passage area.

Furthermore, a comparison of individuals from different origins (long- and short-distance migrants) was planned, as these individuals might also differ in other aspects of their wintering strategy and their sensitivity to anthropogenic disturbances. However, as we had only one potentially breeding individual for the group of short-distance migrants (from Scandinavia – Sweden, see Chapter 9), a meaningful comparison was not possible.

Despite these shortcomings, the findings achieved within the scope of the project objectives will provide fundamental new insights into movement patterns in connection with the feeding ecology of red-throated divers and how this affects the fitness of these birds. This enables the further development of effective conservation measures for this species and the sustainable management of the marine environment and its anthropogenic use.

3.3 Project website

A project website was created under the existing domain www.divertracking.com. This domain was previously used to present the predecessor project DIVER. The results of this predecessor project will continue to be accessible via a menu item. For the DiverLog project, the project homepage was redesigned and the homepage was brought up to the current state of the art. The GPS tracks of the birds were regularly updated on a map (via an interface to the ‘Movebank’ database).

3.4 Acknowledgements

The project underlying this report is funded by the Bundesamt für Seeschifffahrt und Hydrographie (BSH), Funding Code BSH 10053822 & 4500073391. The sole responsibility for the report’s contents lies with the authors.

The project DiverLog was conducted in cooperation with the Justus Liebig University of Gießen (Prof. Dr. Petra Quillfeldt, Department Animal Ecology and Systematics, Research Group Behavioural Ecology and Ecophysiology) and Novia University of Applied Sciences (Stefan Heinänen and Aurélie Noel). We thank all participants of the field work trips, especially Thomas Grünkorn, and OS Energy for their flexibility in providing ships for catching trips. DVM Julius Morkūnas conducted the surgeries/tagging of birds. We also thank Svenja Neumann for her contributions to the project. Thomas Mattern designed and maintained the project website www.divertracking.com.

3.5 Outline of main chapters

In the following, the main chapters of this report are outlined with key points that will be analysed/discussed as well as contributing authors. Also, the number of analysed individuals is provided, as this varied per chapter due to different filtering requirements.

3.5.1 Foraging patterns of red-throated divers in the German Bight and the effect of offshore wind farms

Stephen Salazar, Claudia Burger, Jorg Welcker

In this chapter, the first ever fine-scale assessment of foraging behaviour of red-throated divers is reported using high-resolution GPS and dive-depth data. Birds were captured at sea and equipped with combined GPS and time-depth recorders, allowing the spatial and temporal distribution of diving activity to be quantified (N = 21 individuals). The chapter further examines whether foraging activity and bout characteristics vary with proximity to OWFs. Statistical models were used to analyse foraging characteristics while accounting for individual differences and environmental covariates.

3.5.2 Time-Energy Budgets and Movement Patterns

Stephen Salazar, Claudia Burger, Jorg Welcker

This chapter focuses on describing daily movement patterns and activity budgets of red-throated divers in the focal area. GPS-derived movement data and dive data were used to estimate time spent in three main behavioural states: resting, diving, and flying. Daily activity budgets were calculated for individuals that remained within the focal area for complete days, allowing comparisons of behaviour across days and individuals (N = 22 individuals). Daily energy budgets were estimated using established allometric relationships and activity-specific energetic costs. Statistical models were applied to examine how movement, activity and estimated energy expenditure varied in relation to proximity to OWFs, while accounting for individual variability and temporal factors.

3.5.3 Habitat model

Stephan Heinänen, Aurélie Noel

The habitat models were calculated under the leadership of our project partner Stefan Heinänen from Novia University. Models were calculated for the focal area using a range of potentially relevant parameters like bathymetry, distance to OWF or ship traffic (N = 46 individuals). A new model approach was used to predict the distribution of divers relative to these covariates as well as showing the amount of unexplained variance.

3.5.4 Effects of Ship traffic on Movement Patterns of Divers

Claudia Burger

The GPS data collected as part of the project made it possible to determine a very accurate spatial and temporal distribution of red-throated divers in relation to the presence of ships. Movement patterns (N = 32 individuals) were analysed with regard to the distance from ships, ship speed and size. BSH provided raw AIS-data for a defined area in the eastern German Bight that could be used for analysis.

3.5.5 Migratory Patterns of tagged Divers

Claudia Burger, Vladislav Kosarev, Nanette Gries, Miriam Brandt

In this chapter, the migration routes of the tracked birds (N = 32 individuals) are described with information on the breeding grounds, distance travelled and timing. The use of the German Baltic Sea as staging area is described, and an overview of wintering areas is given.

3.5.6 Using a data-driven individual-based model to investigate the effects of offshore wind farms on the body condition of red-throated divers

Jannis Liedtke, Stephen Salazar, Claudia Burger, Miriam Brandt, Jorg Welcker, Georg Nehls

In this chapter, a spatially explicit individual-based model was developed to assess how OWFs and vessel traffic affect the body condition of spring staging red-throated divers. The model builds on results from the previous chapters and integrates high-resolution behavioural data, derived energetic costs and habitat preferences, also taking prey dynamics, individual variation and avoidance behaviour into consideration. Multiple scenarios with and without OWFs and vessel traffic were simulated to disentangle the mechanistic pathways through which habitat displacement, movement constraints, and density-dependent processes could affect individual body condition and potentially individual fitness of divers.

3.5.7 Implications for Spatial Planning and the development of mitigation measures

Claudia Burger, Georg Nehls

In this chapter, the results from the previous chapters as well as available literature are reviewed with regard to the implications for spatial planning and mitigation. The results of this study are also

complemented with results from other relevant studies to develop recommendations for mitigation measures and site selection.

4 STUDY APPROACH AND METHODS

4.1 Study species red-throated diver (*Gavia stellata*)

The Red-throated Diver (*Gavia stellata*) is one of five extant species belonging to the genus *Gavidae* (divers or loons). Four of these species occur in Europe, but only two are regularly found in the German North and Baltic Seas: The red-throated diver and the black-throated diver (*Gavia arctica*), with the Red-throated Diver being far more common in the North Sea. Both species are distributed circumpolar north of 50° Latitude during the breeding season (CARBONERAS ET AL. 2020).

All divers are migratory, breeding in northern freshwater lakes and spending the winter season at sea (HEMMER 2020). For red-throated diver high site-fidelity was reported in their breeding areas (OKILL 1992), and relatively high consistency was also found with regard to individually chosen migration routes and large-scale wintering areas between years (DORSCH ET AL. 2019; KLEINSCHMIDT ET AL. 2022). There was high variability in individual patterns, however (DORSCH ET AL. 2019; KLEINSCHMIDT ET AL. 2022). In autumn, divers moult their primary feathers, which involves a flightless phase, during which they are especially vulnerable to disturbance. In red-throated divers this flightless period occurs shortly after they have left their breeding areas. In German and Danish waters the peak moulting period occurs between October and November, and the flightless period lasts about two to three weeks (BERNDT & DRENCKHAHN 1990; MENDEL ET AL. 2008).

As breeding habitat red-throated divers prefer small fish-devoid water bodies and search for their food at larger waterbodies or at sea (ERIKSSON 2010; HEMMER 2020; DUCKWORTH ET AL. 2021). In Europe, their main breeding areas are located in Scandinavia and in the Russian Tundra (DURINCK ET AL. 1994). They start breeding at an age of about 3 years (HEMMINGSSON & ERIKSSON 2002) and usually lay 2 eggs (rarely 1 or 3).

The main wintering areas for the red-throated diver in Europe are located in the Baltic, North and Black Sea (DURINCK ET AL. 1994; SKOV ET AL. 1995). The areas with the largest winter concentrations of divers in the North Sea are located in offshore waters less than 30 m deep along the coast west of Schleswig-Holstein, Germany and west of southern Denmark but extend all along the East and West Frisian islands into the Schelde estuary in the Netherlands (SKOV ET AL. 1995). Divers start to arrive in these regions in September and numbers increase in the following months (GLUTZ VON BLOTZHEIM & BAUER 1987). From April onwards, distribution shifts further north with the highest concentrations found in the area west of Schleswig Holstein and Denmark.

In the Baltic Sea, the most important resting area is located in the Gulf of Riga at waters less than 30 m deep (DURINCK ET AL. 1993). Other important areas for wintering divers are the waters off the coast of Lithuania and the Pomeranian Bay, where most divers winter offshore at water depths ranging between 5 and 30 m (DURINCK ET AL. 1994).

Divers are mainly piscivorous birds (especially in wintering areas they almost exclusively forage on fish) strongly linked to aquatic environments. The diet of wintering Red-throated Divers has been investigated in the North Sea as well as in the Baltic Sea (GUSE ET AL. 2009; KLEINSCHMIDT ET AL. 2019). In the Pomeranian Bay, one of their main wintering areas in the Baltic, zander and herring were found to constitute the majority of the consumed biomass of red-throated divers in winter and

spring (GUSE ET AL. 2009). In the North Sea, clupeids, mackerel, gadoids, flatfish and sand lances were the most important prey groups (KLEINSCHMIDT ET AL. 2019). Divers forage by diving and pursuing visually located prey under water. Dives of breeding red-throated divers were reported to consist of pelagic as well as benthic dives, be 3 – 8 m in depth, 22 – 38 sec in duration and occur mainly during the day (DUCKWORTH ET AL. 2021). Information on diving patterns in their wintering areas has been lacking so far.

Red-throated divers are not considered threatened at a global scale. The IUCN categories and the Birdlife International Red List for Europe (BIRDLIFE INTERNATIONAL 2015) consider them as species of Least Concern (LC). Nevertheless, their populations have decreased, and they are among the most vulnerable seabird species to many anthropogenic factors. Being a long-lived species with low reproduction output, Red-throated diver populations are vulnerable towards adult mortality with limited capacity for fast population recovery. The red-throated diver is included in Annex I of the European Union (EU) Birds Directive (EUROPEAN UNION 2010) and is listed in the Agreement on the Conservation of African-Eurasian Migratory Waterbirds (UNEP/AEWA SECRETARIAT 2022). Moreover, the wintering population in the Baltic Sea is considered Critically Endangered (CR) by HELCOM (2013). Among the main threats that affect divers are oil spills, bycatch in fish nets and habitat degradation (MENDEL ET AL. 2008). For example, mercury pollution in lakes may affect their reproduction (e.g. ERIKSSON 2015). Both ship traffic and OWFs have been shown to have negative effects on divers in that the birds show strong avoidance behaviour towards OWFs and intense ship traffic (DIERSCHKE ET AL. 2016; BURGER ET AL. 2019; HEINÄNEN ET AL. 2020; VILELA ET AL. 2020; GARTHE ET AL. 2023).

Population estimates suggest a wintering population of red-throated divers of 210,000 – 340,000 individuals for northwest Europe (1996 – 2019) with a probably decreasing trend between 2009 and 2018 (Wetlands International 2022, AEWA CSR 8, accessed on 29.10.2025).

4.2 Study area

The project DiverLog focused on the north-eastern part of the German and Danish North Sea, where high densities of red-throated divers occur especially during late winter and spring. In order to protect red-throated divers and other seabirds, several large marine areas have been established within the Natura 2000 protected area network in German as well as in adjacent Danish waters (Fig. 4-1). In German waters, a main diver distribution area has been defined by German authorities (BMU 2009). This area is currently on hold from new plannings for OWF (BSH 2025). The area also overlaps with the SPA “Eastern German Bight” which has the red-throated diver listed as one of the key species for that area. High bird densities also extend north into Danish waters (DORSCH ET AL. 2019; SCOTT-HAYWARD ET AL. 2024), but these areas are less well studied.

Within German waters, there are three operational OWFs in the northern part of the study area, Butendiek (80 turbines, 3.6 MW each), DanTysk (80 turbines, 3.6 MW each) and Sandbank (72 turbines, 4 MW each). In the southern part of the study area there is a cluster (“Helgoland Cluster”) consisting of three wind farms, Amrumbank West (80 turbines, 3.6 MW each), Nordsee Ost (48 turbines, 6.15 MW each) and Meerwind Süd|Ost (80 turbines, 3.6 MW each). In Danish waters, there are three operational wind farms (Horns Rev 1 (160MW), Horns Rev 2 (209MW) and Horns Rev 3 (407 MW).

The Eastern German Bight is a shallow shelf sea and consists mainly of sandy sediments and gravel. The 40 m depth contour extends up to 200 km from the coast confining a large shallow water area. In the eastern German Bight a dynamic frontal systems exists in the mixing zone of coastal and riverine waters (SKOV & PRINS 2001). The Elbe plume forms a low-salinity layer that extends north-westward up to 50 km offshore, depending on discharge and wind (RICKER & STANEV 2020). From March to the end of September, when the open North Sea water is thermally stratified, this mixing zone starts at the 30 m depth contour, where it turns towards the coastal shallow waters mixed by wind and tides. Frontal zones are usually associated with increased ecological activity through local enhancement of nutrients, and red-throated divers have previously been shown to prefer the frontal zones between these two water masses in the German Bight (SKOV & PRINS 2001). In a more recent habitat model, factors characterizing the frontal zone, like salinity and chlorophyll, have been shown to be influential parameters (HEINÄNEN ET AL. 2020). This latter study also showed that, when excluding effects of OWF and vessel traffic, the potential suitability of the habitat for divers stretched over a large area in the 20-30 m depth zone across the diver main concentration area (BMU 2009) and reaching further north into Danish waters.

The area is subject to various human activities with several OWFs operating in the area and adjacent Danish waters. There are no larger ports north of the river Elbe and shipping in this part of the German Bight is dominated by fisheries with some other commercial vessels commuting through this area. More recently, vessels used for construction and service of OWFs have also been shown to contribute a significant share to general shipping traffic (BURGER ET AL. 2019).

Red-throated divers were captured and equipped with GPS-transmitters in this known diver hotspot in the German Exclusive Economic Zone (EEZ, Fig. 4-3). For the analyses regarding the non-breeding phase, specific study areas were defined. For analyses on migration routes and timing, all bird localisations were taken into account, depending on the specific questions.

4.2.1 Focal area

For the analysis of diving behaviour, time-energy budgets, OWF effects, the habitat model and the IBM, a focal area (see Fig. 4-1) was defined based on a number of criteria: 1. The area was based on the known main distribution of divers in the eastern German Bight (diver main concentration area; BMU 2009). It was also extended into Danish waters north of the main concentration area, as this is known to be an important resting habitat as well, and tagged individuals were frequently present in this area. 2. The focus of the overall analysis was on the offshore area, where OWF developments are present. Data from individuals close to the coast (<10 km) were not considered in the main analyses as this data could be confounded by several factors. The focal area has a size of 14,859 km².

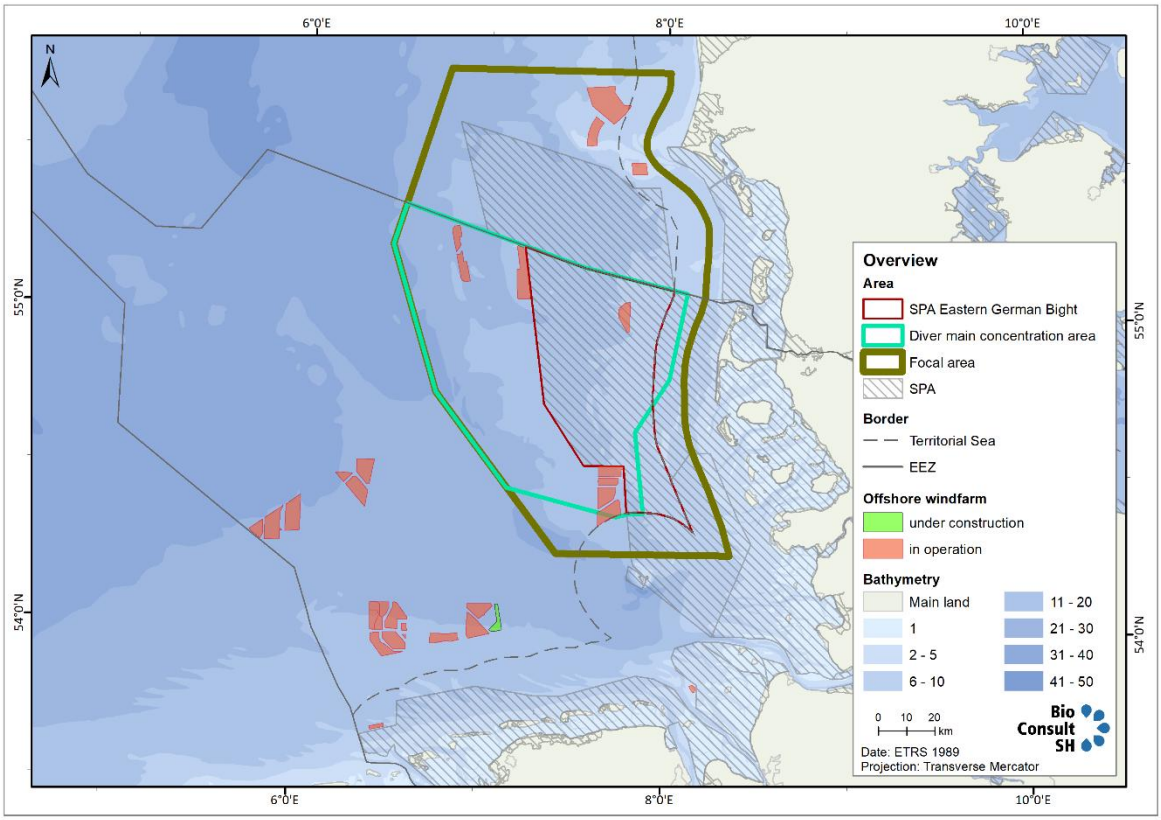

Fig. 4-1 *Overview of the study area in the Eastern North Sea with relevant areas for red-throated divers as well as locations of OWF (status as of 2024).*

4.3 Permits

In cooperation with the animal welfare officer at the University of Giessen, an application for animal welfare approval for the capture and implantation or external attachment of GPS loggers for 75 red-throated divers was submitted to MELUND SH at the beginning of September 2021. The approval was granted by MELUND SH on 29.11.2021 and an extension was granted on 30.08.2023 (Nr. 211129 and 230830).

Furthermore, after submission of the animal welfare permit, the team was granted a capture permit by the Helgoland Bird Observatory to carry out the ringing of the birds.

In addition, an application for permission to catch and tag the red-throated divers was submitted to the Federal Agency for Nature Conservation (BfN) upon presentation of the animal welfare permit. This species protection permit from the BfN is required for the German exclusive economic zone (EEZ) in the North Sea. Permission was granted on 25.02.2022.

4.4 Transmitters and Captures

4.4.1 Diver captures and transmitter deployment

Between 2022 and 2024 in total 68 red-throated divers were captured in their wintering area in the German North Sea and equipped with either implantable GPS-transmitters (38) or external GPS-TDR-transmitters (30). Two additional birds were captured but died during the surgery or did not wake up from anaesthesia. Bird captures took place during three consecutive spring seasons: March – May 2022, April – May 2023 and March - May2024. Birds were captured in the German North Sea in an area between 54.96°N and 54.71°N latitude and 7.28°E and 7.81°E longitude, ca. 30–50 km offshore in the German EEZ (Fig. 4-3). Birds were captured from a boat at sea using the "night lighting technique" (WHITWORTH ET AL. 1997; DORSCH ET AL. 2019). On dark and calm nights birds were searched from a small boat using a bright search lamp. Once found, divers were disoriented by using the bright light which allowed the capture team to approach the diver close enough to catch it with a hand net attached to a pole (Fig. 4-2).

The captured birds were placed into well-ventilated and specially adapted kennels. The kennel floor was covered with towels to keep birds dry and clean; inner walls were padded with soft material to avoid injuries. Only one bird was placed per kennel when transporting, and the kennels were stored outside to prevent birds from overheating. Within minutes after capturing the birds were injected sedative Midazolam by administering approximately 1.5-2 mg/kg. Sedation is necessary for this species as red-throated divers have a tendency of getting stressed. The captured birds were delivered from the small capture boat to a larger ship.

To reduce handling time, the external tagging and surgeries were conducted in a temporary handling and surgery room on board the ship. Transmitters were abdominally implanted with external percutaneous antenna following standard surgical technique used for diving birds (KORSCHGEN ET AL. 1996; MULCAHY & ESLER 1999). Surgeries were done by an experienced veterinarian. Birds were usually released 2–4 hours after completed surgery. Captivity time from the moment of capture to release was on average 6 h (range 4.0 – 11.5 h), which was less than in the previous project DIVER (mean of 7.5 h in 2017). For external tags, captivity time was on average 2:45 h, with a range from 1:30 h to 6:15 h.

We used 4G-GSM loggers from Ornitela Ltd. implanted loggers, which recorded GPS-positions in the focal area every 1 h and had a mass of 45 g, which is below 3% of the mass of a red-throated diver. External loggers, recording GPS positions every 30 min. had a mass of 23 g and were equipped with solar panel and additional TDR, to record dive activity (with 1 s resolution).

Fig. 4-2 *RIB with capture team as it was used for diver captures.*

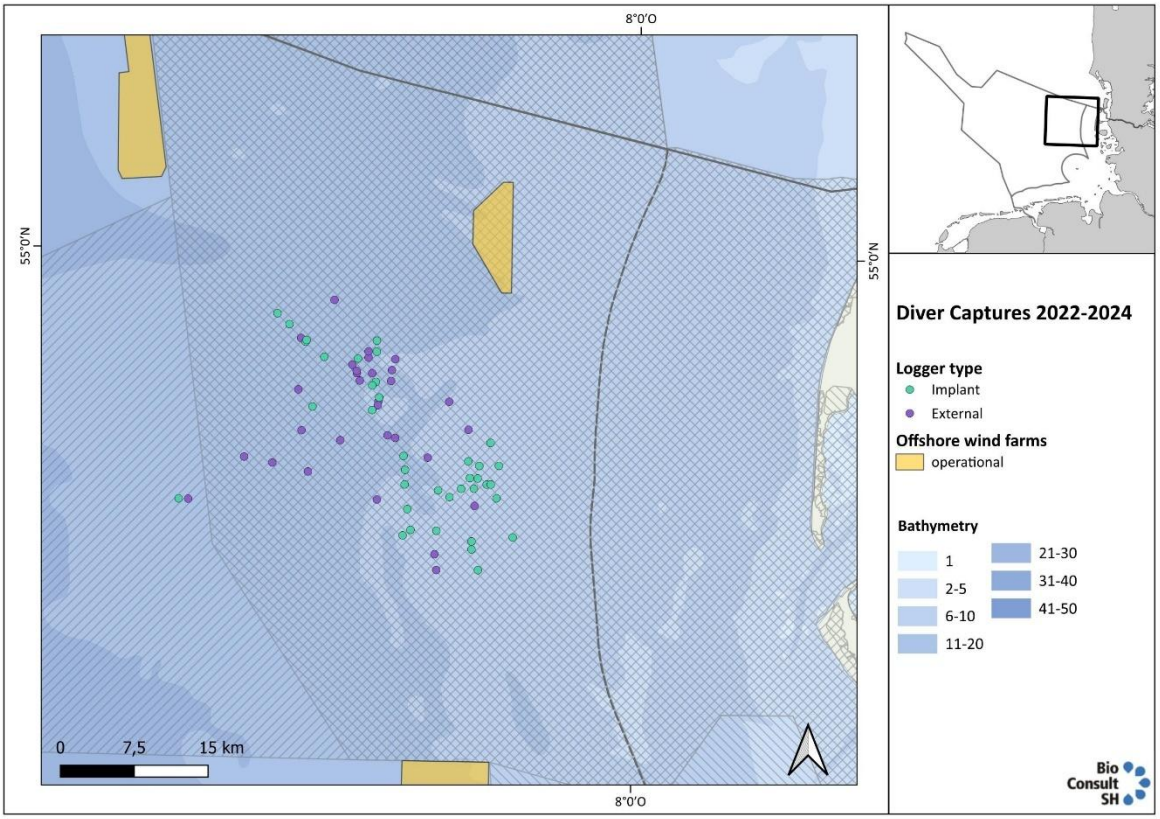

Fig. 4-3 *Capture locations of all 68 divers that were tagged with either external or implanted transmitters, during the three spring seasons of 2022, 2023 and 2024.*

Tab. 4-1 Details on the 30 individuals, which were tagged with external transmitters.

Nr.	TagID	Year	Catch date	End date data	Ring Nr.	Body mass (g)	Sex
1	220660	2022	02.03.2022	NA	J03701	1610	F
2	220659	2022	02.03.2022	NA	J03702	1930	M
3	220661	2022	02.03.2022	15.04.2022	J03703	1700	F
4	220662	2022	03.03.2022	04.04.2022	J03704	1792	F
5	220663	2022	04.05.2022	03.06.2022	J03717	1550	F
6	220664	2022	05.05.2022	19.05.2022	J03721	1700	F
7	220665	2022	05.05.2022	25.05.2022	J03722	1950	F
8	220666	2023	17.04.2023	25.04.2023	J03728	1800	F
9	220667	2023	17.04.2023	NA	J03729	1650	F
10	220668	2023	18.04.2023	NA	J03732	2000	M
11	230458	2023	11.05.2023	18.05.2023	J03733	2260	M
12	230461	2023	13.05.2023	23.05.2023	J03735	1440	F
13	241018	2024	06.03.2024	20.03.2024	J03736	1760	F
14	230452	2024	06.03.2024	27.03.2024	J03737	1635	F
15	241019	2024	06.03.2024	15.03.2024	J03738	1710	F
16	230453	2024	06.03.2024	20.03.2024	J03739	1800	?
17	241020	2024	12.03.2024	10.04.2024	J03740	2000	M
18	241021	2024	12.03.2024	03.04.2024	J03741	1640	F
19	241022	2024	12.03.2024	05.04.2024	J03742	1670	F
20	241023	2024	13.03.2024	27.05.2024	J03743	2235	M
21	241024	2024	13.03.2024	07.04.2024	J03744	1720	F
22	241025	2024	13.03.2024	NA	J03745	1745	F
23	230454	2024	13.03.2024	23.04.2024	J03746	1740	F
24	230455	2024	13.03.2024	22.03.2024	J03747	1555	F
25	230456	2024	13.03.2024	29.03.2024	J03748	1970	M
26	230457	2024	13.03.2024	21.03.2024	J03749	1525	F
27	230459	2024	05.05.2024	14.05.2024	J05203	2050	M
28	244091	2024	05.05.2024	14.05.2024	J05205	1450	F
29	230460	2024	05.05.2024	18.05.2024	J05206	1865	F
30	237444	2024	06.05.2024	28.05.2024	J05210	1590	?

Tab. 4-2 Details on the 38 individuals, which were tagged with implanted transmitters.

Nr.	TagID	Year	Catch date	End date data	Ring Nr.	Body mass (g)	Sex
1	220644	2022	25.04.2022	09.12.2022	J03706	2030	M
2	220648	2022	26.04.2022	26.12.2022	J03707	2100	M
3	220646	2022	26.04.2022	24.05.2022	J03705	2150	M
4	220647	2022	26.04.2022	16.11.2022	J03708	1510	F
5	220645	2022	26.04.2022	NA	J03709	1610	F
6	220650	2022	26.04.2022	18.12.2022	J03710	1650	F
7	220651	2022	26.04.2022	08.12.2022	J03711	1700	F
8	220653	2022	27.04.2022	20.05.2022	J03712	1830	F
9	220652	2022	27.04.2022	13.11.2022	J03713	2050	M
10	220649	2022	27.04.2022	NA	J03714	2100	M
11	220654	2022	27.04.2022	19.10.2022	J03715	1750	M
12	220655	2022	27.04.2022	15.10.2022	J03716	1650	F
13	220658	2022	04.05.2022	09.12.2022	J03718	1650	F
14	220657	2022	04.05.2022	21.12.2022	J03719	1530	F
15	220656	2022	05.05.2022	NA	J03720	1650	F
16	230442	2023	15.04.2023	20.01.2024	J03723	1520	F
17	230437	2023	17.04.2023	18.02.2024	J03724	1680	F
18	230438	2023	17.04.2023	NA	J03725	1520	F
19	230439	2023	17.04.2023	02.12.2023	J03726	1700	F
20	230440	2023	17.04.2023	23.05.2023	J03727	1720	F
21	230441	2023	17.04.2023	08.01.2024	J03730	1680	F
22	230443	2023	17.04.2023	NA	J03731	1770	F
23	230445	2023	12.05.2023	30.12.2023	J03734	1780	F
24	230447	2024	04.05.2024	NA	J05201	1860	F
25	230448	2024	04.05.2024	22.12.2024	J05202	2050	M
26	230446	2024	04.05.2024	17.02.2025	J03750	1590	F
27	230449	2024	05.05.2024	19.05.2024	J05204	1770	M
28	230451	2024	06.05.2024	25.11.2024	J05208	2030	M
29	230444	2024	06.05.2024	NA	J05209	2200	M
30	244020	2024	06.05.2024	27.01.2025	J05211	2260	M
31	244021	2024	06.05.2024	29.03.2025	J05212	1885	F
32	244022	2024	06.05.2024	07.12.2024	J05213	1675	F
33	230450	2024	06.05.2024	NA	J05207	2140	M
34	244023	2024	10.05.2024	15.05.2025	J05214	1860	M
35	244024	2024	10.05.2024	NA	J05215	1900	M
36	244025	2024	10.05.2024	28.05.2024	J05216	1500	F
37	244027	2024	10.05.2024	23.08.2024	J05217	2150	M

Nr.	TagID	Year	Catch date	End date data	Ring Nr.	Body mass (g)	Sex
38	244026	2024	10.05.2024	06.10.2024	J05218	1890	M

4.4.2 Transmitter performance

Data from the transmitters were downloaded automatically onto the online tracking database Movebank (www.movebank.org) and additionally manually from Ornitela logger interface, where also settings could be adjusted as needed. Transmitter performance and data received varied between different transmitters and birds (Table 4.2).

During 2022, 13 of 15 birds with implanted transmitters sent signals on the way to the breeding grounds. Furthermore, 5 of 7 external loggers also sent data, including dive data.

During 2023, 6 of 8 birds with implanted transmitters sent signals on the way to the breeding grounds. Also 3 of 5 birds with external transmitters sent GPS and dive data.

During 2024, 10 of 15 birds with implanted transmitters sent signals, and 15 of 18 birds with external transmitters.

In total, 29 implanted and 25 external transmitters contributed data for the analyses.

Implanted transmitters were transmitting signals up to one year after deployment (range between 4 and 356 days, excluding first 14 days) with an average of 176 days. The external transmitters were only designed to remain attached to the birds for a few weeks and the maximum time period was 73 days but with most transmitters running for a much shorter time (on average 19 days).

In most cases the end of data sampling was due to transmitter battery drain or the transmitter detaching from the bird, but also due to transmitter failure for unknown reasons and mortality. External transmitters fell off the bird after a period of several weeks or months and two transmitters could be retrieved. Surgery or transmitter related mortality cannot be excluded in at least one case, where a tagged bird died within the first two weeks after transmitter deployment.

5 FORAGING PATTERNS OF RED-THROATED DIVERS IN THE GERMAN BIGHT AND THE EFFECT OF OFFSHORE WIND FARMS

5.1 Introduction

Worldwide commitments to reduce carbon emissions have accelerated large-scale developments of renewable energy production (IPCC 2014; FETTING 2020). The rapid development of offshore wind farms (hereon: OWF) is considered pivotal to this renewable energy transition. As the demand for wind energy increases, research efforts have directed at understanding the ecological effects of OWF. This has brought to light a host of different pressures on marine species (BAILEY ET AL. 2014; SCHUSTER ET AL. 2015). This presents profound challenges to governments and policymakers alike and therefore accurate assessment and mitigation of the ecological impacts of OWFs is crucial for their sustainable development.

Currently, many seabird species face direct and indirect negative impacts of anthropomorphic disturbances on themselves and on their habitats (CROXALL ET AL. 2012; FURNESS ET AL. 2013; DIAS ET AL. 2019; PHILLIPS ET AL. 2023). With life-histories characterized by late maturation and low fecundity their populations are markedly sensitive to adult mortality (EVERAERT & STIENEN 2007; SANDVIK ET AL. 2008; FURNESS ET AL. 2013). Seabirds rely on offshore areas for foraging, resting and for migratory transit and these areas are increasingly targeted for OWF developments. While OWF pose mortality risks via direct collision for some seabird species, others stand to face constant and long-term habitat loss due to physical displacement and barrier effects of operating OWFs (EXO ET AL. 2003; HÜPPOP ET AL. 2006; JOHNSTON ET AL. 2014). In addition to habitat loss, individuals from displaced populations may bare additional energetic costs of having to actively avoid OWF or to seek alternative foraging habitats (DREWITT & LANGSTON 2006; FURNESS ET AL. 2013; MASDEN 2015). This has made estimating the avoidance or displacement of populations for resident wintering seabirds a major focus of impact studies over the past decade (BAILEY ET AL. 2014; PESCHKO ET AL. 2020a; GARTHE ET AL. 2023, 2025).

Beyond displacement, OWF could also disrupt seabird foraging patterns and foraging success with the constant presence of visual and auditory stimuli (noise) produced by turbines, causing direct disturbance to birds themselves as well as to their prey species (MASDEN ET AL. 2010; SCHWEMMER ET AL. 2019). For seabirds, maintaining adequate energy intake during the wintering period has been shown to be critical for migration, and breeding preparation (SHOJI ET AL. 2015; FAYET ET AL. 2016, 2017). If foraging becomes more energetically costly due to OWF-related disturbances, by displacing birds into sub-optimal habitats or requiring longer movements due to barrier effects, it could lead to fitness consequences with implications at the population level (NORRIS & TAYLOR 2006; FAYET ET AL. 2016). Large-scale surveys have documented spatial avoidance of OWF by several seabird species (PESCHKO ET AL. 2020a), but no evidence for a population decline was found for one of the most sensitive species, the red-throated diver (e.g. VILELA ET AL. 2021). Although these approaches report important outcomes of OWF developments on seabirds, they lack the resolution needed to identify the behavioural mechanisms linking individual responses to potential population-level impacts. Recent advances in biologging, especially high-resolution GPS combined with additional sensors, enable detailed tracking of individual movements and habitat use (CHUNG ET AL. 2021;

GRÉMILLET ET AL. 2022). These tools provide crucial data that can be used to estimate time-activity budgets, energy expenditure, and subtle behavioural shifts in response to OWF (GILL ET AL. 2001).

The red throated diver (Gavia stellata; hereafter diver) is a protected seabird species with a circumpolar distribution during the breeding phase and migrates to coastal temperate waters during the winter staging. It is a long-lived migratory seabird which breeds along freshwater lakes in the Arctic and northern boreal regions and winters in coastal marine environments. The southeastern (German) North Sea is an important site during the non-breeding phase of this species (GARTHE, STEFAN ET AL. 2015; VILELA ET AL. 2021). Particularly during spring in this region, large numbers of individuals are drawn towards the estuarine fronts associated with the high abundance of their preferred fish prey concentrated around freshwater nutrient discharge of the river Elbe (SKOV & PRINS 2001; KLEINSCHMIDT ET AL. 2019; HEINÄNEN ET AL. 2020; VILELA ET AL. 2021). Accordingly, a special protection area (SPA "Östliche Deutsche Bucht") has been established (BUNDESAMT FÜR JUSTIZ 2017) with divers as one of the focal species and a main concentration area for divers has been defined (BMU 2009). The area is also a site of several OWF. The effects of these OWF on divers and many other seabird species have been under frequent investigation (DIERSCHKE ET AL. 2016; MENDEL ET AL. 2019; PESCHKO ET AL. 2020a; b, 2024; GARTHE ET AL. 2023, 2025). Studies have shown that divers tend to avoid OWFs and are hence not particularly at risk of collisions with wind turbines (GARTHE & HÜPPOP 2004). This however, might deprive the North Sea wintering population of important foraging habitats (GARTHE ET AL. 2025). Although this species is of high conservation relevance and OWF are known to elicit avoidance leading to displacement, its behavioural responses to OWF, particularly foraging behaviour vital for assessing the fitness or energetic costs, remain poorly understood (DIERSCHKE ET AL. 2016; DUCKWORTH 2023).

In this study, we investigate in detail the foraging patterns of divers in a spring-staging area in the North Sea. Previous work on this species have so far described diving behaviour during the reproductive phase (DUCKWORTH ET AL. 2020, 2021). More recently for the first time the foraging behaviour of divers during the non-breeding phase has been documented though with relatively coarse data on location and dive depth (DUCKWORTH ET AL. 2021, 2022; DUNN ET AL. 2024). These studies find that divers exhibit varied foraging patterns influenced by habitat and season and that they may consume a range of different prey species across different trophic levels (DUCKWORTH ET AL. 2024). Divers have been found to predominantly undertake short, shallow dives, typically less than 10 m during foraging bouts that can range from a few minutes to hours. Spatial variations in foraging habits during breeding are evident. For e.g., birds breeding in Finland, forage in freshwater, undertaking longer, deeper dives during extended bouts compared to those in Iceland and Scotland, which forage in marine environments (DUCKWORTH ET AL. 2024). Furthermore, foraging dives during breeding were found to primarily occur during daylight hours in Finland and Scotland, while Icelandic birds show a smaller difference in foraging effort between daylight and twilight. Using stable isotope analysis Duckworth et al have shown that a mix of pelagic and benthic foraging strategies exist. Overall, divers demonstrate spatial and temporal variation in foraging behaviour, suggesting a degree of foraging flexibility that may help them adapt to environmental changes. Nevertheless, detailed assessments using fine-scale data particular of non-breeding birds are largely lacking. This may be a result of the technical challenges involved in capturing birds during breeding and enabling them with tags needed to last year-round until recapture.

We caught and tagged divers at sea within a known concentration area, which is close to several OWF. This approach allows us to obtain suitable data to study their diving behaviour and to relate

these to the presence of OWF. Using high-resolution GPS and dive-depth data from time-depth recorders, we quantify fine-scale characteristics of diving behaviour in this species and describe these behaviours in relation to time of day and sea depth. We identify bouts of foraging behaviour—consecutive dives clustered in time—and assess the characteristics of these bouts. Furthermore, we examine whether and how foraging behaviour varies with proximity to OWF. By applying appropriate statistical techniques, we separate the within- and among-individual components of this potential effect. We aim to explore whether proximity to OWFs is associated with changes in foraging activity or bout structure of divers. We focus on identifying patterns that may indicate altered foraging behaviour, such as differences in the number or duration of dives within bouts near OWF. Given previous evidence of displacement and behavioural sensitivity in this species, we interpret any spatial variation in foraging behaviour in the context of potential disturbance, while acknowledging that the absence of effects does not necessarily imply the absence of ecological impact. Our specific research question therefore was: Do characteristics of diver foraging vary with the proximity to OWF?

5.2 Methods

5.2.1 Fieldwork overview and focal area

We conducted this study on a sample of divers staging in the German Bight of the North Sea during springtime. The site of capture of birds was based on the known main concentration area in the German North Sea around 30 km southwest of the island of Sylt, Germany (BMU 2009; VILELA ET AL. 2021) as well as previous knowledge from the DIVER project (DORSCH ET AL. 2019). Divers were captured in three consecutive years (2022-2024) from the beginning of March until the end of May. In summary, birds were captured on nights around the new moon phase using the night-lighting technique (WHITWORTH ET AL. 1997; SPIEGEL ET AL. 2017; DORSCH ET AL. 2019). For this, short trips were made from a rigid inflatable boat (RIB) despatched from a larger vessel. On capture of one to four birds the RIB returned to the larger vessel for all further handling procedures (ringing, body measurements and tag mounting). The RIB was used to closely approach birds while temporary disorienting them with a single flashlight. Birds were scooped out of the water using a dip net and held in individual plastic kennels until further processing which occurred when the RIB returned to the larger vessel. The kennels were specially adapted to house birds (lined with cushioning material on the sides and base). Birds were ringed, weighed, measured for body morphometry and tagged with an external data logger (see details below) within a cabin of the larger vessel. Feathers were sampled for molecular sex determination. As indoor cabins on the vessel were heated, captive birds were held outdoors in the kennels when not handled, to prevent hyperthermia. For additional details on capture methods see Dorsch et al. (2019) or Heinänen et al. (2020).

For the purpose of this study, a focal area (see Fig. 5-1) was defined based on the known main concentration area in the German North Sea (BMU 2009) and extending into Danish waters, which also hold high numbers in spring (DORSCH ET AL. 2019). The area included ten OWF projects of which all except one were operational in all years of the project (Kaskasi RWE Renewables, began operation in March 2023). The eastern border of the focal area was restricted to 10 km from the coast as these were very shallow and of qualitatively different habitat in which we would assume the (foraging) behaviour of birds to differ from that of more offshore areas as was the focus of this study.

Sea depth data were obtained from the General Bathymetric Chart of the Oceans (GEBCO) online database (GEBCO Compilation Group, 2024; https://www.gebco.net/). The data were accessed via GEBCO's online platform and consisted of a of 15 arc-second interval grid.

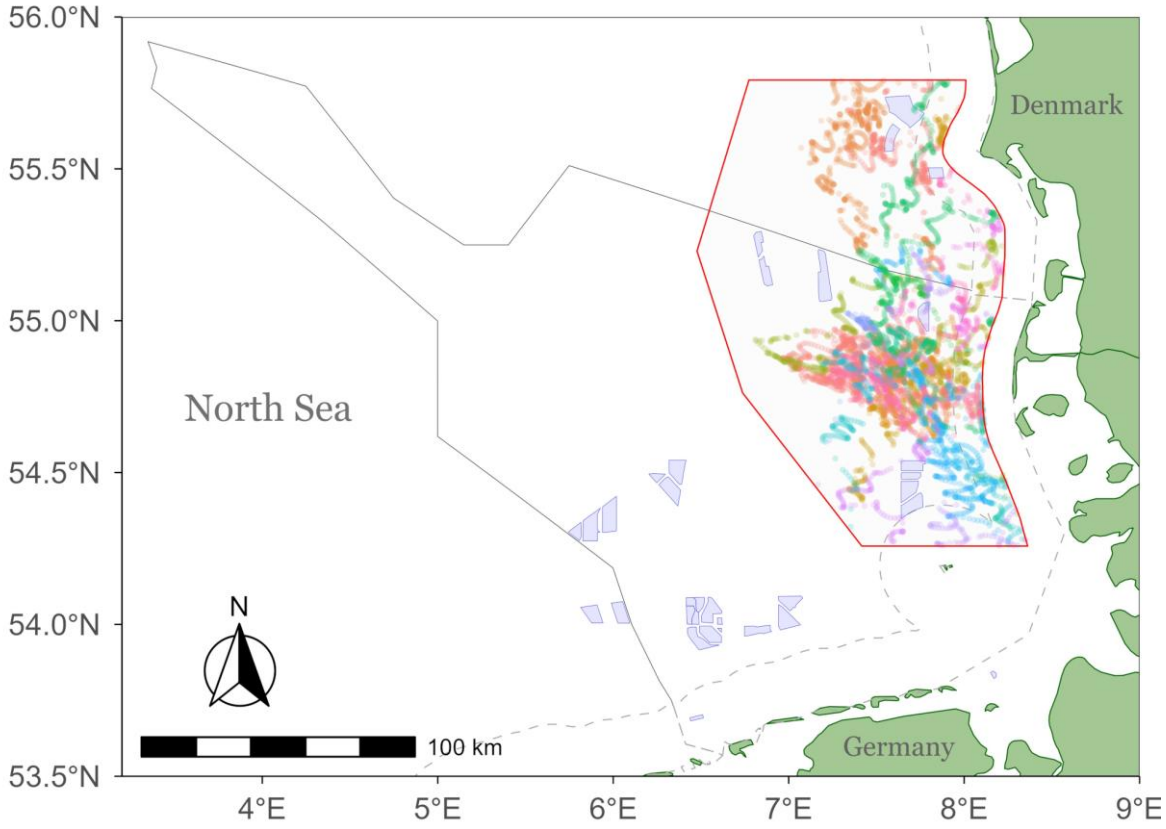

Fig. 5-1 *An Illustrative map of the North Sea indicating the German territorial waters (solid grey line) along with the 12 nautical-mile zone (grey dashed lines). Marked in red is the focal area of the current study along with points in different colours indicating locations of different individual red-throated divers. Shown in blue are the operational OWFs in the area.*

5.2.2 Data loggers

To obtain detailed location and dive data of wintering divers we tagged birds with Ornitrack T25 GPS-GSM loggers (Ornitela UAB, Vilnius Lithuania, https://www.ornitela.com/) equipped with a time-depth recorder (TDR). The loggers were programmed to record a GPS location (hereon fix) once every 30 minutes and record dive depth (in meters) once every second from the time a bird initiated a dive until it returned to the sea surface. The loggers were attached along the longitudinal axis of the birds' dorsal surface onto small back feathers roughly between the scapulae bones. This was done using Tesa™ tape and tape edges were sealed with a UV-cured resin (Solarez™). Each logger weighed 25g which was a maximum of 1.7% of the body mass of the lightest bird (1440 g). The median duration a bird was held in captivity, i.e., between capture and release was 149 minutes (mean ± SD = 167 ± 70 minutes). Handling of birds consisted of a small proportion of this time (c.a. 15 minutes per bird). Birds were released as close as possible to the site of capture from the large vessel while the vessel was kept stationary. All procedures involved in animal capture, ringing and

handling were conducted in adherence to German legislation and approved by BfN (Federal Agency for Nature Conservation; Animal Ethics License: 211129). Data was immediately and continuously recorded from the time of tagging until the loggers detached from the birds by physical action or due to moult ensuring no harm to the birds. Data was obtained remotely via transfer over a GSM network to the logger manufacturer and downloaded via an online portal. We captured and tagged a total of 30 individuals during the three years of study, of which 24 yielded usable data. From these, 21 individuals contributed data within the limits of the focal area.

5.2.3 Data processing

All raw data were processed using the R programming software. We used the 'ExMove' data toolkit (LANGLEY ET AL. 2024; https://exmove.github.io/User_guide.html) which harnesses several R packages such as 'data.table', 'tidyverse', 'lubridate', 'sf', 'here' (BARRETT ET AL. 2006; GROLEMUND & WICKHAM 2011; MÜLLER 2017; PEBESMA 2018; WICKHAM ET AL. 2019), to develop a reproducible workflow for all raw data handling and processing. The toolkit helps integrate metadata of tagged birds (from fieldwork and lab: e.g., capture info, sexing, etc.) with data from loggers as well as to clean, process and filter data for further analyses. To exclude data that represented potential habituation phases to the loggers and therefore aberrant movement and dive behaviour, we discarded the first 24 hours of post-tagging data. This period was calculated starting from the midnight nearest to the bird's post-tagging release time. We then split raw data into GPS fixes and TDR dive data for data type-specific cleaning and processing steps. In short, GPS data were processed to flag and exclude intermittent fixes representing erroneous locations (e.g., 0.00°N, 0.00°E) and unreasonable speeds (>180 km/h). Using the 'redisltraj' function of the 'adehabitatLT' R package (CALENGE 2006) we linearly interpolated these occasional missing (single) fixes and adjusted the fixes such that they were spaced exactly 30 minutes apart. Although the programmed sampling interval was 30 minutes, this step was required as the interval between fixes was not precisely interspaced as birds may have been diving during a scheduled location acquisition or the time required to obtain a GPS signal was extended. Similarly, dive data was processed to identify unreasonably large changes in dive depths or missing depth readings within dives. Such readings which occurred in a small proportion of readings in only 2 individuals, were then adjusted with the mean of the depth values of the preceding and proceeding reading. Data loggers auto-calibrated sea level to zero daily and data showed no visual signs of drift in depth readings. Hence, no zero-offset correction procedure was implemented. Our final dataset consisted of 6,947 fixes obtained from 22 individuals and a total of 23,873 foraging dives from 21 individuals within the focal area (see Tab. 5-1 for detailed overview). Only 2 of the 21 birds (both tagged in 2024) were identified as male and hence we were unable to use sex in any further analyses. For further analyses we included all dives that belonged to a bout that started within the focal area (see dive bouts below).

We used the 'divemove' R package (LUQUE 2007) to recognise the beginning and end times of individual dives from the raw TDR data allowing us to distinguish descent, bottom and ascent phases of each dive (see Fig. 5-2). This is done based on critical quantiles identified for rates of descent and ascent (Luque 2017). Furthermore, the following dive parameters were extracted for every dive using the *DiveStats*() command:

- Dive duration: Total duration of a dive from the start of descent until the end of ascent phases.

- Dive depth: Maximum depth achieved during a dive.
- Post-dive duration: The time spent at the sea surface between the end of ascent of a given dive until the start of descent of the proceeding dive (see Fig. 5-2).

To ensure that our dataset consisted of only dives attributable to foraging attempts (not shorter dives of presumably other functions) we only considered depth readings greater than 1 m and dives that lasted for a duration of 3 seconds or more. For each fix, taken at 30-minutes apart, we counted the total number of dives occurring within the 15 minutes before and after the fix. We thus considered each dive to occur at the location taken nearest in time to the start of the corresponding descent phase. In this way we created two distinct datasets for further analyses: (i) individual fixes with the corresponding number of dives occurring at each assigned location (ii) characteristics of individual dives (dive duration, dive depth, post-dive durations) with their corresponding locations to which each dive was assigned.

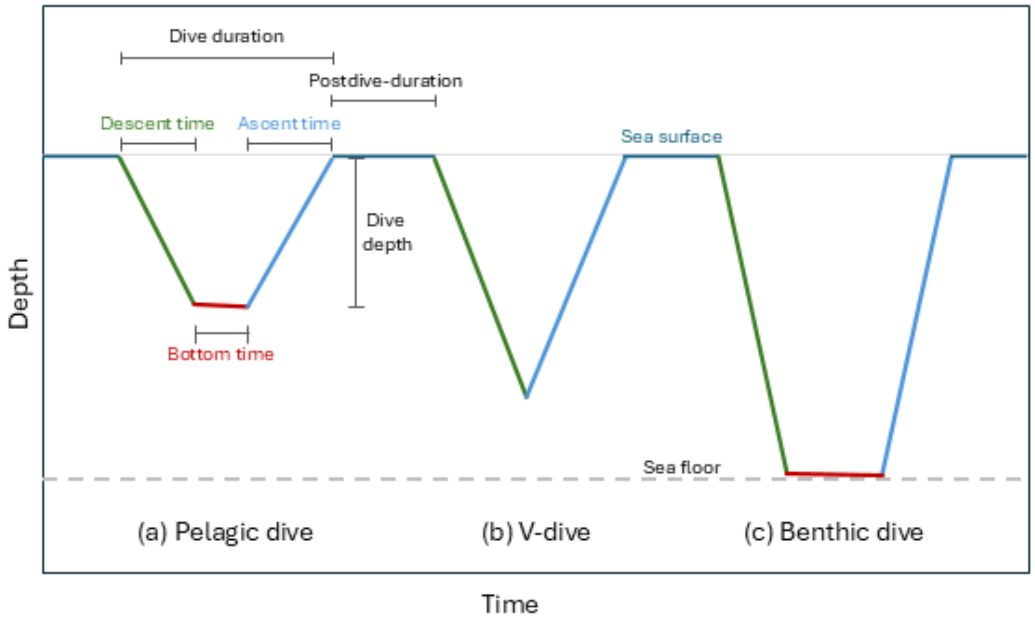

Fig. 5-2 *Illustration of the three types of dives as categorized in this study: (a) Pelagic dives, (b) V-shaped dives and (c) Benthic dives. Shown also are the different phases and characteristics used in different aspects of the analyses.*

To compare diving activity across days varying in the number of daylight hours, we standardized the timing of observations relative to civil dawn, civil dusk, and midnight. We used the centroid of our focal area as the reference location for computing civil dawn and dusk times. Rather than using clock time, which shifts throughout the year, we expressed each observation as a proportion of the day or night based on its position within the dawn-to-dusk or dusk-to-dawn period. For each observation, we first determined whether it occurred during the day (between civil dawn and civil dusk) or night (between civil dusk and the following civil dawn). Observations during the day were standardized as:

$$T_{\text{standardized}} = 6{:}00 + \left(\frac{T_{\text{obs}} - T_{\text{dawn}}}{T_{\text{dusk}} - T_{\text{dawn}}} \times 12\right)$$

where T_{obs} is the original observation time, T_{dawn} is the time of civil dawn, and T_{dusk} is the time of civil dusk. This transformation rescaled daytime observations to a 12-hour window between 06:00 and 18:00, ensuring comparability across days of varying daylight duration. Nighttime observations were standardized using a similar approach but split into two segments:

1. First half of the night (civil dusk to midnight):

$$T_{\text{standardized}} = 18{:}00 + \left(\frac{T_{\text{obs}} - T_{\text{dusk}}}{T_{\text{midnight}} - T_{\text{dusk}}} \times 6\right)$$

2. Second half of the night (midnight to civil dawn):

$$T_{\text{standardized}} = 0{:}00 + \left(\frac{T_{\text{obs}} - T_{\text{midnight}}}{T_{\text{dawn(next day)}} - T_{\text{midnight}}} \times 6\right)$$

This procedure rescaled the entire nocturnal period (dusk to dawn) into a fixed 12-hour window (18:00–06:00), allowing for direct comparisons of activity patterns across different dates. This standardization approach minimized variation in estimated light cycle times while maintaining a biologically meaningful temporal framework. Local civil dawn and dusk times were derived using the *suncalc* R package (THIEURMEL & EL MARHRAOUI 2022), using the centroid's latitude, longitude, along with the individual dive's date and time.

5.2.4 Classification of dive types

We classified all dives as being one of three types—pelagic dives, V-dives or benthic dives—based on guidelines described by Halsey et al., (2007) (see Fig. 5-2). Accordingly, we first calculated the 'broadness index' of each dive as the proportion of the duration of the bottom phase from the total dive duration. Dives with a broadness index < 0.05 were considered as V-dives. These represented dives with very short to no bottom phases and were unlikely to be of foraging function. All other dives, with a broadness index ≥ 0.05 therefore had extended bottom times (also commonly referred to as U-shaped) relative to the total dive time. These were further classified as either benthic or pelagic dives based on the following criteria: Dives with a maximum depth 2 meters from or below the estimated sea depth were considered benthic dives. Deviations between the obtained sea depth and maximum dive depth of a dive at a given location may have resulted from tidal changes or movements of birds within the 30-minute time window. Finally, dives with a maximum depth up to 2 meters of the estimated sea depth were considered as pelagic dives.

5.2.5 Estimation of dive bouts

Foraging behaviour in divers is known to occur over consecutive dives close in time and of similar characteristics forming foraging bouts (DUCKWORTH ET AL. 2020) see Fig. 5-3 for an illustration of bouts). To objectively assign individual dives to bouts we estimated 'bout ending criterion' from the variation in post-dive durations using the framework provided within the 'divemove' package (LUQUE 2007). Accordingly, we first excluded all post-dive durations greater than 30 minutes. We then fit a non-linear least squares "broken-stick" model to the histogram of the log-transformed

frequencies of the post-dive durations. The bin-width for this histogram was chosen as 10. The break point of the 2-step Poisson process model defined a 'bout-ending criterion' defined as the minimum post-dive duration beyond which consecutive dives can be considered as belonging to separate bouts. After defining the bout ending criterion, we assigned all dives into bouts—dives with a post-dive duration less than the bout-ending criterion were considered to be within the same foraging bout (see Fig. 5-3). Furthermore, we calculated bout duration as the time (in seconds) from the start of descent of the first dive, until the end of ascent of the last dive within a bout. From the duration of individual dives and of individual bouts we were able to respectively calculate the total time spent diving and total time spent foraging within a day, within the focal area. For this estimation we included only those days in which individuals spent all 24 hours within the focal area.

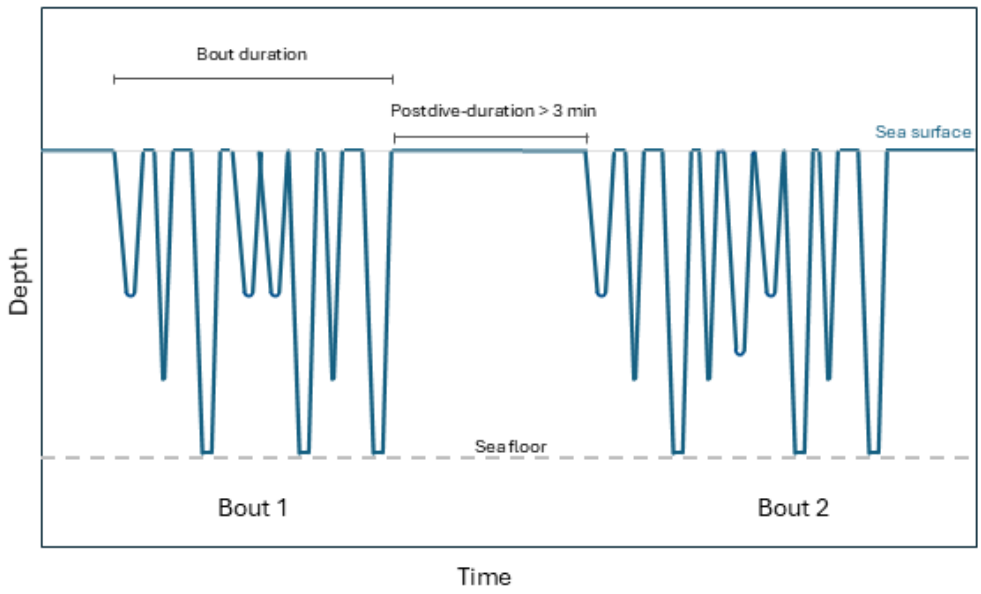

Fig. 5-3 *Illustration of the concept of classifying individual dives into bouts based on the bout-ending criterion.*

5.2.6 Statistical analyses

Summary of modelling workflow

To understand how proximity to offshore wind farms (OWF) affects foraging behaviour in wintering divers we conducted our analyses at two levels: (1) at the level of occurrence of diving behaviour, and (2) studying characteristics of dive bouts. For both levels, we employed a set of generalized linear mixed-effects models (GLMMs), described in detail below.

(1) For the analysis on the level of occurrence of diving behaviour, we restricted data to fixes occurring between 06:00 and 18:00 standardized time (hh:mm; i.e., dawn to dusk of each day). This ensured that absences of diving activity (i.e., zero dive counts) could be interpreted as true non-diving events (i.e., true zeros), rather than artefacts due to nocturnal absence of foraging. This analysis followed a two-step modelling approach. In the first step, we categorized GPS fixes as either having at least one dive (1) or no dives (0). We modelled this binary measure as a response variable using

a binomial GLMM. Each fix was categorized as either having at least one dive (1) or no dives (0). To disentangle within- and among-individual patterns arising from the effects of OWF proximity, we included both the within-individual mean-centred and individual mean distance as separate continuous fixed effects, following the approach of Van de Pol & Wright (2009). Additionally, we included sea depth (in metres), standardized time of day (in decimal hours), and a quadratic term for standardized time of day as continuous fixed predictors. Inclusion of a quadratic term for sea depth showed no significant improvement of model fit and was hence removed from the model. As random effects for individual bird identity we initially attempted to include random intercept and random slope variation for the within-individual effect of OWF distance, but these models failed to converge; the final model therefore included only random intercepts for individual identity. In the second step, we focused on the subset of GPS fixes where diving occurred and modelled the number of dives per fix as a response variable using a negative binomial GLMM. The same fixed effects were included as in the binomial model: the within-individual mean-centred and individual mean distances to OWF, sea depth, and standardized time of day (linear and quadratic terms). In this case, the model included the random effect of individual ID allowing random intercept and random slope variation (for the within-individual OWF distance effect).

(2) For the analysis on the level of foraging bouts we modelled the number of dives occurring within a bout as a response variable using a negative binomial GLMM. The same fixed effects were included as in the previous two models: the within-individual mean-centred and individual mean distances to OWF, sea depth, and standardized time of day (linear and quadratic terms). The inclusion of a quadratic term for sea depth showed no significant improvement of model fit and was hence removed from the model. This model also included the random effect of individual ID allowing random intercept and random slope variation (for the within-individual OWF distance effect). Finally, in a similar model we modelled the duration of a bout (in seconds) as a response variable using a negative binomial GLMM. Once again, the same fixed effects were included as in the previous models: the within-individual mean-centred and individual mean distances to OWF, sea depth, and standardized time of day (linear and quadratic terms). Due to convergence issues this model included the random effect of individual ID only allowing random intercept variation and not random slope variation.

General modelling procedures

All analyses were conducted in the R statistical software environment v4.2.3. All models were run using the 'glmmTMB' R package (BROOKS ET AL. 2017). A significance threshold (α) of 0.05 was applied throughout. The binomial GLMM was fitted with a logit link function, and all negative binomial models used the quadratic parameterization with a log link. The choice of the negative binomial distribution was based on pronounced overdispersion in the count and duration data, which was well captured by the model. In all models we mean centred the standardized time-of-day variable to allow for interpretation of the quadratic term (SCHIELZETH 2010). To account for temporal autocorrelation in the repeated GPS observations within individuals, we applied an Ornstein-Uhlenbeck (OU) correlation structure which allowed for variation in the time between consecutive observations (SANTON ET AL. 2023). We assessed the adequacy of this process by comparing AIC values and visually inspecting autocorrelation function (ACF) plots of residuals, of models with and without applying the OU correlation structure. ACF plots including the OU correlation structure showed rapid decay of temporal autocorrelation. Additional model diagnostics included quantile-quantile

(QQ) plots to visually assess residual normality and plots of residuals versus fitted values to evaluate homoscedasticity. For each model we also used quantile-quantile (QQ) plots along with plots of residual versus fitted values to visually assess normality of residuals and homogeneity of variances.

5.3 Results

5.3.1 Description of diving behaviour

A large proportion of fixes (representing 30-minute intervals) showed absence of diving behaviour (N = 5576; i.e., 80.3%), suggesting that foraging was restricted to specific locations and times within the day (Tab. 5-1). The spatial pattern showed that foraging dives were concentrated in the central and northern-eastern regions of our focal area, in some cases also in close proximity to the OWFs Butendiek and Horns Rev 1, 2 and 3 (Fig. 5-4). When diving occurred, the number of dives ranged between 1 – 82 dives per 30-minute interval with an average of 17.5 dives per fix (median = 13; Fig. 5-5, Fig. A 1). Diving behaviour was largely restricted to daylight hours (Fig. 5-6) with 99.7% (23796 of 23873 dives) of all dives occurring between civil dawn and civil dusk. Using our method of time standardization, it was observable that diving behaviour increased sharply around the time of civil dawn, tapering off towards time of local dusk (Fig. A 2). The mean number of dives per hour during the daytime (dawn to dusk) was 8.9 ± 7.03 (median = 8.2) and during the night (dusk to dawn) was 0.12 ± 0.3 (median = 0).. Median dive duration was 23 seconds (mean ± SD = 25 ± 16 seconds, range = 3 – 103 seconds; Fig. 5-7). While the median sea depth where dives occurred was 20 meters, dives were on average considerably shallower within the water column (median = 5.2 meters; mean ± SD = 7.0 ± 5.6 meters; range = 1.0 – 29.5 meters; Fig. 5-8).

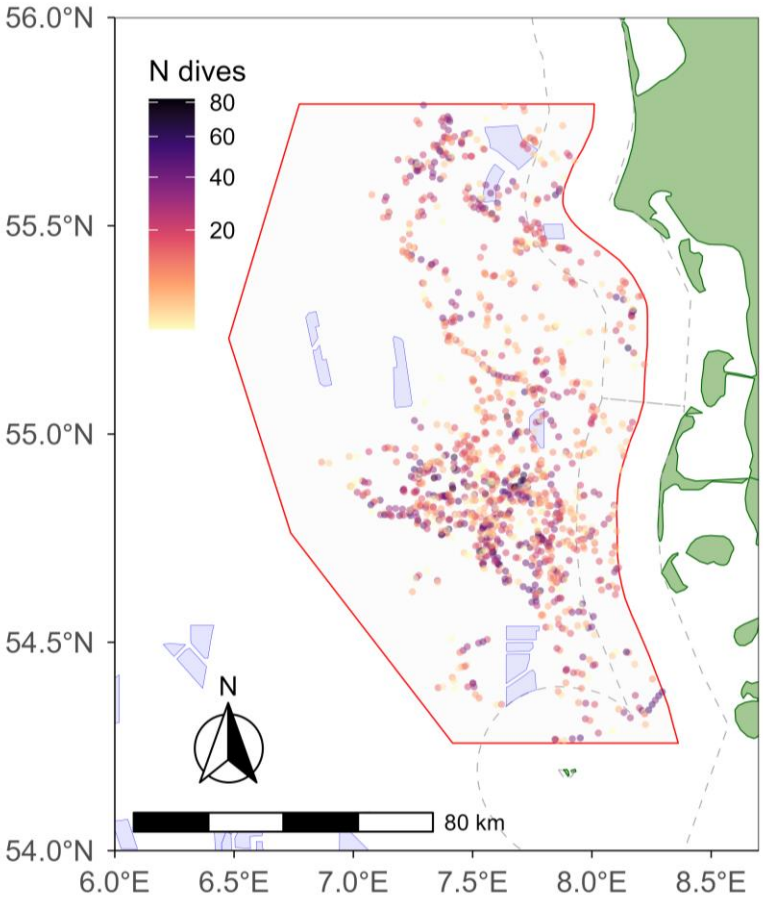

Fig. 5-4 *A map showing the spatial pattern of diving behaviour within the focal area in which points indicate the locations of dives. Colour scale of the points represents the number of dives occurring at a location, where dives ranged between 1 and 82 dives. Shown are only those locations where dives occurred.*

Tab. 5-1 *A summary of individual birds included in this study along with their individual contributions to the total dataset and characteristics of their diving behaviour*

	Bird ID	Year	Sex	N Days	N Dives	Mean dive depth	Std dev dive depth	% of all dives in dataset	N bouts
1	220661	2022	F	33	6247	5.60	4.24	26.2	273
2	220662	2022	F	30	7592	5.87	4.77	31.8	196
3	220663	2022	F	7	185	9.05	5.30	0.8	22
4	220664	2022	F	7	209	7.40	4.37	0.9	26

	Bird ID	Year	Sex	N Days	N Dives	Mean dive depth	Std dev dive depth	% of all dives in dataset	N bouts
5	220665	2022	F	2	165	7.15	4.67	0.7	15
6	220666	2023	F	5	112	3.82	1.47	0.5	17
7	230461	2023	F	10	1376	7.13	2.85	5.8	44
8	230452	2024	F	2	72	5.50	2.67	0.3	5
9	230453	2024	?	3	1087	6.55	4.66	4.6	41
10	230454	2024	F	13	1755	14.72	7.80	7.4	120
11	230455	2024	F	3	335	12.37	8.33	1.4	47
12	230459	2024	M	2	80	8.82	2.19	0.3	6
13	230460	2024	F	3	53	1.72	0.62	0.2	14
14	237444	2024	?	6	647	7.74	2.55	2.7	24
15	241018	2024	F	2	180	5.03	3.88	0.8	25
16	241019	2024	F	6	837	7.50	4.56	3.5	33
17	241020	2024	M	4	493	9.73	7.97	2.1	39
18	241021	2024	F	5	636	4.35	4.90	2.7	51
19	241022	2024	F	2	75	9.51	7.23	0.3	13
20	241024	2024	F	8	1265	9.48	6.66	5.3	49
21	244091	2024	F	8	472	6.37	3.82	2	41

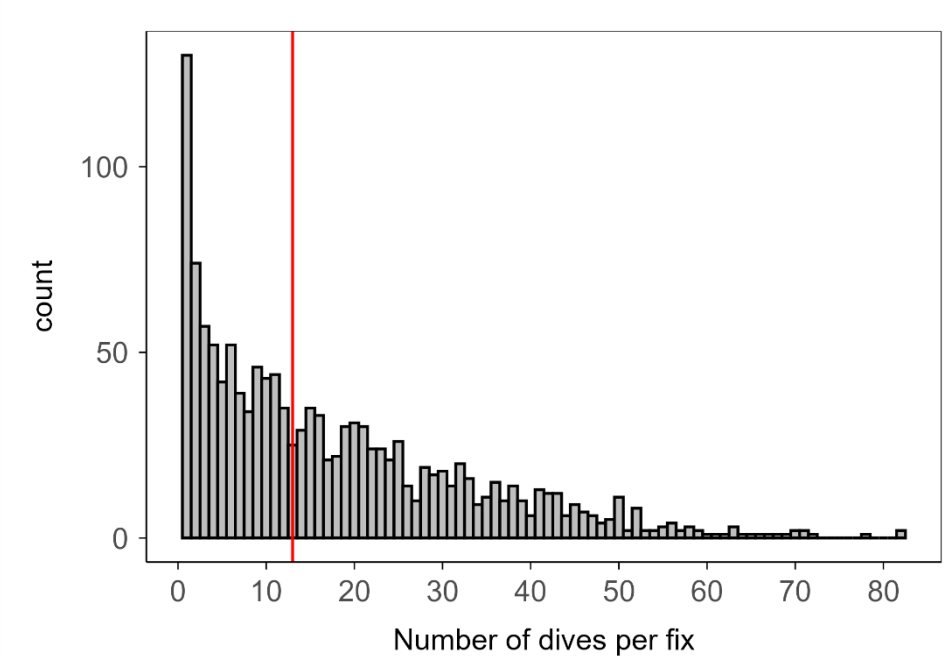

Fig. 5-5 *A histogram of the number of dives occurring per GPS fix, when considering only locations where at least one dive occurred. Note the large zero inflation due to the large number of fixes which showed no diving behaviour. Indicated in red is the median number of dives per fix (13).*

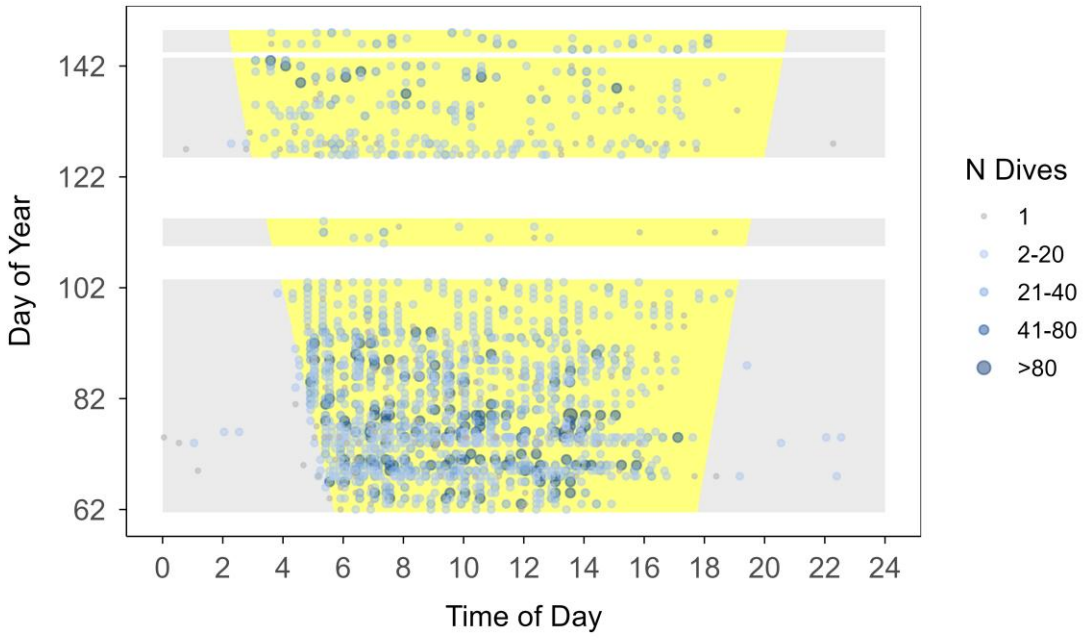

Fig. 5-6 *Figure showing the intensity of dive behaviour (number of dives at a location) over the time of day (X-axis) across days of the year with increasing daylight hours (Y-axis). Darker blue shades and larger points indicate more dives at a location.*

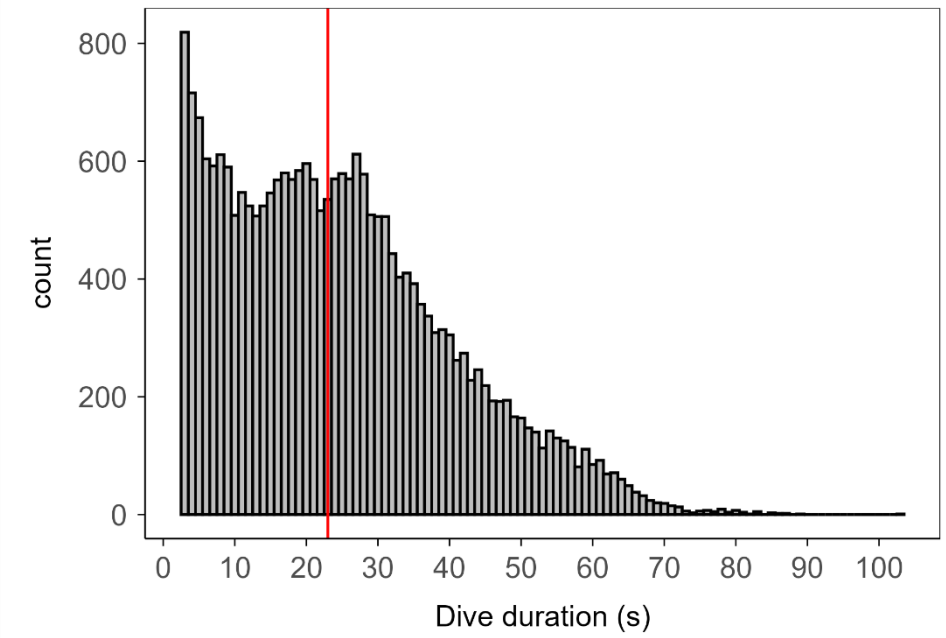

Fig. 5-7 *A histogram of dive durations of dives within our dataset. Indicated in red is the median dive duration (23 seconds).*

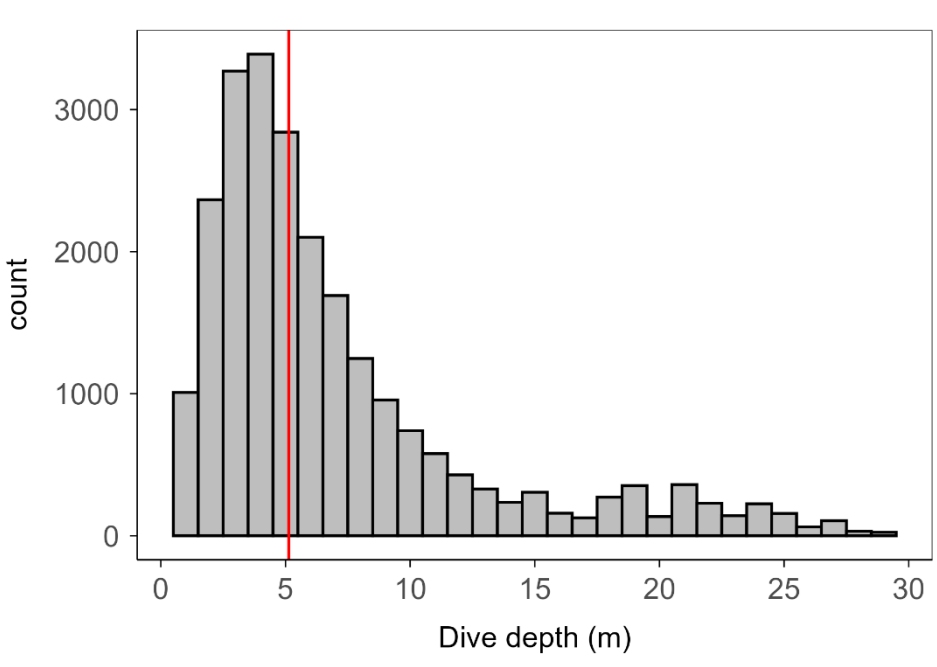

Fig. 5-8 *A histogram of dive depths within our dataset. Indicated in red is the median dive depth (5.2 meters).*

5.3.2 Dive types

Most dives within our dataset were classified as pelagic dives (N = 16474; 69.0%), with fewer V-shaped dives (N = 4666; 19.6%) and least of all benthic dives (N = 2733; 11.4%;Tab. 5-2; Fig. 5-9). While most dives were restricted to daylight hours (see details above), no benthic dives occurred outside of the dawn to dusk period (range: 06:24 – 17:19), dives being on average the shortest and benthic dives being of the longest duration (see Fig. 5-10, Fig A-4; Tab. 5-3). Of the total time spent diving for all dives in our dataset, 51.4 % consisted of pelagic dives, 25.7 % consisted of V dives and 22.9 % consisted of benthic dives (Tab. 5-2).

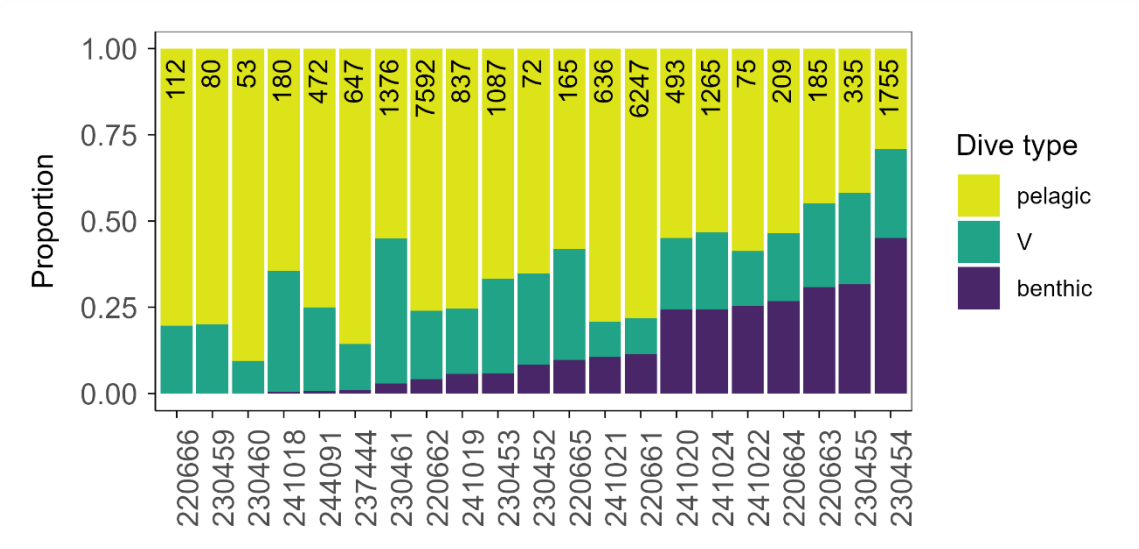

Fig. 5-9 *Proportional breakdown of total dives per individual across different dive-type categories.*

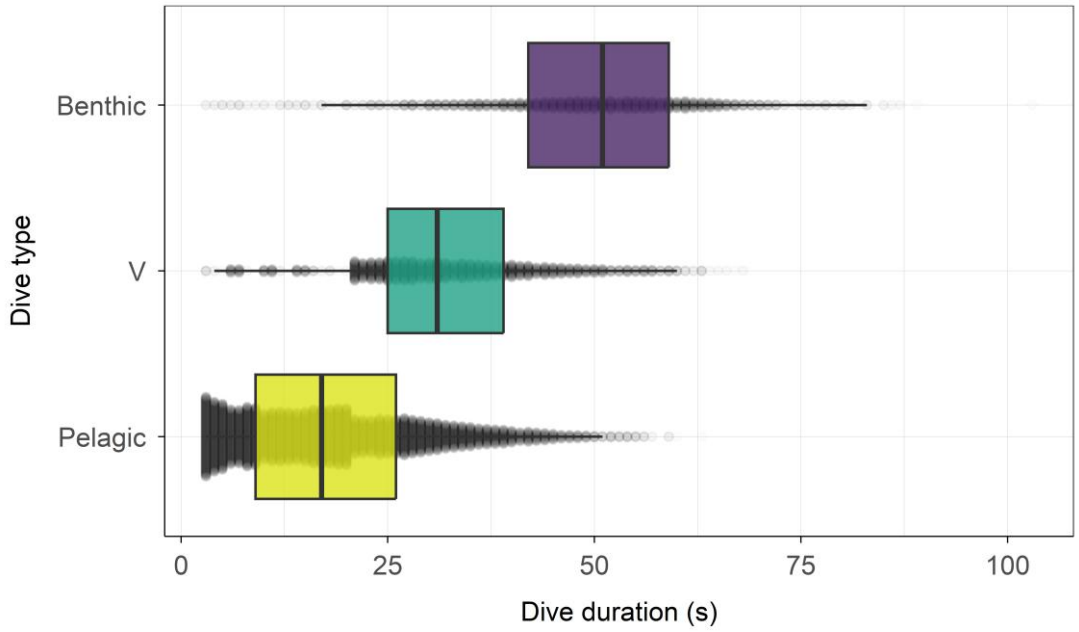

Fig. 5-10 *Differences in dive durations between the three different types of dives as classified in this study. Dive durations between each of the three dive types were found to be significantly different from the other with pelagic dives being of the shortest duration, V-shaped dives being longer and benthic dives being the longest. See also Table 3*

Tab. 5-2 *Percentage distribution of dives classified into Pelagic, V-shaped, and Benthic types, along with their corresponding contributions to total dive duration*

Dive type	% of total dives	% of total dive duration in dataset
Pelagic	69.0	51.4
V	19.6	25.7
Benthic	11.4	22.9

5.3.3 Dive bouts

Bout ending criteria was estimated at 181 seconds (ca. 3 minutes) allowing us to allot the 23873 dives into 1101 foraging bouts. The number of dives within a bout varied greatly (see Fig. 5-12; range: 1- 348). Foraging events consisted of 21.7 ± 33.5 dives (median = 8) with a considerable proportion of all of these consisting of a single dive (N = 247; 22.4%;Fig. 5-12). Single dives (as opposed to dives within bouts of more than 1 dive) made up only 1.0% of the total number of dives. Single dives were most often pelagic (N = 196; 79.4%) or V-shaped (N = 47; 19.0%) dives but rarely benthic dives (N = 4; 0.01%). All other dives belonged to bouts of two or more dives which lasted between 4 seconds to 176 minutes, with the average bout lasting 17.4 ± 23.1 SD minutes (median = 8.4 minutes). The median post-dive duration within a bout was 16 seconds. From a total of 108 complete bird-days of monitoring within the focal area we estimated the total time spent foraging per day as 2.31 ± 1.43 hours (mean ± SD, median = 2.45 hours or 02:15 hh:mm; Fig. 5-13). From

birds in which consecutive days of data were present it was apparent that time spent foraging over consecutive days varied in a roughly cyclic manner, with phases of intense or greatly reduced foraging effort (see example in Fig. 5-14). Individual dives within a bout were found to have highly correlated depths and durations.

Tab. 5-3 *Summary of the pairwise-comparisons of dive durations of the three dive types. Estimates and P-values are derived from a linear mixed-effects model with dive duration as a response variable and dive type taken as a predictor with 3-levels. Bout ID nested within Individual ID were included as random effects. See also Fig. 5-10*

Contrast	Estimate ± SE	P value
Pelagic – V	-7.04 ± 0.15	<0.0001
Pelagic - Benthic	-20.58 ± 0.27	<0.0001
V – Benthic	-13.55 ± 0.27	<0.0001

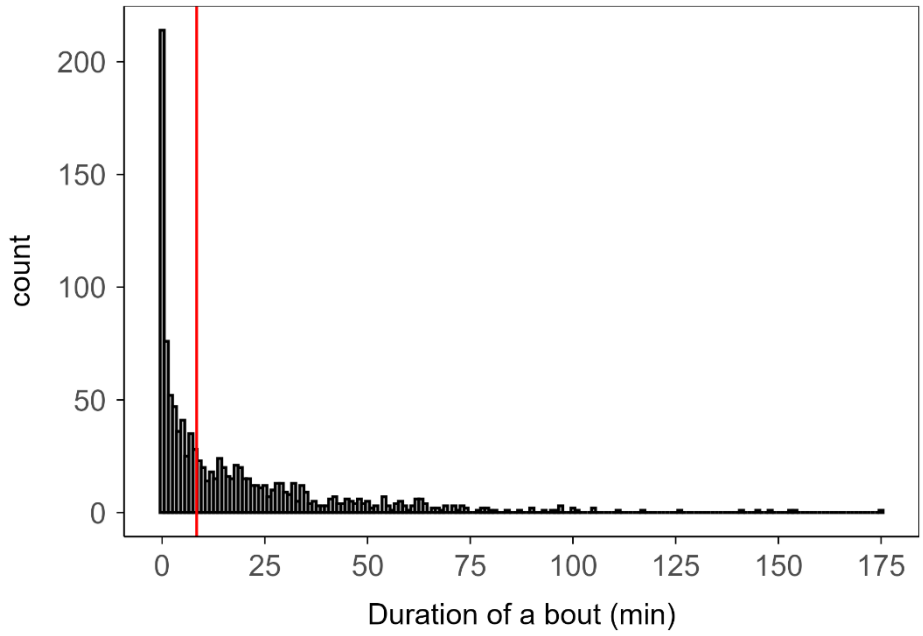

Fig. 5-11 *A histogram of bout durations within our dataset. Indicated in red is the median bout duration (8.4 minutes).*

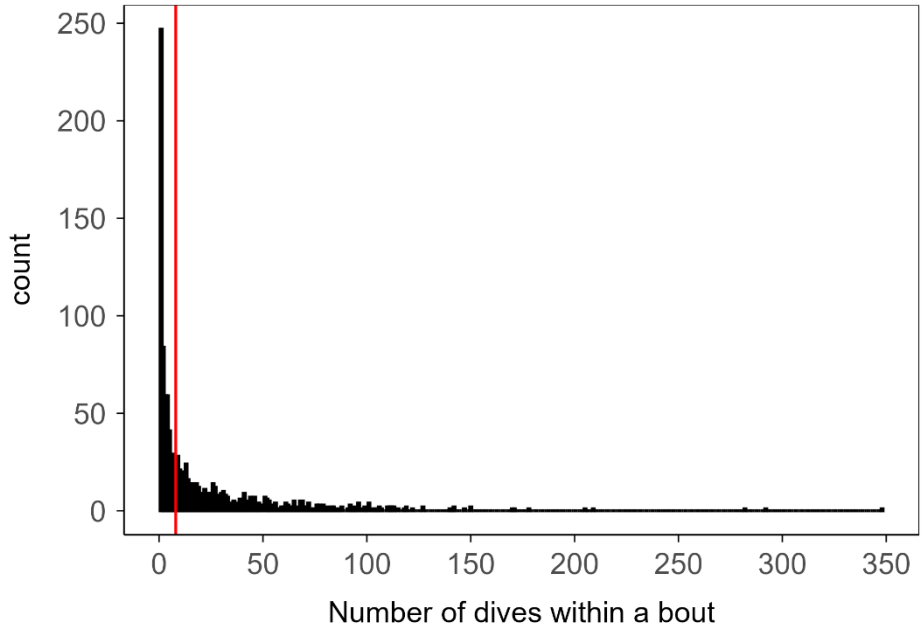

Fig. 5-12 *A histogram of the number of dives within a bout in our dataset. Indicated in red is the median number of dives occurring in a bout (8).*

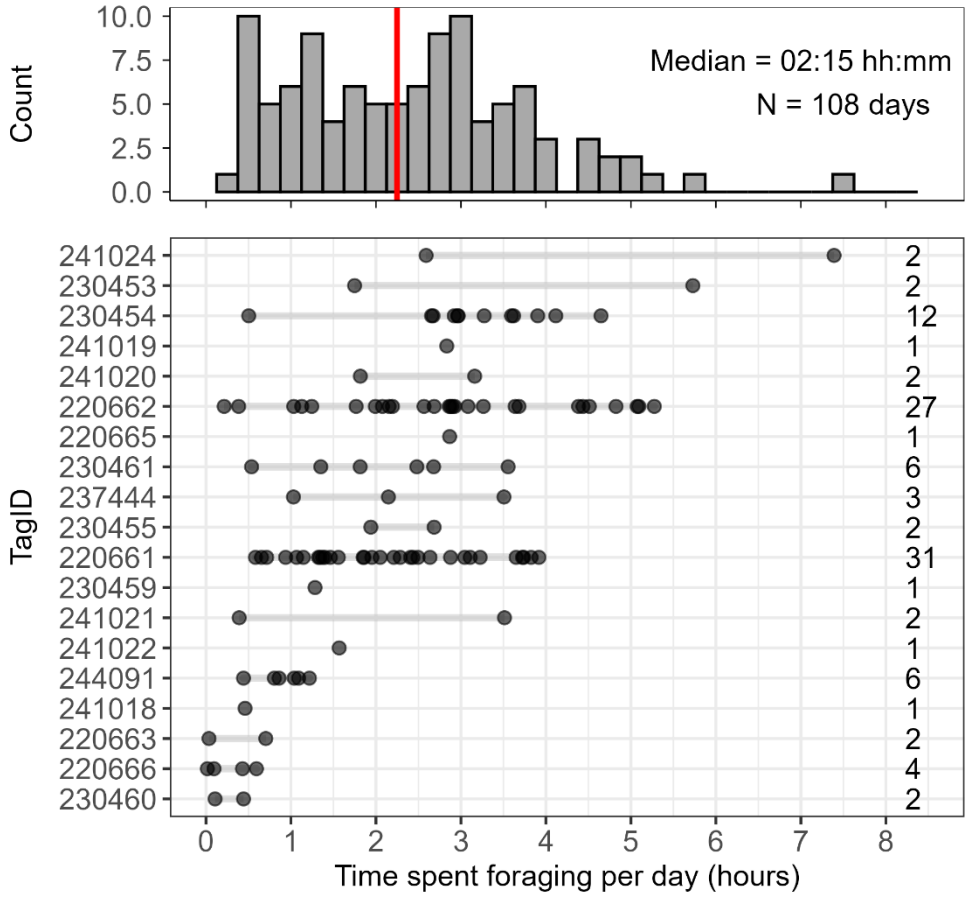

Fig. 5-13 *The total time spent foraging per day for different individuals (dotplot) calculated from those days (N = 108) in which individual birds (N = 19) spent all 24 hours of a day within the focal area. The total number of days sampled per individual is indicated on the right. Shown above is the distribution (histogram) of the time spent foraging per day combined for all birds, with the median indicated in red (2.31 hours).*

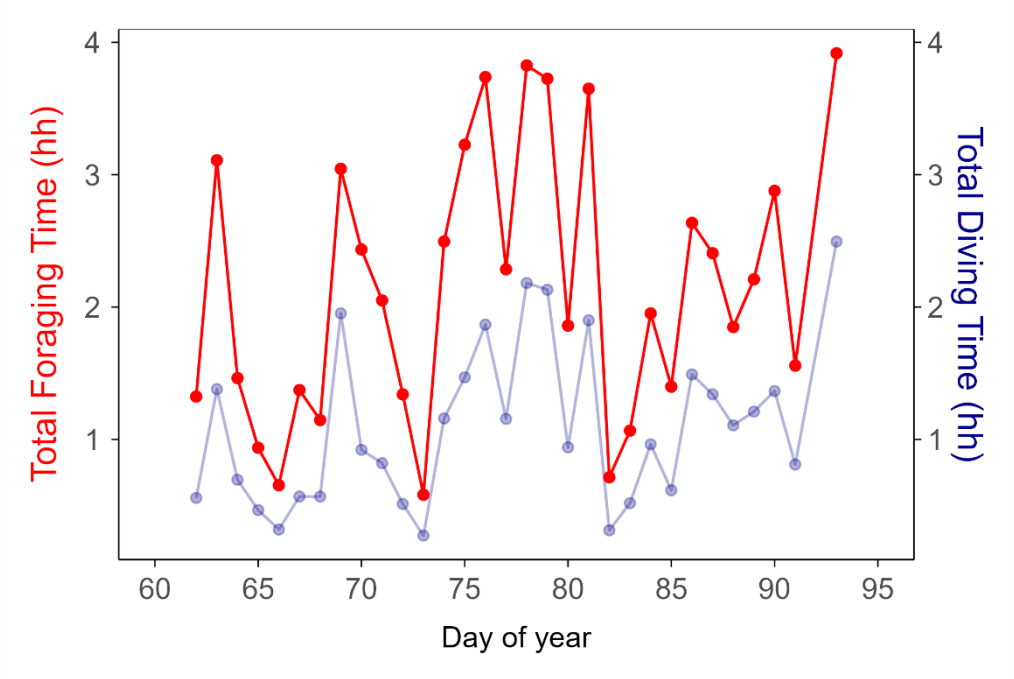

Fig. 5-14 *An example of the time spent foraging (dive durations + post-dive durations within a bout) and corresponding time spent diving (dive durations only) by an individual bird (ID: 220661) over consecutive days of monitoring within the focal area.*

5.3.4 Occurrence of dives in proximity of OWF

We found a significant among-individual increase in the probability of diving nearer to OWF (Tab. 5-4)—Individuals approaching nearer to OWFs had a higher probability of diving than those located away from OWF. We found no evidence that individual birds decreased their probability of diving nearer to OWF (Tab. 5-4). The number of dives at a location showed neither among- nor within-individual patterns with the distance to OWF (Tab. 5-5). Both the probability of diving and the number of dives showed a significant decrease with increasing sea depth (Tab. 5-4 & Tab. 5-5). Both response variables also showed a significant negative curvilinear (squared) term over the dawn to dusk period (Tab. 5-4 & Tab. 5-5). Model outputs using a dataset restricted to locations within 20 km of the OWF produced largely similar patterns with among- and within-individual effects of distance to OWF as well as with the other predictors included.

Tab. 5-4 *Summary of the binomial GLMM modelling the among- and within individual effects of the distance to the nearest OWF on the occurrence of dives at a given location. The data consist of N = 4209 locations. Sea depth and standardized time of day (linear and quadratic effects) were fitted as additional fixed predictors. Bird identity (N = 22) was fitted as a random effect. Significant effects are marked with an asterisk (*)*

Fixed predictors	Estimate	Std. Error	P Value
Intercept: Probability of diving	2.962	0.899	<0.001*
Distance to OWF (among-ind; km)	-0.206	0.050	<0.001*
Distance to OWF (within-ind; km)	-0.003	0.009	0.765
Sea depth (m)	-0.02	0.014	0.171
Std. time of day (hour decimal)	-0.3055	0.025	<0.001*
Std. time of day ² (hour decimal)	-0.052	0.007	<0.001*
Random effects	Intercept variance		
Bird ID	0.779		

Tab. 5-5 *Summary of the negative binomial GLMM modelling the among- and within- individual effects of the distance to the nearest OWF on the number of dives at every location where a dive occurred. The data arise from counts at N = 1335 locations. Sea depth and standardized time of day (linear and quadratic effects) were fitted as additional fixed predictors. Bird identity (N = 21) was fitted as a random effect. Significant effects are marked with an asterisk (*)*

Fixed predictors	Estimate	Std. Error	P Value
Intercept: N dives	3.158	0.437	<0.001*
Distance to OWF (among-ind; km)	-0.002	0.024	0.937
Distance to OWF (within-ind; km)	-0.002	0.011	0.836
Sea depth (m)	-0.027	0.008	<0.001*
Std. time of day (hour decimal)	-0.029	0.009	<0.01*
Std. time of day ² (hour decimal)	-0.013	0.003	<0.001*
Random effects	Intercept variance	Slope variance	Correlation
Bird ID	0.062	0.001	0.056
Dispersion parameter	1.687		

5.3.5 Bout characteristics in proximity of OWF

Both, the number of dives within a bout and the duration of a bout showed similar patterns with regard to the set of predictor variables (Tab. 5-6 & Tab. 5-7). We found no evidence that individuals decreased their dives within a bout nor that they decreased their bout durations closer to OWFs (i.e., no within-individual effect; Tab. 5-6 & Tab. 5-7). We also found no evidence that individuals foraging closer to OWF had shorter bouts or bouts with fewer dives (i.e., no among-individual effect; Tab. 5-6 & Tab. 5-7). Bout durations and the number of dives within a bout decreased at deeper sea depths. Both bout characteristics also showed a significant negative curvilinear (squared) and

increasing (linear) effect over the dawn to dusk period (Tab. 5-6 & Tab. 5-7). Model outputs using a dataset restricted to bout locations within 20 km of the OWF produced similar (null) patterns with among- and within- individual effects of distance to OWF as well as with the other predictors included.

Tab. 5-6 *Summary of the negative binomial GLMM modelling the among- and within- individual effects of the distance to the nearest OWF on the number of dives within a bout. The data consists of N = 1101 bouts. Sea depth and standardized time of day (linear and quadratic effects) were fitted as additional fixed predictors. Bird identity (N = 21) was fitted as a random effect. Significant effects are marked with an asterisk (*)*

Fixed predictors	**Estimate**	**Std. Error**	**P Value**
Intercept: N dives within a bout	4.138	0.646	<0.0001*
Distance to OWF (among-ind; km)	-0.016	0.034	0.640
Distance to OWF (within-ind; km)	0.002	0.013	0.859
Sea depth (m)	-0.054	0.013	<0.001*
Std. time of day (hour decimal)	-0.009	0.013	<0.001*
Std. time of day ² (hour decimal)	-0.02	0.003	<0.001*
Random effects	Intercept variance	Slope variance	Correlation
Bird ID	0.081	0.001	0.005
Dispersion parameter	0.852		

Tab. 5-7 *Summary of the negative binomial GLMM modelling the among- and within-individual effects of the distance to the nearest OWF on the duration of a bout (in seconds). The data consists of N = 1101 bouts. Sea depth and standardized time of day (linear and quadratic effects) were fitted as additional fixed predictors. Bird identity (N = 21) was fitted as a random effect. Significant effects are marked with an asterisk (*)*

Fixed predictors	**Estimate**	**Std. Error**	**P Value**
Intercept: Bout duration	8.405	0.524	<0.001*
Distance to OWF (among-ind; km)	-0.039	0.027	0.148
Distance to OWF (within-ind; km)	-0.002	0.007	0.788
Sea depth (m)	-0.042	0.012	<0.0001*
Std. time of day (hour decimal)	0.047	0.014	<0.01*
Std. time of day ² (hour decimal)	-0.024	0.003	<0.001*
Random effects	Intercept variance		
Bird ID	0.001		
Dispersion parameter	0.591		

5.4 Discussion

This study provides the first fine-scale assessment of the foraging behaviour of the red-throated diver, a species of high conservation concern, in an important staging habitat in the North Sea which overlaps with several OWF developments. Below, we discuss the ecological and conservation implications of our findings.

A main finding of this study is the relatively short amount of daily time (2.31 ± 1.43 hours; Fig. 5-13) that individuals spent foraging within our focal area. While our "foraging" estimate takes post-dive durations into account, the time spent solely on diving amounted to only 1.13 ± 0.83 hours (Fig. 6-4). These values are considerably lower than what is reported for most other diving seabirds during the non-breeding season (DUNN ET AL. 2024). As there is strong seasonal variation in diving activity (DUCKWORTH 2023; DUNN ET AL. 2024), it is important to compare similar time periods, whenever possible. For example, common guillemots in the general North Atlantic region and around the same time of year as our study period, are reported to spend an average of 5.62 ± 0.43 daylight hours diving (DUNN ET AL. 2020). Our estimate also lies well below published estimates for a migratory population of red-throated divers wintering in the North Sea, where birds spent 28% of daylight hours diving (DUNN ET AL. 2024). Only for the non-migratory diver population in Iceland, values where in the same range or lower during winter and spring. Adult great northern divers (*Gavia immer*) were reported to spend between 30 and 44% of daylight hours under water in their wintering area off the southern U.S. Atlantic coast (KENOW ET AL. 2023). The comparatively low dive investment observed in our study therefore suggests that prey resources in the staging area were sufficiently abundant to allow birds to meet energetic requirements with relatively little effort. In diving seabirds, time spent underwater is commonly used as a proxy for foraging effort and prolonged bouts are often interpreted as indicators of increased search costs under poorer feeding conditions (CHIVERS ET AL. 2012). Reduced foraging effort has been documented in other seabirds during periods of high prey availability. For instance, breeding common guillemots reduce both dive frequency and bout duration in years with abundant prey, reflecting increased foraging efficiency (MONAGHAN ET AL. 1994). Relatively low dive investment observed in our study therefore suggests that prey resources in the staging area were sufficiently abundant to allow birds to meet energetic requirements with minimal effort. The apparently favourable foraging conditions in our study may also explain why divers from vastly different breeding grounds (see Chapter 9) concentrate in the study area during springtime.

Despite generally low foraging effort, time spent diving varied considerably between days, with individuals showing phases of increased and reduced foraging activity. From the two birds that yielded a continuous time-series of data over several weeks within the focal area, it was evident that the time spent foraging per day fluctuated between consecutive days (e.g., Fig. 5-14). Such day-to-day variability suggests that divers adjust their foraging effort flexibly in response to short-term changes in prey availability, weather conditions or oceanographic processes such as tidal fronts (FINNEY ET AL. 1999). This flexibility may be particularly important during the pre-migratory staging period examined here, when individuals must balance the need to accumulate energy reserves with minimizing unnecessary energetic expenditure. Areas that allow birds to rapidly meet energetic demands may therefore be of disproportionate value, even if total daily foraging time is low. Future studies on movement and habitat selection could explore whether these cycles correspond to environmental drivers such as oceanographic or weather conditions (but see SKOV & PRINS 2001).

We also found that divers exhibit strongly diurnal foraging with 99.7% of all dives occurring during daylight hours. Foraging activity roughly peaked in the early hours past dawn and tapered down towards dusk. While diurnal foraging is common among pursuit-diving seabirds, the pattern appears more pronounced for species of divers (DUCKWORTH ET AL. 2020, 2021; KENOW ET AL. 2023) and puffins (SHOJI ET AL. 2015) than others. For example, Common guillemots (*Uria aalge*) and Razorbills (*Alca torda*), are known to flexibly extend diving activity into crepuscular or nocturnal periods (REGULAR ET AL. 2010, 2011; ELLIOTT & GASTON 2015), although the deepest dives are usually performed during the day (HEDD ET AL. 2009). The near absence of nocturnal foraging activity observed in our study suggests a strong preference for visual prey detection in red-throated divers. This interpretation is further supported by the predominance of shallow, pelagic dives in the upper water column (depths <10m), where prey capture is likely to depend on good visibility. Additionally in this regard, water clarity, another related parameter to visual prey detection, has been suggested to impact foraging efficiency for visual predators such as divers. As noted in work on a related species (THOMPSON & PRICE 2006; PIPER ET AL. 2024), turbidity can negatively affect prey detectability, particularly for pelagic foragers.

Most dives in our dataset were classified as pelagic, with benthic dives accounting for only 11% of total dive duration. Previous studies on foraging behaviour and diet suggest divers to be opportunistic predators with flexible foraging strategies based on prevailing habitat conditions (KLEINSCHMIDT ET AL. 2019; DUCKWORTH ET AL. 2021). Data on moulting divers have been used to coarsely identify dives as benthic or pelagic based on the uniformity of "intra-depth zone" dives within a bout (DUCKWORTH ET AL. 2024). Accordingly, foraging dives at consistently similar depths presumably reaching the sea floor are considered benthic dives and those that are variably are considered as pelagic foraging (DUCKWORTH ET AL. 2024). In the latter study, a considerable proportion (45%) of dives could be classified as benthic dives, suggesting that benthic foraging constitutes a significant proportion of the diet of some individuals during moult. In our study the combination of high-resolution TDR data coupled with the GPS positions allowed us to study dive types relative to the sea depth and thus classify dive types with a finer grain. The dominance of pelagic dives within our dataset further emphasises the importance of visual prey detection, driving a general preference for foraging in shallower depths. Pelagic foraging behaviour also aligns with earlier studies on the diet of divers in the same area. Specifically, energy-rich juvenile clupeid fish were the most frequently detected species group in the diet (KLEINSCHMIDT ET AL. 2019). This family of fish is known to be planktivorous and to form schools in the upper strata of the water column. Benthic dives accounted for a small proportion of total number of dives and dive duration (Tab. 5-2 & Tab. 5-3) possibly suggesting a shift to more predictable benthic prey when pelagic fish are scarce despite higher energetic costs of benthic diving. Our data hint at inter-individual foraging preferences, with considerable differences in the number of benthic vs pelagic and V-dives (see Fig. 5-9.). Such inter-individual foraging niche specialization has been documented across a number of seabird species (CEIA & RAMOS 2015; PHILLIPS ET AL. 2017). Nevertheless, given that there is very little temporal overlap in sampling days across individuals it would be difficult to rule out the effect of variation in environmental conditions and prey-type available to different individuals driving such patterns.

Dive bouts were highly variable in both duration and number of dives. This suggests that although prey availability in the concentration area may be generally high it may fluctuate in space and time. This is typical of oceanographic features of tidal fronts. The variation in daily foraging time further supports this idea, with prey conditions possibly varying greatly between days. In other assessments of diver foraging behaviour during the breeding season the number of dives within a bout and the

bout duration for divers was found to broadly differ with geographic region (DUCKWORTH ET AL. 2021). The authors suggest that these metrics reflect the effort needed for successful prey capture with shorter bouts indicating quicker prey capture success due to greater prey abundance. Contrastingly, in studies on breeding European shag (*Gulosus aristotelis*) Carlsen et al. (2021, 2023) posit that runs of similar dives within a bout indicate successive successful prey capture events. In a rare study using a combination of TDR data and visual identification of prey type at nests of Thick-billed murres (*Uria lomvia*), Elliott et al. (2008) show that smaller prey items tended to be caught on bouts with fewer dives, whereas bouts with many dives indicated pursuit of larger prey.

In the current study we use variation in foraging characteristics as a means to study the possible disturbance effects of OWF on foraging behaviour. A key finding was the general lack of variation in foraging patterns as an effect of OWF proximity. Specifically, we found no evidence that the number of dives, bout durations and number of dives within a bout decreased with distance to OWF, at both the among- and within-individual levels. Notably, however, we find an among-individual difference in foraging decision, with increased willingness of some individuals to forage closer to and within OWF. This suggests that individual birds differ in how close they may be willing to approach a wind farm. Overall, this study provided important baseline data on foraging patterns of red-throated divers in a non-breeding area of high conservation concern. Taken together with previous studies, our results suggest that although in general divers are disturbed by OWF, their presence is unlikely to disrupt fine scale characteristics of diver foraging behaviour. Furthermore, OWF presence may not have a uniform displacement effect on all individuals, possibly leaving some bold or more habituated individuals undeterred by OWF presence. However, earlier population-level studies on displacement have found no signature of diver habituation to a Danish windfarm, even five years past construction (PETERSEN & FOX 2007; PETERSEN ET AL. 2008). Thorough analysis of such a question would require multi-year individual-level telemetry data. Finally, our findings highlight the importance of high-resolution tracking data and of decomposing among- and within-individual patterns when assessing impacts of renewable energy infrastructure on wildlife populations.

6 TIME-ENERGY BUDGETS AND MOVEMENT PATTERNS

6.1 Introduction

Physiological energy is a fundamental factor shaping an animal's ecology. The amount of energy available influences short-term processes such as daily behavioural decisions and long-term life-history events like reproduction, ultimately affecting fitness (BROWN ET AL. 2004; GRÉMILLET & DESCAMPS 2023). Quantifying energy expenditure therefore provides a mechanistic link between individual behaviour and population-level outcomes. Estimating an individual's energy expenditure over a given period requires accounting for the energy allocated to activities such as flight, foraging, diving and resting, each with distinct metabolic costs (BIRT-FRIESEN ET AL. 1989; FORT ET AL. 2011; DUNN ET AL. 2023).

For diving seabirds like red-throated divers, both flight and diving are energetically demanding because of a high wing loading and reliance on foot propulsion (LOVVORN 2001; ELLIOTT 2025). Consequently, divers tend to minimise flight during staging and wintering periods unless migrating. Repeatedly induced flight by flushing from ships (BURGER ET AL. 2019) or to avoid OWF (FURNESS ET AL. 2013) may impose cumulative energetic costs. Quantifying how time and energy are distributed across behaviours is therefore essential for understanding responses to environmental change and anthropogenic disturbances (GRUNST ET AL. 2025). Detailed activity and energy budgets can reveal which behaviours dominate energy expenditure, how schedules vary across contexts (e.g., breeding vs. non-breeding), and how external pressures may alter these patterns (TOMLINSON ET AL. 2014; COLLINS ET AL. 2016; DUNN ET AL. 2020).

The accelerating expansion of offshore wind energy across northwest European seas is transforming extensive marine habitats of a number of seabird species (FURNESS ET AL. 2013; DIERSCHKE ET AL. 2016; PESCHKO ET AL. 2024; GARTHE ET AL. 2025). Among these species, the red-throated diver (*Gavia stellata*) has repeatedly been identified as particularly sensitive to offshore wind farm (OWF) development, showing marked avoidance during both construction and operational phases (PETERSEN & FOX 2007; GARTHE ET AL. 2014, 2023, 2025; MENDEL ET AL. 2019; BELLEBAUM 2020). Substantial reductions in diver densities around OWFs have been documented across multiple national sectors of the North Sea, typically extending several kilometres beyond turbine arrays (LAMB ET AL. 2024). If displacement forces birds to relocate to sub-optimal habitats, increase commuting distances, or alter foraging patch use, then even in the absence of direct mortality, incremental sublethal energetic costs may accumulate over time. Such subtle sublethal effects may indirectly affect survival and reproductive outcomes, but are challenging to quantify (DREWITT & LANGSTON 2006; SEARLE ET AL. 2018).

Recent advances in analytical frameworks and biologging technology now enable empiricists to estimate field energetic values directly from behavioural data (FORT ET AL. 2011; ELLIOTT 2025). This provides empiricists with a powerful tool to investigate the potential energetic costs of anthropogenic disturbances such as OWF. For example, Dunn, Duckworth, and Green (2023) have developed a general framework to quantify marine bird energetics, emphasising how activity-specific costs can be integrated across temporal scales to evaluate environmental effects. Similarly, Dunn et al. (2020; see also , 2022) demonstrated how seabirds adjust their energy budgets across annual cycles, and in a further study Duckworth et al. (2024) described divers' foraging and habitat preferences during

moult, highlighting the species' sensitivity to habitat change. In parallel, modelling studies have predicted how displacement or barrier effects may elevate energetic demands, with even modest increases in flight distance or changes in foraging habitat potentially affecting overwinter condition (MASDEN ET AL. 2010; WARWICK-EVANS ET AL. 2018).

Several behavioural mechanisms could impose costs for the red-throated diver. First, displacement from the vicinity of OWF either by swimming or by flight can elevate energy expenditure (GARTHE & HÜPPOP 2004; MENDEL ET AL. 2019). Second, exclusion from high-quality feeding areas may force individuals to exploit suboptimal or deeper foraging grounds, resulting in longer or more frequent dives. Third, disturbance or increased vigilance near OWFs could reduce foraging efficiency and resting opportunities, further increasing energetic demands. Studies quantifying such potential costs under field conditions in the non-breeding phase remain sparse (WARWICK-EVANS ET AL. 2018), primarily due to the challenge of acquiring appropriate datasets.

Individual divers may differ in their behavioural and physiological responses to environmental cues such as prey availability as well as anthropogenic disturbance, reflecting among-individual variation in strategies observed across many seabird species (KLEINSCHMIDT ET AL. 2022). Such heterogeneity means that OWF disturbance is unlikely to affect all birds equally: some individuals may consistently forage far from turbines, while others may routinely use areas next to OWF. Distinguishing changes that occur *within* individuals—as they move closer or farther from OWF—from differences *among* individuals provides essential insight into whether OWF trigger behavioural adjustment or simply reshape habitat use by subsets of the population. Statistically accounting for these differences in telemetry data is important, because individual-level variation can strongly influence exposure, energetic costs and ultimately survival (VAN DER KOLK ET AL. 2021).

The combination of GPS and time-depth recorders (TDRs) offers detailed insight into movement and foraging behaviour and furthermore to reconstruct basic activity budgets. This in turn allows for the estimation of time-specific energy expenditure using established activity-specific metabolic rates (FORT ET AL. 2011; DUNN ET AL. 2023). Although displacement of red-throated divers from OWFs is well supported by survey and tracking studies (GARTHE & HÜPPOP 2004; MENDEL ET AL. 2019; HEINÄNEN ET AL. 2020), very few studies have quantified how such displacement translates into changes in behaviour and daily energy expenditure at the level of individual birds. Most existing assessments rely on theoretical models that estimate increased flight distances or reduced foraging access (MASDEN ET AL. 2010; WARWICK-EVANS ET AL. 2018), but direct field measurements linking OWF proximity, activity budgets and energetics remain scarce—particularly during the non-breeding season. By combining GPS, diving data and activity-specific energetic estimates, this study provides one of the first empirical tests of whether OWF-associated displacement leads to measurable energetic costs for divers during the non-breeding phase.

Here, we use high-resolution GPS and TDR data from red-throated divers in the non-breeding period to broadly address the question: Do red-throated divers experience increased energetic costs as they move in proximity to OWF? Accordingly, we first (i) describe general movement patterns and activity budgets in terms of flight, diving, and resting behaviour in a known diver concentration-area in the German North Sea. We then (ii) assess how individuals' movement and activity budgets vary with proximity to OWF. Finally, we (iii) investigate the energetic implications of this variation. By linking movement, behaviour, and energetics we aim to determine whether OWF-related displacement translates into measurable energetic consequences. Such consequences could be

further used to inform population-level analyses and provide inputs for evidence-based maritime spatial planning (WARWICK-EVANS ET AL. 2018; BUCKINGHAM ET AL. 2026).

6.2 Methods

6.2.1 Fieldwork overview, focal area and data logger settings

The fieldwork for the current study is described in detail in chapter 4. In short, we studied red-throated divers (*Gavia stellata*) resting in the German Bight of the North Sea during spring (March-May) 2022-2024. Birds were captured at sea during nights around the new moon using night-lighting from a small boat operating from a larger vessel in the main 'concentration area' southwest of Sylt, Germany. Captured individuals were ringed, measured, and equipped with Ornitrack T25 GPS-GSM loggers with time-depth recorders, attached dorsally using tape and resin. Loggers were programmed to obtain location fixes and instantaneous ground-speed recordings every 30 minutes along with dive data from TDRs (time-depth recorders) at the rate of 1 Hz, every time a bird dived 1m below sea level, for more than 3 seconds. The focal study area encompassed German and Danish offshore waters (excluding near-coastal shallows) containing ten wind farm sites. In total, 30 birds were tagged (≤ 1.7% of body mass), yielding usable data from 24 individuals (21 within the focal area). All procedures were authorized and followed German animal welfare regulations. For more details see Chapter 4.

6.2.2 Data processing

Location and dive data were processed as in chapter 4. As in the previous chapter, to account for varying daylight hours during the study period we created a transformed time variable in which dawn and dusk times were standardized to 06:00 and 18:00. Thereafter, for each individual, data was divided into 30-minute intervals or steps, each assigned to the location marking the start of the 30-minute interval. Accordingly, the step length (straight-line distance between a given location and the next) and the total time spent diving were assigned to each step. Note that this was different from the previous chapter as here all dives occurring within the 30 minutes prior to a given acquired location were assigned to the corresponding step. Furthermore, in this chapter we considered the time that a bird spent submerged under water for more than three seconds and at depths greater than 1 m as the time spent diving. Our total sample size included 6,948 steps from 22 individuals. Of these, 19 individuals spent at least one complete day within the focal area, resulting in a total of 112 complete days over three sampling years (see Tab. 6-1).

6.2.3 Estimating daily time-activity budgets

To study the daily activity budget of red-throated divers within our focal area, we made use of the combination of location TDR data and instantaneous ground speed readings. Our objective was to estimate the time spent in each of three broad behavioural categories—diving, resting and flying—first per 30-minute interval and then as a total daily activity budget. For this, we first assigned all dives occurring within a 30-minute step to that step. In this way, the TDR data directly provided the total duration spent diving within each interval, while the step length represented the total distance

travelled in 30 minutes. We estimated the speed of movement during diving from those steps in which the majority of the time was spent diving (1.0 km/h). We estimated the corresponding flying time using an assumed average flight speed of 51.0 km/h. We selected this value after examining the distribution of instantaneous speed readings which showed a distribution distinct from that of the slower, more numerous speed readings. Furthermore, we confirmed that it aligned with published estimates of red-throated diver in-flight speeds (NORBERG & NORBERG 1971). Because seabirds such as divers drift passively with ocean currents or wind even when not making active directed movements via swimming or flying, we set resting speed at 1.6 km/h. We determined this value from the mean of instantaneous speed readings obtained from the loggers, after excluding data assignable to flying based on a 20km/h cutoff. We used the resting speed to calculate the maximum distance a bird could travel without flying during the non-diving period, and adjusted the value based on the time spent diving. When the observed step length exceeded the distance attainable by resting speed and diving speed, we attributed the excess distance to flight. The remaining non-diving time was classified as 'resting', which encompassed all activities not attributable to diving or flying. This procedure enabled us to partition each 30-minute interval into diving, flying, and resting components, thereby deriving an activity budget for each individual. To ensure convergence on a consistent solution, we refined this allocation iteratively over six successive steps. In each iteration, we updated the remaining non-diving time by subtracting the newly estimated flying time and re-calculated the expected distance. We repeated the process until the residual unexplained distance was minimized and a stable partitioning of the 30-minute interval into diving, flying, and resting components was achieved. Although this procedure tended to overestimate the number of steps within a day in which flight occurred (observed when plotting data), it assigned a small but seemingly accurate proportion for the total time spent flying within a day and across days. This was verified with the proportion of steps assignable to flying using the instantaneous ground speed readings. For days in which individuals spent the entire 24-hours cycle within the focal area, we estimated the respective daily activity budgets, by adding up daily time spent in that respective behaviour and thereafter calculated the proportion of time spent in each activity per day.

Tab. 6-1 *A summary of individual birds included in this study along with their individual contributions to the total dataset and the number of complete days spent within the focal area.*

	Bird ID	Year	Sex	N steps	N days within focal area
1	220661	2022	F	1541	31
2	220662	2022	F	1404	27
3	220663	2022	F	226	2
4	220664	2022	F	274	0
5	220665	2022	F	185	3
6	220666	2023	F	252	5
7	230461	2023	F	378	6
8	230452	2024	F	29	0
9	230453	2024	?	121	2
10	230454	2024	F	622	12
11	230455	2024	F	128	2
12	230456	2024	M	31	0

	Bird ID	Year	Sex	N steps	N days within focal area
13	230459	2024	M	77	1
14	230460	2024	F	230	4
15	237444	2024	?	213	3
16	241018	2024	F	85	1
17	241019	2024	F	157	1
18	241020	2024	M	186	2
19	241021	2024	F	129	2
20	241022	2024	F	60	1
21	241024	2024	F	288	2
22	244091	2024	F	332	5

6.2.4 Estimating daily energy expenditure

Using the framework set up by Dunn et al (2023), we translated the above daily activity budget into daily energy expenditure (hereon DEE) using estimated basal metabolic rate (hereon BMR) and activity-specific multipliers. Accordingly, we first estimated individual BMR from the average of two allometric scaling equations both of which use an individual's mass as input. Next, we calculated activity-specific energy expenditure as the product of an individual's BMR, the time spent per day in each activity and an activity-specific BMR multiplier. Although the framework provides multipliers for five different behaviours for foot-propelled diving seabirds such as our study species, our biologging equipment allowed to discern only three of the five possible behaviours. Specifically, for behaviours other than flying and diving we averaged the multipliers of the remaining three behaviours and assigned it to a time spent 'resting'. Thus, it may be important to note that the resting category incorporates all water-surface activity not assignable to diving or flying (such as resting, swimming, preening etc.).

Heat loss in cold seawater can elevate metabolic rates beyond those associated with locomotion (ELLIS & GABRIELSEN 2002; FORT ET AL. 2011). Thus, as also suggested by the adopted framework (DUNN ET AL. 2023) we estimated activity-specific thermoregulatory costs. For this we calculated the lower critical temperature (see definition below), extracted relevant daily sea surface temperatures and calculated thermal conductance (TC) for activities in which birds were on (resting) and under water (diving). As pointed out by Dunn et al. (2023) and Duckworth (2024) excessive heat produced from active flapping may accommodate thermoregulatory needs during flight and were therefore omitted from the calculation. The lower critical temperature (LCT) i.e., the temperature below which an individual incurs an additional thermoregulatory cost, was also calculated using the equation provided by Dunn et al (2023). Using the 'rerddap' package (CHAMBERLAIN 2025) we extracted year-specific daily sea-surface temperatures at the centroid of our focal area as representative for the entire focal area. Daily sea surface temperature (SST) from days sampled were retrieved from the NOAA (National Oceanic and Atmospheric Administration, Government of USA) Optimum Interpolation Sea Surface Temperature (OISST) v2 dataset. Data were accessed via the NOAA ERDDAP (https://www.ncei.noaa.gov/erddap/index.html) server using 'griddap' function of rerddap R package. Thermoregulatory costs were thus calculated for all days, i.e., days on which sea surface

temperature was below individuals' lower critical temperature using the following equation (DUNN ET AL. 2023):

$$Thermoregulatory\ costs\ =\ degrees\ below\ LCT\ \times\ \frac{body\ mass}{1000} \times\ TC\ \times\ time\ in\ activity$$

DEE was thus estimated as the sum of its activity-specific energy expenditure and corresponding thermoregulatory costs, for days in which individuals spent the entire 24-hour cycle within the focal area.

Because BMR was derived from body mass using allometric equations (DUNN ET AL. 2023), we corrected individuals' DEE for differences in their mass for use in the analysis using the following equation (as in DUCKWORTH 2023):

$$DEE\ per\ unit\ mass\ (Kg) =\ DEE\ kJ\ \div\ Mass\ in\ Kg^{0.7545}$$

This equation divides DEE by mass raised to 0.7545, which is the mean of the exponents used in the two equations to derive BMR from body mass (DUCKWORTH 2023; DUNN ET AL. 2023). DEE per unit mass was used in further statistical analyses.

6.2.5 Statistical analyses

In line with our broad research aims our analysis followed three main steps described below:

(i) To study the movement patterns of red-throated divers we first analysed variation in step length as a response variable using a GLMM with a gamma distribution and a log link function. For this analysis we restricted our dataset to the continuous time series of data from individuals until the bird first left the focal area. This allowed us to use the simpler first-order autoregressive process to account for temporal autocorrelation, rather than the more complicated Ornstein-Uhlenbeck process used for interrupted data. To disentangle within- and among-individual patterns arising from the effects of OWF proximity on step lengths, we included both the within-individual mean-centred and individual mean distance as separate continuous fixed effects, following Van de Pol & Wright (2009). This approach resolves whether birds that generally range closer to OWFs in our dataset, differ from those that remain farther away, while separately and simultaneously testing whether a given bird changes its behaviour or energetics on days when it is closer or farther from OWFs than usual. We included sea depth (in metres) to test if the depth at a current location influenced the step length away from that location. Additionally, we included a circular time of day variable to explore diel periodicity and to estimate peak time of movement activity (IANNARILLI ET AL. 2025). For this we applied trigonometric (sine and cosine) functions to our standardized measure of time of day (IANNARILLI ET AL. 2025) which followed a circular distribution. Peak movement time (increased step lengths) was calculated from the fitted harmonic (phase angle from the sine/cosine coefficients) and reported on a 24-h scale (IANNARILLI ET AL. 2025). Individual identity was included as a random intercept. An additional model testing for a bimodal activity pattern using additional trigonometric predictors explained no additional variation in the data and was discarded (following Iannarili et al. (2025); Tutorial: https://hms-activity.netlify.app/).

(ii) To study how activity-specific patterns were affected by the proximity to OWFs we modelled the proportion of time spent per day in each of the three behavioural activity categories—diving, flying

and resting— in separate GLMMs. In each of these models the response variables consisting of proportion data were modelled with a beta distribution and a logit link function. To obtain a daily distance of the individual from the nearest OWF we calculated the centroid of the daily coordinates of each individual and measured the corresponding distance to the nearest OWF. Using these we calculated an individual's mean distances to OWFs and within-individual mean-centred distances to OWFs across days. These were included as fixed predictors. We also included the day of year as a continuous variable to account for potential seasonal variation in behavioural activity. We included the random effect of individual ID. Calculations of daily distance to OWFs based on daily centroids were highly correlated with the mean distance of all fixes within a day ($r = 0.948$, $t = 31.30$, $df = 110$, $P < 0.001$), and model outputs (including below mentioned model) were near identical regardless of which distance metric was used. For the model on the proportion of time spent diving, an additional zero-inflation term was included to allow for the beta model to accommodate zeros from the few days (N = 5 from a total of 112 days) on which no diving behaviour occurred.

(iii) Finally, to assess how the interplay of different activities might have a combined effect on total energy expenditure of divers in relation to OWF presence, we modelled the total DEE per unit diver mass as response variable in a linear mixed effects model with a gaussian distribution and identity link function. As in the set of models of the previous step we included fixed predictors for the individual's mean distances and their corresponding within-individual mean-centred distances to OWFs across days. We also included the day of year as a continuous variable to account for potential seasonal variation in energy expenditure. Individual ID was also included as a random effect in this model.

All models were run using the '*glmmTMB*' package (BROOKS ET AL. 2017) in the R statistical software environment. In all models, inclusion of random slopes in addition to random intercepts for individual ID resulted in model convergence issues. We thus retained the random intercept-only models. We set our significance threshold (α) at 0.05. All models were diagnosed for adherence to assumptions using the 'performance' R package (PERFORMANCE 2021).

6.3 Results

6.3.1 General patterns of movement, activity and energy use

On average path lengths of birds were 43.5 ± 12.3 (mean ± SD) km per day (Fig. 6-1), with most half-hour steps spanning less than a kilometre (Fig. 6-2). Daily movement patterns revealed a significant time-of-day effect on step length (Tab. 6-2; Fig. 6-2), with greater step lengths occurring within day-light hours. Phase calculations based on model coefficients indicated peak movement activity at 09:41 on the standardized time scale (roughly 3.5 hours past civil dawn; see Tab. 6-2). The sea depth at a given location showed no detectable influence on proceeding step length (Tab. 6-2).

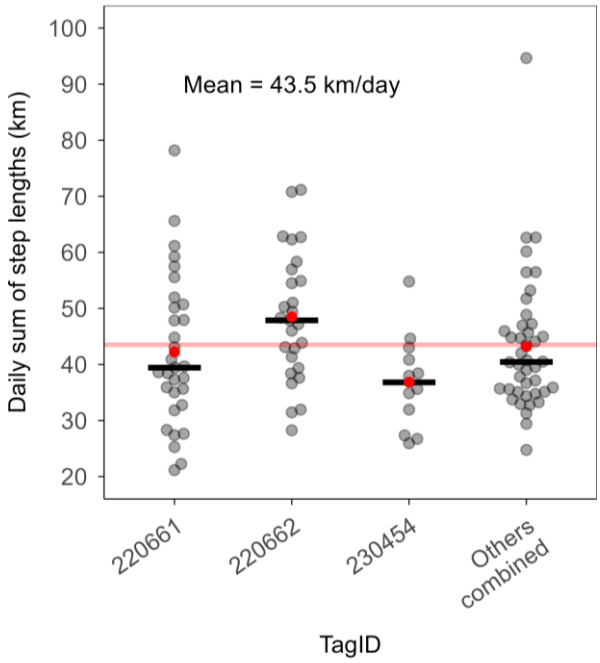

Fig. 6-1 *Daily path lengths travelled by divers within the focal area shown as points. Shown are the medians (horizontal black bars) and means (red points) with the overall mean (horizontal re d line) of 43.5 km/day. Data from three individuals with the most sampling days shown separately with all other individuals shown in a combined category. See Tab. 6-1 for sampled days per individual.*

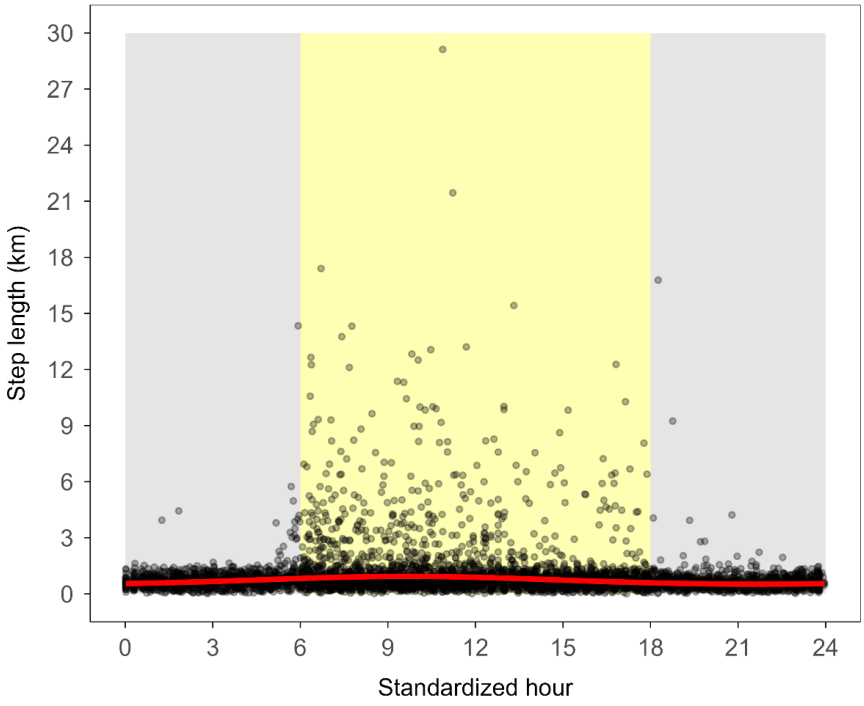

Fig. 6-2 *Step lengths (points) plotted against the standardized hour of day. Shown in red is the predicted line of the trigonometric functions estimating the peak and trough of step lengths over the diel period taken from the model presented in Tab. 6-2.*

Activity budgets showed that divers in the focal area spent a vast majority of the 24-hour cycle in resting behaviour (Fig. 6-3 and Fig A-7). Both diving and flying activity took up far lower proportions of the time of day than resting behaviour (Fig. 6-3, Fig. 6-4, Fig. A 7). The daily time spent in the two more energetically intense activities flying and diving were weakly yet significantly positively correlated ($r = 0.24$, $t = 2.63$, $df = 110$, $P = 0.01$) suggesting that individuals had days of relatively high or low combined activity. None of the three activities covaried with progression of the season (day of year; Tab. 6-3, Tab. 6-4 and Tab. 6-5).

In general, DEE varied considerably within individuals with the largest difference between highest and lowest values being 433 kJ (Bird ID: 220662; Fig. 6-6). DEE tended to roughly vary as days of high or low energy expenditure (e.g. time series of bird ID 220661; Fig. 6-7), with no clear pattern. DEE averaged at 1959 kJ (Tab. 4-1). When correcting for differences in mass, it averaged at 1380 $kJ/Kg^{0.7545}$ (Tab. 6-6). DEE decreased significantly with progression of the season (i.e., day of year; Fig. 6-5;Tab. 6-6).

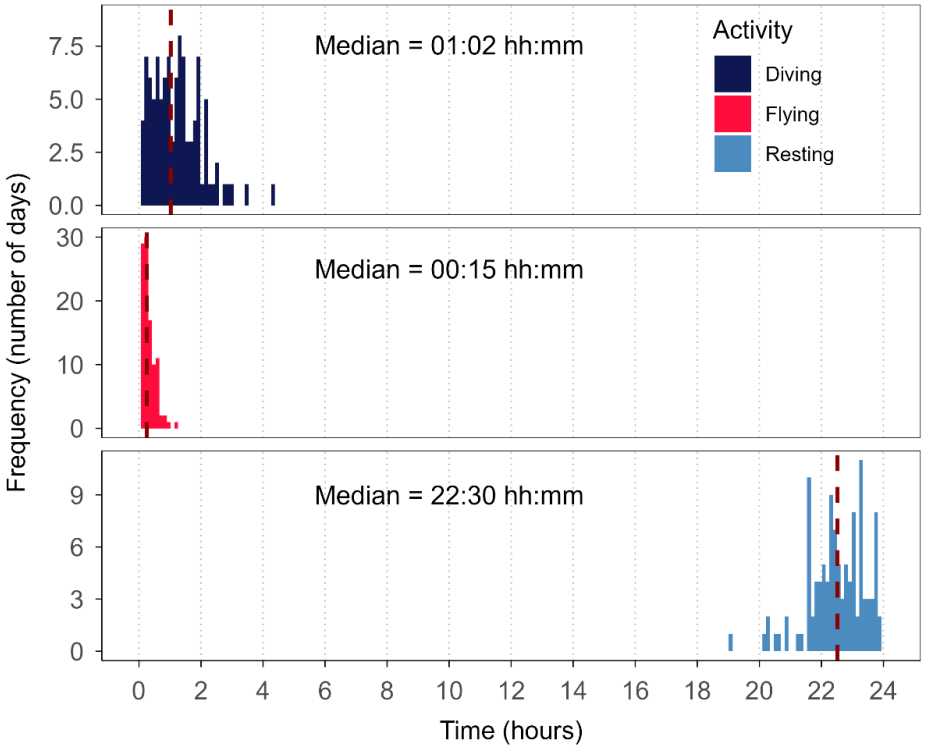

Fig. 6-3 *Histograms showing the daily time spent in diving, flying and foraging behaviours as estimated from our time-activity budget calculations. Marked in dashed red lines are the median time spent in each behaviour per day.*

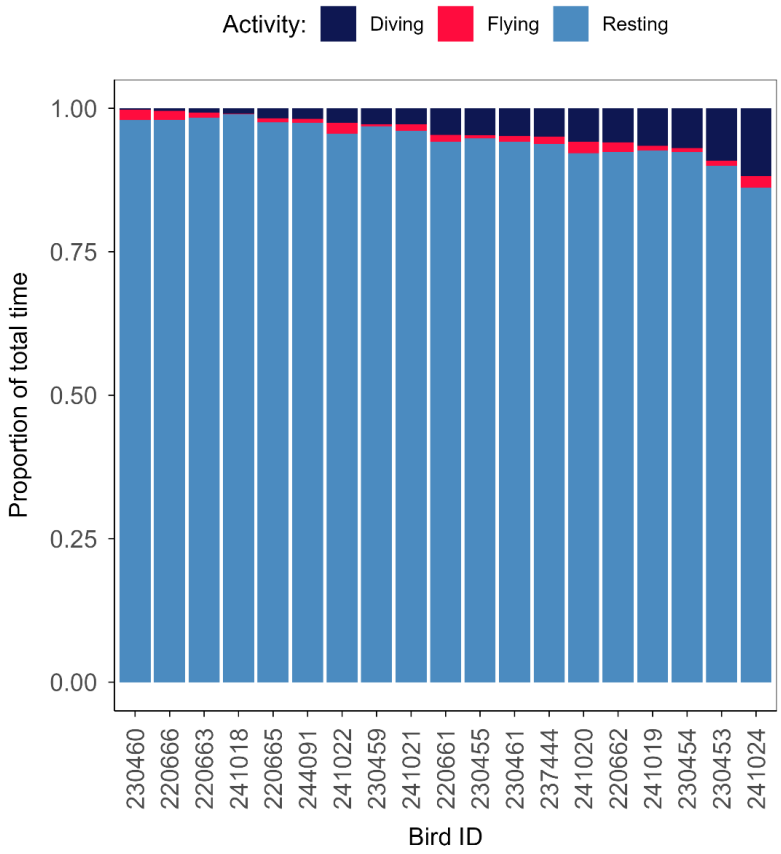

Fig. 6-4 *Proportions of the total time spent in different activities by different individuals within the focal area*

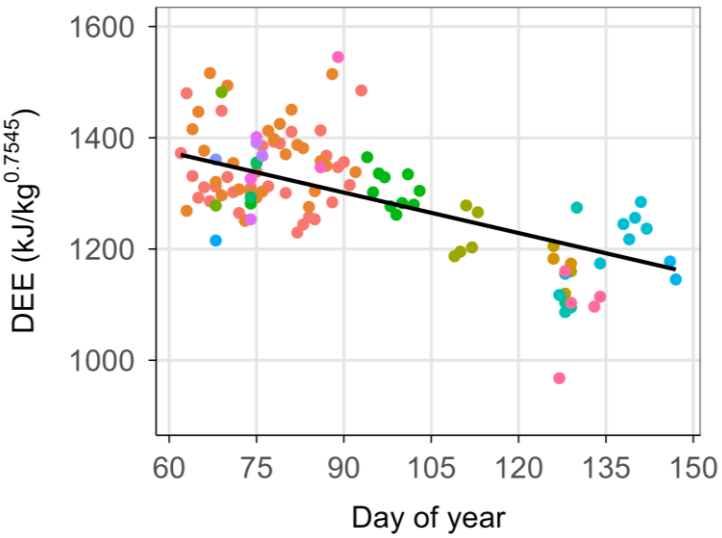

Fig. 6-5 *Seasonal variation in daily energy expenditure over the sampled period. Shown is a significant decrease in daily energy expenditure (DEE) with progression of the season (beginning early March) as indicated by the solid black line. Colours represent different individuals. Predicted line is based on the model presented in Tab. 6-6.*

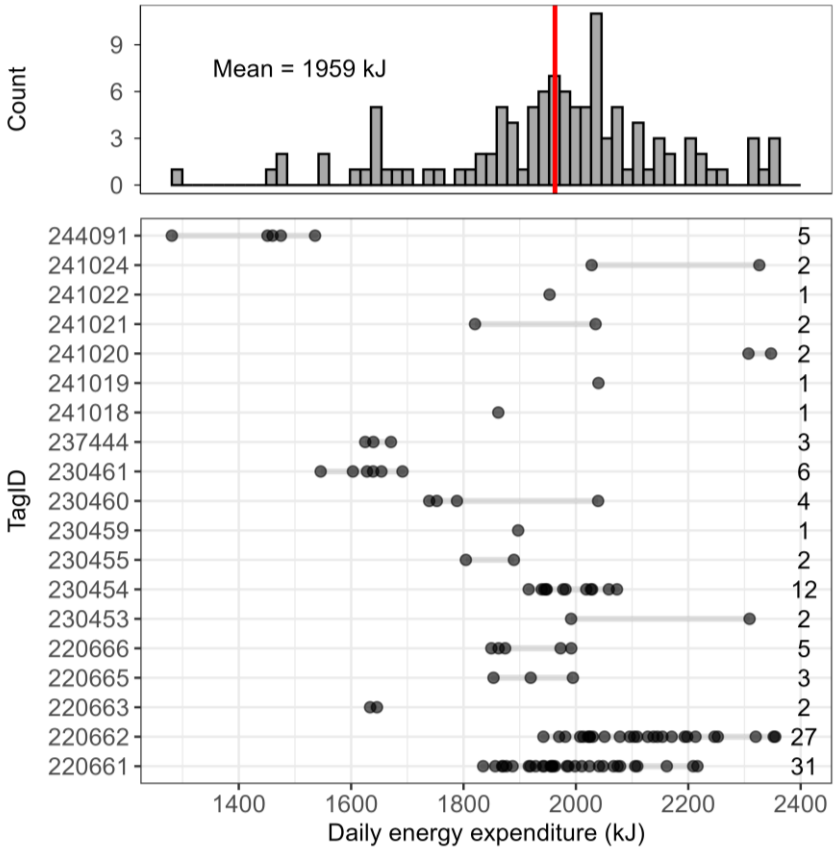

Fig. 6-6 *DEE (kJ) of individuals (points) calculated from days (N = 112) in which individual birds (N = 19) spent all 24 hours of a day within the focal area. The total number of days sampled per individual is indicated on the right. Shown in the top panel is the corresponding distribution of the DEE across all individuals, with the mean indicated in red.*

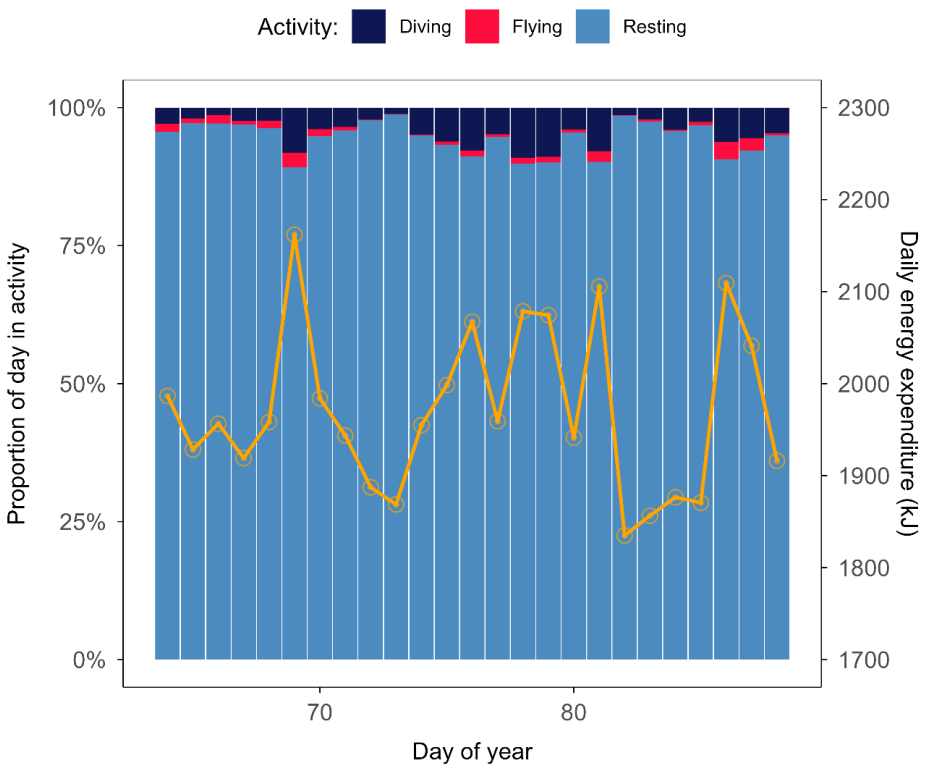

Fig. 6-7 *An example of variation in the daily time spent in different activities and the corresponding variation in daily energy expenditure of a single individual (ID: 220661) over consecutive days of monitoring within the focal area. The stacked bars show the proportion of consecutive days spent in different activities, while the orange points and line indicate the corresponding daily energy expenditure.*

6.3.2 Movement, activity and energy expenditure variation in proximity to offshore wind farms

Neither the among-individual nor within-individual effects of OWF distance significantly predicted step length (Fig. 6-2, Tab. 6-2).

Tab. 6-2 *Summary of the GLMM modelling the among- and within-individual effects of the distance to the nearest OWF on step lengths. The data consist of N = 4780 steps. Sea depth and standardized time of day (with trigonometric transformations) were fitted as additional fixed predictors. Bird identity (N = 22) was fitted as a random effect. Significant effects are marked with an asterisk (*)*

Fixed predictors	Estimate	Std. Error	P Value
Intercept: Step length (km)	-0.203	0.114	0.073
Distance to OWF (among-ind; km)	-0.009	0.006	0.168
Distance to OWF (within-ind; km)	0.004	0.004	0.243
Sea depth	0.002	0.004	0.644
sin(2π × time of day/24)	1.166	0.031	<0.001*
cos(2π × times of day/24)	-0.239	0.031	<0.001*
Random effects	Intercept variance		
Bird ID	<0.001		
Residual	<0.001		
Dispersion parameter	0.13		

Birds that generally ranged closer to OWFs spent significantly more daily time diving overall (Tab. 6-4). Within-individual deviations in daily diving behaviour were not significant (Tab. 6-6), suggesting that diving behaviour was driven more by persistent among-individual differences between birds than by day-to-day changes in OWF proximity (see Discussion section for detailed interpretations). In contrast, the flying-time model revealed no significant among-individual effect of OWF distance (Tab. 6-6). However, at the within-individual level, birds spent more time flying on days when they were closer to OWFs (Tab. 6-3). This indicates a short-term behavioural response rather than a stable individual-level difference. Birds that generally ranged farther from OWFs spent more time resting (Tab. 6-5). A similar positive effect occurred within individuals: on days when a bird was farther from OWFs than its own average, it spent a greater proportion of time resting (Tab. 6-5). Thus, both individual differences and daily fluctuations indicated reduced resting behaviour with closer OWF proximity.

Tab. 6-3 *Summary of the GLMM modelling the among- and within-individual effects of the distance to the nearest OWF on the proportion of daily time spent flying. The data consist of N = 112 days. Bird identity (N = 19) was fitted as a random effect. Significant effects are marked with an asterisk (*)*

Flying: Fixed predictors	Estimate	Std. Error	P Value
Intercept:	-4.27	0.32	<0.001*
Distance to OWF (among-ind; km)	-0.01	0.02	0.589
Distance to OWF (within-ind; km)	-0.02	<0.01	0.030*
Day of year (days)	<-0.01	<0.01	0.821
Random effects	Variance		
Bird ID	0.06		
Dispersion parameter	167.09		

Tab. 6-4 *Summary of the GLMM modelling the among- and within-individual effects of the distance to the nearest OWF on the proportion of daily time spent diving. The data consist of N = 112 days. Bird identity (N = 19) was fitted as a random effect. Significant effects are marked with an asterisk (*)*

Diving: Fixed predictors	Estimate	Std. Error	P Value
Intercept:	-2.17	0.49	<0.001*
Distance to OWF (among-ind; km)	-0.08	0.03	0.024*
Distance to OWF (within-ind; km)	-0.01	<0.01	0.268
Day of year (days)	0.01	0.01	0.187
Zero inflation intercept	-3.06	0.46	<0.001*
Random effects	Variance		
Bird ID	0.39		
Dispersion parameter	52.53		

Tab. 6-5 *Summary of the GLMM modelling the among- and within-individual effects of the distance to the nearest OWF on the proportion of daily time spent resting. The data consist of N = 112 days. Bird identity (N = 19) was fitted as a random effect. Significant effects are marked with an asterisk (*)*

Resting: Fixed predictors	Estimate	Std. Error	P Value
Intercept:	2.17	0.32	<0.001*
Distance to OWF (among-ind; km)	0.04	0.02	0.041*
Distance to OWF (within-ind; km)	0.02	0.01	0.021*
Day of year (days)	<0.01	<0.01	0.666
Random effects	Variance		
Bird ID	0.11		
Dispersion parameter	50.63		

We found a weak but significant negative within-individual effect of OWF proximity on DEE (Fig. 6-8; Tab. 6-6), indicating that birds expend slightly more energy on days spent closer to OWFs. For a typical 1.8 kg diver, this corresponds to an increase of approximately 4.08 kJ/day (2.201 kJ/ $kg^{0.7545}$ × $1.8^{0.7545}$) with every km increase towards an OWF. We also found that birds that were generally in closer proximity to OWFs, had significantly higher DEE (i.e., among-individual effect; see Tab. 6-6; Fig. 6-8).

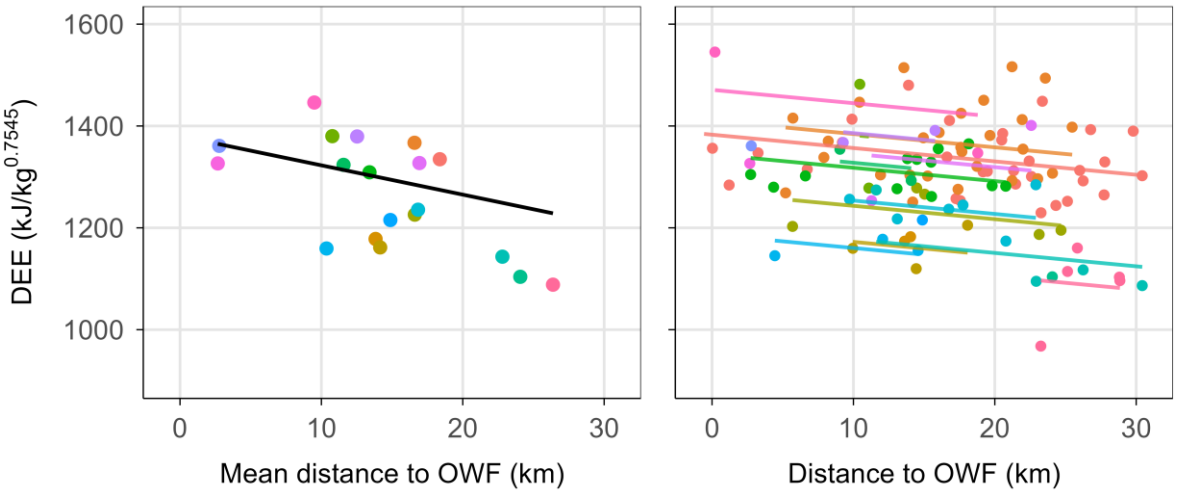

Fig. 6-8 *Among- and within-individual effects of the distance to offshore wind farms (OWF) on daily energy expenditure (DEE). Left panel: Mean DEE plotted against individuals' mean distance to OWF; the solid black line indicates the significant negative predicted effect. Right panel: Raw individuals' DEE values plotted against daily distances to OWF. Coloured lines show significant individual-specific predicted intercepts and slope, illustrating changes in DEE with day-to-day variation in distance to OWF. Colours represent different individuals throughout. Predicted lines are based on the model presented in Tab. 6-6.*

Tab. 6-6 *Summary of the LMM modelling the among- and within-individual effects of the distance to the nearest OWF on the daily energy expenditure of individual divers. The data consist of N = 112 days. The day of year was fitted as an additional fixed predictor. Bird identity (N = 19) was fitted as a random effect. Significant effects are marked with an asterisk (*)*

Fixed predictors	Estimate	Std. Error	P Value
Intercept: DEE per unit mass	1380.26	36.19	<0.001*
Distance to OWF (among-ind; km)	-5.75	2.28	0.012*
Distance to OWF (within-ind; km)	-2.62	1.01	0.010*
Day of year (days)	-2.43	0.47	<0.001*
Random effects	Intercept variance		
Bird ID	861.8		
Residual	4493.0		

6.4 Discussion

This study reports on fine-scale movement and activity patterns of spring-staging red-throated divers in the German North Sea. By integrating GPS and TDR biologging data, we quantified time allocation to different behavioural activities and assessed how activity budgets and corresponding energy expenditure varied with proximity to OWFs. We detected both among- and within-individual behavioural responses to OWF proximity and show that these responses are associated with small but statistically significant increases in DEE. Together, these findings provide insights into a potential mechanistic pathway via which OWFs may influence individual energy balance, complementing existing evidence of spatial displacement.

We find that diver baseline activity budgets reflect an energetically conservative strategy during the non-breeding period. Within an important spring staging area, divers spent the vast majority of their time (>22 hours per day) at the water surface engaging in low-energy activities other than flying and diving such as passive drifting and slow surface swimming. Establishing this baseline is essential, as it highlights how even small shifts toward more energetically costly behaviours, particularly flight, can disproportionately influence DEE. Given the high wing loading of red-throated divers and the substantial energetic cost of flight (ELLIS & GABRIELSEN 2002; ELLIOTT ET AL. 2013), the pronounced minimisation of flight aligns with expectations for foot-propelled diving seabirds. Comparable activity budgets have been reported for Finnish, Scottish, and Icelandic wintering diver populations, where birds similarly spent around 20 hours per day in low-energy surface activities (DUCKWORTH 2023; DUCKWORTH ET AL. 2024; DUNN ET AL. 2024), suggesting a broadly conserved energy-conserving strategy prior to spring migration.

Movement exhibited a clear diel structure, with longer step lengths during daylight hours and reduced movement at night. This pattern indicates that energetically costly active relocation, including flight and directed surface movement, occurs predominantly during daylight, whereas nocturnal behaviour is characterised by passive drift. Similar diel patterns have been reported across a range of seabird species and are generally attributed to visual foraging constraints and circadian organisation of activity (DUNN ET AL. 2020). Mean daily movement distances (43.5 km) exceeded estimates from an earlier study based on coarser ARGOS data (DORSCH ET AL. 2019), highlighting the value of high-resolution tracking for quantifying fine-scale movement. We also found that divers spent on average 9% of available daylight hours diving, placing dive effort at the lower end of reported estimates for the wintering phase of this species in the North Atlantic (DUNN ET AL. 2024). This relatively low dive effort suggests that the focal area provides favourable foraging conditions that do not require intensive search behaviour, reinforcing its importance as a key non-breeding concentration area. By comparison, wintering Common Loons (*Gavia immer*) have been reported to spend substantially more time engaged in underwater foraging, accounting for approximately 20–40% of daylight activity budgets in nearshore habitats (DAUB 1989; FORD & GIEG 1995) and up to around 40% of daylight hours spent underwater in offshore wintering areas (KENOW ET AL. 2023).

Behavioural responses to OWFs differed between within- and among-individual scales. Individuals that generally occupied areas closer to OWFs spent more time diving, suggesting persistent differences in habitat use or foraging strategy among birds. In contrast, flight behaviour showed a clear within-individual response: birds flew more on days when they were closer to OWFs than their own average. This pattern is indicative of short-term behavioural adjustment rather than fixed individual specialisation. Elevated flight activity near OWFs is consistent with avoidance behaviour, relocation

between foraging patches, or responses to associated vessel traffic—patterns that have also been documented in divers exposed to ships and other offshore infrastructure (BRADBURY ET AL. 2014; FLIESSBACH ET AL. 2019). At the same time, reduced resting time near OWFs suggests that disturbance may compromise opportunities for low-cost behaviours, and thus have energetic consequences.

Flight was the most energetically expensive behaviour in the activity budgets, far exceeding the costs of diving or resting (ELLIOTT ET AL. 2013; COLLINS ET AL. 2016). Consequently, even minor increases in flight time translated into detectable increases in DEE. Within individuals, DEE increased significantly as birds occurred closer to OWFs (β = 2.62 ± 1.02 kJ per day per km), corresponding to an increase of approximately 0.2% in DEE per kilometre closer to an OWF, or roughly 2% over a 10 km approach, relative to an average mass-corrected DEE of ~1380 kJ. When placed in a broader context, these energetic costs are an order of magnitude smaller than those predicted for breeding seabirds in barrier-effect models. For example Masden et al., (2010) predicted increases of several percent, and in some cases more than 10–20% of DEE, under scenarios involving repeated avoidance flights during central-place foraging. The comparatively small proportional increases observed here are therefore consistent with the absence of repeated commuting flights during the non-breeding season and suggest that existing OWFs do not function as major energetic barriers for wintering red-throated divers. These findings align with empirical estimates of baseline non-breeding energetic demands. Duckworth (2023) reported mass-corrected DEE values for wintering red-throated divers between 1130 and 1482 kJ per day (during December), providing important energetic context for interpreting OWF-related effects. Against this baseline, the proportional increases associated with OWF proximity observed in the current study are small at the daily scale but may be biologically relevant if experienced repeatedly over extended periods. Although population-level impacts cannot be inferred directly from our analysis, the behavioural mechanisms identified here resemble those assumed to influence overwinter survival in demographic and individual-based models (WARWICK-EVANS ET AL. 2018; VAN KOOTEN ET AL. 2019). Integrating empirically derived activity budgets and energetic costs into such models represents an important next step for assessing longer-term ecological consequences.

In addition to OWF-related effects, day of year emerged as a strong predictor of DEE, reflecting increasing daylight hours and a strong negative correlation with SST ($r = -0.71$, $t = -10.54$, $df = 110$, $P < 0.001$). SST increased from approximately 6 °C at the start of the sampling period to 15 °C at its end, implying higher thermoregulatory costs during colder early-season conditions. Consequently, energetic consequences of OWFs are superimposed on a seasonally structured energetic baseline driven primarily by environmental conditions. Pronounced seasonal variation in energy expenditure aligns with findings from other seabirds, where baseline environmental factors structure daily energetic demand and behavioural adjustments drive variation around that baseline (COLLINS ET AL. 2016; BUCKINGHAM ET AL. 2023). Interpreting OWF effects within this broader seasonal context is therefore essential, as anthropogenic disturbance operates on top of an environmentally defined energetic landscape rather than in isolation. Notably, we detected no seasonal trends in the proportion of time allocated to diving, flying, or resting, suggesting that seasonal variation in DEE is driven largely by thermoregulatory costs rather than changes in foraging effort.

Several considerations are important for interpreting these results. As with many biologging studies, the dataset was characterised by uneven individual contributions, with a disproportionate number of complete observation days originating from a small subset of individuals (WEBSTER & RUTZ 2020). Increasing sample sizes and achieving more balanced individual representation in future

deployments would strengthen inference. In addition, activity budgets and energetic estimates depend on modelling assumptions, including behavioural classification thresholds and activity-specific metabolic multipliers (DUNN ET AL. 2023). While these assumptions introduce uncertainty into absolute DEE values, relative differences associated with OWF proximity are likely robust to moderate deviations in behavioural cost functions.

While this analysis provided important estimates for the time-activity budgets as well as energy expenditure of these birds in the focal area, a key next step will be to integrate these empirically derived activity and energy budgets into individual-based models to assess how repeated energetic costs interact with environmental variability to influence individual fitness and population viability. Such approaches will be critical for identifying thresholds beyond which behavioural flexibility can no longer buffer energetic costs, thereby informing evidence-based maritime spatial planning.

7 HABITAT MODEL

7.1 Introduction

The German Bight is a core area for staging red-throated divers in spring (VILELA ET AL. 2021; GARTHE ET AL. 2023). The area is also intensively used by humans, and red-throated divers have been shown to be highly sensitive to anthropogenic pressures (e.g. GARTHE ET AL. 2025). Describing and understanding the habitat used by red-throated divers is therefore crucial for effective management and conservation.

The environment in the German Bight is highly dynamic and influenced by river outflows and tides (STANEV ET AL. 2019). Red-throated divers have previously been shown to favour the ecologically productive frontal zone between coastal and more saline North Sea water masses (SKOV & PRINS 2001; HEINÄNEN ET AL. 2020), where they feed on small pelagic and benthic fish (KLEINSCHMIDT ET AL. 2019). Divers have also been shown to display a high degree of avoidance from offshore wind farms (OWFs) and ship traffic (e.g. BURGER ET AL. 2019; HEINÄNEN ET AL. 2020). A combination of a dynamic environment and mobile prey makes the task of describing the habitat challenging. Outstanding questions are for example: How much of the variation in diver distribution can be explained with environmental parameters related to the frontal zone as well as static parameters like water depth? How important are anthropogenic parameters like distance to OWF and ship traffic? How much of the variation appears to be random?

The fine resolution telemetry data collected in this project allow us to map the distribution of divers in relation to covariates and to evaluate the findings of previous research. In the predecessor DIVER project (DORSCH ET AL. 2019) the telemetry and survey data were analysed utilizing Generalized Additive Mixed Models (GAMMs) which can account for spatial and temporal autocorrelation in the model residuals. In this study we utilize an algorithm similar to GAMMs, sdmTMB, that is further capable of including spatial (spatio-temporal) random fields (ANDERSON ET AL. 2024; MONIER 2024). The spatial random fields allow for mapping spatial patterns unexplained by the fixed effects, which further allows us to interpret also the unexplained distribution and to map distributions including both fixed effects and unexplained spatial variation. The main aim of this study is to assess the drivers of habitat suitability and distribution patterns in the core spring area of diver occurrence.

7.2 Material and methods

7.2.1 Study area

The study area was defined to include the core area of red-throated diver distribution in the German Bight based on information from previous studies (Fig. 7-1). The area also contains several OWFs. Near shore habitats were excluded as the ecological processes in the near shore areas can be very different from offshore and could therefore complicate modelling. If near shore areas are of interest, different models could be fitted for those.

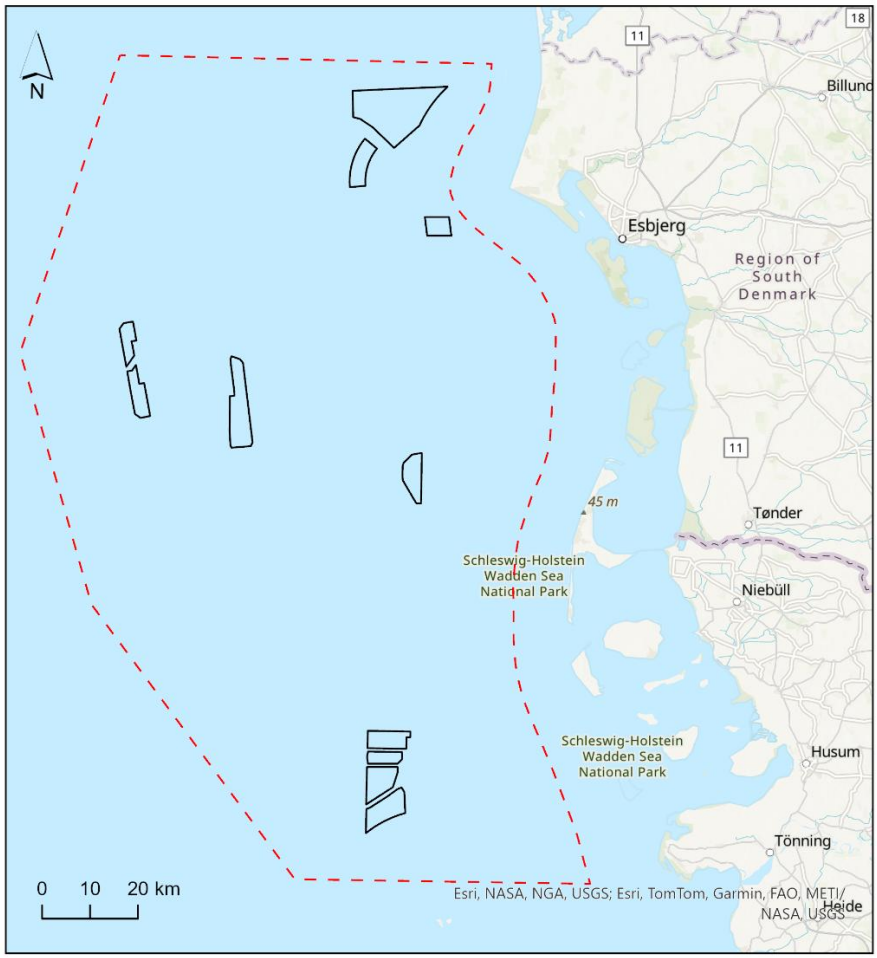

Fig. 7-1 Study area, all analyses in this chapter are based on data from within the red dashed area.

7.2.2 Telemetry data

Telemetry data were collected from March to May across three years (2022–2024). The data set included 46 individuals recorded within the study area (Fig. 7-2). For more details see Chapter 4.4.

As a generalized linear mixed modelling approach, a logistic regression, was used. We generated 10 pseudo-absence points per bird and timestep to be able to model the binomial response (0 or 1). As the study area was overall considered as suitable habitat in general, the pseudo-absence locations were distributed randomly within the study area.

The environmental data, described below, was extracted to match the bird data set based on position and time. Before modelling, the bird presence locations were classified into night and day (day including dawn and dusk), only daytime presence locations were used in modelling. The classification was done utilizing the R package “suncalc” (THIEURMEL & EL MARHRAOUI 2022).

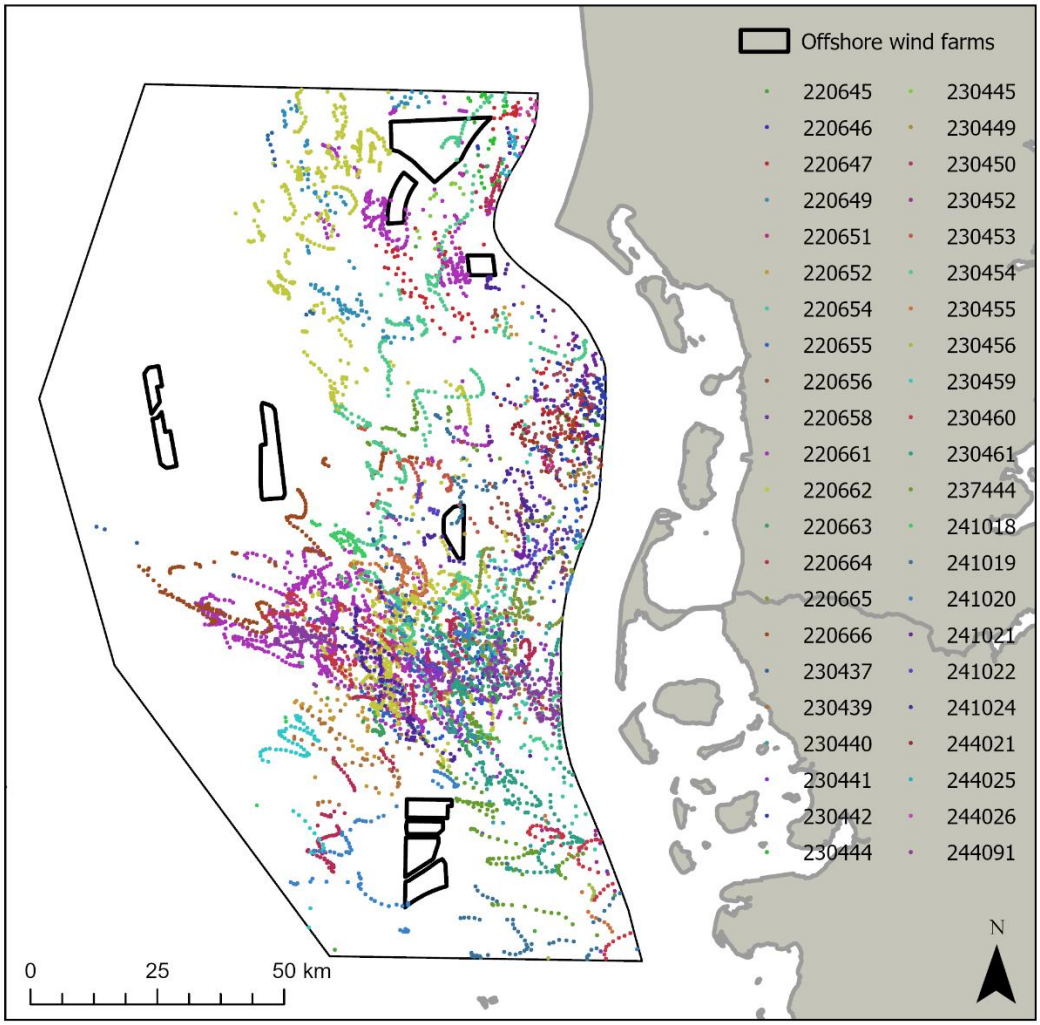

Fig. 7-2 *Daytime locations of tagged red-throated diver individuals included in the modelling (individual ID:s indicated in the legend). Ten randomly pseudo-absence locations were generated for each presence location (these can be called availability locations as they we available but not utilized). The availability locations are not visualised as they are all over the study area and would make the figure difficult to interpret.*

7.2.3 Environmental and anthropogenic data

The inclusion of covariates (environmental and anthropogenic) was based on a priori knowledge: static water depth, surface salinity (at 3m), chlorophyll-a (at 3 m), shipping and fishing hotspots, and distance to OWFs. Chlorophyll-a was considered as a representation for productivity and frontal area. Salinity was included as a proxy for water masses and therefore also the frontal zone. The temporal resolution of salinity and chlorophyll-a, was daily, and the spatial resolution 0,01° (~1.1 km). Chlorophyll-a and salinity data was downloaded from E.U. Copernicus Marine Service (Product Title*. E.U. Copernicus Marine Service Information (CMEMS). Marine Data Store (MDS).* DOI: 10.48670/moi-00059 (Accessed on 22-08-2024)).

Data on ship presence were downloaded from Global Fishing Watch (https://globalfishingwatch.org/map; accessed September 13, 2024). The data is based on AIS-data and the spatial resolution of the layer is 0.01° (~1.1 km) and temporal resolution daily.

Ship presence was further analysed using the "Optimized Hot Spot Analysis" tool in ArcGIS Pro (https://pro.arcgis.com/en/pro-app/latest/tool-reference/spatial-statistics/how-optimized-hot-spot-analysis-works.htm). The hot spot analysis is based on Getis-Ord Gi* statistics, a high positive value of the resulting Z-score indicates a hot spot for ship activity, and a high negative score indicates a cold spot. The covariate included in the model is therefore called AIS hotspots. Daily presence of ships was also assessed for inclusion in the models, however, static representations of shipping activity (i.e. hotspots) was chosen to be included in the final model, based on interpretation of patterns. Distance to OWFs was estimated using the Euclidean distance tool in ArcGIS Pro and grouped into distance classes and included as a factor variable in the model.

To be able to map model predictions, a mean for all three modelled spring months (March to May) and three years 2022-2024 was calculated. All covariate data were further extracted to a prediction grid covering the complete study area (Fig. 7-1). The predictor variables are mapped in Fig. 7-3 to *Fig. 7-6*.

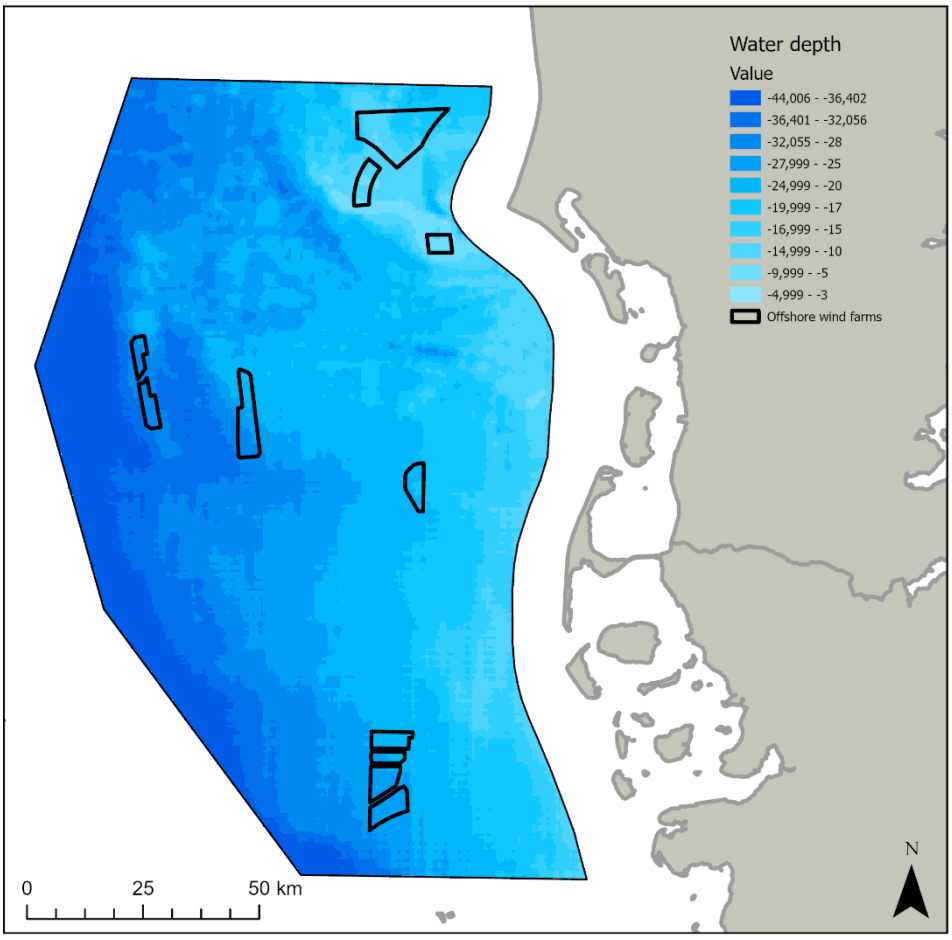

Fig. 7-3 Water depth used as a static predictor in the model

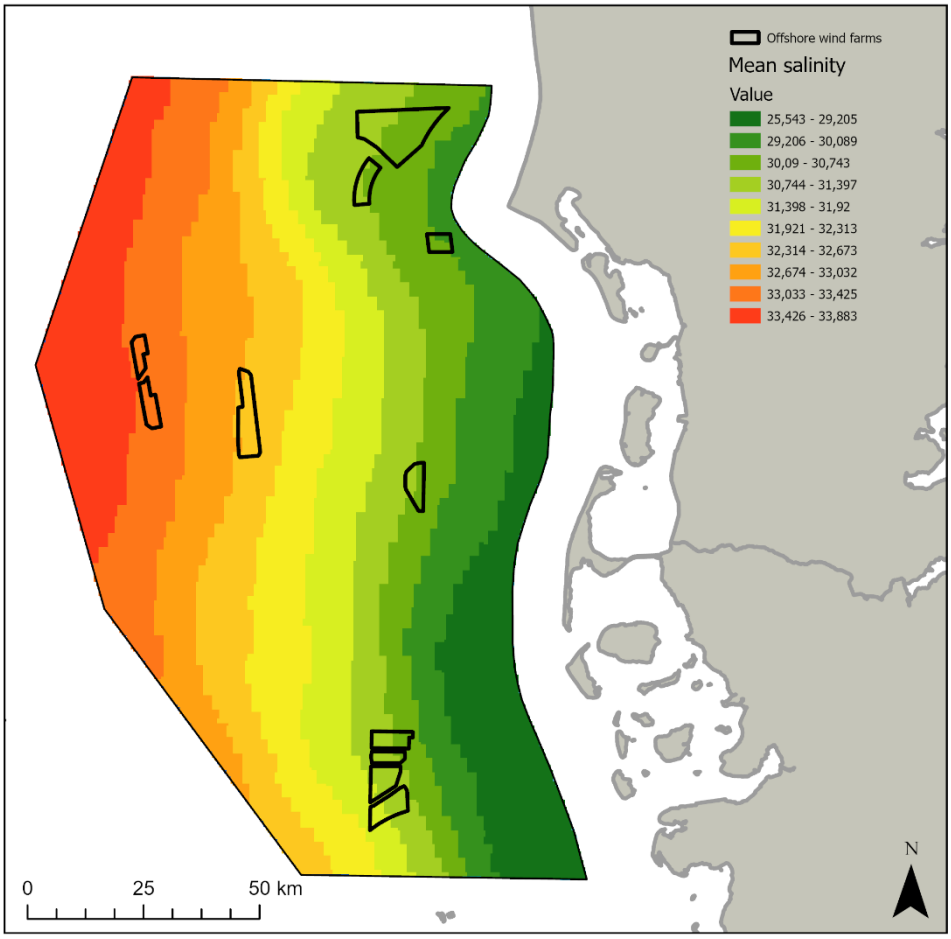

Fig. 7-4 *Visualised mean salinity for all periods used for generating the predictions. Daily salinity values were extracted and used for fitting the model*

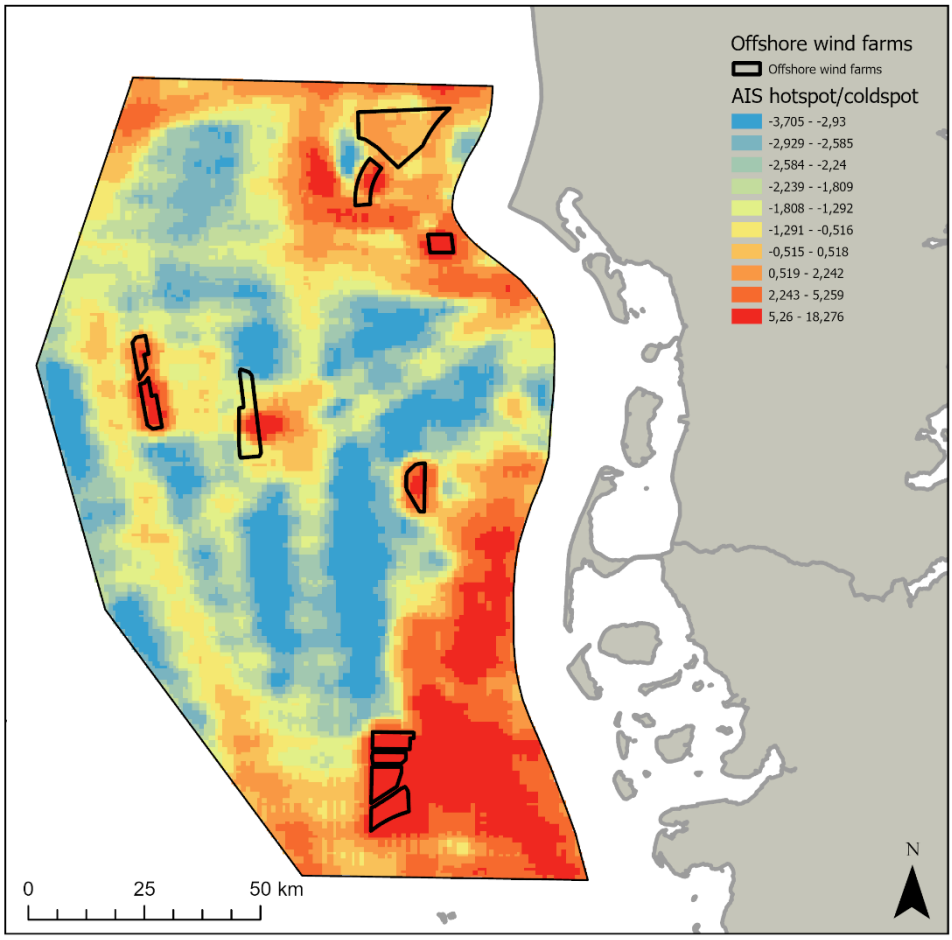

Fig. 7-5 *Estimated mean hotspot and coldspot values for AIS locations in the study are used for predictions. Models were fitted utilizing seasonal averages.*

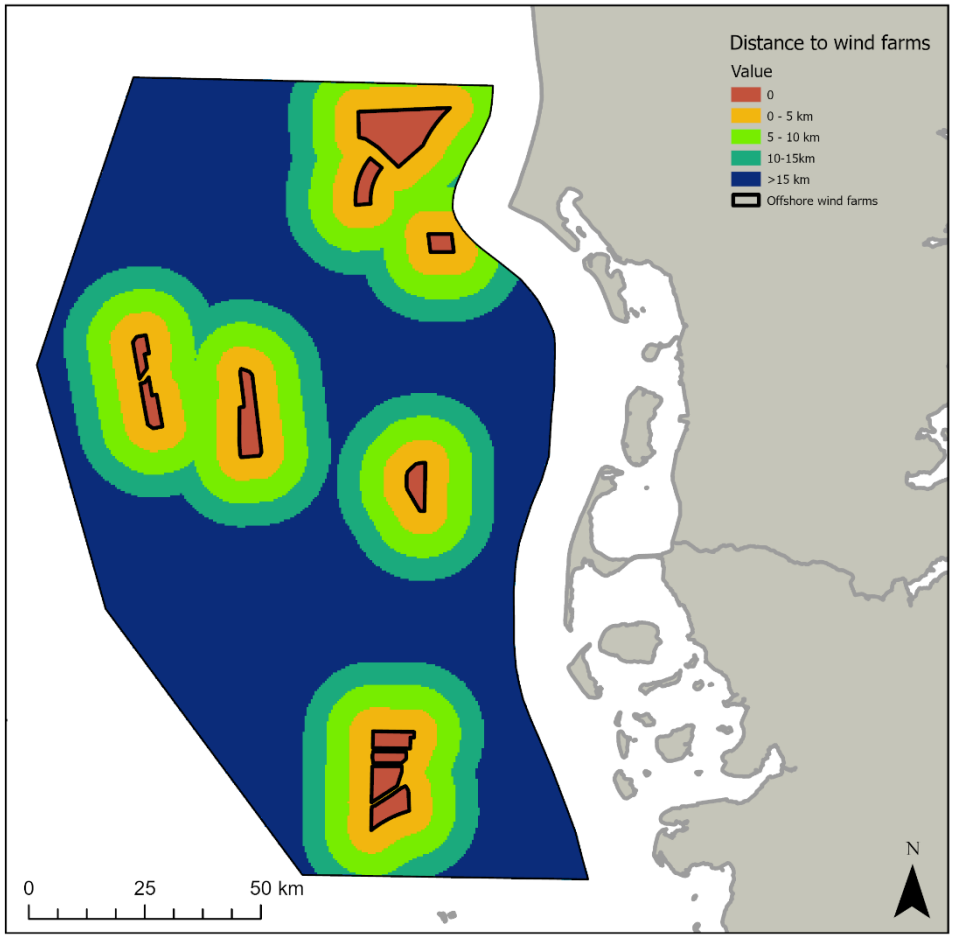

Fig. 7-6 Distance bands indicating distance from OWF used as predictor in the modelling.

7.2.4 Habitat suitability modelling – model fitting

Prior to model fitting correlation between variables were checked. Chlorophyll-a was dropped from the models as it was highly correlated with salinity (Fig. 7-4). The correlation is also relatively high between depth and salinity but regarded not to be too high for inclusion as in line with the generally used threshold value of 0.7 (DORMANN ET AL. 2013).

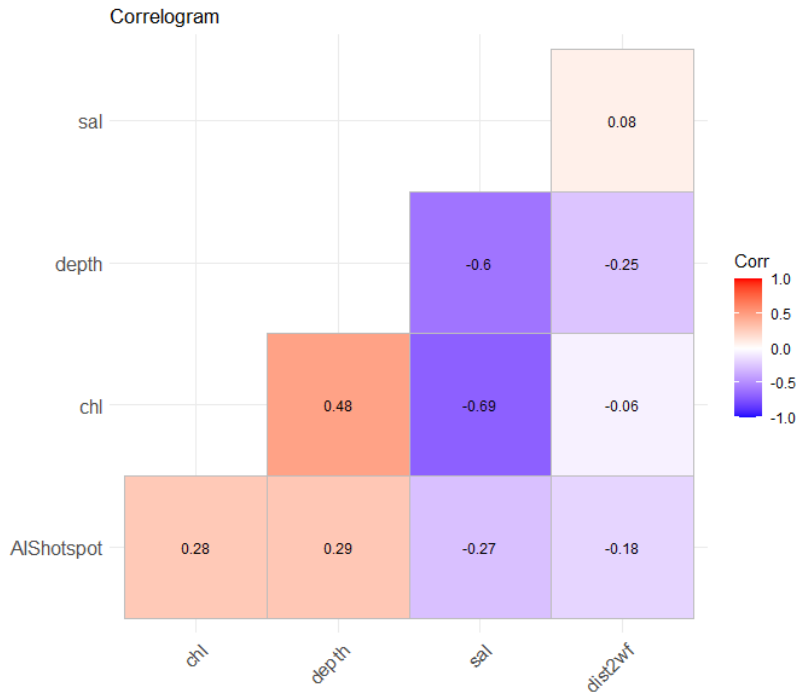

Fig. 7-7 Collinearity between covariates

Generalised linear mixed effects models (GLMMs) with Gaussian Markov random field using a SPDE (stochastic partial differential equation) based approach were fitted using the sdmTMB package (ANDERSON ET AL. 2024) in R (R Core Team, 2024). For fitting a sdmTMB model with the SPDE-approach a mesh is required, defining the spatial domain for where the spatial random field is approximated. The mesh is constructed based on a chosen cutoff distance that controls the resolution of the spatial predictions. The cutoff value for the mesh was set to 3-4 km (Fig. 7-5) and was the finest possible mesh resolution possible for fitting. A mesh is specific for a data set used in the modelling. Tag ID, an identifier for each tagged bird was included as a random term in the model.

Two sets of models were fitted:

A **full model** based on day-time presence location and related pseudo-absence locations.

A set of **10 subset-models** based on subsampling 5 presence locations per individual bird and day (daytime locations) and 10 absence locations per bird and day of the full data set 10 times. The subsampling is a means of reducing potential spatial autocorrelation not accounted for by the spatial random fields. The mesh for the full model was constructed with a cutoff value of 4 km and lower sample size in the sub models allowed for a finer mesh with a cutoff value of 3 km. In addition to reducing the spatial autocorrelation in the data set, the set of sub-models gives a means to assess the robustness of the models. The model can be defined as robust if they sub-model results generate similar responses and patterns.

All models were fitted with the following formula:

Response:

$$PA_i \sim \text{Bernoulli}(p_i), \text{where } PA_i = 1 \text{ for presence and } 0 \text{ for availability.}$$

Link function:

$$\text{logit}(p_i) = \eta_i$$

Linear predictor:

$$\eta_i = \beta_0 + f_1(\text{depth}_i) + f_2(\text{sal}_i) + \beta_3 \cdot \text{AIShotspot}_i + \beta_4 \cdot \text{owf}_i + b_{\text{tag}_i} + \omega(s_i)$$

Where:

$f_1(\text{depth})$and $f_2(\text{sal})$are smooth functions (splines) with $k = 5$ basis dimensions.

$\beta_3, \beta_4$are fixed-effect coefficients for categorical or continuous predictors.

$b_{\text{tag}_i} \sim N(0, \sigma^2_{\text{tag}})$ is the random intercept for tag_id.

$\omega(s_i)$ is the spatial random field modeled via SPDE (Gaussian Markov Random Field).

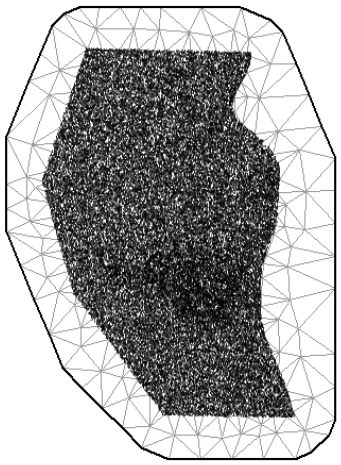

Fig. 7-8 The mesh used in the modelling when including all daytime models, the cutoff value was set to 4 km

7.2.5 Predictions by fitted models

The models, fitted on all data and the 10 sub-models were predicted on a grid covering the whole study area (Fig. 7-1). Average values of all three spring periods (March to May) and the years 2022-2024 was calculated for all variables. The predict() function in the sdmTMB R package was used and resulted in an overall estimate, estimates excluding random effects as well as estimated random

spatial effects. All these three prediction outputs were mapped using ArcGIS pro with a resolution of 500 x 500 m.

7.3 Results

Initial explorative analysis of the response variables indicated that the difference between presence location and availability location are rather small regarding the spread and central tendency values of the environmental covariates (Fig. 7-6, Tab. 7-1). The ratio between presence and availability within different distance bands (intervals of 5 km) from OWFs indicate that few red-throated divers are within or close to the OWFs in comparison to further away from OWFs (Fig. 7-7).

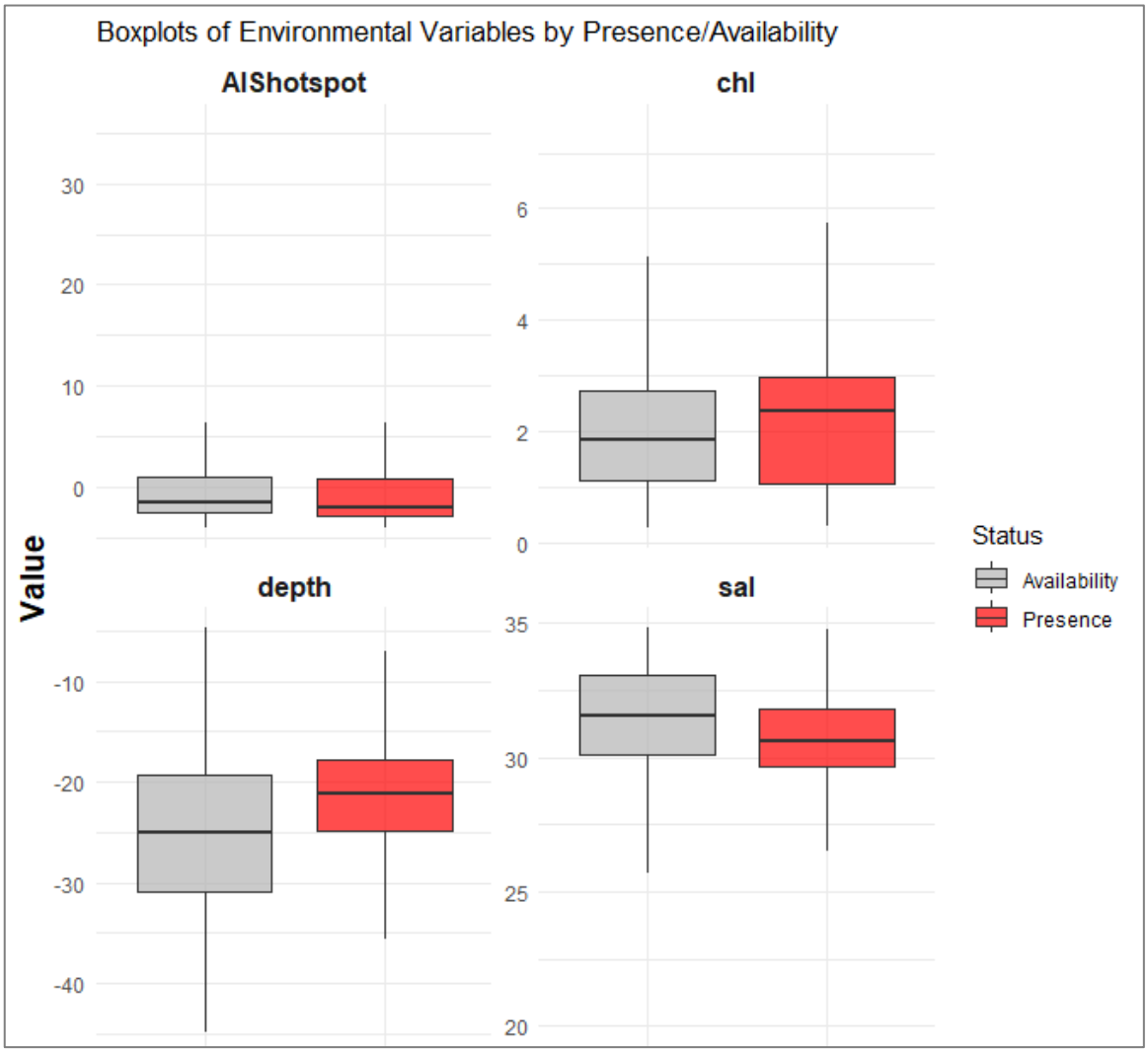

Fig. 7-9 *Box plot visualizing the variability of the covariates grouped by presence location of red-throated divers and locations indicating availability.*

Tab. 7-1 Mean values as well as minimum and maximus values for the covariates

Covariate	Available	Presence
Mean chloropyll-a (min - max)	1.99 (0.25–7.51)	2.21 (0.29–6.65)
Mean depth (min -max)	-25.5 (-44.9 – -4.72)	-21.2 (-41.1– -6.14)
Mean salinity (min - max)	31.2 (19.8 – 34.8)	30.6 (21.1–34.8)
Mean AIS hotspot z-value (min-max)	-0.0174 (-4.10–35.9)	-0.490 (-3.98–27.9)

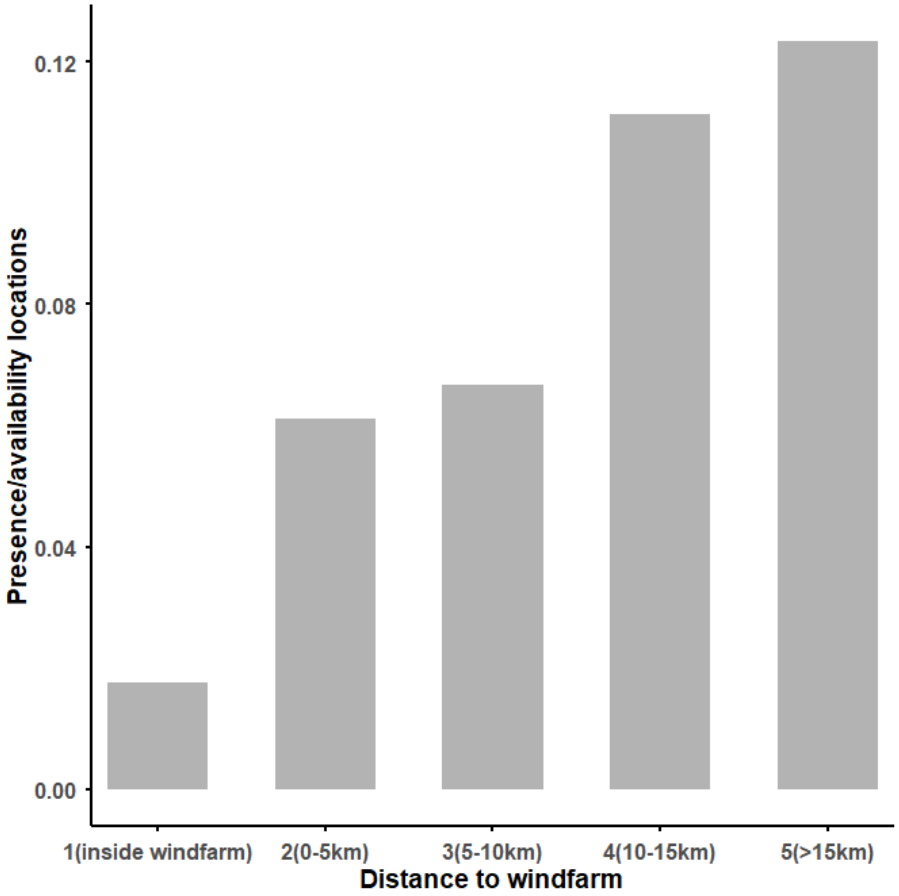

Fig. 7-10 The ratio between presence and availability points within different distance zones from OWFs, indicating increased presence points in relation to availability with increasing distance from OWFs.

7.3.1 Full model results

The sdmTMB model fitted based on all data (full model) showed relatively strong temporal auto-correlation in the model residuals (tested with the acf() function) while a variogram analysis indicated no spatial autocorrelation in the residual and estimates. Evaluating the model results we considered the individual “track effect” to be too high and the model therefore overfitted and we

therefore do not present the results of the full model here. Instead, we continued with the subset-models.

7.3.2 Subset model results

Results from the 10 sub-models were similar to the full model, however, a bit more general due to the reduced influence of individual bird tracks. Print screens of model results can be found in the Appendix (A.3), most important results are highlighted here (Tab. 7-2). Two of ten models showed no significant results with depth. Salinity, AIS hotspots and distance to OWFs, on the other hand, were relatively consistent across all models (Fig. 7-11). All models indicated an increase in probability of presence of red-throated divers outside to wind farm footprints, increasing with distance from the footprint. In most models the probability of presence (Wald test) was significantly higher outside the footprint, also indicated by the mean coefficient (± SE) in Tab. 7-2. The estimated odds ratio indicate that the probability of diver presence is 3.4 time higher in the distance class from 0-5 km away from the footprint and about 6 times higher 15 km away (Fig. 7-12).

The high similarity between response curves indicate that the models are robust. The predictions were averaged across all models and mapped, overall suitability (Fig. 7-13), only fixed effect (Fig. 7-14) and unexplained spatial variation (Fig. 7-15). A variogram analysis indicated that none of the models had residual spatial autocorrelation. However, an acf() graph indicated that there was some temporal autocorrelation still remaining in the residuals. For the subset model, this was regarded as acceptable and the predictions resemble the observed patterns well (Fig. 7-14).

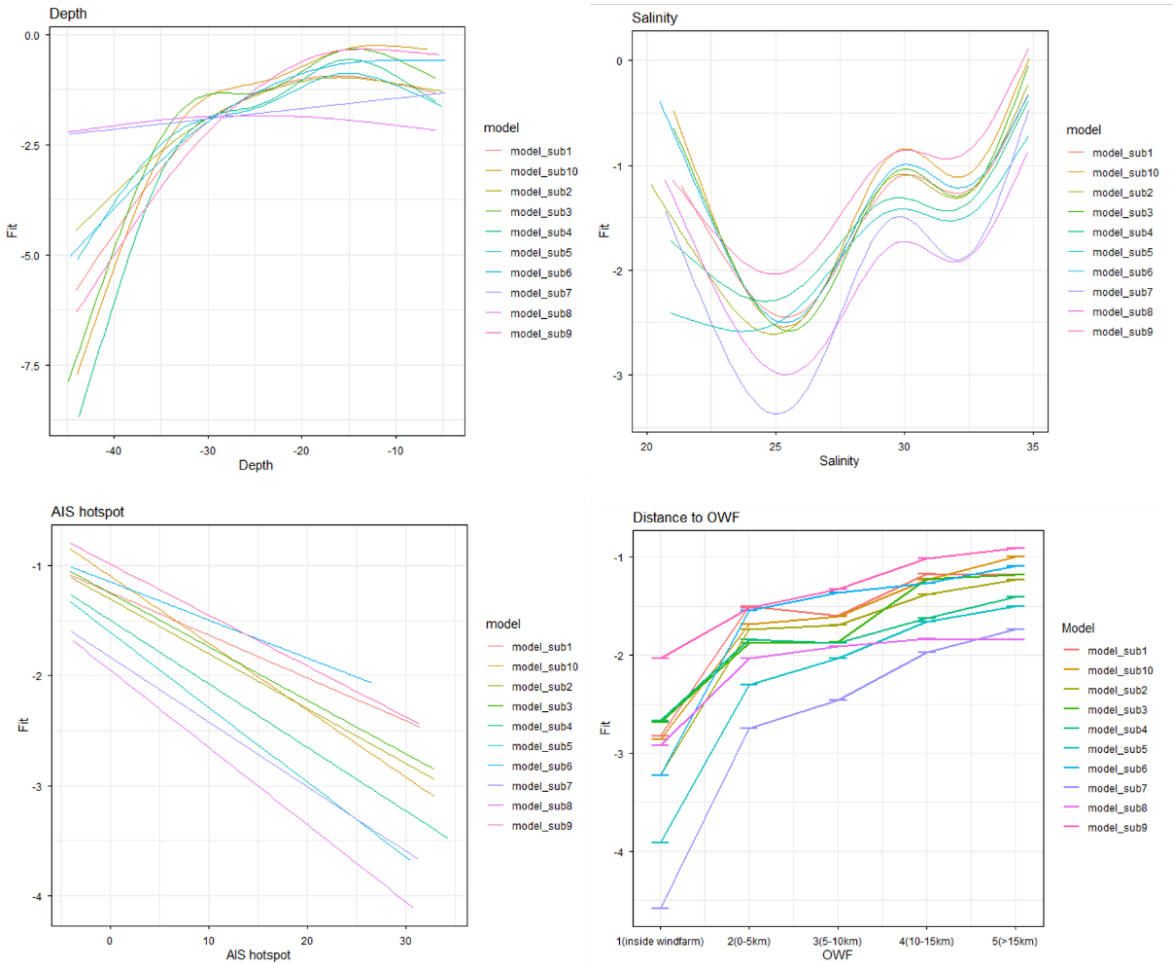

Fig. 7-11 Response curves of all 10 sub-models, showing highly consistent responses.

Tab. 7-2 Mean estimates (±SE) for the covariates used in the sub-models.

Covariate	Mean estimate	Mean std.error
(Intercept)	-3.665	1.039
AIShotspot	-0.053	0.0191
owf2(0-5km)	1.216	0.545
owf3(5-10km)	1.322	0.584
owf4(10-15km)	1.660	0.622
owf5(>15km)	1.787	0.656

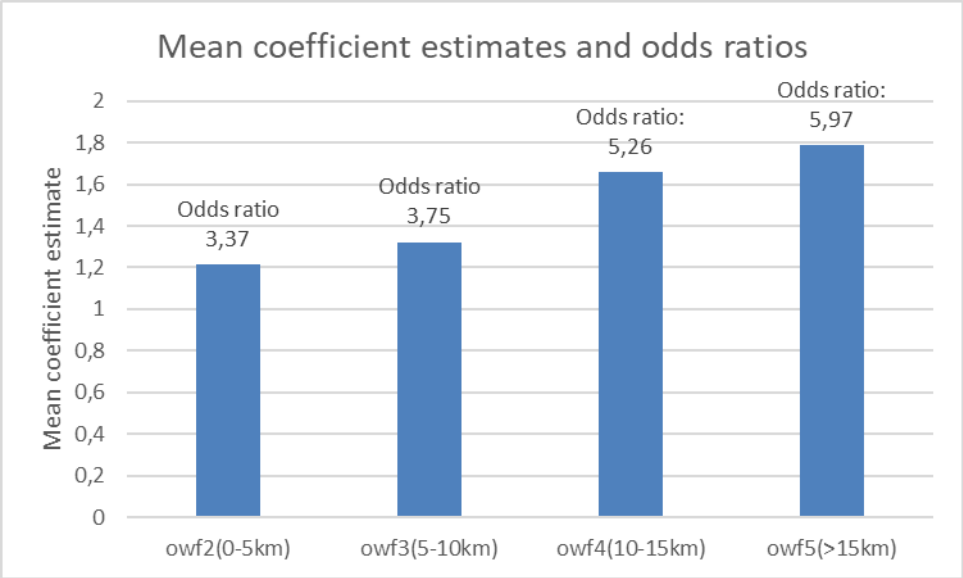

Fig. 7-12 *Estimated coefficients for the distance bands from OWFs. Odds ratios for each distance band is indicated.*

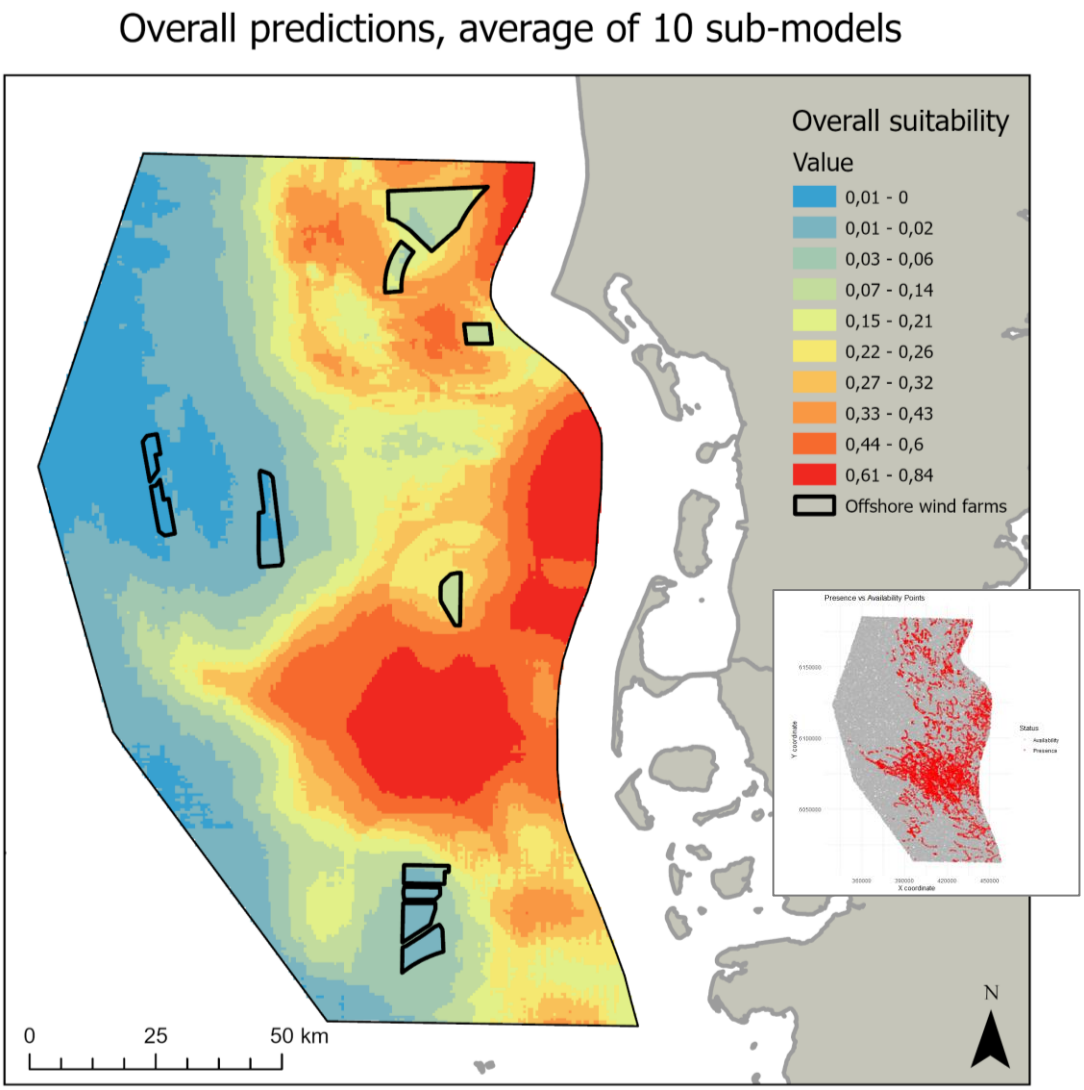

Fig. 7-13 Average model prediction of all 10 subset full models, including both fixed and spatial effects.

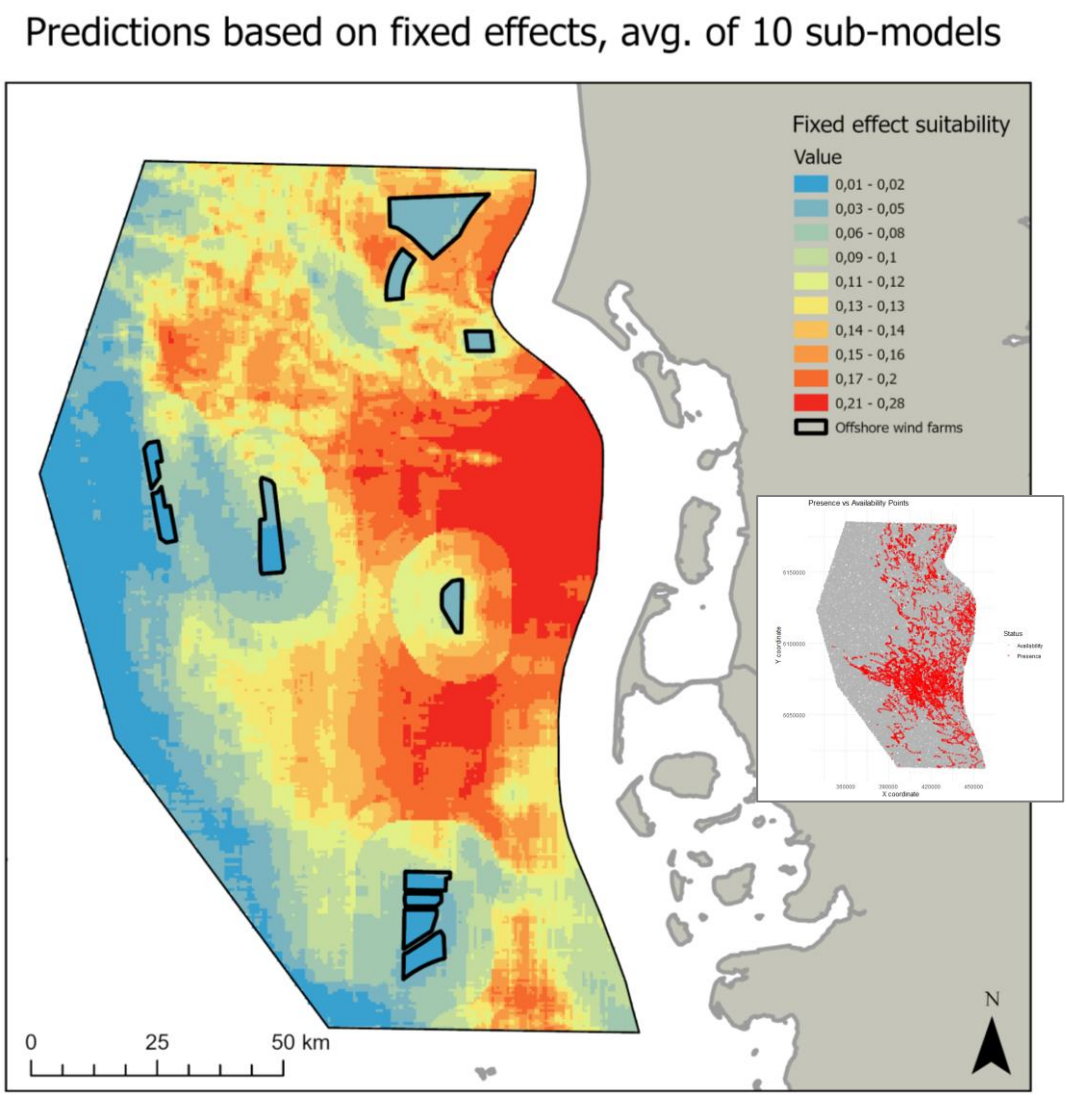

Fig. 7-14 Average 10 subset model predictions based solely on fixed terms.

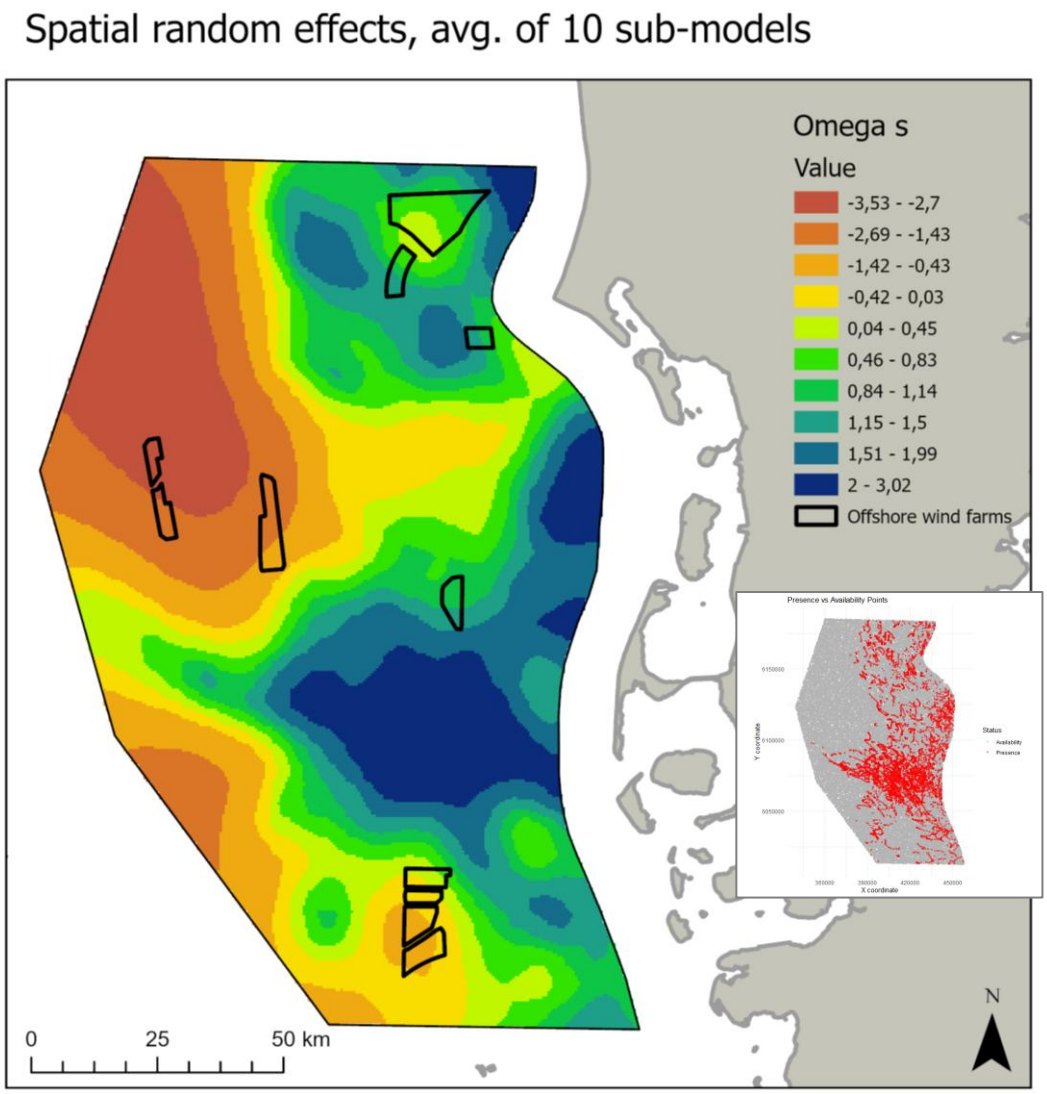

Fig. 7-15 *Average mapped spatial random effects of 10 subset models. Negative values are lower than expected based on fixed terms only and positive values indicate higher than expected based on fixed terms.*

7.4 Discussion

7.4.1 Interpreting patterns

This study, based on distribution modelling of 45 tagged divers within the defined study area are in agreement with previous results based on both tagging and aerial surveys (HEINÄNEN ET AL. 2020). The area predicted to be most suitable, the area between the OWFs Butendiek and Dan Tysk in the north and the Helgoland Cluster in the south, fits well with the areas of highest red-throated diver density mapped in previous studies (VILELA ET AL. 2021; GARTHE ET AL. 2025). The relatively "weak" patterns estimated by the fixed terms included in the models are not surprising when looking at the relatively small differences in the central tendency and spread of the values in the presence and availability data (Fig. 7-10). Nevertheless, the average of the 10 sub-models produced realistic responses and predictions. The mapped random spatial terms and the discrepancy between the

overall predictions and fixed effect predictions indicate clearly that there is a lot of unexplained variation in the data. This can be due to, for example, prey availability driven by some unknown environmental parameters. Not much is known about small-scale prey availability in this area, as it is notoriously difficult to measure. Also, conspecific attractions as a result of learning behaviour (MONIER 2024), predator-prey interaction (FAUCHALD 2009) and individual variation could play a role. The possibility within the sdmTMB R package to easily plot the spatial random effects in combination with and separate from the fixed effects enables us to better understand what is known and unknow in relation to observed patterns. Including spatial random effects also improves the mapping and interpolation of the observed patterns.

Directly comparing suitability patterns and patterns of occurrence with density patterns is not advisable as processes resulting in high densities of birds might be driven to some extent by other factors than of occurrence (HEINÄNEN ET AL. 2017). The patterns are nevertheless relatively similar.

Modelled relationships

The modelled responses and the relationship with both environmental and anthropogenic pressures were similar to previous studies (HEINÄNEN ET AL. 2020), even if telemetry data is often, correctly so, described as showing distribution patterns based on "only" a limited number of individuals. Telemetry data can be challenging to model in the framework for species distribution modelling because of high degree of autocorrelation and lack of absence locations. It is therefore useful to compare models utilizing different data sets and even to some degree different algorithms. The models used in this study and results from the DIVER study (HEINÄNEN ET AL. 2020), conducted roughly within the same study area, show relatively consistent response, confirming the effects of anthropogenic pressures and environmental variables.

Salinity

The importance of the frontal zone between coastal and North Sea water masses for red-throated divers is once again indicated by the model (SKOV & PRINS 2001; HEINÄNEN ET AL. 2020). The frontal zone is highly dynamic as can be seen in the extracted daily variation from the Copernicus data portal (Fig. 7-16). We extracted and modelled the relationship to salinity based on a daily temporal resolution. However, predictions were calculated on an average for the whole modelled period.

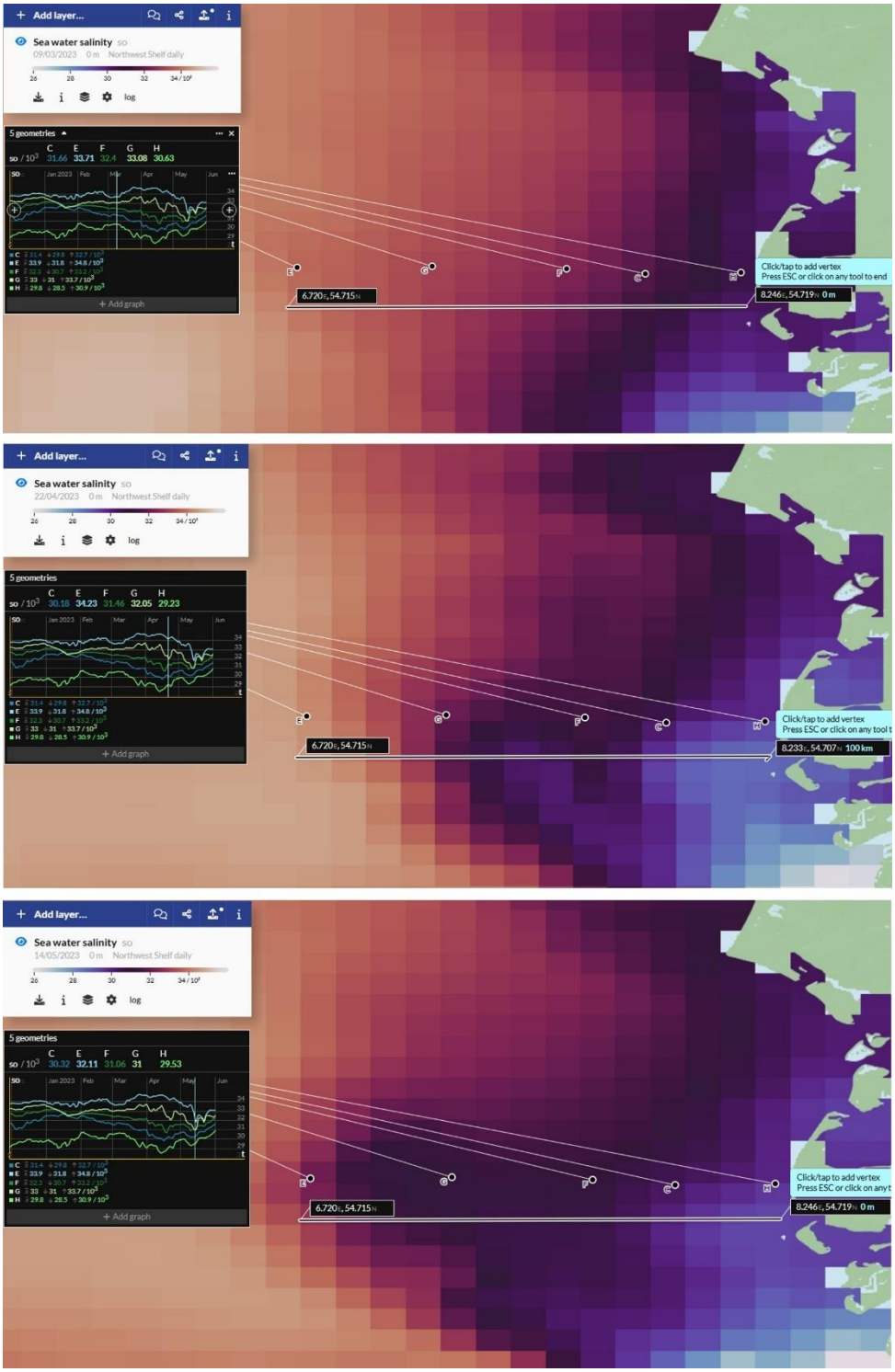

Fig. 7-16 *Snapshots of Copernicus salinity data used in the modelling. The 3 different maps visualize a transect consisting of 5 points starting from the coastal area close to Sylt extending approximately 100 km offshore, displaying the variation in salinity over the spring period. The frontal area can be seen as the darker colours with salinities extending beyond 30. The position of the front is dynamic, however, often closer to the coast in the northern parts of the study area https://doi.org/10.48670/moi-00059.*

Water depth

The response to water depth suggests that red-throated divers tend to prefer shallow areas, although this predictor is less robust than others (Fig. 7-11). This result matches previous findings for telemetry data (HEINÄNEN ET AL. 2020), however, it differs somewhat from results of survey data analysis, where water depths of around 20 m seemed to be preferred. Both datasets however showed reduced diver densities in depths of >30m. In chapter 5, no dive depths of more than 30 m were found. Waters of less than 30 m depth thus still provide access to both pelagic and benthic prey (KLEINSCHMIDT ET AL. 2019), thereby maximizing the likelihood of successful foraging.

Distance to OWFs

The response to OWFs indicates that red-throated divers are significantly displaced from the footprint, i.e. the probability of presence is significantly higher outside the footprint in comparison with inside. Similar to earlier modelling results (HEINÄNEN ET AL. 2020), the probability of presence of red-throated divers, according to the 10 sub models, increase with distance from the OWF and is highest >15 km away. The relationship is however not very strong and might by due to different reasons. A decline in the displacement effect has been indicated by a recent study on the OWF "Butendiek", using long-term aerial survey data (BURGER ET AL. 2025). For the area of the SPA, speed limits and a reduction of OWF service traffic have been implemented by the regulator since 2021 during springtime. This has reduced the disturbance by ship traffic and thus might be an explanation for the observed patterns. This study does not examine whether the effects of different OWF differ, but previous work suggests regional and temporal variations in the displacement effect (VILELA ET AL. 2020). As most datapoints in this study were generated within the SPA, any effects might mostly reflect patterns in this area and might not be generally transferable to other regions.

Shipping and fishing vessels

Avoidance of AIS hotspots, although a weak relationship, suggests that red-throated divers avoid areas frequently visited by vessels. Also, the analysis in chapter 8 suggests, that divers avoid ship encounters, which often result in red-throated divers being flushed (FLIESSBACH ET AL. 2019).

7.4.2 Challenges, uncertainties and potential next steps

Modelling telemetry data presents challenges, as the data is highly autocorrelated and consists of only occurrence locations. In this study, we focused on distribution patterns and therefore applied the sdmTMB approach, which falls into the class of resource selection functions. The ability of sdmTMB to incorporate random spatial effects gives us an opportunity to assess the random patterns and discuss causes for the unexplained variation. Other approaches focusing more on movement, e.g. step-selection functions (FLORKO ET AL. 2025), are available and could be a promising alternative modelling approach partly because of the relatively fine scale we are working on.

8 EFFECTS OF SHIP TRAFFIC ON MOVEMENT PATTERNS OF DIVERS

8.1 Introduction

During the non-breeding season, red-throated divers are found in many coastal and offshore areas of the North and Baltic Sea. At the same time, various anthropogenic uses take place in these areas, like energy production, fisheries and other activities. In the eastern German Bight, ship traffic is frequent. Cargo ships mostly cross the area on defined shipping routes, while fishing vessels engaged in fishing navigate across large parts of the area, especially towards the coast. Wind farm-related vessels also cross the area with sometimes high speeds (BURGER ET AL. 2019). Red-throated divers are known to strongly respond to ship traffic (BELLEBAUM ET AL. 2006; BURGER ET AL. 2019; FLIESSBACH ET AL. 2019). Divers frequently flush and escape by flight over a long distance, and flight distances from survey vessels of on average 1 km have been found. Recent analyses using transect survey data (BURGER ET AL. 2019; MENDEL ET AL. 2019) found effects of ships on divers reaching up to 5 km. Burger et al. (2019) also showed that higher ship speeds have stronger disturbance effects than slow-sailing vessels. Tracking data has so far been used only in very limited ways to investigate such effects, due to the need for high-resolution data. In the previous DIVER project (Dorsch et al. 2019), the analysis of tracking data showed already some effects of the number of ships in the vicinity of the birds on relocation distances. However, precision of data from satellite tracking was rather limited and the resolution in time was coarse. In other species, mainly marine mammals, such analyses have been used successfully to estimate ship disturbance (see e.g. FRANKISH ET AL. 2023). For red-throated divers, behavioural responses to shipping are therefore still not well understood. As divers are expected to mainly react to the visual stimuli of shipping, differences in their behavioural responses may exist between day and night, something that has also not yet been investigated. Such new insights may allow for improved mitigation measures to reduce disturbance on these birds in sensitive areas and during critical time periods. Here, we analysed an extensive dataset of red-throated diver movement data that was intersected with raw AIS-data using a newly developed package (PIGEAULT ET AL. 2024) in order to answer the questions below:

- Up to what distance can a response be detected?
- What ship types (size and speed) have the largest effects on flight or avoidance behaviour of the birds?
- How does the response differ between day and night?

8.2 Methods

We used GPS-data from 32 birds tagged during the years 2022 and 2024 (for the time periods 01.03. – 31.05.). GPS-fixes are obtained every 30 min (external tags) or 1 hour (implanted tags). The first 24 h of data (external tags) or the first 14 days (implanted tags) were removed for the analysis (see Chapter 4). Furthermore, only GPS-data for the spring period when birds were within the focal area was used. Limiting data in the east to the border of the focal area was done to avoid spurious results due to coastal data, near ports etc.

Raw AIS-data was provided by BSH for the spring periods (01.03. – 31.05.) of the years 2022 and 2024. These years were selected, as the most GPS-data of individuals was available for these time periods (2023 less data was available). The area for which data was provided was between Lat 54.09094 and 55.5038 and Lon 6.41925 and 8.59937 (rectangular shape). In a later step, this area was restricted in the east to the border of the focal area (see above).

We used the newly developed R package *AISanalyze* (PIGEAULT ET AL. 2024) to intersect AIS-data and GPS-data (see example, Fig. 8-1). For each GPS-position, a time period of 15 minutes before and after was defined as the timeframe to look for nearby ship traffic. The search radius was 10 km around each GPS-position to also include radii further than the expected extent of the response.

The package *AISanalyze* also allows interpolation of gaps in the dataset. Gaps were interpolated for up to 2 hours. In the offshore area, gaps between the AIS-signals are common, but the time was limited to avoid erroneous calculations (conservative approach). The search radius for connecting trajectories of individual ships was limited to 20 km. Furthermore, ship speeds of >80 km/h were excluded from the dataset.

For GPS-data, relocation distances to the next position were calculated, using R package *adehabitatLT* (CALENGE 2019). Calculations were limited to data where timestamps were less than 3700 sec. (ca. 1 hour) apart. Relocation distances were subsequently corrected for the duration of each time step. Furthermore, the square-root of relocation distance was used as the response to improve model performance. Effects of ships on the relocation distance were investigated using mixed effect models in R 4.2.2 (R CORE TEAM 2022) with individual ID as random effect. For ship presence/absence, generalized linear mixed models were used (R package *lme4*), while for analyses using ship distance, speed and length (of the nearest ship), GAMMs (R package *mgcv*) were used to allow for non-linear patterns, as have been found before (Burger et al. 2019).

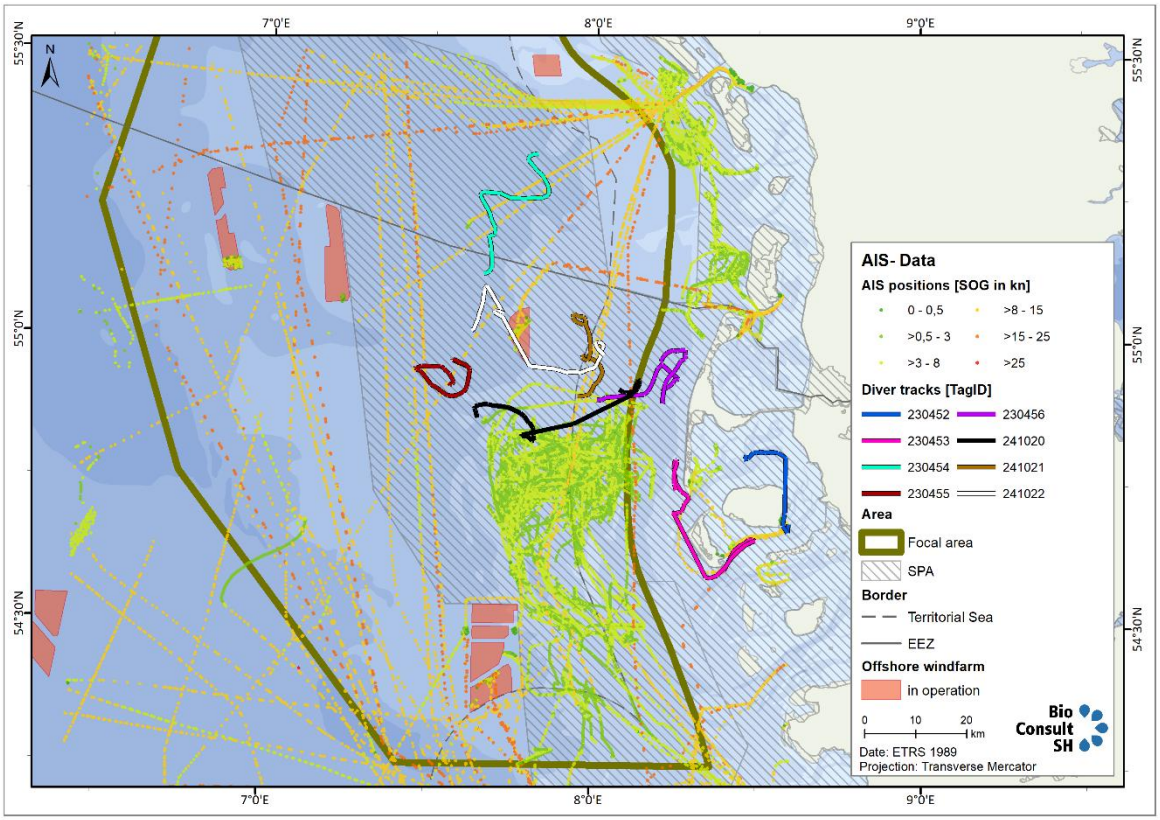

Fig. 8-1 *Example of AIS-data (with speed (SOG) categories) plotted with corresponding GPS-positions of divers for one day (14.03.2024).*

8.3 Results

Of 7062 GPS-positions in the dataset (spring 2022 and 2024), only 743 were identified (10.52 %) where one or more ships were present in a 10 km radius in the 15 min before and after the timestamp. Close encounters (< 1km) occurred only in 0.16% of all cases.

During day, relocation movements in the study area covered a distance of on average 2.42 km/h. When ships were absent within a 10 km radius, the distance covered was 2.3 km/h. When ships were present, distance increased to 3.52 km/h, on average. This was an increase of around 50%. These movements also included cases of flight which could explain the strong increase in the presence of ships.

Tab. 8-1 Overview of the relocation distances (in km/h) for cases with ships being either present or absent in a 10 km radius and for day and night.

Relocation distance (km/h)	Day	Night
Ships present	3.52	1.42
Ships absent	2.3	1.42
Overall	2.42	1.42

The presence of ships within a 10 km radius was significantly related to higher diver relocation distances as compared to cases when no ship was present. However, when analysing day and night data separately, this effect was only significant for data during day ($p<0.001$). Closer inspection revealed, however, that this pattern seemed to be mainly driven by two individuals showing a strong response and high relocation distances overall.

When limiting data to cases when ships were present within 10 km, during day no significant relationship between relocation distance and the distance of the closest ship within the 10 km radius was found. Also, the number of ships within 10 km, as well as speed and size (length) of the closest ship had no significant effect. During night, the relocation distance significantly decreased with increasing distance from the closest ship ($p=0.028$). However, this effect seemed to be influenced strongly by one high value (high relocation distance when a ship was close by). When excluding this value, no significant effect is seen. As during daytime, speed and ship size of the closest ship had no significant effect.

Effects of ships on divers so far have only been shown to reach to a maximum distance of 5 km (MENDEL ET AL. 2019). When limiting data to cases with only ships present within 5 km, during day a significant relationship between relocation distance and the distance of the closest ship was found ($p<0.05$, Fig. 8-2). As before, ship speed and length showed no significant effect. During night, no significant effect of either relocation distance, ship speed or length was found.

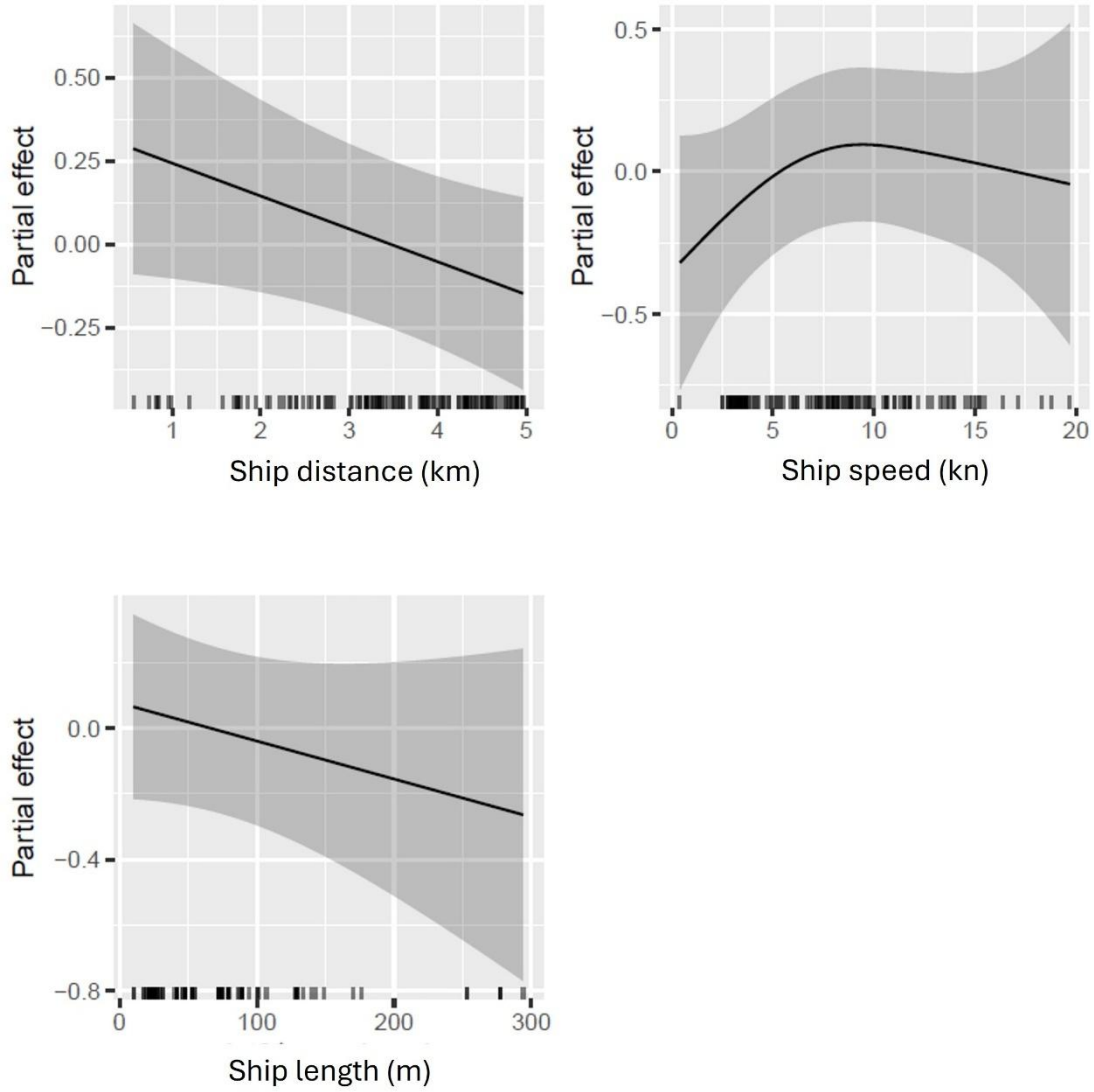

Fig. 8-2 *Effects of ship distance, speed and length on relocation distances of red-throated divers during day.*

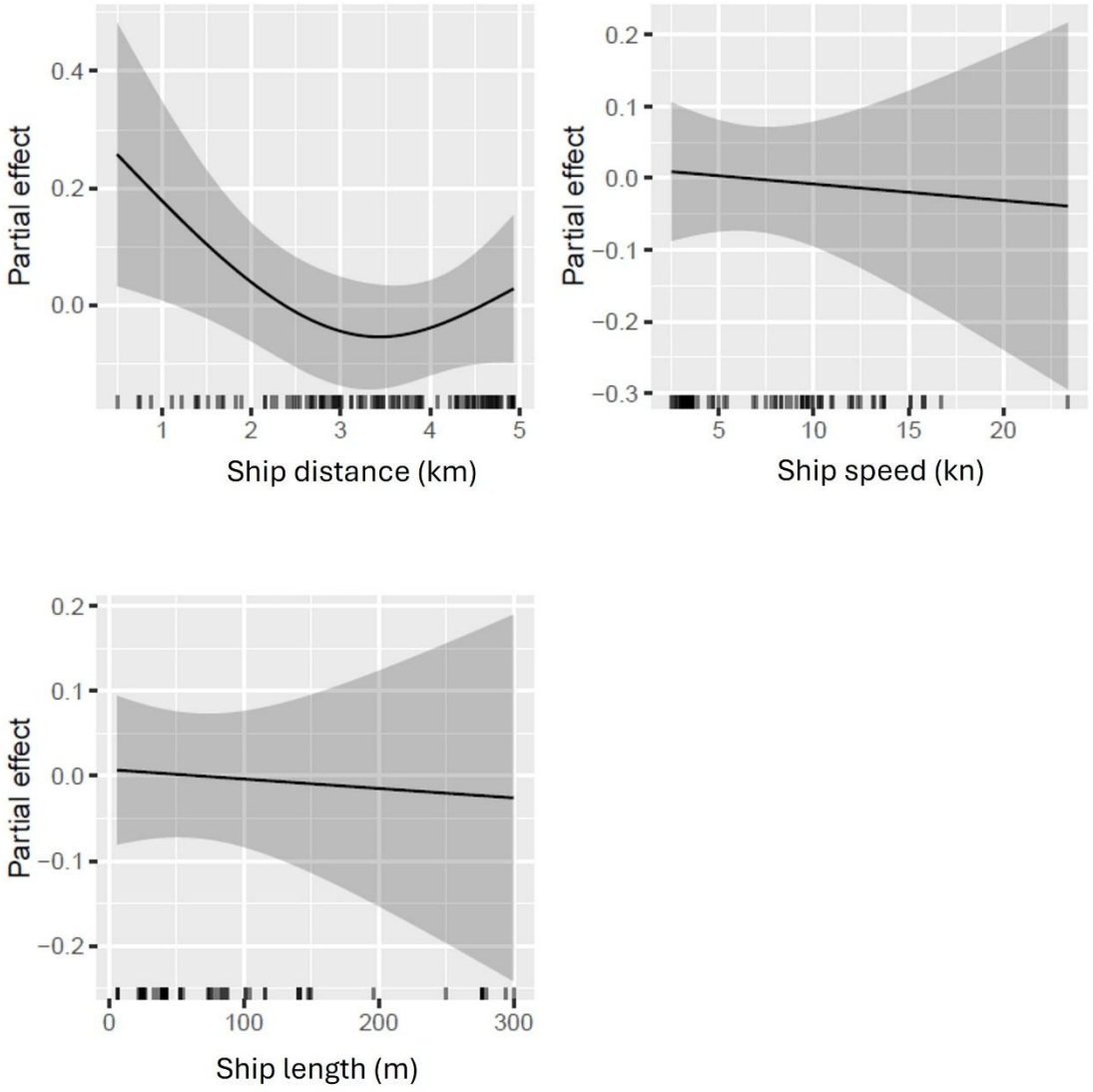

Fig. 8-3 *Effects of ship distance, speed and length on relocation distances of red-throated divers during night.*

8.4 Discussion

The analyses showed effects of the presence of ships in the vicinity of divers on their movements. Birds moved over longer distances when one or more ships were present within a 10 km radius, indicating some disturbance effects. However, this effect was only found for movements during daytime. At night, birds generally moved less and did not show a general response within the 10 km radius. This pattern of reduced activity during night is also described in Chapter 6. It is likely also connected to the low visibility of ships during night, although ships are equipped with navigational and other lights. For OWFs, it has been shown previously that divers also avoid these during the night, possibly due to the lights (DORSCH ET AL. 2019). Lights from ships, however, are positioned at

a lower height and are thus visible only at a short distance. The ship presence/absence model for the 10 km radius had a high number of zero's, indicating that the tagged birds had little interactions with ships.

A more detailed analysis of the effects, taking into account the distance, speed and size of the ships, yielded less clear-cut results than expected. This may be due to the limited sample size, as there were only a few cases in which ships were in close proximity to the birds' GPS positions. This could indicate that birds in general avoided areas with high ship traffic, as has been shown previously for shipping lanes (SCHWEMMER ET AL. 2011). Furthermore, the relocation data was very variable, especially during daytime. It appeared that relocations over longer distances also occurred in the absence of ships and were possibly related to birds switching foraging habitat or movements related to migration.

When analysing only data with ships being present within the 10 km radius, the distance of ships to the position of the birds had no significant effect on the relocation distances. However, when limiting the dataset to a radius of 5 km, during daytime, a significantly negative effect was found with closer ships resulting in larger relocation movements. At night, there was also a marginal (n.s.) effect of ship distance on relocation distance, but this was mostly driven by one individual that moved a long distance after a close encounter with a ship. Overall, this shows that the strongest effects of ships occur within a 5 km radius at maximum and during daytime, but there are no clear indications that this effect reaches even further, although the presence/absence model suggested shorter relocations in distances greater 10 km from ships. Due to only very few bird-ship interactions in close proximity, no smaller radii could be tested for possible effects of e.g. ship speed and size.

As ship traffic and habitat quality are not uniformly distributed over the study area (see Chapter 7), differences in relocation movements at greater distances might also be influenced by other environmental factors. For example, birds might generally move less in certain areas with high food abundance which are also rarely frequented by ships. The habitat model (Chapter 7) indicated indeed that birds chose areas with little overall ship traffic, rather than showing short-term responses to single ships.

In our dataset, there were very few cases of high-speed vessels approaching birds closely (two cases with ship speed >15 kn within 1 km radius). This might be a result of mitigation measures that were in place during spring (March and April) for a large part of our study area (within the SPA Eastern German Bight). Here, a general speed limit of 9 kn was imposed for this area (BSH 2021), besides other measures, e.g. reduced OWF service-traffic (for OWF Butendiek) and channelled routes for these vessels. This could partly explain the lack of strong effects as have been found in previous analyses in the DIVER project (BURGER ET AL. 2019). In the latter study, the strongest displacement effects have been found for high-speed vessels.

A new study by Burger et al. (2025) showed that a decrease in displacement effects from the OWF "Butendiek", located within the SPA Eastern German Bight, during recent years, was related to a reduction in OWF-related service traffic. These results suggest that reductions in ship traffic, but also in ship speed can be successfully used to mitigate the impacts of OWFs in sensitive areas with high densities of divers.

Even though the resolution of our GPS-data was high, an even higher resolution would be desirable for such an analysis, as movements (of ships and divers) between time steps of 30 min (external loggers) or 1 h (implanted loggers) can be large. For AIS-data, it is also important to note that gaps frequently occur for data in the offshore area and thus precision of data is limited. Also, only large ships are required to transmit AIS-signals, while small boats, e.g. fishing vessels <15m in length might be missed in this dataset. However, as our study area is located far offshore, small boats without AIS are rather rare, as compared to coastal areas with higher amounts of recreational traffic.

In conclusion, we could confirm that divers show a behavioural response to ships within a radius of 5 km. Also in previous studies displacement has been suggested to reach up to this distance (BURGER ET AL. 2019; MENDEL ET AL. 2019). This study showed that the responses were generally stronger during daytime than during night. However, the data also indicates that divers seem to avoid any encounters with ships by choosing areas with low overall ship traffic, making it difficult to investigate direct interactions.

8.5 Acknowledgements

We thank the German Federal Maritime and Hydrographic Agency (BSH) for providing AIS data from the European Maritime Safety Agency (EMSA).

9 MIGRATORY PATTERNS OF TAGGED DIVERS

9.1 Introduction

It has long been known that the German Bight represents an important wintering area for red-throated divers (SKOV ET AL. 1995; GARTHE ET AL. 2015) and it was speculated that this may be due to frontal zones leading to favourable feeding conditions (SKOV & PRINS 2001; GUSE ET AL. 2009). Until recently, however, there was little knowledge about what breeding populations these birds belong to, what migration routes they follow, where they moult and how flexible individual birds are in their choice of breeding, moulting and wintering area. The rapid development of offshore wind farms (OWFs) in the North and Baltic Seas over the last decade, the overlapping of these OWFs with wintering habitat of red-throated divers (GARTHE ET AL. 2015) and the documented strong avoidance of OWFs and associated shipping traffic by these birds (BURGER ET AL. 2019; MENDEL ET AL. 2019; HEINÄNEN ET AL. 2020) have raised concerns about the consequences of these industries on the populations of European red-throated divers. If red-throated divers are excluded from vital winter foraging grounds or from essential moulting areas, this could potentially reduce individual fitness and lead to carry-over effects into the breeding season, meaning that birds may show decreased breeding success, which eventually may affect a populations' viability. If we are to evaluate the impact of anthropogenic activities on red-throated diver populations, knowledge about the complete annual cycle of a birds' behaviour and habitat use are essential. Birds may face a range of different anthropogenic activities in the various habitats they use throughout their annual cycle, and how flexible a population is in its use of habitats and choice of migration strategies will affect its resilience towards environmental change and human impacts.

Red-throated divers breed throughout the Arctic tundra regions north of 60° latitude and after breeding migrate to marine habitats that they use for moulting and wintering. Red-throated divers are known to simultaneously moult their flight feathers in autumn sometime between September and December (CRAMP & SIMMONS 1977; BERNDT & DRENCKHAHN 1990; MENDEL ET AL. 2008) and are then flightless for period of about three weeks. This period presents a critical time when divers are bound to a particular location and may be particularly sensitive to disturbance (MENDEL ET AL. 2008). Red-throated divers were found to be highly faithful with regard to their breeding sites (OKILL 1992), while, until recently, little was known regarding site fidelity towards their wintering and staging areas.

There have been some winter recoveries of red-throated divers ringed as chicks in Scotland (mainly on the Orkney and Shetland islands) from around coastal areas of the UK and Ireland and a few also from the coast of France and Holland, suggesting a partial migratory strategy of this breeding population (OKILL 1992). Furthermore, some birds recovered at the south-eastern coast of England could be linked to breeding populations in Greenland, Sweden and Finland, and it was speculated that they were associated with the important wintering area in the southern North Sea and the Helgoland Bight (OKILL 1992). However, as most recoveries were of dead birds caught in fishing gear, such data may be highly biased towards fishing intensity in a given region (OKILL 1992). The invention of animal tracking devices and isotopic signatures provided a much better suited method for studying the routes of migratory birds and the different habitats they use throughout their annual cycle. Over the last decade some studies used these methods to investigate the migratory

behaviour of European red-throated divers and shed some light on the use of spring staging, moulting and wintering grounds of these birds.

During the DIVER project (DORSCH ET AL. 2019) red-throated divers were caught in the eastern German Bight between February and April and fitted with satellite tags. For 33 of these individuals the breeding region could be identified. Most of the birds moved to breeding areas in Northern Russia (25 ind.), two birds moved to Greenland, two to Svalbard and four to Norway (KLEINSCHMIDT ET AL. 2022). With a minimum migration distance of over 1,000 km for most birds (88 %), they performed a long-distance migration, with only the ones breeding in Norway moving less than 1,000 km. Of the 25 birds moving to northern Russia, 19 moved to the Siberian Arctic and five to the European part of Northern Russia. Birds migrating to Northern Russia did so along the Baltic Sea, either moving along the Bothnian Bight or the Finish Bight, with some individuals using both. There was only one exception when a bird moved along the Northern Cape. Spring migration was a relatively slow stepwise migration with several spring staging sites in the North Sea for birds moving to Greenland, Svalbard and Norway and in the North and Baltic Sea for those moving to Russia. Important spring staging sites were located in the Gulf of Bothnia (especially the Gulf of Riga), the Pomeranian Bay and the Skagerrak/Kattegat. Migration from breeding areas was in most cases (77 %) separated into moulting migration and autumn migration, but some individuals undertook a direct migration using the same general area for moulting and wintering. Tracking data and stable isotope analyses revealed that birds found moulting in the Baltic Sea all bred in Russia, birds moulting in the North Sea came from breeding populations in Scandinavia and from Russia. Of eleven birds that could be tracked during the moulting period after returning from the breeding area, two used the German Bight as a moulting area. In the Baltic Sea, especially the Gulf of Riga turned out to also be an important moulting area. Also, the Gulf of Bothnia was used as a moulting area. Wintering areas could be analysed in some detail for ten individuals that were tracked long enough for analysing their habitat use after returning from the breeding site. One of these birds bred in Svalbard and used the Eastern German Bight for wintering, the other nine bred in northern Russia and varied in their winter habitat use. Four individuals used mainly the Eastern German Bight, two used mainly areas in the Baltic Sea, one the Irish Sea, two the Southern Bight of the North Sea (UK coast and French coast) and one moved extensively along the eastern North Sea coast from the West Frisian Islands up to Denmark. Of the 10 birds tracked, six used the German Bight either as a wintering site during the complete season or temporarily. This shows that the German Bight serves as an important moulting, wintering and staging area for red-throated divers from the Russian and probably also Scandinavian breeding population of red-throated divers.

With red-throated divers from the breeding population in Northern Russia distributing over various different staging and wintering areas with only limited overlap between home ranges, this population showed only low migratory connectivity (KLEINSCHMIDT ET AL. 2022). With regard to individual strategies, it turned out that migration routes and wintering sites are quite consistent between years (KLEINSCHMIDT ET AL. 2022).

Departure time from wintering areas correlated with latitude but not with longitude, also travelling time was correlated with longitude but not with distance travelled. Birds that had longer travelling times also had longer durations of staging and more staging stops.

Duckworth et al. (2022) analysed winter locations of red-throated Divers from three European breeding populations fitted with light-based geolocator tags and, other than what Kleinschmidt et

al. (2022) found for the breeding population from Northern Russia, they found high migratory connectivity within these population with no mixing of birds from these three populations throughout their annual cycle. Birds from Iceland (16 birds) stayed in the local Icelandic waters during winter only moving up to about 200 km from the breeding site in some cases. Scottish birds from Orkney and Shetland islands (14 birds) showed a partly migratory strategy, with some birds remaining in the waters around Orkney and Shetland throughout the winter and some moving a little further south to the coastal waters of Scotland and Northern Ireland. In contrast, red-throated divers from Finland (8 birds) were fully migratory and moved westwards through the Baltic in early winter and on to the North Sea in late winter. Stable isotope analyses taken together with locations obtained during the breeding and wintering period suggested that the three populations also differ in their moulting areas, with Finish birds moulting in the Baltic Sea and the other two populations in different areas of the North Sea (DUCKWORTH ET AL. 2022).

Taken together, these two studies show that European breeding populations of red-throated divers differ substantially in their migration strategies. While some only perform short movements between the seasons (from Scotland and Iceland), others show short distance migrations into the North Sea (from Norway) and others show medium to long distance migrations into the Baltic and/or North Sea (from Greenland, Spitzbergen, Finland and Russia). Data suggest that populations undertaking medium to long distance movements at least partly mix in their staging and wintering areas.

While knowledge on migration in red-throated divers accumulates, there are still knowledge gaps considering the reasons for their choice of different migration strategies and the importance of the German Bight and especially the German Baltic Sea as a staging and/or wintering ground for the different populations. Previous data showed that the Pomeranian Bay was used by some birds as a staging area on their way to and from Russia (KLEINSCHMIDT ET AL. 2022), however, its importance for the different breeding populations remains largely unclear. Also, only few birds could be tracked stemming from the Norwegian breeding population, and it is unclear whether they are fully migratory and use the German Bight as a wintering area to a large degree, or whether they may be partly migratory, with some individuals staying closer to their breeding areas or use differing wintering sites. To understand the importance of German waters for the differing breeding populations it is essential to understand how flexible these populations are in their choice of staging and wintering areas. Also, the energetic constraints on short-distance migrants may be substantially different to long-distance migrants, as they do not have the need to store up on food reserves during long-distance migration and may also be more flexible in their choice of wintering habitat. In this study we aimed to

1) Describe the migration routes of red-throated divers wintering in the German Bight and compare it to previous findings

2) Determine the distance travelled to breeding grounds and identify short- versus long distance migrants

3) Describe the timing of individual birds from the different breeding areas with a focus on their time spent in the German Baltic Sea

4) Discuss the overlap of winter movements with OWFs across Europe

9.2 Methods

Similar to all other analyses, for birds with implanted loggers, the first 14 days after tagging were removed, and for birds with external loggers the first 24 hours, to avoid any effects from the tagging still affecting the movement of birds. After this time period, birds were assumed to resume their normal behaviour. This resulted in some tracks not starting in the catching area but only after the birds moved already away on their migration.

9.2.1 Migration maps

Maps showing the migratory trajectory were plotted separately per individual as well as combined per year. Trajectories were divided into a spring/summer period, lasting from March to July, and an autumn/winter period, lasting from August to February (following KLEINSCHMIDT ET AL. 2022). For individuals which showed potential breeding (star-shaped GPS-positions over a longer time period on land, indicating a nesting location), this was indicated in the map. For individuals present in a potential breeding region but mainly moving within larger water bodies, no breeding was assumed.

9.2.2 Distance calculation

For calculation of migration distances to breeding grounds, one GPS-position per day was used. Distances were calculated from catching area to potential breeding area and in autumn from breeding area to catching area. If birds did not return to that area the distance to the closest staging area was used. As the first 14 days are not used for analysis for implanted birds, the distance between the catching area and the first position after this time period was used for the distance calculation.

9.3 Results

In total, 52 of the 68 tagged individuals transmitted signals. Individual tracks of all birds can be found in the Appendix A.4.1. Of these, 32 individuals transmitted data from (the start of) migration outside of the catching area (outside of the German and Danish North Sea). Thirty birds reached potential breeding areas, while still being tracked, and 21 of these birds were likely breeding.

9.3.1 Migration routes and breeding areas

Most individuals (70%) migrated to breeding grounds in northern Russia (21 of 30), six birds (20%) migrated to Norway, one bird migrated to Sweden, one bird to Greenland and one bird to Svalbard. Below, maps are shown separate for spring/summer and autumn/winter as well as separate per tagging year. Tab. 9-1 provides detailed information on timing and breeding areas for all individuals migrating to potential breeding grounds and (partly) for their autumn migration.

Birds migrating to Siberia show mainly three routes when crossing Scandinavia and the Baltic Sea: either following the Norwegian coastline around the northern cape, or a more direct route into the Baltic Sea and then migrating either through the Finish Bay or the Bothnian Bay, before crossing over land into the White Sea (Fig. 9-1, Fig. 9-3, Fig. 9-5). In 2022, one bird taking a route along the Norwegian coastline moved northward towards Svalbard (Fig. 9-1). On their autumn migration,

most birds used these same routes, but with some individual variations (Fig. 9-2, Fig. 9-4, Fig. 9-6). The “Svalbard-bird” for example, performed a loop migration, using a more westerly route towards UK in autumn (Fig. 9-2).

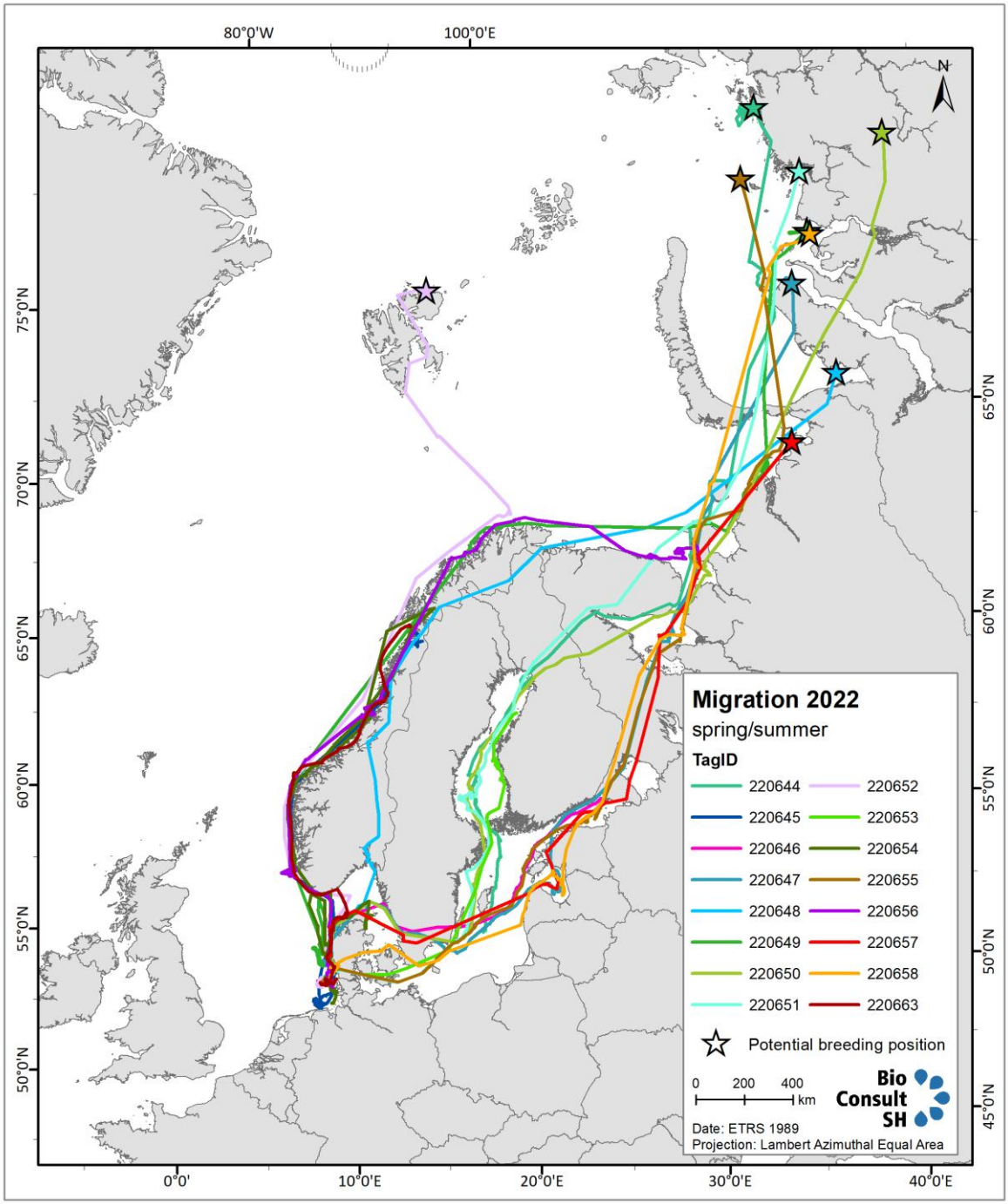

Fig. 9-1 Migration routes of individual red-throated divers during spring/summer 2022

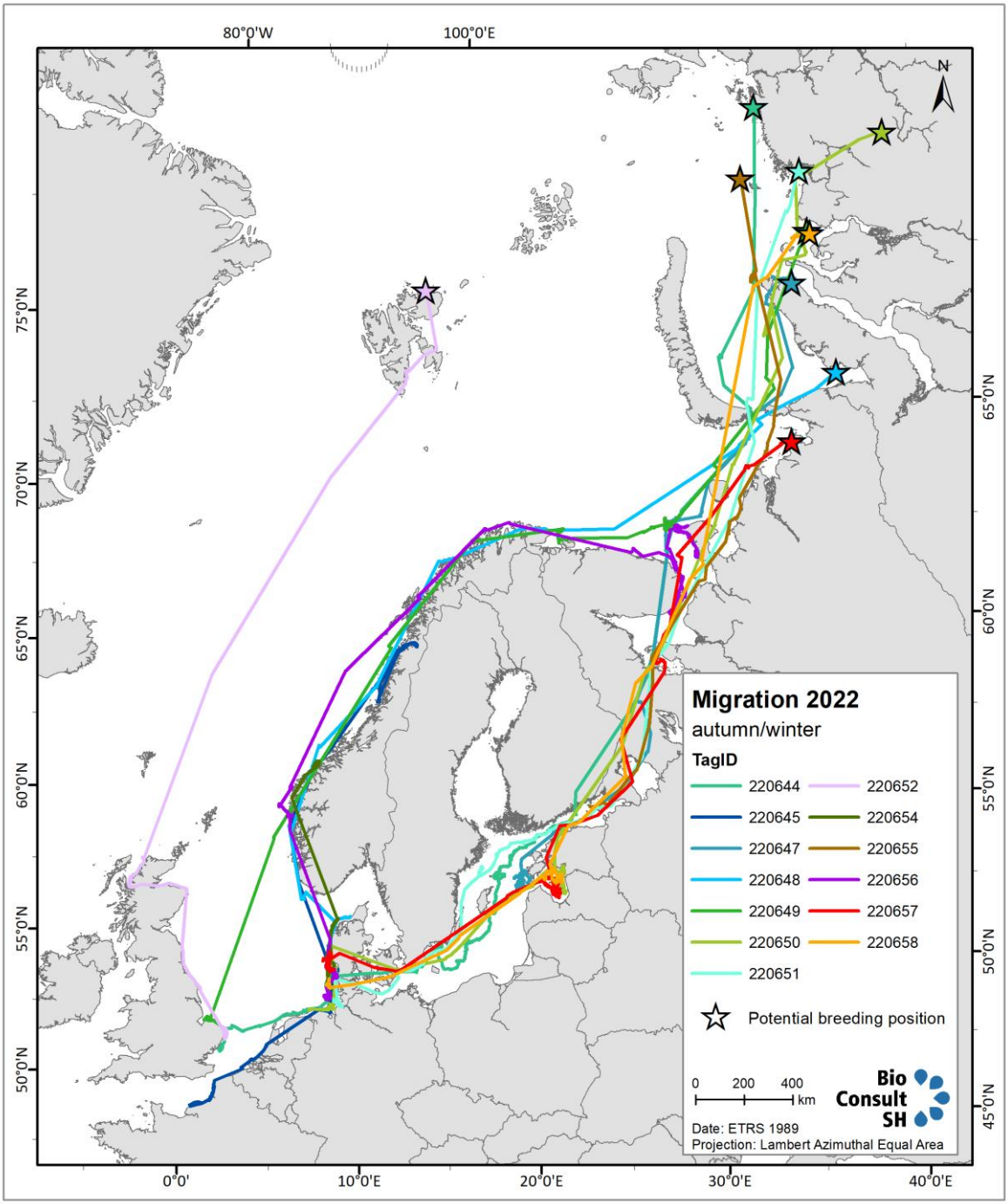

Fig. 9-2 Migration routes of individual red-throated divers during autumn/winter 2022

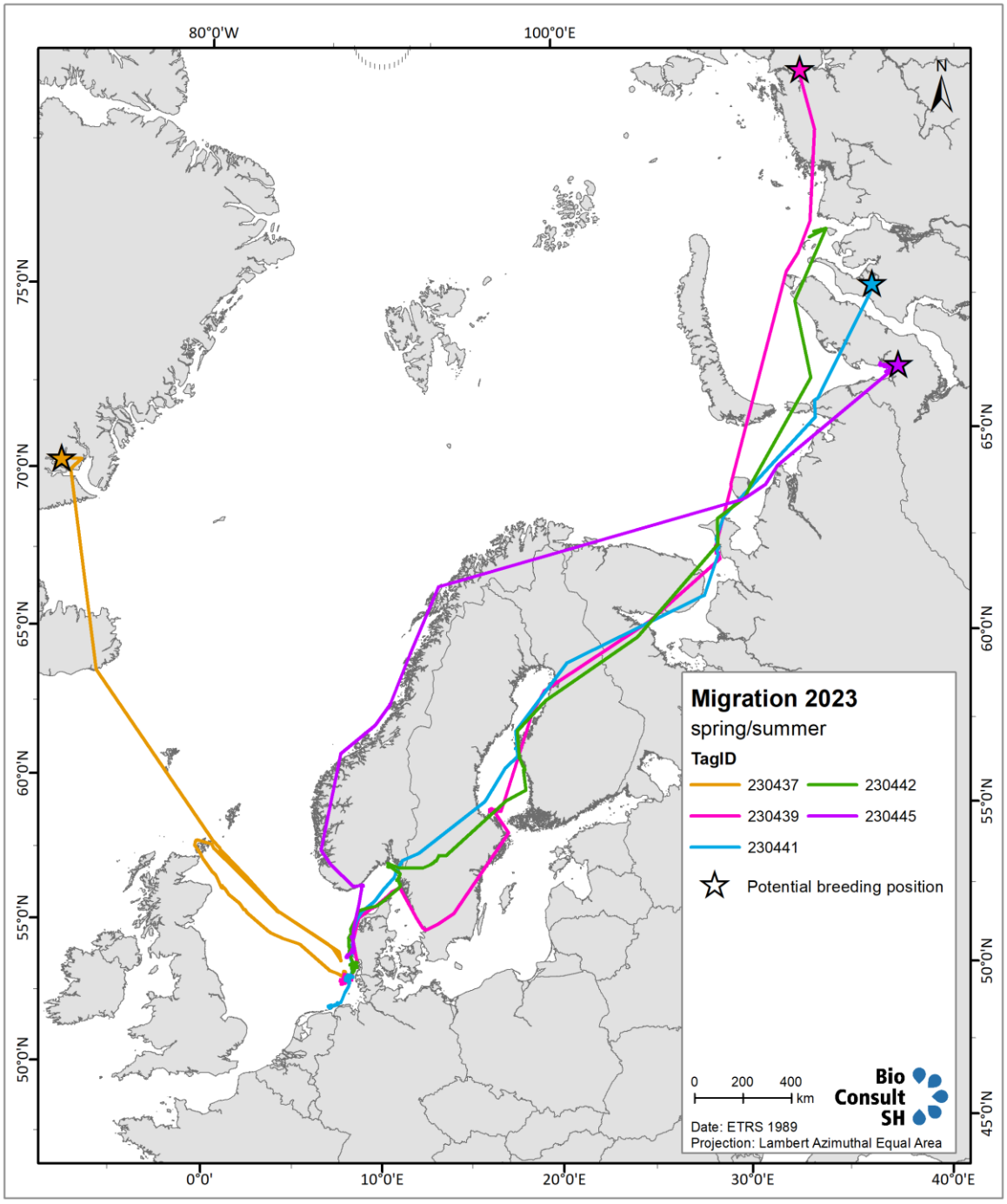

Fig. 9-3 Migration routes of individual red-throated divers during spring/summer 2023

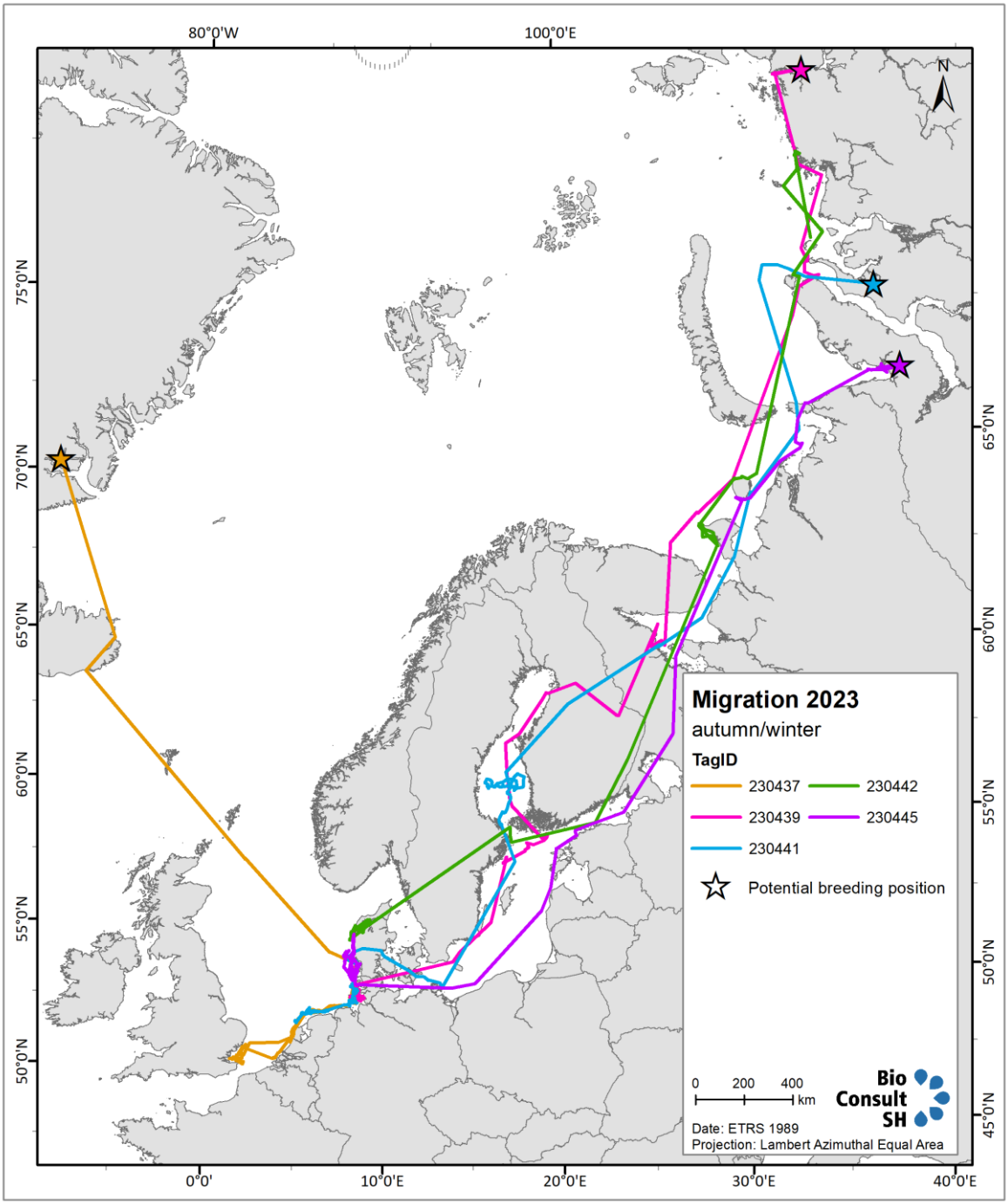

Fig. 9-4 Migration routes of individual red-throated divers during autumn/winter 2023

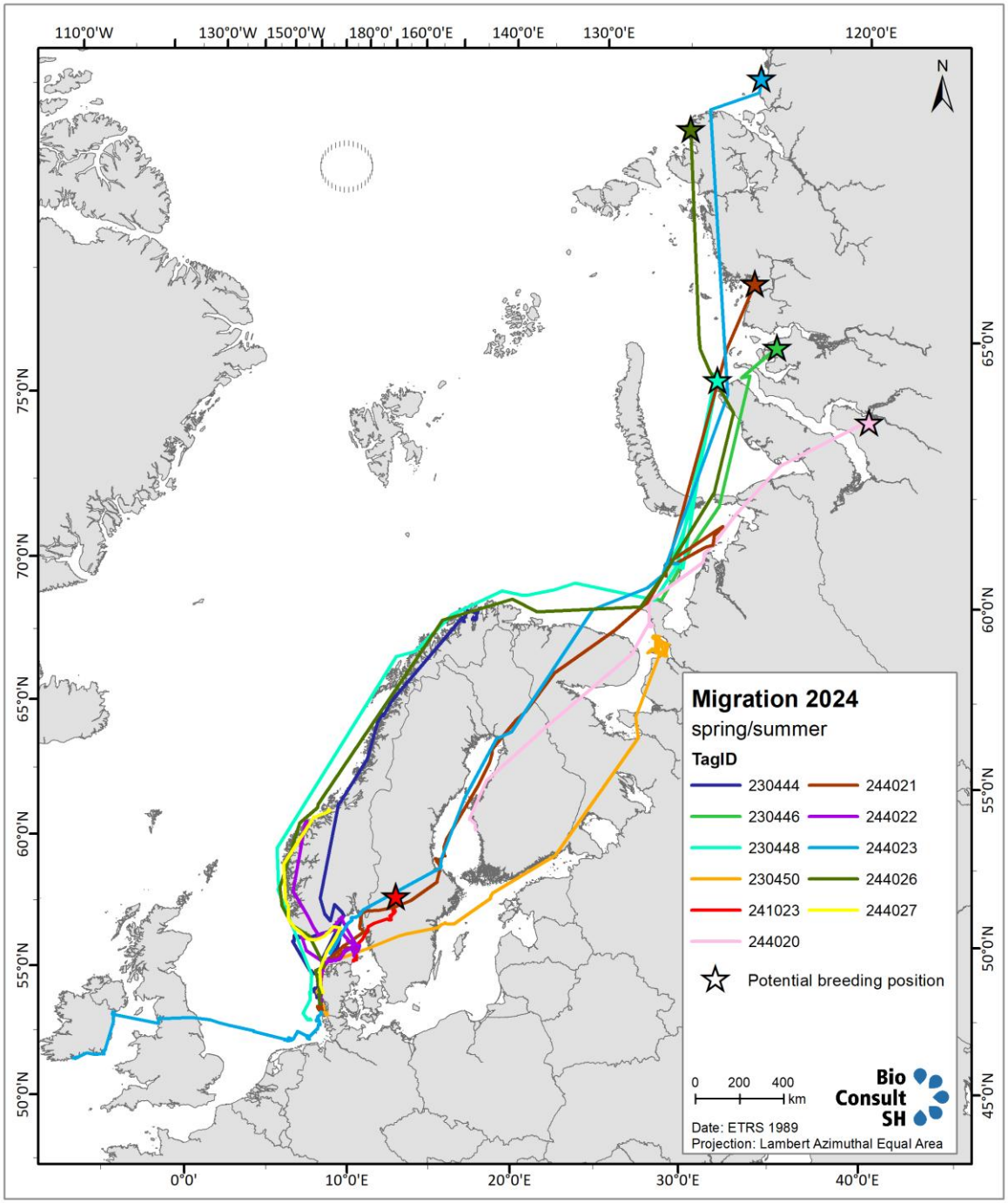

Fig. 9-5 Migration routes of individual red-throated divers during spring/summer 2024

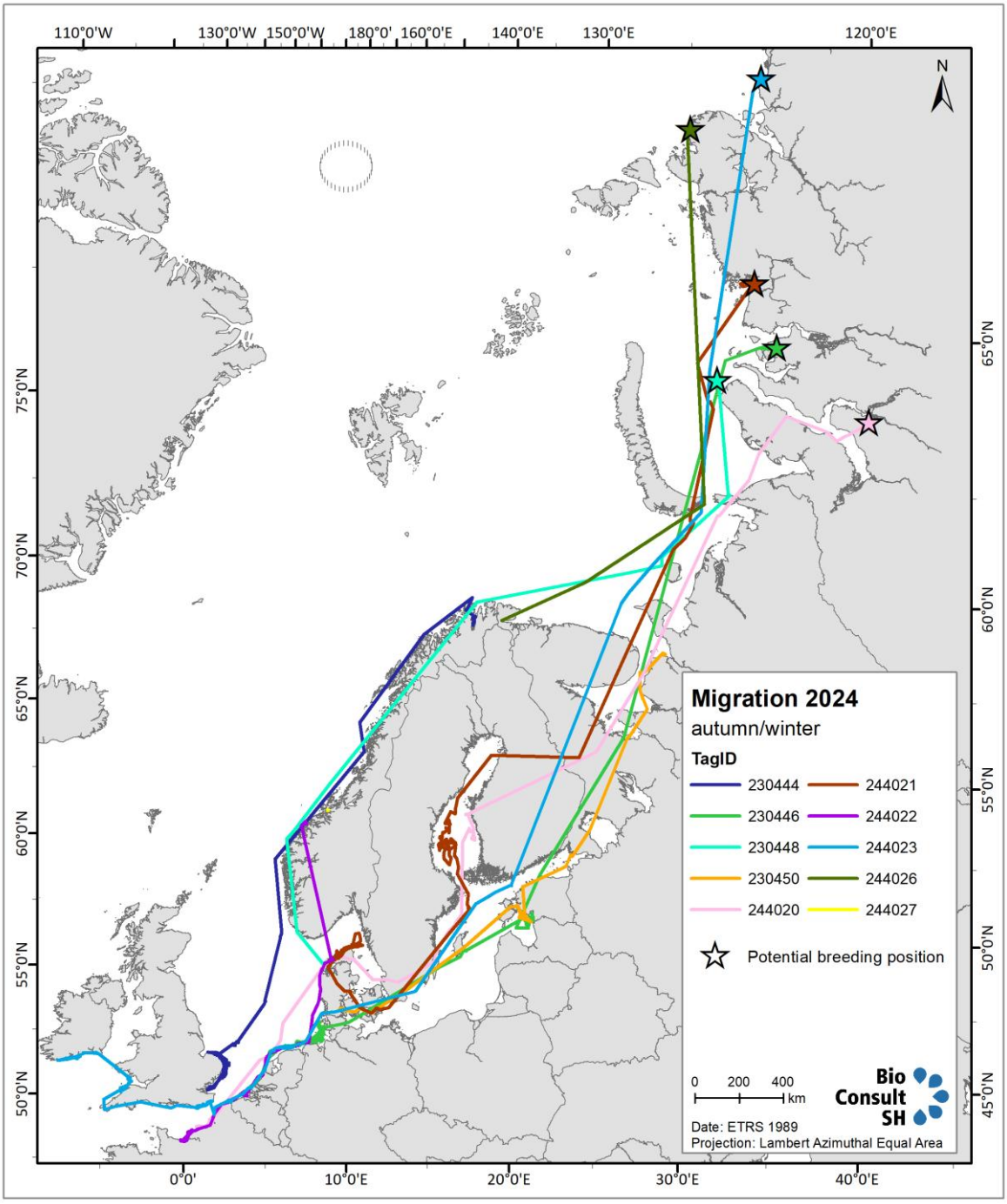

Fig. 9-6 Migration routes of individual red-throated divers during autumn/winter 2024

Tab. 9-1 Overview of migration for 24 individuals reaching breeding areas and providing data for autumn migration/wintering.

Tag ID	Sex	Spring departure	Breeding area_arrival	Breeding area	breeding_area_ comments	Breeding area_depar-ture	Autumn migr_arrival	autumn_route	wintering_area_ furthest_away
220644	M	10.05.2022	19.06.2022	Taymyr	lake 1 km from coast, July - Sep, range of movements about 100 km visiting waters off-shore	07.09.2022	18.11.2022	White Sea, Finnish Half, across Germany	UK, south-east
220645	F	03.06.2022	14.06.2022	mid Nor-way	fjord in mid Norway, movements within rang of 40 km	03.09.2022	15.09.2022	along coast of Norway and Denmark	Fr, La Manch
220648	M	26.05.2022	11.06.2022	Jamal	small lake on Jamal 2 km inland	05.09.2022	25.10.2022	along coast of Norway and Denmark	DK, western coast
220649	M	25.05.2022	15.06.2022	Jamal	3 lakes on the island, 1.5 km from the coast	14.09.2022	18.10.2022	along coast of Norway and Denmark	UK, south-east
220650	F	11.05.2022	08.06.2022	Taymyr	river and lakes 385km from coast, south of Taimir	04.09.2022	29.11.2022	White Sea, Finnish Half, across Germany	Ger, south North Sea
220651	F	20.05.2022	15.06.2022	Taymyr	small island in river delta at the coast	17.09.2022	11.10.2022	White Sea, Finnish Half, across Germany	Ger, south North Sea
220652	M	19.05.2022	06.06.2022	Spitzber-gen	islands northern Spitz-bergen, several areas max 1.7 km from the coast	11.09.2022	25.09.2022	across Norwegian Sea to northern Scotland, across Scotland to North Sea and till south UK	UK, south-east

Tag ID	Sex	Spring departure	Breeding area_arrival	Breeding area	breeding_area_ comments	Breeding area_depar-ture	Autumn migr_arrival	autumn_route	wintering_area_ furthest_away
220654	M	26.05.2022	08.07.2022	mid Nor-way	large movements in mid Norway in Jun - Aug, 08.07.2022 is the furthest point	08.07.2022	19.09.2022	along coast of Norway and Denmark	Ger, south North Sea
220656	F	31.05.2022	30.06.2022	White Sea	Jul - Oct in the en-trance to White Sea, east and west coasts	27.10.2022	14.11.2022	along coast of Norway and Denmark	Ger, south North Sea
220657	F	19.05.2022	01.06.2022	Novaja Zemlja	small lake 2.5 km in-land	05.09.2022	03.12.2022	White Sea, Finnish Half, across Germany	DK, western coast
220658	F	20.05.2022	10.06.2022	Jamal	island 30 km from coast and there sev-eral lakes 8 km from shore	17.09.2022	03.12.2022	White Sea, Finnish Half, across Germany	Ger, Sylt North Sea
230437	F	20.05.2023	13.06.2023	Green-land	fixes are not every day, 06.09.2023 on breeding ground, 14.09.2023 on Iceland	06.09.2023	03.10.2023	Iceland, north Scot-land, Germany, Sylt North Sea	UK, south
230439	F	09.05.2023	06.06.2023	Taymyr	river 100 km inland, before autumn migra-tion flew several time to the coast and back inland	03.09.2023	19.10.2023	White Sea, Botnic Half, across Germany	Ger, south North Sea
230441	F	18.05.2023	02.06.2023	Jamal	2 lakes 60 km inland, very small range	17.09.2023	05.12.2023	White Sea, Botnic Half, across Germany	NL, south North Sea
230442	F	21.05.2023	14.07.2023	Jamal	moved along the coast east of Jamal, no breeding?	18.08.2023	05.12.2023	White Sea, Finnish Half, across Germany	DK, western coast

Tag ID	Sex	Spring departure	Breeding area_arrival	Breeding area	breeding_area_ comments	Breeding area_depar-ture	Autumn migr_arrival	autumn_route	wintering_area_ furthest_away
230444	M	27.05.2024	19.07.2024	north Norway	moved in fjords north of Norway, about 200 km range	30.09.2024	02.11.2024	along coast of Nor-way, across North Sea	UK, south
230445	F	03.06.2023	16.06.2023	Jamal	lakes 50 km inland and coastal areas	12.09.2023	19.10.2023	White Sea, Finnish Half, across Germany	Ger, Sylt North Sea
230446	F	08.06.2024	15.06.2024	Jamal	lake 30 km inland by Leskino	14.09.2024	09.12.2024	White Sea, Finnish Half, across Germany	NL, south North Sea
230448	M	20.05.2024	26.06.2024	Jamal	small island north of Jamal, 3-5 km inland	05.09.2024	08.10.2024	along coast of Norway and Denmark	Ger, Sylt North Sea
230450	M	04.06.2024	20.06.2024	White Sea	on water at the en-trance to White Sea	28.09.2024	24.12.2024	White Sea, Finnish Half, across Germany	DK, western coast
244020	M	20.05.2024	11.06.2024	Jamal	river and lakes 30 km inland	20.09.2024	30.10.2024	White Sea, Botnic Half, across Skona, along coast of Den-mark	Fr, La Manch
244021	F	24.05.2024	30.06.2024	Jamal	river delta 25 km in-land	10.09.2024	30.11.2024	White Sea, Botnic Half, across Germany	DK, western coast
244022	F	04.06.2024	28.06.2024	mid Nor-way	island in southern Nor-way	31.08.2024	02.09.2024	along coastline from Denmark to France	Fr, La Manch
244023	M	24.05.2024	14.06.2024	Taymyr	lake 10 km inland	05.09.2024	14.10.2024	White Sea, Finnish Half, across Germany	Ireland

9.3.2 Distance to breeding grounds (long- vs. short-distance migration)

Migration distances to (potential) breeding grounds reached from 372 km for a bird breeding in Sweden to 5374 km for a bird breeding in far eastern Siberia (ID 244023). On average, spring migration distance was 3506 km. Only two birds (ID 241023 and ID 244027) migrated less than 1000 km (here termed as short-distance migrants), one to Sweden and one to southern Norway (Tab. 9-2).

For individuals with a complete autumn migration (reaching the catching area or another wintering area), distances to the first wintering location were on average slightly longer, but comparability is limited as loggers often stopped working before the end of the winter season and thus not all movements could be included. Several individuals, after passing the catching area, moved south-west to France and UK, with Ireland (ID 244023) being the furthest western wintering area. The latter individual also showed the longest spring migration.

Tab. 9-2 Migration distances for spring and (if available) autumn migration (to first wintering site) as well as location of the potential breeding area.

Tag ID	Distance spring (km)	Distance autumn (km)	Breeding area
220644	4954	4771	Taymyr
220645	1594	1505	mid Norway
220647	4068	-	Jamal
220648	3198	3548	Jamal
220649	4865	4051	Jamal
220650	4797	5345	Taymyr
220651	4413	4228	Taymyr
220652	3370	3473	Svalbard
220654	2956	1638	mid Norway
220655	4220	-	Jamal
220656	2728	2979	White Sea
220657	2624	3658	Novaja Zemlja
220658	4116	4048	Jamal
220663	1603	-	mid Norway
230437	4216	2627	Greenland
230439	4896	5547	Taymyr

Tag ID	Distance spring (km)	Distance autumn (km)	Breeding area
230441	3730	4869	Jamal
230442	4102	4640	Jamal
230444	2941	2567	north Norway
230445	3690	3901	Jamal
230446	3678	4444	Jamal
230448	5374	3638	Jamal
230450	2065	2555	White Sea
241023	372	-	Sweden
244020	3470	4485	Jamal
244021	4769	5106	Jamal
244022	1357	646	mid Norway
244023	4935	5074	Taymyr
244026	5193	-	Taymyr
244027	890	-	southern Norway

9.3.3 Timing of migration

Birds migrating to Sweden, Norway, Svalbard and Greenland were investigated separately from birds migrating to Siberia.

Timing of the northward migrating individuals is shown in Fig. 9-7 and Fig. 9-8. Fig. 9-7 shows that the only bird (with external logger) migrating to Sweden (ID 241023) left the area already at the beginning of April. However, comparison with implanted individuals is difficult as catching of all other birds occurred later in the season. The individual migrating to Svalbard (ID 220652) departed around mid May and then quickly moved North without any long stop-overs. In comparison, ID 230444 moving to northern Norway, showed much slower progress with some staging roughly half-way through the migration.

In autumn, most birds left the breeding grounds between the beginning and mid of September, while ID 230444 only started moving South in October.

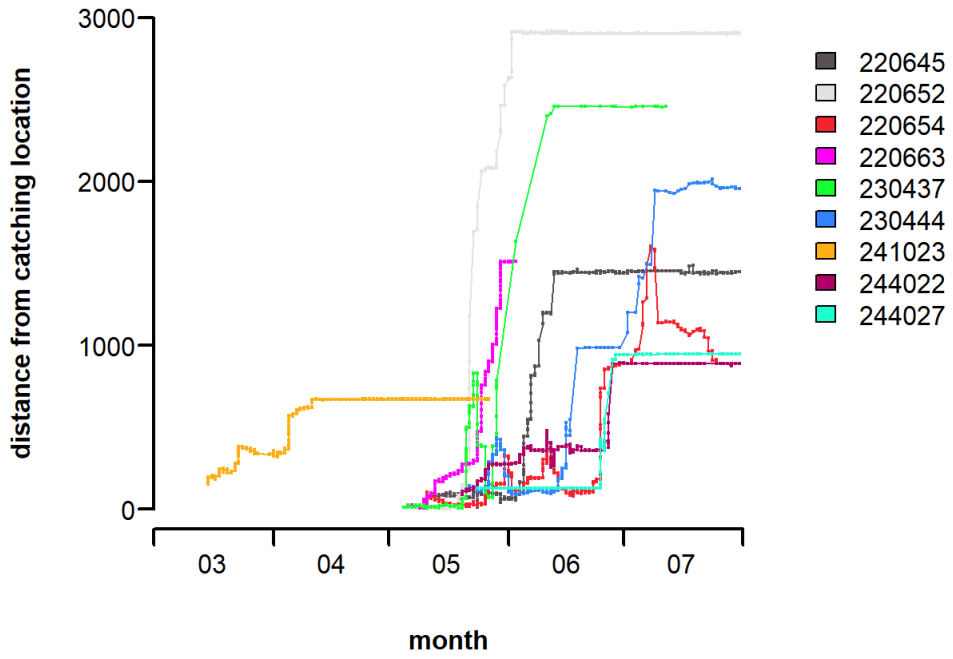

Fig. 9-7 *Timing of spring migration for northwards migrating individuals*

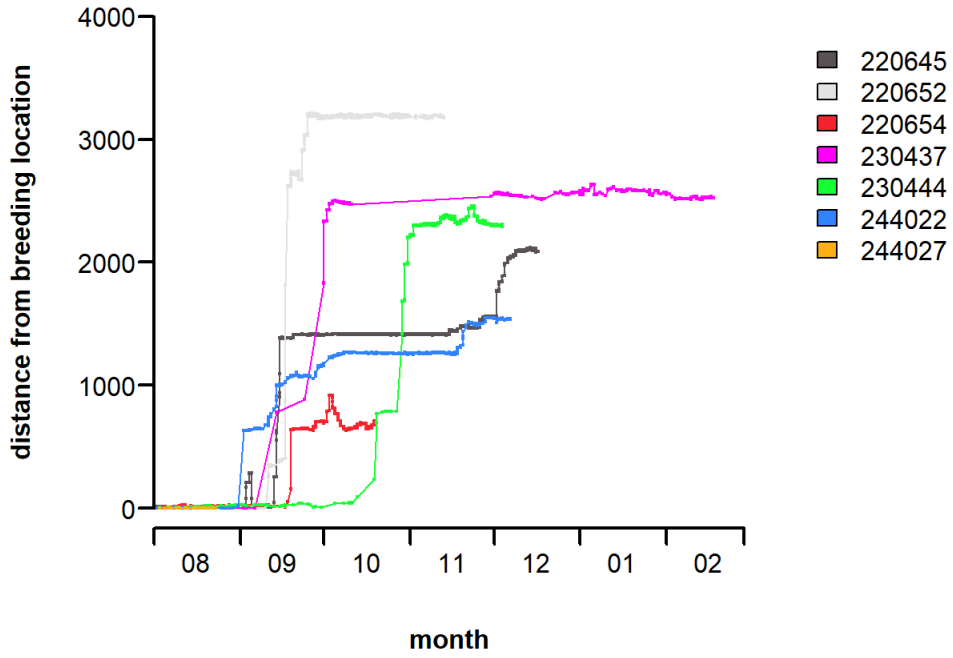

Fig. 9-8 *Timing of autumn migration for northwards migrating individuals*

Birds migrating to Siberia showed rather high similarities in their timing and movements (Fig. 9-9, Fig. 9-11, Fig. 9-13). This was except for two birds (ID 220656 in 2022 and ID 230450 in 2024), which left the area relatively late in the beginning of June and moved a shorter distance to western Siberia

(not breeding). All other individuals reached potential breeding areas between the beginning and the end of June.

In the beginning of September, the first birds started their autumn migration to the moulting areas and later onwards to wintering locations further west (Fig. 9-10, Fig. 9-12, Fig. 9-14). While initial departure was quite synchronous between individuals, movements later on showed strong individual differences, reflecting the different wintering locations that birds visited. Exceptions were again the two (non-breeding) birds staging at the coast in western Siberia during the summer. These left the area only in late October/beginning of November.

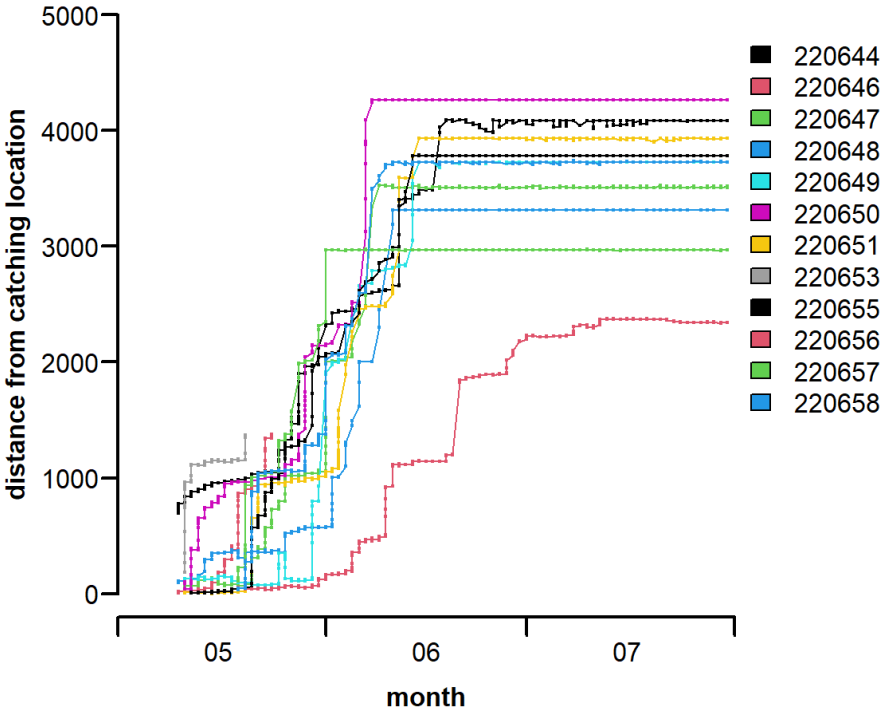

Fig. 9-9 *Timing of spring migration for individuals migrating to Siberia in 2022*

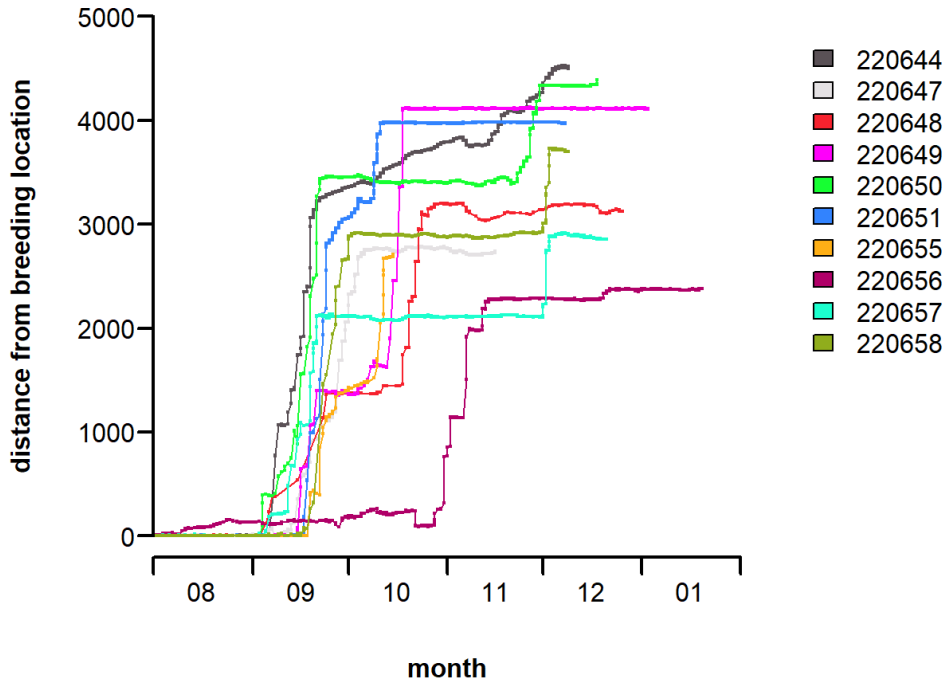

Fig. 9-10 Timing of autumn migration for individuals migrating to Siberia in 2022

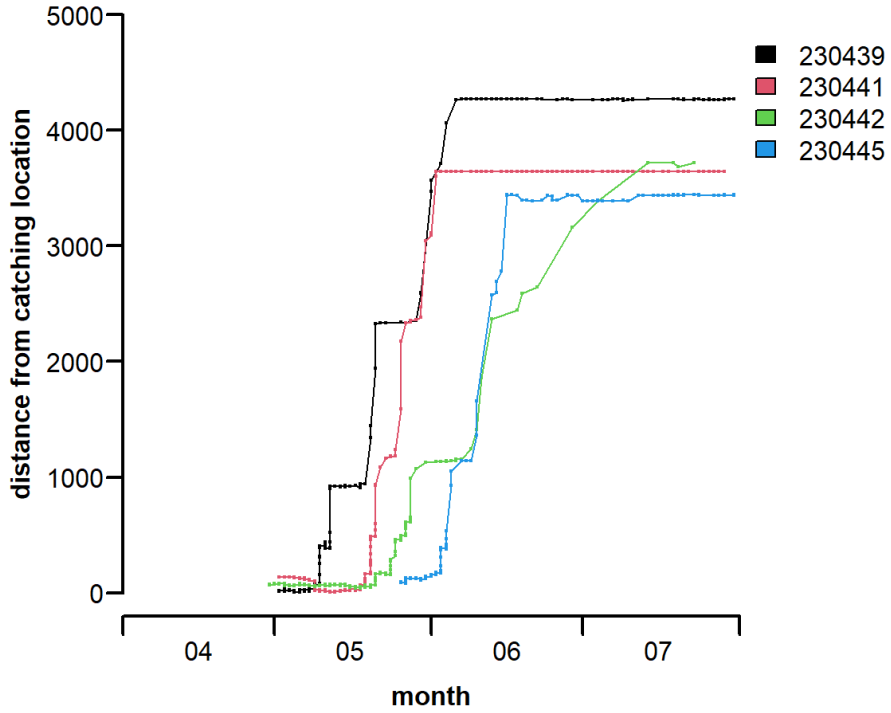

Fig. 9-11 Timing of spring migration for individuals migrating to Siberia in 2023

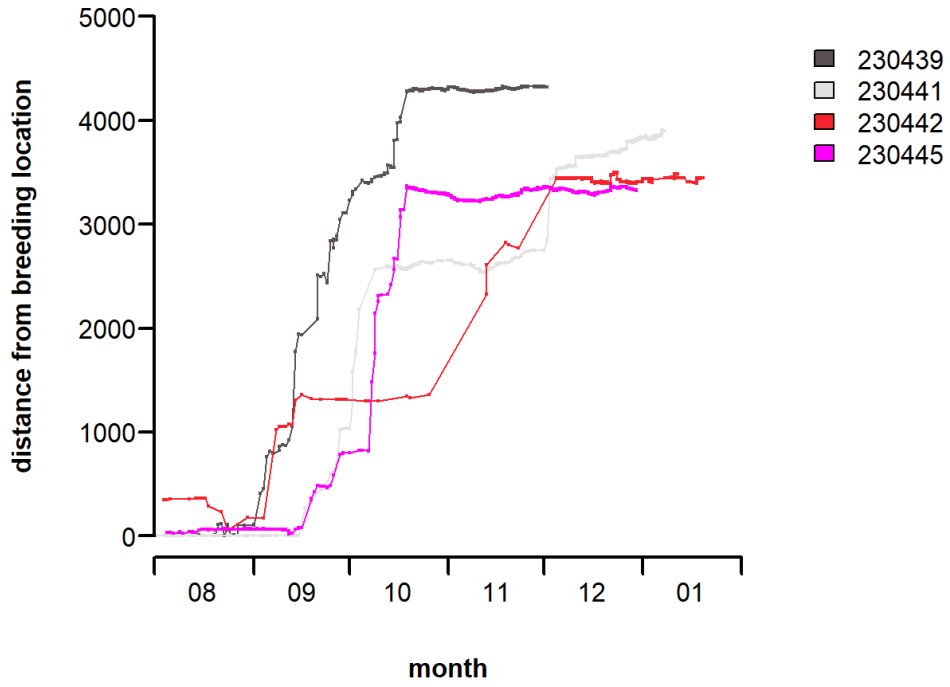

Fig. 9-12 Timing of autumn migration for individuals migrating to Siberia in 2023

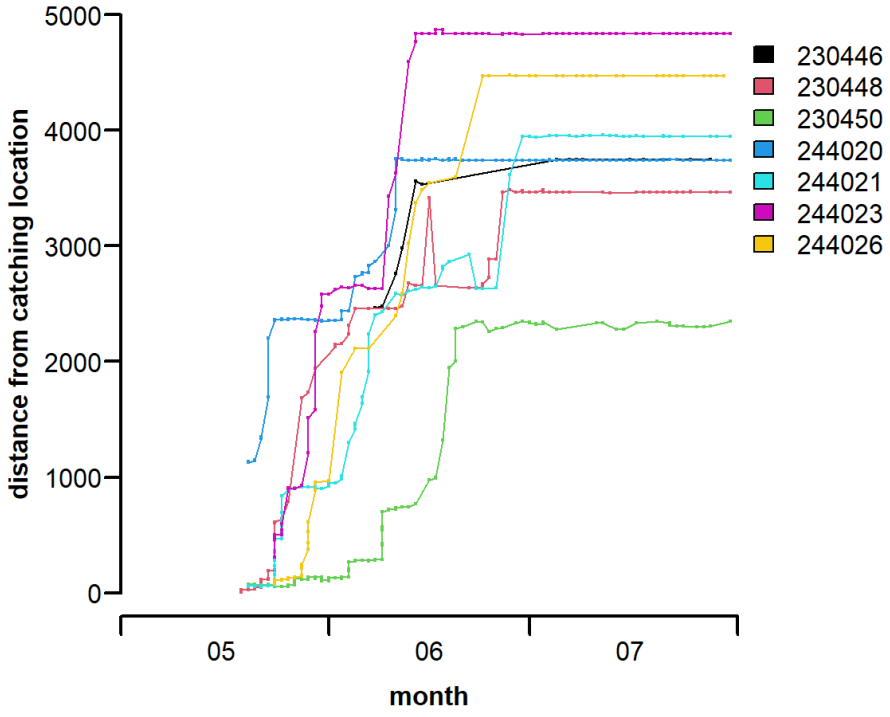

Fig. 9-13 Timing of spring migration for individuals migrating to Siberia in 2024

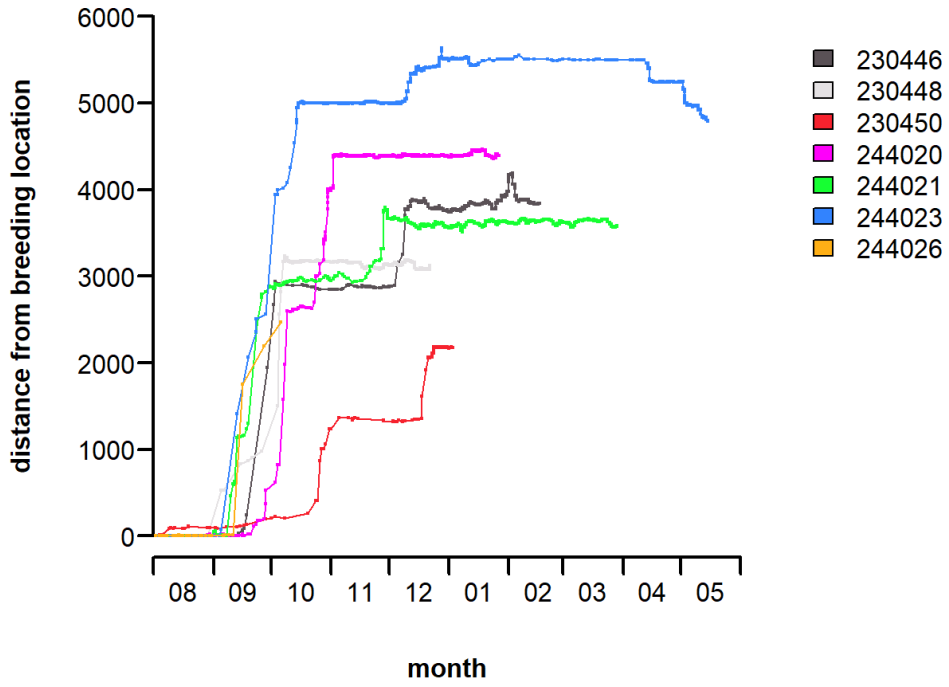

Fig. 9-14 Timing of autumn migration for individuals migrating to Siberia in 2024

9.3.4 Use of the German Baltic Sea

Of all tracked individuals (32), only six birds used the German Baltic Sea on their way to or from the breeding grounds (Tab. 9-3). Only one bird (230457, Fig. 9-15) spent several days in this region, migrating via Fehmarnbelt to coastal locations at the Darss and then moving further east to the southern coast of Rügen, before the logger signal was lost on 21st March 2024. Another individual (241022, Fig. 9-16) spent almost two weeks in the Danish part of the Fehmarnbelt with only a few positions in German waters. The other four birds were registered on their return flight in autumn to cross the German Baltic Sea in transit to their wintering area (for individual maps see appendix A.4.1). Also, a number of additional birds used the Danish parts of the Baltic Sea for transit and staging.

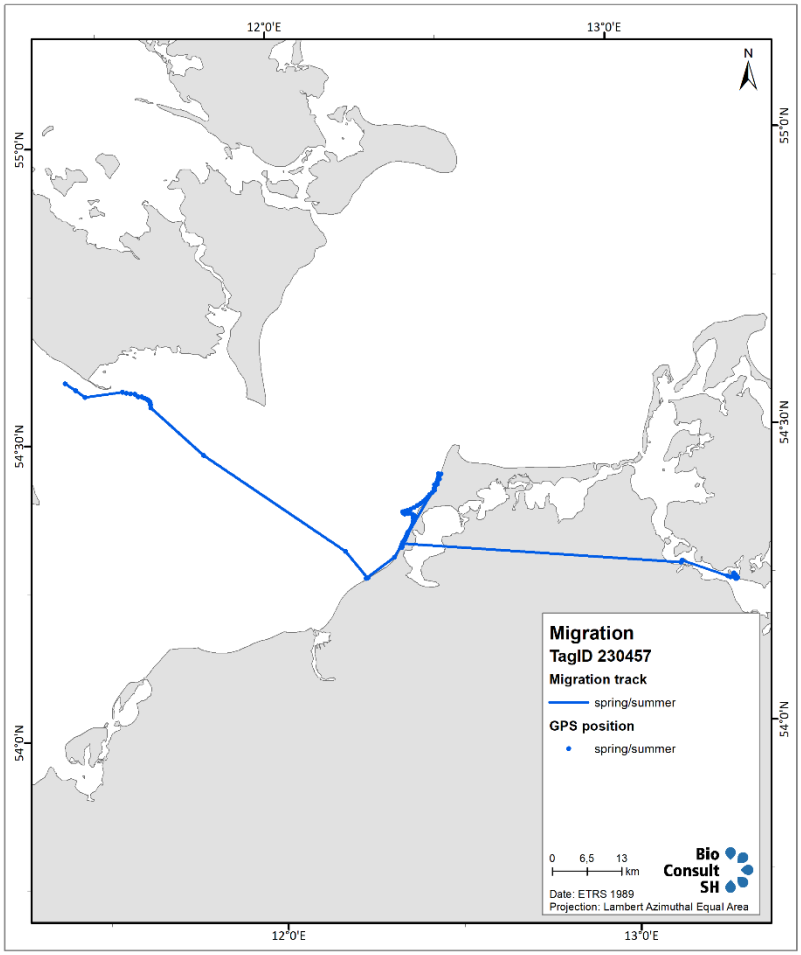

Fig. 9-15 Track of tag ID 230457 in the Baltic Sea

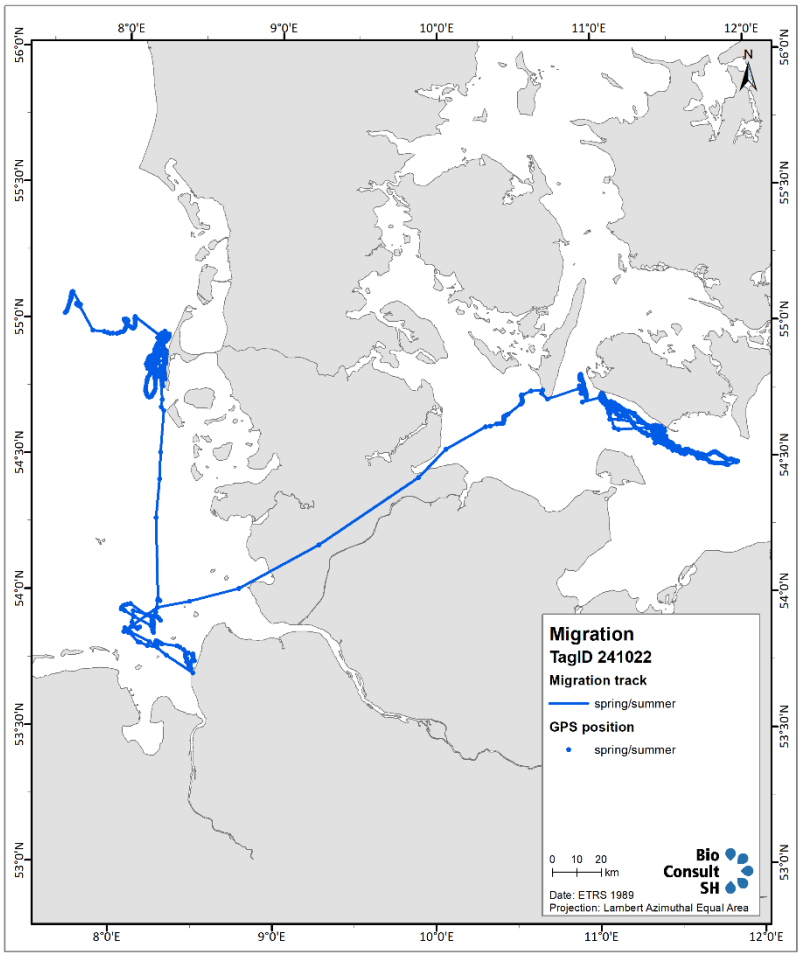

Fig. 9-16 Track of tag ID 241022 in the North and Baltic Sea

Tab. 9-3 Overview of the individuals that spent time in the German Baltic Sea during spring or autumn migration with the number of fixes in this area.

ID	N fixes	Spring arrival (Date&Time)	Spring departure	Autumn arrival	Autumn departure	Details on location
220651	11	-	-	2022-10-10 14:36:21	2022-10-11 00:36:42	transit
230441	20	-	-	2023-12-03 19:53:34	2023-12-04 21:53:07	transit
230445	2	-	-	2023-10-17 18:05:21	2023-10-18 02:06:32	transit
230446	4	-	-	2024-12-09 03:48:09	2024-12-09 06:48:09	transit
230457	69	2024-03-17 06:19:00	2024-03-20 19:17:18	-	-	Tag in Baltic Sea from 2024-03-16 till 2024-03-21

ID	N fixes	Spring arrival (Date&Time)	Spring departure	Autumn arrival	Autumn departure	Details on location
241022	5	2024-03-23 15:35:35	2024-03-25 07:38:16	-	-	Mainly in danish FehmarnBelt till end of transmitting in 2024-04-05

9.3.5 Overlap of winter movements with OWFs across Europe

For the autumn/winter period of divers (for the second spring period there was insufficient data), GPS-tracks were plotted on maps including OWFs under construction or in operation, to show potential overlap of migration routes and wintering area with existing OWF developments (Fig. 9-17, Fig. 9-18, Fig. 9-19). While this overlap was discussed in the previous chapters for the Eastern German Bight, areas further west along the North Sea coast and English Channel, as well as the British coast, also show certain overlaps with existing developments. One example is ID 230437, which staged in the Thames Estuary, with the larger area hosting several OWFs (Fig. 9-18). During winter, individuals mainly moved and staged close to the coast and thus coastal developments might show the strongest overlap with diver habitat.

When intersecting GPS-fixes for the winter period (December to February) with existing and planned OWFs across Europe, only few positions were found inside (planned) OWF footprints. The highest number of 14 fixes were found for the planned OWF Dunkirk in France. Overall, only 0.2% of all fixes were found in planned OWFs during winter. For OWFs in operation or under construction, 0.3% of fixes were found inside the footprints, with the most fixes inside OWF Horns Rev 3.

Across all years and all GPS-fixes, the operational OWF Horns Rev 3 and Vesterhav Nord/Syd (before construction) had the most fixes inside the (planned) footprints.

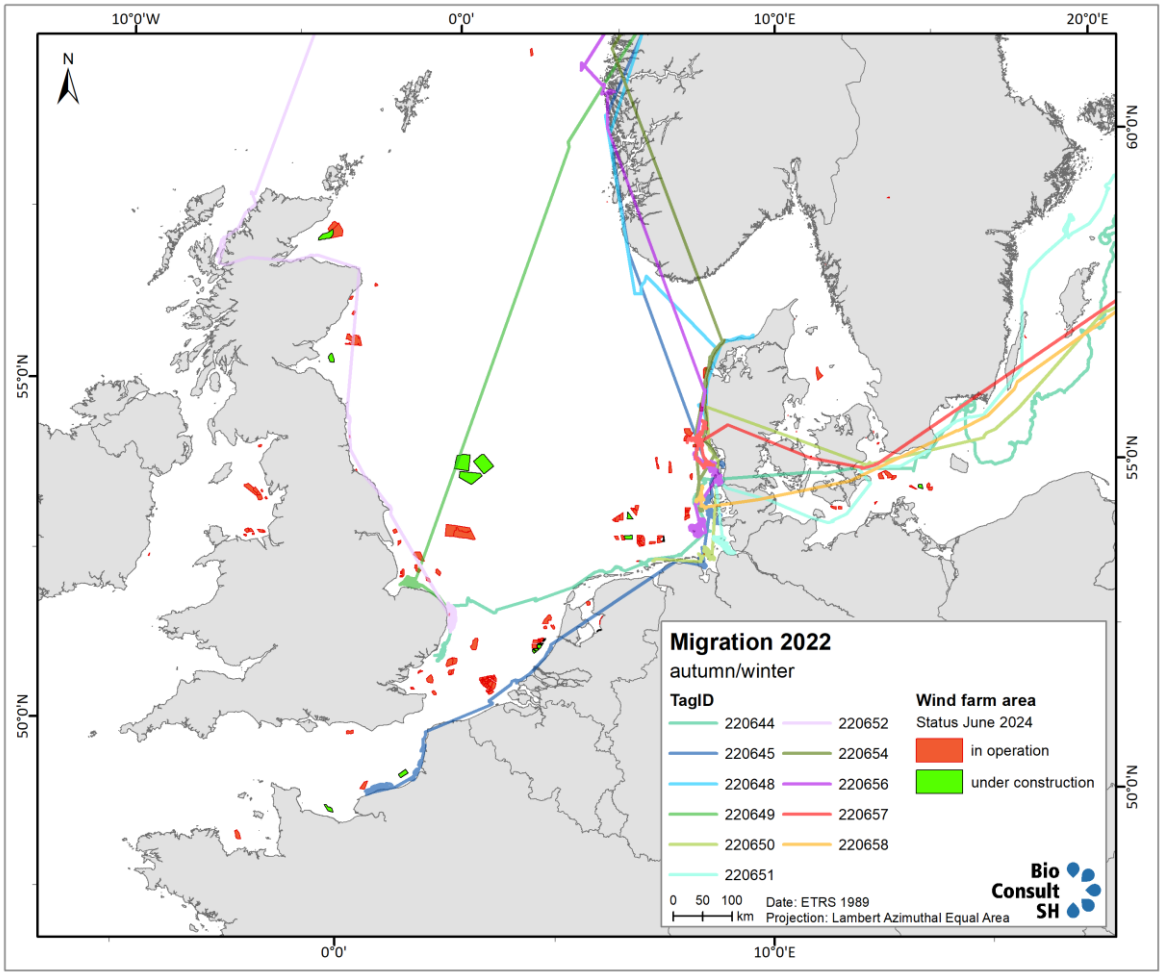

Fig. 9-17 Individual tracks during autumn and winter 2024, including existing OWF developments.

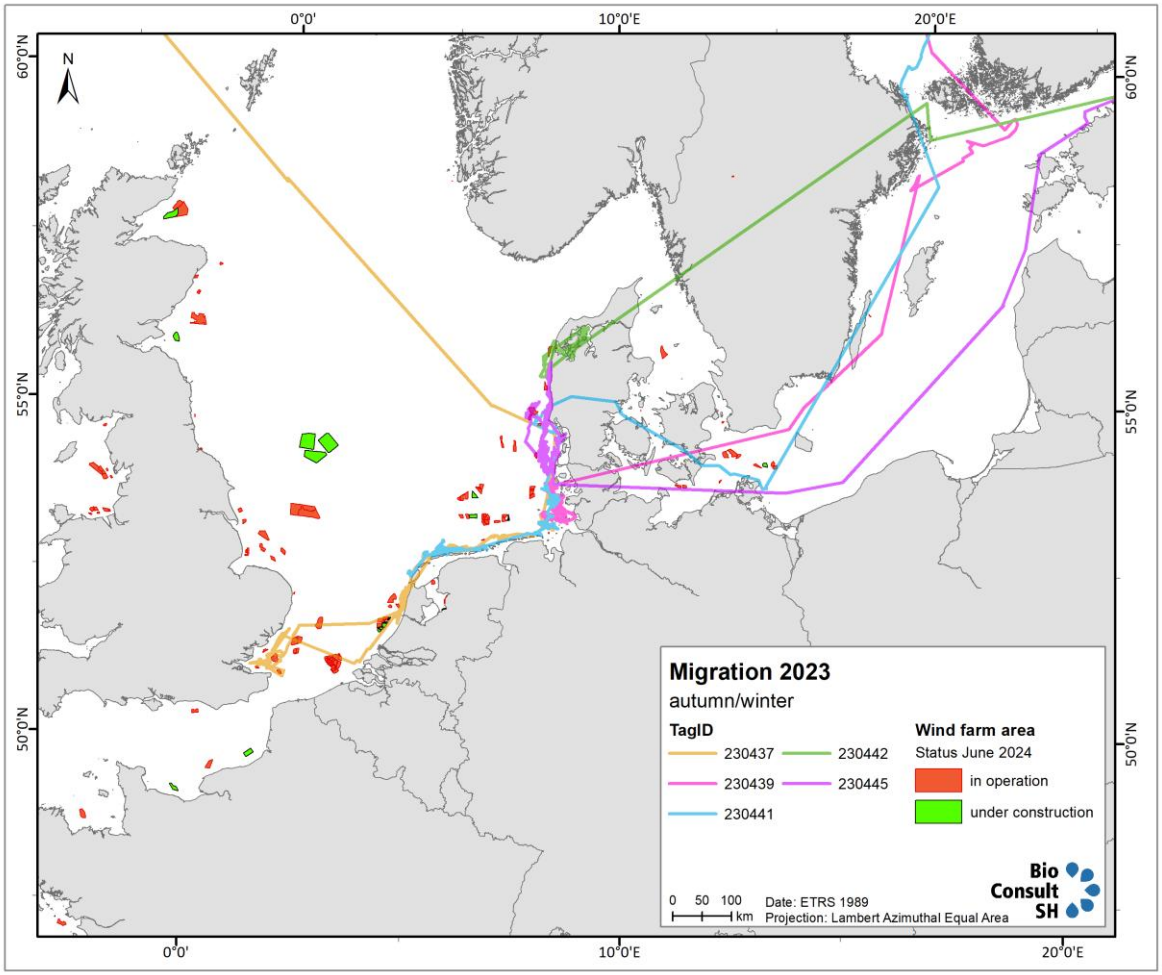

Fig. 9-18 Individual tracks during autumn and winter 2023, including existing OWF developments.

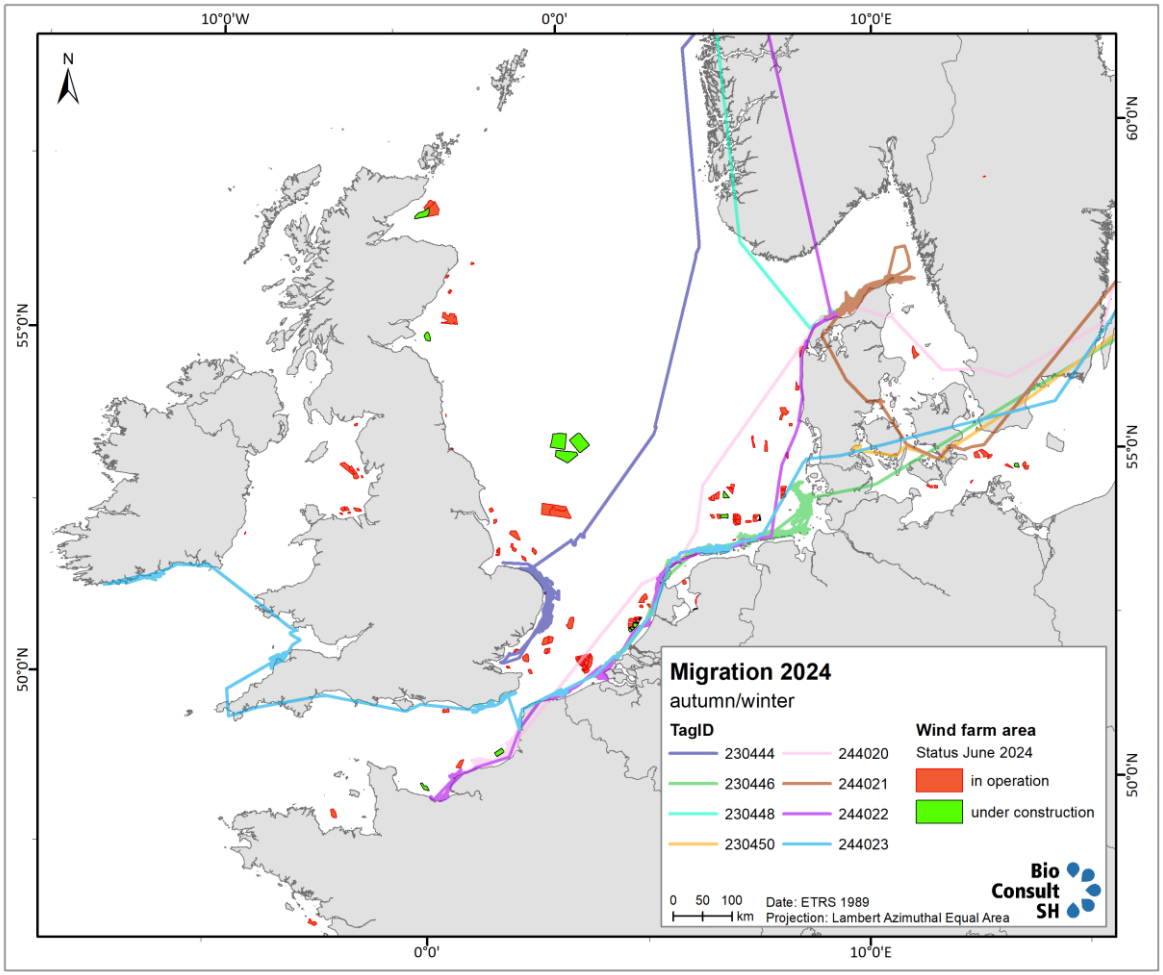

Fig. 9-19 Individual tracks during autumn and winter 2024, including existing OWF developments.

9.4 Discussion

In the current study, breeding locations as well as migration routes of divers were very similar to the previous DIVER project. In the current study 70% of birds moved to northern Russia, in the previous diver project it was 74%. This shows that our sample size was representative of showing the full range of breeding locations of birds staging in the focal area. With respect to migration routes, in the current study, 6 out of 21 individuals (29%) migrating to breeding grounds in northern Russia, used the route around northern Norway, while this route was rarely used in the previous DIVER project (n=1; KLEINSCHMIDT ET AL. 2022). In this study, we also identified the shortest migration distance (to Sweden) as well as the longest migration distance (far eastern Siberia) towards confirmed breeding grounds. Again, only few short-distance migrants (< 1000 km) were identified, suggesting that birds breeding in (southern) Scandinavia are not using the focal area to a large extent. However, a study by Duckworth et al. (2022) showed that birds breeding in Finland migrated into the North Sea in winter, but geolocator data did not allow exact determination of wintering areas.

We hypothesised that long- and short distance migrants might differ in their use of the focal area due to different energetic needs when preparing for migration. However, due to the small sample size of short-distance migrants (n=2), no detailed comparison with long-distance migrants was possible.

In this study, the German part of the Baltic Sea as well as the western Baltic Sea in general were used only to a low extent, with very few GPS-position in German waters. The eastern Baltic Sea was used more frequently for staging and during autumn moult (especially Bothnian Bay and Bay of Riga). Kleinschmidt et al. (2022) also showed that during autumn/moult, areas in the eastern Baltic Sea (e.g. Bothnian Bay) were used frequently, while during winter, only few individuals used the western Baltic Sea as staging area. Monitoring data from the western Baltic Sea however identified several key areas (MENDEL ET AL. 2008; SKOV ET AL. 2011), although densities are usually much lower as compared to the Eastern German Bight.

Both studies (DIVER and DiverLog) confirmed that, after frequently staging for moult in the eastern Baltic Sea (for Siberian breeders), most individuals moved further west, into the focal area or further on along the southern coast of the North Sea towards UK and France. The staging time in the focal area in autumn and winter varied largely between individuals. For spring staging, no data was available in this study, but previous work suggests that site use within individuals is rather consistent in consecutive years, although the length of stay varied largely between individuals (KLEINSCHMIDT ET AL. 2022).

With the ongoing expansion of OWF developments all across Europe, divers migrating and staging in coastal and offshore waters will be increasingly impacted by OWF developments all along their migration routes. While the main concentration area in the German North Sea is located quite far offshore and overlapping with OWF installations, other key areas for divers in western Europe are located closer to the coast. In the current project, overlaps of diver GPS-fixes and OWF footprints were found mainly for one recently installed OWF (Horns Rev 3 in Denmark) and inside the planned footprints for OWF Versterhav Nord/Syd (before construction) and Dunkerque in France. However, overall the direct overlap was less than 0.5% of all GPS-fixes for planned as well as for operational OWFs. Nevertheless, the potentially large disturbance ranges of OWF installations have to be taken into account. At nearshore locations, disturbance from ship traffic (from nearby harbours, fishing, recreation etc.) might be an important factor, even in the absence of OWF installations. Thus, the cumulative effect of all these anthropogenic pressures as well as possible alterations in prey availability need to be considered when estimating the long-term impacts on this species.

10 USING A DATA-DRIVEN INDIVIDUAL-BASED MODEL TO INVESTIGATE THE EFFECTS OF OFFSHORE WIND FARMS ON THE BODY CONDITION OF RED-THROATED DIVERS

10.1 Introduction

The red-throated diver (*Gavia stellata*) has been found to be particularly sensitive to the presence of offshore wind farms with significant avoidance distances reaching up to about 16 km (DORSCH ET AL. 2019; MENDEL ET AL. 2019; HEINÄNEN ET AL. 2020; GARTHE ET AL. 2023). Red-throated divers are also sensitive to shipping vessel traffic (BURGER ET AL. 2019; FLIESSBACH ET AL. 2019; JARRETT ET AL. 2020), which tends to increase within areas of wind farm development. These effects have raised concern about the consequences of such habitat exclusion on the viability of European red-throated diver populations. OWF developments could possibly displace the wintering population from vital habitats, potentially reducing the physiological condition of individuals and compromising their condition prior to migration as well as their ability to breed and raise offspring. Almost two decades after construction of the first offshore wind farms within the German Bight, in an area known to be of high importance to wintering red-throated divers (BMU 2009; GARTHE ET AL. 2015), it was shown that this development has caused a marked redistribution of wintering red-throated divers in this area (VILELA ET AL. 2021). Whether such a redistribution inflicts fitness effects on the population is still not known. However, spring abundance of divers within the German Bight have fluctuated between years but remained relatively constant over the period 2001 to 2021 and did not decrease when compared to the years before offshore wind farm construction occurred. Although such monitoring data allows the accurate estimation of effect sizes and changes in abundance, the underlying biological mechanisms behind these effects cannot be inferred.

If individual divers staging int the German Bight belong to several different breeding populations, as evidence suggests (DORSCH ET AL. 2019; KLEINSCHMIDT ET AL. 2022; see also Chapter 9), it may take many years for the negative effects on a birds' condition during the non-breeding season to become detectable at the population level. This is because the different breeding populations with their varying migration strategies may be subject to a variety of differing constraints that also vary between years. Furthermore, for a long-lived seabird with a low reproduction rate, such as a red-throated diver, impacts of breeding performance take longer to manifest at the population level than in short-lived species with a high reproductive rate. Monitoring the breeding success of the different populations of red-throated divers wintering in the German Bight is notoriously difficult, however, for various reasons (geographic access, the species extreme sensitivity towards disturbance, etc.). Thus, it is desirable to be able to predict how populations may change due to different stressors, based on the behavioural responses that can be observed.

A tool that is increasingly being used to achieve such simulation is individual-based modelling (IBM). It is meant to provide a link between animal behaviour and population dynamics, in that aspects of the population ecology of species such as population size, migrating systems and the response of populations to ecological change, can directly and realistically be related to behaviour (SUTHERLAND 1997). An IBM is a type of computational model that simulates the behaviour and interactions of many individuals, based on inputs from observed individuals, with the aim to understand how this scales up to patterns at the population level. In cases, such as with the red-throated divers wintering

in the German Bight, where many aspects of a species behaviour and its responses to a particular stressor and the physiological constraints are known, or at least can be derived from theoretical frameworks, IBM can prove to be a powerful tool to predict population level consequences of disturbance (e.g. Speakman et al. 2025). IBMs have been used in the past to predict population level consequences in seabirds such as the common guillemot or northern gannet (WARWICK-EVANS ET AL. 2018; VAN KOOTEN ET AL. 2019) and Duckworth (2023) demonstrated how it may be used for red-throated divers.

IBMs offer conceptual and practical advantages over classical statistical approaches. Conventional regression-based models are typically calibrated within the bounds of observed data and therefore exhibit limited predictive reliability when extrapolated to novel or extreme environmental conditions (OLIVER & ROY 2015; AUSTIN 2007). Extrapolation beyond the calibration domain is associated with increasing uncertainty, particularly when system dynamics are governed by unobserved thresholds, nonlinear responses, or context-dependent interactions (YATES ET AL. 2018). Furthermore, these methods cannot account for individuals' interactions with their environment and with other conspecifics. Such processes are critical for understanding and predicting population-level responses to environmental variability and change, as emergent dynamics often arise from individual-level decisions and interactions (JELTSCH ET AL. 2025). IBMs are specifically designed to address these limitations by mechanistically representing individual organisms and their behavioural rules, physiological constraints, and decision-making processes, thereby allowing population-level patterns to emerge from bottom-up dynamics. When appropriately parameterised and validated, IBMs can explicitly incorporate both direct and indirect interactions among individuals (SUTHERLAND 1997), as well as responses to spatially and temporally heterogeneous environmental conditions, including anthropogenically induced stressors such as offshore wind farms (JELTSCH ET AL. 2025).

Studies using IBMs to understand seabird ecology have mainly investigated breeding individuals/ pairs, which are obligate central place foragers (LANGTON ET AL. 2014; WARWICK-EVANS ET AL. 2018). IBMs for the wintering period use rather simplified assumptions due to the lack of e.g. behavioural data (VAN KOOTEN ET AL. 2019). In this study we investigated divers during spring staging in the North Sea using high-resolution data on movements and behaviour. Like non-breeding vagrants they are free to choose their foraging sites which might result in different movement patterns in contrast to central place foragers. These circumstances may make them less vulnerable towards environmental or anthropogenic impacts such as OWFs, because they may be able to move out of the areas of high impact. Here, the aim was to assess how the presence of OWFs and its known consequences for the birds' behaviour may change an individual's ability to find sufficient food resources for maintaining a sufficiently good body condition, measured as body condition, for subsequent migration and breeding.

It is assumed that the presence of OWFs leads to 1) additional movement when birds have to move between profitable foraging patches (barrier effect) and limits their choice of feeding areas; 2) reduced foraging efficiency if birds are displaced into suboptimal habitats; 3) increased density dependent effects due to evasive movements of prey. These points might ultimately be associated with additional energetic costs for these birds. Estimating the extent of these costs is the focus of this study. In an IBM developed by Duckworth (2023 thesis chapter 7) they investigated such negative effects by assuming i) a reduced foraging efficiency and ii) cost of additional flights. The authors meticulously estimated the associated cost and estimated the effect on the overall energy budget of divers under these circumstances showing that with a given reduction in foraging efficiency

(>50%) the population size may be reduced by 50%. However, in that study the authors assume that foraging efficiency is negatively affected by the presence of OWFs and that divers may compete over these resources. Given that divers show large avoidance distances of OWFs, it seems reasonable to assume a reduction in foraging efficiency, however, the effect size remains unknown. Competition over food resources in wintering divers, however, has not yet been demonstrated. We believe it unlikely that divers, which occur in only low densities (rarely > 5 individuals per km^2), directly decrease prey density by removal of their prey. However, potential evasive behaviour of fish schools under increasing predation pressure, may lead to temporal redistribution in space, reducing local prey density and thereby foraging efficiency. Divers may respond to this change in local prey density by moving to better locations themselves, thereby reducing the negative effect of reduced foraging efficiency. In any case, such predator prey interactions, intra-specific density depended effects and displacement effect of anthropogenic nature, are depending on spatial configurations; in this case how predators and prey are distributed in space relative to the OWFs.

To this end we develop a spatially explicit model in which agents could move freely within a defined focal area of the North Sea meaning they were not constrained to specific locations but could relocate anywhere within that area. By allowing individuals to move within this area, we could determine to what extend negative effects of displacement (directly or via increased density dependent effects) may be compensated by divers redistributing themselves and how likely population viability may be affected due to a possible reduction in body condition. The main focus of the analysis is on a possible difference in body mass between a scenario with the currently present OWFs and a scenario without OWFs. A possible difference in the average body mass at the end of the simulation can then be attributed to the presence of OWF. In addition, we also accounted for differences due to vessel traffic by including or excluding this parameter. To simulate the system as realistically as possible we feed the IBM with data obtained from tracking data (GPS and dive logger) and corresponding energy expenditure calculated in previous chapters.

Tab. 10-1 Table of the different scenarios simulated in this study showing the combination of the effects of offshore wind farms and ship vessel traffic within the focal area used in each scenario.

Scenario	OWF	Vessel traffic
A	✓	✓
B	✗	✓
C	✗	✗

10.2 Methods

This section generally follows the Overview, Design concepts and Details (ODD) protocol established by Grimm et al. (2010) as a framework for objectively describing individual-based models. We adapted the protocol to better match the present IBM.

For improved readability, parameters are written in *italics*.

10.2.1 **Purpose**

The purpose of our IBM is to implement a causal mechanistic model to better understand the potential effects of the presence of OWFs in the North Sea on the viability of diver population overwintering there. Our specific research question is: Does the apparent displacement effect of OWFs on divers have a negative effect on their body mass during the period of their stay in the focal area (see Fig. 4-1). Do the energetic costs of habitat displacement by the current configuration of OWFs in the German Bight have the potential to reduce the fitness of overwintering divers by significantly affecting the individual body mass? To address this question the results of two different models will be compared: scenario A that includes all OWFs currently present within the focal area and scenario B without any OWFs. All other parameters within these two models will be identical, so that any differences in body mass of divers at the end of simulation can thus be regarded as to be caused directly or indirectly by the presence of the OWFs.

However, a significant proportion of shipping traffic in the focal area is attributed to OWF-related maintenance work. Since this vessel traffic is mainly in or near the OWFs themself, the effects of OWFs and shipping traffic on diver distribution cannot easily be disentangled. Unfortunately, it is not possible to differentiate between different types of vessel activity within the data set available to us. Consequently, we decided to run a third model (scenario C) excluding both OWFs and all vessel traffic, being aware that this will also remove effects of vessel traffic unrelated to OWFs. The comparison between the scenarios will allow to deduct that the true influence of OWFs plus the OWF-related vessel activity will be somewhere between the effect-size of the two-by-two comparison of scenario A including OWFs and vessel activity with scenario B including vessel activity only, and the comparison of scenario B (vessel activity only) with scenario C excluding both stressors.

10.2.2 **Basic principles**

The basic principle of the model is that individuals can move and forage freely within a simulated 2-dimensional focal area. This virtual focal area is divided into a matrix of square grid cells each (5 × 5 km) with characteristics based on physical parameters (area, OWF proximity, sea depth) of the real focal area. Relocation of divers was allowed to occur from one grid cell to the next. Individual divers move using either a random walk for local movements or, for longer relocations, an alternative stochastic process described in detail below (see paragraph ‘Movement’). These movements incur energetic costs but enable individuals to reach areas of highest overall suitability, based on the integration of both stressors and attractors. These movements impose energetic costs on individuals but enable them to reach locations of higher “value", determined by a combination of different environmental factors.

The model is parametrized with morphological and behavioural patterns of the simulated individuals which are based on those estimated in the other chapters of this report. Through the implemented decision tree (see below) individuals seek to remain in locations that yield higher payoffs in terms of foraging. Foraging success at a location depends on prey density and on the presence of conspecifics depleting prey within the same grid cell. This causes grid-cell suitability to vary over time. Consequently, individuals continually adjust their location in response to these changing conditions.

10.2.3 **Objectives**

The objectives of the modelling exercise were to assess the impacts of OWF presence on the fitness of individuals of the wintering population of divers in the focal area. Here we used body mass as an indicator for individual fitness, which is quantified as body mass (in grams) at the end of the simulated period. In the first scenario, i.e. including OWFs, we selected parameter values such that, on average, individuals' final body mass would be similar to their starting body mass - thus their body mass remains constant over the period of their stay in the focal area. This was done as we had no previous information on body mass changes over time in the current environment including OWFs. In a second scenario all OWFs were removed and the difference in mean final body mass between the two scenarios was compared. This difference was thought to reflect the effect of the OWFs on body mass of divers. Because substantial variation among individuals arises from stochastic processes within the simulation, we treat the mean final body mass as the primary performance metric.

In addition, following Duckworth et al. (2023) at the end of the simulation we evaluate the proportion of individuals whose body mass fell below a threshold, defined as two-thirds of their initial body mass value (compare also VAN KOOTEN ET AL. 2019; BUCKINGHAM ET AL. 2026). Individuals which fall below this threshold were considered as not being able to maintain a sufficiently good body condition for subsequent migration and breeding. These individuals were not removed from the simulation but included to estimate mean body mass and a general survival rate at the end of the simulation.

10.2.4 **Process overview and scheduling**

Initializing

At the beginning of a simulation run, parameters were set (see list of parameters: Tab. 10-2) and the population created with characteristics as described below. Individuals were randomly assigned starting grid cells within the focal area. To record individual attributes across simulated time steps, a set of data frames—referred to as storages— was created to record individual attributes (e.g., location, energy level) and environmental variables (e.g., prey density, local predation pressure).

Because grid cell suitability varied substantially across the landscape, some individuals required several time steps to relocate to an appropriate position within the focal area. This resulted in elevated movement early in the simulation and, consequently, artificially inflated movement costs. To avoid bias from this initial redistribution phase, we excluded the first *nD_int* days of each simulation as a burn-in period, allowing the model to reach a stable state before data were used for analysis.

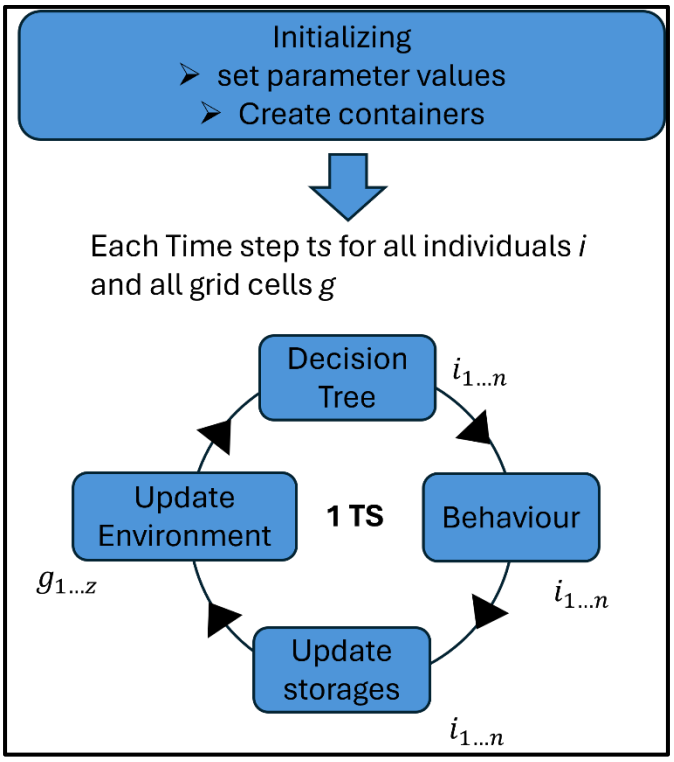

Fig. 10-1 *Process overview. The figure shows the general workflow of the simulation with the first step being the initialization which is executed once per simulation and followed by four steps which are repeated for each time step (TS). During each time step for all individuals ($i_{1...n}$) and each grid cell ($g_{1...z}$) these processes are consecutively executed.*

Tab. 10-2 *Table of parameters which were changed during the tuning of the parameter space. Other parameters which were held constant (e.g. number of time step per hour or basal metabolism rate) are not listed here.*

Parameter	Definition: Function	Value in final model	Unit
N	Number of individuals	500	Integer
nD	Number of Days	28	Integer
sBM	starting average body mass	1700	gram
sBMsd	standard deviation of sBM	200	gram
uBM	upper limit of body mass (4/3 of sBM)	sBM * 4/3	gram
lBM	lowest body mass below which individuals are considered to not be able to survive to reproduction (2/3 of sBM)	sBM * 2/3	gram
E_start	energy level at start of simulation	1700	kJ
E_low	threshold of energy level below which individuals will have to rest	170	kJ
E_max	multiplier of *E_start* giving the upper labile energy beyond which the birds are satiated	1.2	Number
cs	Gives net energy gain from a successful foraging attempt	317	kJ

Parameter	Definition: Function	Value in final model	Unit
cp	'catch probability' making catching more or less likely	0.85	Number (0 - 1)
sat_limit	Satiation limit: threshold upon which the birds are satiated	350	KJ
ppt	Predation pressure tolerance: threshold upon which prey will escape and leave the grid cell for 'ed' time steps	5	integer
ed	escape duration in time steps	36	integer
h_prey_update	defines how often (every x hour) prey density will be 'updated'	6	integer
prey_sd	give the SD of prey density during 'prey_update'	0.1	Number (0 - 1)
sat_check_dur	The number of time steps prior to the current for which catch success is evaluated to simulate digesting duration	12	integer
check_catch_suc	defines how many of the latest predation events where successful in order to decide if birds dive again or moves on	3	integer (1 - 6)
move_check_dur_loc	defines how many steps in the past individuals will check if they done any short flights in that area	66	integer
move_loc_max	Gives the max number of local movements allowed before an individual decides to make a long flight	2	integer
move_check_dur_long	defines for how many steps in the past individuals will check if they done any 'long flight'	12	integer
a	weighting parameter for avoidance effect	1	Number (0 - 1)
b	weighting parameter for bathymetry	1	Number (0 - 1)
p	weighting parameter for prey density	0.3	Number (0 - 1)
v	weighting parameter for vessel traffic	1	Number (0 - 1)

After model initialization, each time step comprised several sequential processes (see Fig. 10-1). In the first step, via the decision tree (see below), the behaviour of all individuals (1…N) was determined. In the second step, these behaviours were executed sequentially for each individual. The order of individuals was randomized at each time step to avoid artefacts arising from sequential updating, such as earlier-processed individuals experiencing density-dependent effects less frequently than those processed later. In the third step, the individual-level storages were updated to record actions taken and current state variables. Finally, environmental storages were updated for each grid cell (1…Z), capturing changes in prey density, predation pressure, diver density, and other relevant conditions.

Decision tree

The decision tree operates through a sequential set of queries that examine both environmental conditions and the individuals' state at the current, and in some cases previous, time steps. The process begins by determining whether it is day or night. If it is night 'night behaviour' is executed as described below. If it is daytime, the model checks the behaviour tracker (i.e., the behaviour storage for the current time step) to see whether a behaviour has already been assigned, for example because a previously initiated behaviour such as flight or diving could extend across multiple time steps.

If no behaviour has yet been assigned, the decision process continues by evaluating the individual's blood energy level i.e. labile energy. If this level is below a defined threshold (*E_low*), the individual rests in an exhausted state for at least one time step. If the energy level is adequate, the model checks whether the individual is satiated; if so, the individual rests in a satiated state. Satiation could be reached either through a 'full stomach', i.e. the individual is still digesting, or reaching the upper limit of the labile energy given by parameter *'E_max'*. If neither condition applies, the individual will proceed with either a dive or a movement.

To determine which of the two actions occurs, the model evaluates the individuals' recent foraging success. Within the past hour, the latest '*check_catch_suc*' dives in the current grid cell are evaluated. If these have been without success (i.e. no fish caught), the individual moves to a different location. If no dives have occurred in this location within the past hour, or if at least one dive has been successful, the individual will dive again in the same grid cell.

If movement is selected, the model next determines whether the individual performs a local movement or a long-distance movement. First, it checks whether a long flight has occurred recently (within '*move_check_dur_long'* time steps). If so, the individual performs a local movement.

If no long flight has occurred within that period, the model evaluates how many local movements the individual has already made at or next to the current location. If the number of local movements exceeds a defined threshold ('*move_loc_max*'), the individual initiates a long-distance movement. If the threshold has not been reached, the individual performs a local movement.

Behaviour execution

After the decision tree loop, the behaviour loop is called in which the behaviour of the divers will be executed. The following behaviours are possible and are described in detail below:

- Rest exhausted
- Rest satiated
- Move local (local movement and escape responses)
- Move long (long flight)
- Dive initial

- Dive continuous
- Night behaviour

Storages update

After the behaviour loop storages are updated (see table Tab. 10-3), the individuals' storages are updated followed by environmental storages.

Tab. 10-3 Storages

Storage	Function	unit
Individuals' storage per time step		
Body mass	Body mass	Gramm *g*
Labile energy	Energy in blood such as sugar or ATP	*kj*
Location log	Location	ID of grid cell (1: 658)
Distance moved	Distance covered by movement	*km*
Behaviour tracker	Keeps track what behaviour was decided on during decision tree	Character string (abbreviations for behaviour categories such as 'dive')
Catch success	Amount of net gain energy obtained due to successful hunting	*kj*
Recent catch success	Accumulating catch success over recent 'sat_check_dur' time steps. If > sat_limit, individual is regarded as satiated	*kj*
Environmental storage per time step		
Predation attempts	Number of foraging attempts for current time step at this location (i.e. grid cell). Sums up how many individuals dived in this gird during this time step.	integer
Recent predation press	Summing up all foraging attempts at this location for the last hour (6 time steps)	integer
Conspecific density	Number of divers per grid cell	integer
Prey density	Prey density per grid cell	Number between 0 and 1

After all storages have been updated the model continues to the next time step until the end of the predetermined duration (number of timesteps).

Entities, state variables and scales

In the model *N* individual divers are simulated for a given number of days *nD*. Each individual has multiple fixed characteristics i) ID, ii) an internal preference for bathymetry and iii) an internal avoidance tendency towards OWFs. The latter two characteristics are based on findings of previous

studies using aerial survey data. In both cases actual preference curves (given by model outputs) for population averages and their variation were taken and used in a sampling process to generate individual preference curves. In the IBM these mean curves were used as the mean from which the sample was taken with a variance matching roughly the observed variance in the data. For bathymetry we used the results provided by Heinänen et al. (2020) (see Fig. 10-2 A).

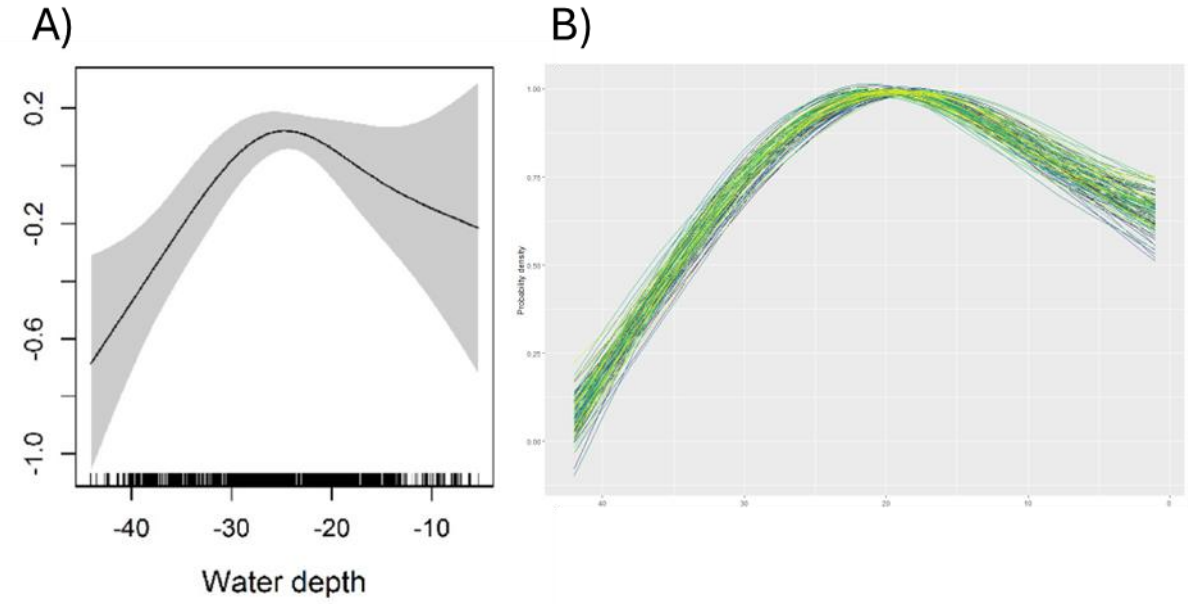

Fig. 10-2 *Water depth preference curves: A) as found in Heinänen 2020 and B) an example of 100 simulated curves based on A). Each line represents an individual preference of one diver in the IBM. Please note that the variance in A) is much larger at the extreme values than in B). This greater variance is due to model uncertainty caused by the small sample size at water depth below -40 and above -10 m.*

Individual avoidance rate values (Fig. 10-3) are based on data from previous work (VILELA ET AL. 2021). Following results from these analyses a maximum negative effect distance of 13 km was implemented in the IBM. We used the population mean avoidance curve and sampled individual avoidance curves with a given variation around that mean to introduce individual variation which roughly represents the variation found in nature. This process resulted in individual avoidance curves which give the reduced propensity to move to a grid cell with a given distance to OWFs (Fig. 10-2). In general, the closer the grid cell is to the OWFs the less likely divers would enter it. Within wind farm the preference was 0.15 % ± 0.1 % (SD). For grid cells adjacent to those containing OWFs the preference was ≤25% from what it is at a distance of > 13km. During parameterization (see below) we compared the diver density within grid cells including OWFs with the density given in reference grid cells to verify that the densities match our expectations. Reference grid cells were selected according to two criteria: (i) cells had to be located beyond the disturbance distance defined by the mean avoidance curve (maximum effect distance: 13 km; Fig. 10-3); and (ii) cells could not exceed a distance of 30 km from the OWFs to reduce potential spatial confounding effects (e.g. bathymetric gradients). Accordingly, all reference cells were situated between 13 and 30 km from the OWFs (Fig. 10-4). In total, 52 grid cells overlapped with the OWFs, and 282 grid cells were used as reference cells.

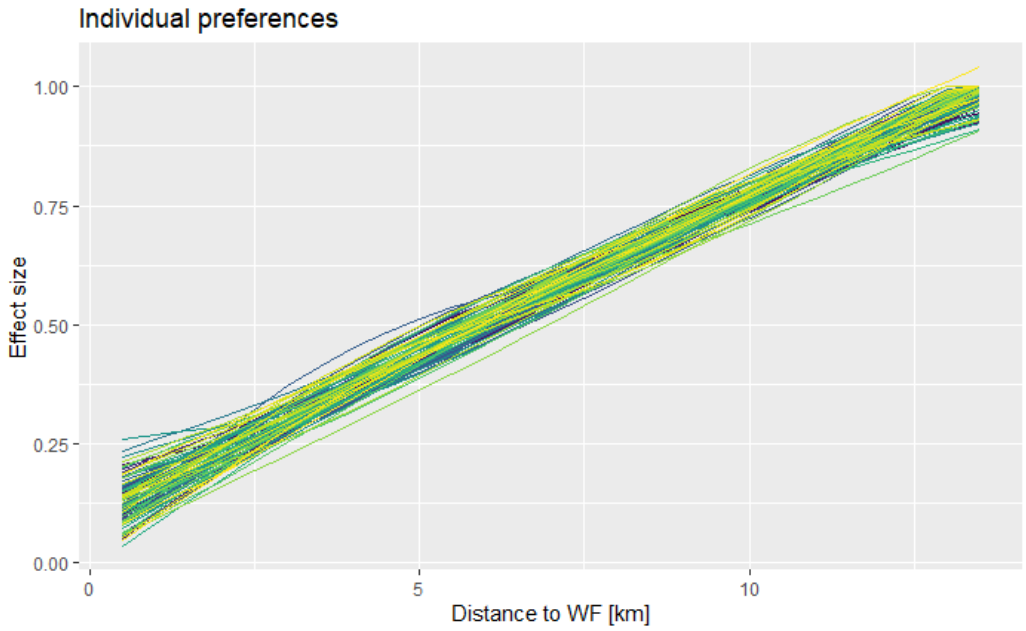

Fig. 10-3 *Avoidance curves: each line represents an individual avoidance curve. The y-axis represents the reduction in the tendency to move toward a location, as a function of the distance from an OWFs shown on the x-axis: the closer the location is to the OWFs the less likely divers would move there. Next to OWF the preference was <= 25% from what it is at a distance of > 13km. Within wind farm the preference was 0.15 % ±0.1 % (SD).*

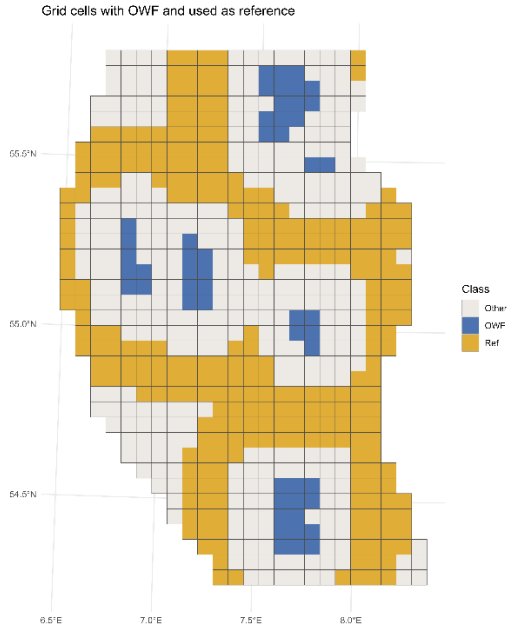

Fig. 10-4 *Grid cells used for comparison of diver 'densities within grid cells including OWFs (in blue) and reference cells (in ochre). Other grid cells (in grey) were either too close or too far away from OWFs to be used as reference.*

The fourth characteristic assigned to each individual within the IBM was preference for dive duration, derived from a normal distribution with a mean of 4 min. and SD of 2 min. To ensure positive values the minimum was set to 2 min. These values were taken from dive logger data (see chapter 5) and represents the summed duration of dives within bouts rather than single dives.

Furthermore, individuals within the IBM were assigned the following two starting characteristics, which were identical or similar in all individuals: 1) starting body mass: random value drawn from normal distribution with mean of *sBM* and SD of *sBMsd* and 2) starting labile energy: 1700kj.

At the beginning of the simulation divers were randomly assigned a location (i.e., a grid cell) within the focal area.

Movement:

General idea: Most of the time divers move only passively on the water surface. In the IBM we assume that if divers actively move, it is mainly for foraging reasons. In particular, we assume that they move away from their current position after a number of unsuccessful dives (given by parameter `*check_catch_suc*´) within the last hour. They can either make a local movement, basically towards one of the adjacent grid cells, or make a long movement. For the latter the distance is given from a (Weibüll-) distribution (with shape = 2 and scale = 20000) that is set to give a close match to results from the tracking data analysed in chapter 6.

Whether a diver performs a local or a long movement depends on its recent movement history, defined by the parameters *move_check_dur_loc* and *move_check_dur_long*. If an individual exceeds the threshold *move_loc_max* for local movements within the respective evaluation period, it will switch to a long movement. This mechanism reflects the assumption that a bird repeatedly searching (i.e., diving) unsuccessfully for prey within a location and its surroundings, will relocate to a more distant area where prey density—and thus hunting success—may be higher.

However, tracking data indicate that divers seldom perform multiple long flights consecutively (unpublished data). To reflect this behaviour, the IBM prevents an individual from undertaking another long movement if it has already performed one within the past *move_check_dur_long* time steps. In such cases, the diver will make a local movement regardless of how many local movements it has recently executed in that area.

The only other reason for active movement unrelated to foraging occurred when divers drifted into the area of an OWF during the night (see below).

Random walk:

If the decision tree determines that an individual should move, the movement function is executed. This function assesses whether movement will occur and, if so, identifies the destination grid cell. Local movements are modelled using a random-walk algorithm that incorporates the basic

principles of the Metropolis algorithm (METROPOLIS ET AL. 1953), as commonly applied in simulation studies (CODLING ET AL. 2008). This approach ensures that individuals relocate to neighbouring cells with probabilities proportional to each cell's value, while still retaining the ability to explore all locations within the spatial domain, including those with comparatively lower value.

In our implementation, one candidate grid cell is randomly selected from the set of cells adjacent to the individual's current cell. If the value of the candidate cell exceeds that of the current cell, the individual will move to the candidate cell. If the candidate cell has a lower value, the individual will move there only with a probability equal to the ratio of the candidate cell's value to the current cell's value. Consequently, the lower the candidate cell's value relative to the current location, the less likely the individual is to move into it. Over time, this mechanism results in grid cell occupancy patterns that reflect their value.

During `long´ movements two processes are executed. First, as described above, a new destination within the focal area is selected by drawing a movement distance from a Weibull distribution and assigning a random direction from the individual's current position. After determining this destination point, the grid cell containing the point, along with its neighbouring cells, is treated as the set of potential candidate cells. From this set, the cell with the highest value is selected as the movement target (prey density is not considered at this stage; see below). We adopted this approach to ensure that, once the decision tree has determined that the diver initiates a long movement—i.e., begins a long flight—it will reliably relocate to a new location regardless of the relative values of the candidate cells.

During the night, divers rest; however, they are passively displaced by water currents and therefore drift to new locations. Vindenes et al. (2018) measured substantial variation in tidal currents in the North Sea but reported a mean current speed of 0.3 m s^{-1}, which corresponds to an average drift distance of approximately 12960 m over a 12-hour night—the value used in our model. Drift distance was generated by drawing a random number from a normal distribution with this mean and a standard deviation of 1296 m. The resulting distance was applied to move the individual, with drift direction randomly sampled from angles between 90°–180° or 275°–360°, producing a general NEE to SWW displacement pattern.

If the resulting location fell outside the focal area, the individual was reassigned to one of the nine grid cells (and therefore within the focal area) closest to the projected position.

If the drifted location fell within a wind farm, the diver initiated an escape response at the start of the following morning. In this case, the individual randomly selected one of the nine nearest grid cells located outside the wind farm but still within the focal area and moved there immediately.

Grid cell values:

The value of each grid cell was determined by multiple static environmental factors (Fig. 10-5). To facilitate handling within the IBM and to improve comparability among factors, all natural environmental variables were normalized to a range between 0 and 1, with 1 representing the highest suitability for divers and 0 providing no contribution to habitat value. Anthropogenic stressors, like presence of OWF and vessel traffic, were also normalised between 0 and 1 but used to multiply the

grid cell values. Consequently, when these factors had a value of 1 the grid cells' value did not change. The smaller these factors became, the stronger the resulting negative effects were, leading to a greater reduction in the grid cell value. During movement, divers 'inspected' neighbouring grid cells using the random-walk procedure (see paragraph 'movement'). For each inspected cell, a composite value was calculated as the sum of the normalized values of all habitat quality factors (Bathymetry and prey density) multiplied by the 'stressor' avoidance and vessel traffic. To ensure that no grid cell would have a value of zero a minimum of 0.05 was introduced for the vessel traffic value. To allow adjustment of the relative importance of these factors, each one could be weighted by a parameter (*a*, *b*, *p and v*), enabling flexible tuning of their influence in the value calculation.

$$grid\ cell_i =$$

(bathymetry_preference*b + prey-density*p) * ((1 - a) + a *avoidance_preference) * ((1 – v) + v * vessel traffic)

Although vessel traffic is inherently dynamic, we simplified this component by averaging data across the study period (see chapter 7). Data on ship presence were downloaded from Global Fishing Watch (https://globalfishingwatch.org/map; accessed September 13, 2024). The data is based on AIS and the spatial resolution of the layer is 0.01° (~1.1 km) and temporal resolution daily. Ship presence was further analyzed using the "Optimized Hot Spot Analysis" tool in ArcGIS Pro (https://pro.arcgis.com/en/pro-app/latest/tool-reference/spatial-statistics/how-optimized-hot-spot-analysis-works.htm). The hot spot analysis is based on Getis-Ord Gi* statistics, a high positive value of the resulting Z-score indicates a hot spot for ship activity, and a high negative score indicates a cold spot.

Please note, in order to consider natural variation in avoidance behaviour towards OWFs and preference of bathymetry, individual differences in these factors were implemented in the model.

In addition to the static environmental factors, prey density was implemented as a dynamic variable. At regular intervals of '*h_prey_update'* time steps, prey density in each grid cell was updated based on the cell's bathymetry-derived preference value. Cells with higher preference values exhibited higher expected prey densities. Specifically, prey density was drawn from a normal distribution with a mean equal to the cell's bathymetry preference value and a standard deviation defined by the parameter *prey_sd*. This procedure introduced temporal variability around the cell-specific mean, ensuring that a given cell was not consistently higher or lower in prey density than its neighbours.

This temporal variation is intended to capture, at a coarse scale, the natural fluctuations in prey availability observed in the North Sea. Moreover, incorporating dynamic variation in cell values is important in spatially explicit modelling, because in the absence of such variability, individuals would tent to stay in a local optimum.

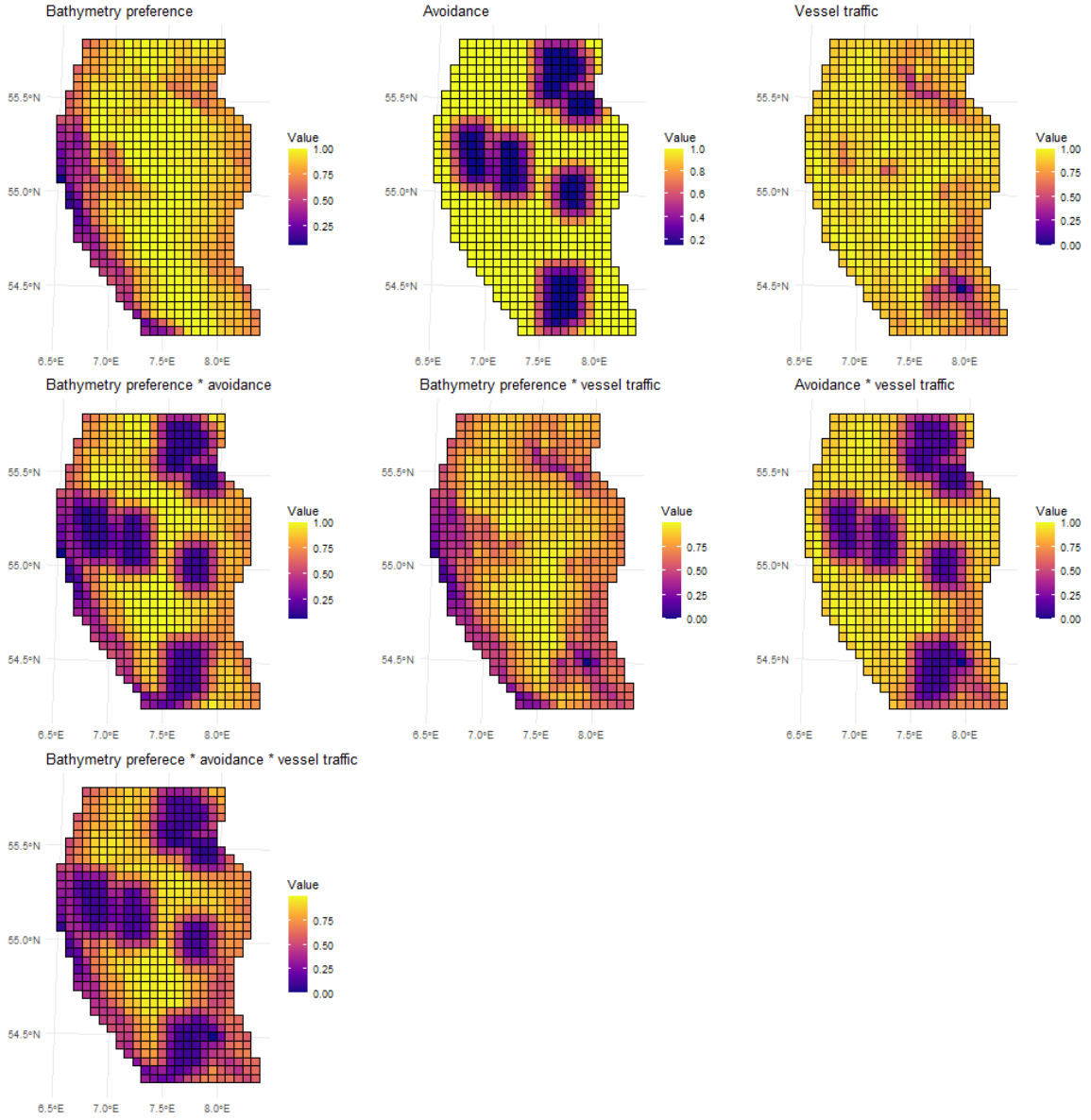

Fig. 10-5 *Value of grid cells for single environmental factors (top row), combined values for factors (middle row) and for all three factors combined (bottom row). Please note that here mean values are given, however, for bathymetry and avoidance individual differences are implemented in the model.*

Distances in the IBM are expressed on a metric scale, i.e. in metres or kilometres. Grid cells have a side length of 5 × 5 km. Due to computational constraints, a finer spatial resolution was not feasible. Because individuals were always positioned at the centre of a grid cell, they needed to move more than half the cell's side length to enter an adjacent cell. Consequently, movements of less than 2.5 km were not detectable when plotting diver tracks. Movement costs, however, were assigned per time step in which movement occurred, irrespective of whether the individual crossed into a new grid cell or moved within the same cell.

Time in the IBM is represented in discrete 10-minute intervals, each corresponding to one time step. Any durations specified in other units (e.g. minutes or hours) were converted into 10-minute

equivalents. Only daytime was subdivided into discrete time steps, with daylength fixed at 12 hours, resulting in 72 time steps per day. Nighttime was modelled as a single time step, reflecting the assumption that divers rest during this period.

Diving and predation

During the day, if divers are neither resting due to saturation or exhaustion nor engaged in movement behaviour, they dive to obtain energy by catching fish. Dive duration (in minutes) is drawn from a normal distribution with a mean determined by the individual's internal preference (Dive_dur; see above) and a standard deviation of 1 minutes. This duration is then converted into 10-minute time steps, which defines the number of time steps allocated to the current dive bout.

In nature, dive bouts consist of multiple dives of varying duration and depth (see chapter 5). In the IBM, we simulate diving at coarser level only, with dive durations ranging from a minimum of 10 min. to a maximum of 40 min. The energetic cost of diving is set at 24 kJ per time step (i.e. per 10-minute interval), consistent with values presented in chapter 5.

We do not model the number of fish caught explicitly; instead, energy gain is represented as a single value, defined by the parameter *cs*, which specifies the energetic reward (in kJ) received if a dive is successful. Success depends on prey density and the catch-probability parameter (*cp*).

Prey density within each grid cell is determined by bathymetry. Specifically, based on the bathymetry preference curve reported by Heinänen et al. (2020), prey density is highest in grid cells with water depths corresponding to the species' optimal range (approximately 23–25 m). This reflects the assumption—supported by other studies (e.g. HEINÄNEN ET AL. 2020)—that bathymetry serves as a proxy for habitat quality for divers. For each grid cell, prey density is drawn from a normal distribution with a mean equal to its normalized bathymetry preference value (ranging from 0 to 1) and a standard deviation determined by the parameter *prey_sd*. Prey density is updated every *h_prey_update* time steps to introduce temporal variability in resource availability.

To account for the high mobility of prey—divers predominantly feed on small, agile fish—we assume that prey species temporarily vacate a grid cell when predation pressure exceeds a threshold. This threshold is governed by the parameter *ppt* (predation pressure threshold), which specifies the number of predation attempts by divers on prey species occurring within a one-hour period, irrespective of whether the attempts involve one or multiple individuals or whether they are successful. If predation attempts exceed *ppt*, prey are assumed to have dispersed from grid cell and prey density in that cell is set to zero for *ed* time steps, rendering the cell temporarily prey-depleted. Divers cannot detect this depletion directly; instead, they experience reduced foraging success when diving in these affected cells. During the night, prey density in all grid cells is reset based on the bathymetry preference curve, such that at the start of each morning prey distribution again reflects habitat suitability.

It is important to note that this mechanism introduces intraspecific negative density dependence: the more individuals forage within the same grid cell, the more likely predation pressure will exceed the threshold, temporarily reduce prey density and thereby lowering catch success for all

individuals using that cell. The strength of this density dependence is controlled by the parameter *ppt* in relation to number of individuals simulated (*N*).

Labile energy and body mass

Within our model, we distinguish between two forms of energy storage. The first represents the readily available metabolic energy (e.g. ATP or blood glucose), measured in kilojoules, which supports the individual's immediate energetic demands. We refer to this storage as the '*labile energy'*. Each diver starts the simulation with an initial amount of energy (*E_start*). All behaviours incur energetic costs per time step (see Tab. 10-2), which are directly deducted from this storage. When the labile energy falls below a threshold (*E_low*), individuals are considered *exhausted* and must rest.

While resting in an exhausted state, individuals replenish their labile energy from a second storage compartment representing body fat reserves, referred to as '*body mass'* and measured in grams of fat (g). We assume an effective energy density of 33 kJ per gram of body fat tissue, which accounts for its non-lipid components (e.g. water and structural material). During metabolic conversion of fat to readily usable energy, we assume a 5% loss, such that 1 g of fat yields 31.65 kJ of metabolically available energy.

During each resting time step, exhausted individuals gain kilojoule twelve times the amount of basal metabolism rate (BMR), reflecting that the most energetically demanding behaviour in the model—flight—costs 12 times the BMR. For example, if divers rest five time steps, they regain sufficient energy to fly for five time steps afterwards.

For simplicity, divers may initiate a long flight whenever their current labile energy is sufficient to sustain one time step of flight, even though long flights typically last multiple time steps and therefore may require more energy than presently stored. As a consequence, individuals may become exhausted immediately after completing a long flight and must rest to rebuild their labile energy. In nature, some bird species are able to convert fat to ATP during flight (SCOTT ET AL. 1994), suggesting that real divers may experience shorter post-flight exhaustion periods or even none at all. Nevertheless, long flights are rare both in nature and in our simulation, and divers spend most of the day resting; therefore, any slight mismatch between natural physiology and our simplified post-flight recovery dynamics is expected to have negligible influence on overall model outcomes.

Divers obtain energy through successful foraging events (i.e. successful dives; see paragraph "Diving" above). Following a successful capture, individuals are assumed to digest the prey over a defined number of time steps (*sat_check_dur*) (compare LANGTON ET AL. 2014). The full energy content of the prey (*cs*) is added immediately to the individual's labile energy.

At the end of each day, if the current labile energy exceeds the starting energy level (*E_start*), the surplus is converted into body fat (in grams) and added to the individual's body mass. Conversely, if the labile energy at day's end is below *E_start*, the deficit is replenished by drawing energy from the body mass, following the same conversion rules applied when exhausted individuals rest.

Tab. 10-4 Energetic cost per behavioural category

Behaviour category	Energy demand per hour as found in chapter 6 for average sized bird (1.761 kg) given in *kj*	Energy per 10min interval in IBM	Explanation
BMR	28.33	4.72	Basal metabolism rate; assumed for energy expenditure during night where divers rest inactively in the model
Active on water	66.01	11	"resting" during daytime including preening, short movements and resting. It is an average for when neither diving for flying
Diving	144.48	24	One average value for diving independent of water depth and temperature
Flying	354.13	59	Average energy demand for flight, aggregated across all flight phases.

Night behaviour

During the night, individuals were subject to passive drift as described earlier (see Movement). After drift, energy exchange between the labile energy ('blood energy') and body fat reserves was conducted according to the rules outlined above (see Labile energy and body mass).

At the first time step following night, the model checked whether any individuals had drifted into an OWF. Those that had entered an OWF initiated an escape response. A random cell from the nearest nine grid cell outside the OWF was chosen as the new location. This reflects the assumption that, during an escape response, individuals prioritise rapid avoidance of stressors over habitat selection based on other environmental factors.

Emergence

The decision rules when and where to go and when to dive or rest are implemented in a way that the overall probability of these behaviours are emerging from environmental circumstances. While the duration of single dives and the distance of single local or large movements are given by the distribution as found from the tracking data, the sum of dives and their summed duration as well as the frequency and distance moved within one iteration is an emerging property of the model rather than predetermined values. In principle, parameter settings could be tuned so that individuals dive or move almost constantly or, conversely, hardly at all.

We selected parameter values that yielded overall behavioural budgets consistent with those observed in the tracking data (see chapter 6), under current environmental conditions, including the presence of OWFs. While the energetic expenditure per behavioural category per unit time is based

on empirical data, the total energy expenditure depends on the duration of each behaviour and is therefore also an emergent property of the model.

The spatial distribution of divers within the focal area also emerges from environmental conditions and is not predetermined. Although the value of each grid cell changes over time due to fluctuations in prey density, the long-term distribution of divers is expected to reflect the underlying spatial pattern of grid-cell value.

It should be noted that the weighting of individual environmental characteristics that determine each grid cell's value can be adjusted through model parameters (namely *a*, *b*, *p, v*). This enables the landscape value to vary between scenarios and consequently influences the resulting distribution of divers.

Adaptation

There are no evolving adaptive traits in the model. The model simulates only a restricted duration during spring staging time. No reproduction is implemented. However, as described above, individuals are able to adapt their behaviour to environmental conditions by i) perceiving predation success which depends on prey density and ii) evaluate gird cell values integrating stressors (distance to OWF and fishing effort) and attractors (bathymetry as proxy for habitat quality and prey density). We assume that divers can perceive external cues that act as proxies for prey density, such as the presence of other piscivorous seabirds, chlorophyll concentrations, or other indicators of frontal zones, all of which are associated with elevated prey availability. We treated prey density as an imperfect and variable predictor of habitat suitability. Accordingly, we set the parameter p=0.3, such that prey density contributed only 30% of its maximum influence on the overall grid-cell suitability during movement. This weighting reflects the assumption that prey density is less accurate and less temporally stable than the other environmental predictors considered.

Learning

As described above, divers can assess how much they have dived during the previous hour and how many of those dives were successful. This mechanism is intended to mimic learning from recent experience.

Divers also register the extent of their recent local movements and whether they have undertaken any long flights. While the first mechanism represents a form of learning or short-term memory, the latter is not intended to mimic learning. Instead, it reflects a physiological state that captures the species' apparent inherent reluctance to engage frequently in long-distance flights.

Prediction

Divers cannot predict future environmental conditions.

Sensing

Divers can perceive the distance to the OWFs, the local fishing effort, the bathymetry of the area and prey density, with the latter two serving as a proxy for habitat quality.

Interaction

Intraspecific interactions occur indirectly, as described above, through the temporary displacement of prey from a grid cell when local predation pressure exceeds a defined threshold. This reduction in prey density affects all individuals currently within that cell, as well as those entering it during the period in which the prey has abandoned the area.

Observation

We recorded all behaviour executed of all individuals per time step. Each physiological parameter of individuals (e.g. body mass or saturation) is noted throughout the simulation as well as all changes in the environmental parameters subject to temporal changes.

Parameterisation

During parameterisation, we systematically adjusted model parameters and evaluated their effects across multiple performance metrics. The overarching objective was to ensure that the simulated individuals' time budgets, movement patterns, and spatial distributions matched as close as possible those observed in natural populations. To identify an appropriate parameter space, we combined systematic variation of individual parameters with logical and causal inference regarding their direct and indirect effects, informed by our understanding of the model's internal mechanisms.

For some parameters, the expected effects were straightforward. For example, increasing the energetic gain of a successful dive beyond the saturation threshold inevitably reduced the number of dives, as a single dive bout became sufficient to satiate an individual. Reduced diving activity consequently led to increased resting time and decreased movement. In contrast, the effects of increased density-dependent predator–prey interactions on movement patterns and spatial distributions were less intuitive. In such cases, parameters were varied systematically over a wide range to explore their effects, whereas for more predictable parameters it was possible to constrain suitable values more narrowly.

Parameter interactions substantially increased the complexity and duration of the parameterisation process. For instance, increasing the saturation limit allowed for higher energetic gains per successful dive, which in turn increased the overall body mass of the diver population.

As stated above, the final parameter set was selected based on the closest simultaneous agreement with empirical observations of diver energetics, time budgets, movement patterns, and spatial distributions. Because these aspects of diver behaviour and physiology were well documented in this project, we are confident that all remaining parameters fall within biologically realistic ranges. For example, unrealistically high energetic gains per dive bout would result in excessive resting behaviour, whereas unrealistically low gains would require simulated divers to dive far more frequently than observed in tracking data.

10.2.5 Validation

We validated the model using multiple complementary approaches.

First, we assessed whether the simulated spatial distribution of divers matched theoretical expectations. This was done by visually inspecting density maps of simulated diver locations and comparing them with the theoretically expected spatial pattern derived from grid values based on aggregated environmental predictors, namely distance to OWFs, bathymetry, and fishing effort (see Fig. 10-5).

Second, we compared the simulated distribution with empirical distributions reported in studies based on count data of actual divers in the focal area (Vilela et al. 2021, Scott-Hayward et al. 2024). These empirical distributions closely match the theoretically expected pattern described above. However, natural variability—both between years and between days—is better captured and evaluated using count-based data.

Third, we compared movement and activity metrics derived from tracking data with those generated by the simulations. Specifically, we evaluated the mean and distribution of daily movement distances and the proportion of available daytime spent moving. In addition, we compared time spent diving and the number of dives per day. These comparisons were conducted both at the population level (mean values) and with respect to between-individual variability.

Fourth, we evaluated movement patterns by visually comparing simulated movement tracks with empirical tracks obtained from tagged divers in the focal area.

Finally, we examined the temporal dynamics of all stored state variables (Tab. 10-3) to ensure that the simulated sequences were biologically plausible. For example, even if the mean daily diving time of an individual matched the population mean, a strongly skewed temporal pattern—such as diving occurring predominantly during the first half of the simulation but largely ceasing thereafter—would not be realistic. Tracking individuals' step by step throughout the simulation allowed us to verify that the underlying mechanisms operated as intended and produced coherent behavioural trajectories.

Due to the high number of parameters used in this model a rigorous global sensitivity analysis as introduced by Sobol (2001) was not feasible. We therefore identify influential parameters by individually changing parameters values and inspected by how much this increment would change mean and variance (compare Morris 'Elementary Effects' method; MORRIS 1991) of following outputs:

1. the mean body mass and the percent of individuals staying above lower body mass
2. mean of distance moved per day
3. percent of time spent flying during daytime
4. percent of time spent diving during daytime

We focused on parameter where we did not have strong indication of the parameter value from real world data as found in chapter 6, e.g. step length of flight, or body mass. We used a biological

sensible parameter variation for investigating the effect size of candidate parameters. For example, the parameter *cs* stands for energy gained from successful feeding. Logically it was always positive, and we set an upper limit during sensibility analysis to about double the DEE of an average bird. We deemed it highly unlikely that birds can regularly catch enough fish within 10 min to sustain the birds for two complete days. As seen from the dive data, normally divers dive multiple times per day.

Since the simulations are subject to stochasticity we run multiple iterations. During the exploration phase, i.e. fine tuning of parameter space, we used 3 to 5 iterations and inspected the variance between iterations. With the final parameter setting we run 10 iterations and estimated mean and variance over the set of iterations. This ensured that we covered the whole variation in the data caused by random starting conditions (such as location of individuals or their individualized avoidance rate and preference for bathymetry values).

The final model used to compare the two scenarios (i.e. with and without OWF) was run with 500 individuals and for 28 days (with additional four days burn-in time).

Estimating the exact number of individuals present in the focal area for a period of four weeks during spring is virtually impossible, as there are currently no methods available to distinguish individuals at that spatial and temporal scale. Although the total population size may remain relatively constant around a given value (e.g. ~5,000 individuals), we cannot reliably quantify the turnover of individuals entering and leaving the area during specific periods.

Due to computational constraints, we were unable to simulate more than 500 individuals per scenario, which is clearly below the expected natural population size in the focal area. However, the use of so-called *super-individuals* (SCHEFFER ET AL. 1995), a common practice in individual-based modelling (STILLMAN 2008; BUCKINGHAM ET AL. 2026), allows each simulated individual to represent multiple individuals in nature. In the present study, one simulated individual might for example represent 10–20 natural individuals, resulting in an effective population size of approximately 5,000–10,000 individuals, which is a plausible approximation of natural population sizes during the study period.

Density dependence in the model was explicitly controlled by the parameter *ppt*, which defines the tolerance of prey to predation pressure within a grid cell. When this threshold is exceeded, prey temporarily leave the cell; therefore, tuning *ppt* allows population-size effects to be adjusted independently of the number of simulated individuals. Consequently, patterns observed at a given population size (e.g. $N = 250$) would be expected to occur under increased population sizes when using the same parameterisation, provided *ppt* is scaled accordingly. It should be noted that density dependence scaled only approximately linearly with *ppt*. Therefore, doubling the number of individuals would yield comparable results with a *ppt* value slightly lower than twice the original setting.

10.3 Results

No single ppt parameter value yielded the best performance across all main calibration metrics of the IBM, including body mass, time spent diving or flying, daily distance moved, spatial density distribution, and ethograms. Overall, the best resemblance to tracking data was observed for ppt values between 5 and 7.

Spatial distributions, tracks, and ethograms were assessed visually. For all three ppt values, which regulates the negative density dependency, the spatial distribution corresponded well with expectations (see Fig. 10-6). Individual tracks and ethograms reproduced the generally similar patterns as those of tracking data, although at a coarser temporal and spatial resolution (see Fig. 10-7; Fig. A 8).

The remaining four metrics (mean body mass, proportion of daytime spent diving, proportion of daytime spent flying and distance travelled per day) were evaluated quantitatively by calculating the percentage deviation of the IBM outputs from the expected values derived from the tracking data (see Tab. 10-5). Based on the sum of those differences, the best agreement between the IBM outputs and the tracking data was obtained for a ppt value of 5. Accordingly, this setting was used to compare scenarios with and without the presence of offshore wind farms (OWFs) to infer possible effects on the diver population.

In scenario A, which included the effects of both OWFs and vessel traffic, the mean daily distance moved was 39.77 km [95% CI: 39.28, 40.25], mean time spent diving was 15.88% [95% CI: 15.75, 16.01], and mean time spent flying was 2.08% [95% CI: 2.03, 2.13]. The mean body mass at the end of the 28-day simulation period was 1689.7 g [95% CI: 1683.84, 1695.56] and therefore close to the assumed initial body mass of 1700 g.

In scenario B, without OWFs but with effect of vessel traffic, the mean daily distance moved was 36.56 km [95% CI: 36.29, 36.82], mean time spent diving was 15.29 % [95% CI: 15.23, 15.36], and mean time spent flying was 1.72% [95% CI: 1.69, 1.75]. The mean body mass after 28 days was 1720.67 g [95% CI: 1713.24, 1728.10] and therefore slightly above the assumed initial body mass of 1700 g.

A direct comparison of the mean body mass found in of scenario A and B (1689.7 g versus 1720.67 g) showed that the body mass was 1.8% higher in the scenario B, i.e. the scenario without OWFs. The non-overlapping confidence intervals indicate that this difference is significant. In contrast, no significant difference was observed in the proportion of individuals staying above a critical body mass, i.e. a body mass greater than or equal to two thirds of their initial body mass, after 28 days. Although this proportion was slightly higher in the scenario without OWFs (99.18% [95% CI: 98.8, 99.56]) than in the scenario with OWFs (98.90% [95% CI: 98.6, 99.2]), the overlapping confidence intervals, indicate a non-significant difference.

In scenario C, wherein both anthropogenic stressors, i.e. OWF and vessel traffic effects, were excluded, the overall picture was similar to scenario B. For most metrics considered, the difference between these two scenarios were not significant.

Only a slight but statistically significant reduction in time spent flying was observed between scenarios C and B, with divers flying less when vessel traffic was excluded (1.72% [95% CI: 1.69–1.75]

versus 1.64% [95% CI: 1.59–1.68]). However, the confidence intervals were nearly overlapping, suggesting that minor changes in parameter settings could render this difference non-significant.

The comparison with Scenario A (including OWFs) showed qualitatively similar results across all ppt values. Notably, however, the confidence intervals for the percentage of the population remaining above the lower body mass threshold showed only minimal overlap (0.006%) between Scenario A (98.90% [95% CI: 98.59–99.20]) and Scenario C (99.40% [95% CI: 99.19–99.60]) at a ppt value of 5—the value that produced the best overall model fit. This minimal overlap indicates that even small adjustments in parameter settings could result in a statistically significant difference in this metric, implying that population-level effects in natural systems should not be dismissed a priori. This is corroborated by the finding that, at a ppt value of 4, the proportion of individuals exceeding this threshold is significantly greater in scenario C compared to scenario B, and significantly greater in scenario B compared to scenario A (Tab. A 5).

Tab. 10-5 *The table presents the (mean) results for four calibration metrics of the IBM evaluated at three different ppt values. The sum of differences represents the aggregated deviation between the model results and the target values for each metric. Lower values indicate a better agreement between the IBM and the tracking study data.*

Metric	IBM result	Aim (based on tracking data)	|% Diff|	Sum of Differences
ppt 5				
Body mass	1689.702	1700	0.61	98.12
% Time diving	15.88	9.4	68.94	
% Time flying	2.08	2.6	20.00	
Distance per day	39.77	43.5	8.58	
ppt 6				
Body mass	1721.39	1700	1.26	111.24
% Time diving	14.94	9.4	58.94	
% Time flying	1.72	2.6	33.85	
Distance per day	36.018	43.5	17.20	
ppt 7				
Body mass	1774.06	1700	4.36	135.72
% Time diving	13.44	9.4	42.98	
% Time flying	1.12	2.6	56.92	
Distance per day	29.814	43.5	31.46	

When observing plots of the spatial distribution within the focal area it becomes obvious that in both scenarios (A and B) divers distribute evenly under higher intra-specific competition. Notably, in the scenario including OWFs this includes the area of the wind farms (Fig. 10-6).

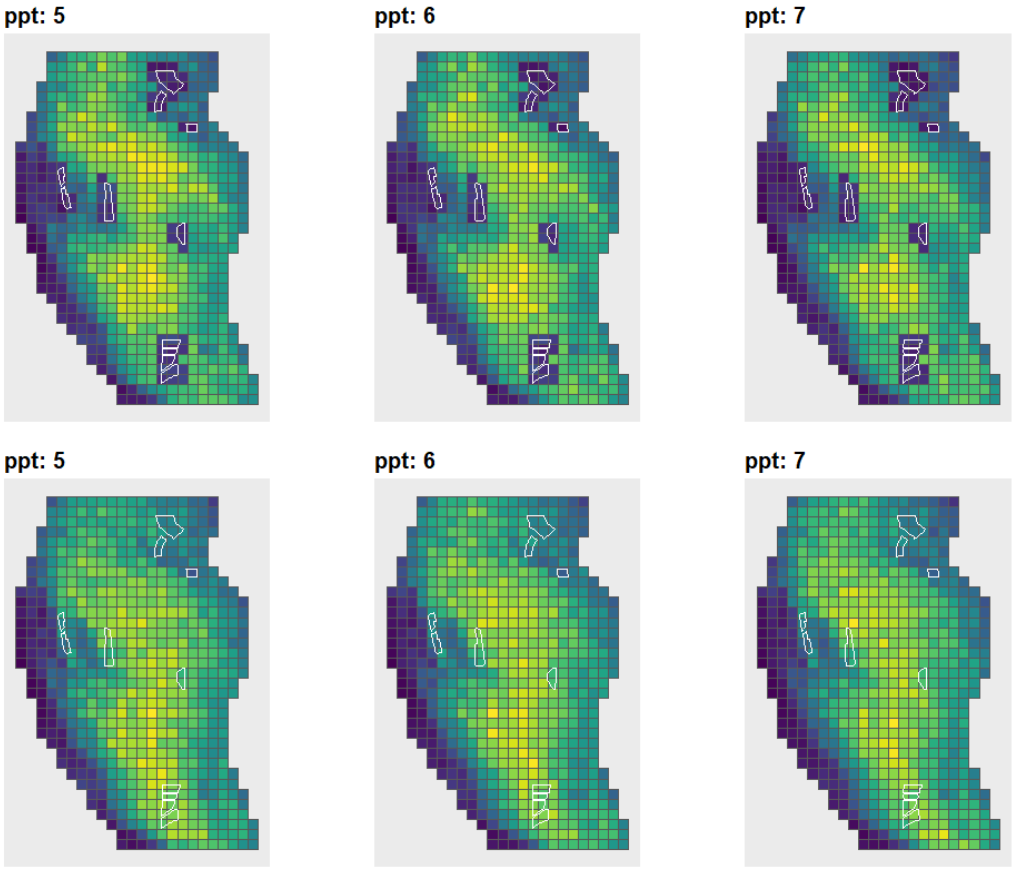

Fig. 10-6 *Spatial density of divers per 5 × 5 km grid cell in the focal area after 28 days of simulation with different ppt values (5 - 7). Density increases from dark to brighter colours. White polygons denote installed offshore wind farms (OWFs). Upper row shows the density of divers after simulation including avoidance behaviour in response to OWFs in combination with vessel traffic (scenario A). Lower row shows simulation without avoidance behaviour (scenario B); OWF boundaries are shown for visual comparability only. Note that while direct comparisons between model scenarios are valid, quantitative comparisons between simulated densities and naturally occurring densities are not possible because the model uses super-individuals, each representing multiple divers. However, a qualitative comparison of spatial distribution is valid.*

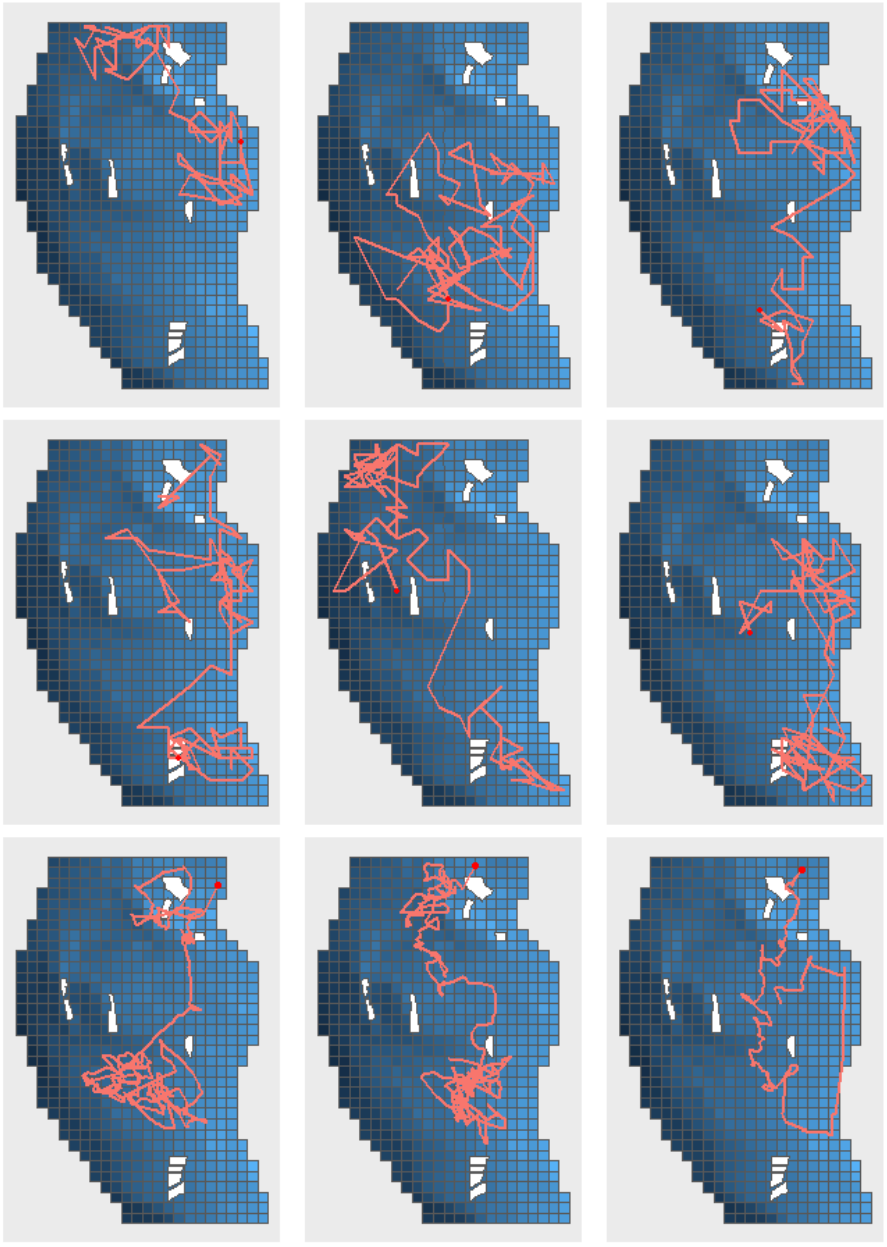

Fig. 10-7 *Simulated tracks are shown in the top two rows, and three tracks from tagged divers are shown for comparison in the bottom row. The top two rows present six randomly selected simulated individual tracks over the 28-day simulation period. Because individuals were assigned to grid-cell centres, only movements between grid cells are displayed. Movements within grid cells are not shown, but they were included in the calculation of individual movement distances. The bottom row shows three tracks from tagged divers that remained in the focal area for longer periods (31, 27, and 12 days, respectively). White polygons indicate installed offshore wind farms (OWFs).*

10.4 Discussion

We created one of the first mechanistic IBMs for a seabird species outside the breeding season, examining the mechanism by which OWFs may influence body condition, with implications for the long-term viability of the population. Parameterisation of the model with the currently most detailed behavioural dataset available for red-throated divers during the non-breeding season allowed us to closely mimic the natural patterns and identify important drivers through which displacement from OWFs could translate into negative fitness effects.

The results of the IBM indicate that the presence of OWFs has a slight negative effect on the mean body mass of simulated spring staging divers. Because the extent of both negative density dependence and food constraints during the non-breeding phase in diver populations in nature is currently unknown, it remains speculative to what degree the modest negative effect observed in the IBM translates into possible long-term consequences for population viability (i.e. over multiple years). Nevertheless, the results suggest that any reduction in foraging efficiency within the focal area is likely to amplify the negative effects of OWFs and may result in significant impacts.

In the following section, we discuss these findings in greater detail. We first examine the outcomes of the IBM under the parameterisation that best reproduces empirical metrics observed in nature. We then compare model runs that include and exclude vessel traffic as an additional key anthropogenic stressor which is partly correlated with OWFs making it difficult to disentangle the effects.

When parameterizing model scenario A, we set the energy expenditure so that most individuals would not fall below a lower threshold of body mass and the mean body mass would stay constant over the course of their time in the focal area. This decision was based on our real data of captured individuals in which we found no evidence that body mass of individuals varied with date of capture over the season (chapter 4.4.1). We also found no existing information on variation in body condition of red-throated divers within the non-breeding phase. We therefore treat this scenario A as our (impacted) baseline, assuming that the mean body mass of the spring staging population stays constant over the simulation period. A higher body mass in scenario B (without OWFs) as compared to scenario A would then indicate a negative effect of OWFs. Thus, more important than an exact estimation of body mass change is the comparison of results deriving from the different scenarios with and without OWFs. However, for verification of our model, it is also essential to compare the values of our study with other available studies. In a recent study, the body mass change in overwintering guillemots was estimated to be about 2g per day under undisturbed condition (BUCKINGHAM ET AL. 2026). If we would upscale this number to the size of red-throated divers, we might expect a daily gain of about 4.5g. As we simulate 28 days this would result in a gain of about 126g on average. The results of our IBM under conditions excluding OWFs indicate a slightly lower gain of only 21g to 84g for the simulation runs with ppt values ranging from five to seven. While this increase in body mass is a little lower than expected when assuming similar patterns as for auks it shows that the assumptions of only a minor change in body mass in our system seems realistic. Extending the duration of the simulations might, however, be worthwhile, as small differences between scenarios may become more pronounced over longer time periods. We had no clear information on how long divers on average stage in the focal area in spring nor on the turnover rate, but data from a previous study indicated that staging time can vary among individuals from between one day to several months (DORSCH ET AL. 2019). However, peak diver numbers are known to occur

between end of March and end of April (BioConsult SH, own observation) and thus a time period of 28 days seemed reasonable.

Mean body mass differed slightly but significantly between scenarios even across several different ppt conditions, consistently showing that average body condition of simulated divers degrades when OWFs are present. However, when examining the proportion of individuals maintaining a set minimum body mass, little to no difference is observed between scenarios with and without OWFs, as the confidence intervals overlap in all but one case. Notably, for ppt = 4 the confidence intervals do not overlap, indicating that under certain conditions this metric may also become significant. This indication is further supported when considering the third scenario, in which vessel traffic was also excluded. Under these circumstances, the differences in mean become more accentuated. While for a ppt value of 5 the difference in mean was still not significant, the CI only marginally overlapped. This suggest that even small adjustments in parameter settings could result in a statistically significant difference here, too. Overall, the combined effect of OWFs and vessel traffic may therefore lead to a small but statistically significant reduction in the individuals' body mass. It should also be noted that the lower body-mass threshold applied in this study (two thirds of the initial body mass) may be too conservative. Under natural conditions, divers likely experience substantial fitness costs even above such a threshold, as has been shown for other species. Yet, it should also be considered that, under natural conditions, divers may be better able to compensate for reduced feeding efficiency than assumed in the simulation. Improved knowledge of predator–prey interactions, feeding efficiency, and digestion times in divers would enable a more realistic representation of the system.

Furthermore, under scenarios B and C the population accumulates higher mean body mass over time during their stay in the focal area, whereas mean body mass under scenario A remains approximately constant. Consequently, simulating a prolonged stay will inevitably amplify differences in mean population metrics among scenarios, increasing the likelihood of statistically significant effects. Although we considered a four-week stay in the focal area to be the most plausible average duration, it is evident that the actual time an individual spends in the area will strongly influence the magnitude of anthropogenic stressor effects on its condition. Improved empirical knowledge of staging time during spring would substantially enhance the precision of our model estimates and reduce uncertainty in projected effect sizes.

Under the current simulated duration and best-fitting parameter setting (ppt 5), mean body condition of the model birds is reduced by approximately 1.80 % when comparing scenario A (with OWFs and vessel traffic) with scenario B (without OWFs but including vessels) and 2.09 % between scenario A and C (without OWFs and without vessels). Whether this reduction alone has consequences for survival later in the season or negatively affects the reproductive success would require detailed demographic modelling and could not be addressed within the scope of this study.

An advantage of our mechanistic IBM is that it allows closer examination of the processes underlying our finding of reduction in body mass due to OWF presence. Within our model framework, the reduction was primarily linked to increased movement distances. Under OWF scenarios, divers exhibited greater movement for several interacting reasons. First, displacement from OWF areas led to locally increased diver densities in surrounding grid cells, thereby intensifying negative density dependence. In the model, higher foraging pressure within a cell increased prey evasive behaviour, which in turn reduced local foraging efficiency. As foraging efficiency declined, divers were more

likely to move to alternative grid cells, resulting in greater overall movement distances and higher associated energetic costs. In addition to this density-mediated mechanism, OWFs also acted as barriers to movement. When flying between locations, divers occasionally encountered OWFs and were forced to detour around them, increasing travel distances. However, because flight events were relatively infrequent—occurring on average only every few days—this barrier effect likely contributed little to the overall increase in energetic expenditure; a result in line with findings of a previous IBM of migrating divers (TOPPING & PETERSEN 2011). Interestingly, when reducing negative density dependency to an extent where it had almost no effect at all on foraging efficiency, divers still moved significantly more when OWFs where present, which is likely associated in part to the barrier effect. The increased energy expenditure of the simulated birds, however, could apparently be compensated by increased diving effort resulting in a body mass not or only slightly different between the scenarios at the end of the simulated 28-day period. In an IBM on breeding northern gannets in the English Channel, cumulative negative impacts of the barrier effect on the fitness of individuals have been found (WARWICK-EVANS ET AL. 2018), suggesting that this effect might be much stronger during the breeding season when birds have to commute between foraging and breeding locations.

Another aspect which might partly explain the increased movement of divers is drifting. In the simulation divers are subject to drift caused by water currents. During night hours drift caused relocation distances of about 13km. If divers drift into OWFs they escaped the perceived threat by flying to another location further away from the OWFs. While these situations are relatively rare in the model, they will increase the overall movement of divers over time in scenarios including OWFs.

Time spent flying constitutes another aspect of movement behaviour. In the IBM, flight is used to cover larger distances, with mean flight distances similar to those observed in the tracking data within the focal area. In nature, divers are known to initiate flight in response to perceived threats (e.g. approaching vessels; FLIESSBACH ET AL. 2019), but the decision rules governing flight within and outside this context remain poorly understood.

The resulting time spent flying in the IBM closely matches that observed in the tracking data. Nevertheless, we may have overestimated the propensity of birds to initiate flight in response to declining foraging success, while underestimating flight triggered by external disturbances such as vessel approaches (see also 'limitations' below). Although this distinction does not affect the overall energy budgets as flight cost the same amount of energy in both cases, it may influence the interpretation of the mechanisms through which displacement affects population viability. For example, if the increased vessel traffic within and around OWFs induces the increased probability of flight, then careful planning of maintenance work for OWFs might reduce vessel traffic and hence the energy spent flying by divers. If, however, displacement is mainly induced by the presence of the turbines, a loss of foraging habitat might still force divers to fly more often to find suitable locations. It has been shown that the OWF displacement effect is a combination of vessel traffic and turbine presence, with vessel traffic accounting for about 14% of the effect in a 3km radius in an analyses by Mendel et al. (2019) and that a reduction of vessel traffic results in significant reduction of the displacement effect (BURGER ET AL. 2025). Future studies would therefore benefit from a more realistic representation of vessel traffic, as well as improved empirical knowledge of prey distribution and behaviour, which likely shape the spatio-temporal dynamics of diver movements. Overall, however, because flight contributes only a small part (~6%) to total energy expenditure, moderate

changes in its time budget—whether driven by anthropogenic or natural factors—have only limited effects on the energy budgets.

In addition to movement, time spent diving was another key metric used to calibrate the model. Tracking data indicated a mean dive time of approximately 9% of daylight hours, whereas the IBM produced a higher value of around 16% under the parameterisation that yielded the best overall agreement across all calibration metrics. This discrepancy is likely at least partly attributable to the limited temporal resolution of the model, which operates on a 10-minute time step. Individual dives are substantially shorter than this interval; therefore, the model does not represent single dives but rather dive blocks of a certain duration per time step. This coarse temporal resolution likely leads to an overestimation of total dive time. As with other behavioural metrics, relative differences between model scenarios are more relevant than absolute agreement with tracking data. Thus, while the model seems to slightly overestimate absolute dive duration, this mismatch is unlikely to compromise the primary conclusions of the study. Moreover, the variance in time spent diving overlapped substantially between simulated and empirical data, indicating that the model produces generally realistic patterns of diving behaviour.

Finally, although resting has the lowest energetic cost per unit time among the behaviours considered, it accounts for the largest share of total energy expenditure simply because divers spend more than 90% of their time resting. In the tracking data, however, it is not possible to distinguish between passive and active movement while birds are swimming. Consequently, this behavioural category was termed ‘resting’ and its energetic cost represents a mean estimate of both passive drifting and active swimming. Following the slight overestimation in time spent diving and flying, time spent resting was underestimated proportionally. Given that resting typically occupies approximately 22–23 hours per day, changes in resting duration of some minutes have little effect on overall energy expenditure and consequently should not influence the overall picture found in this study.

10.4.1 Spatial distribution

As noted above, the parameterisation that best reproduced time and energy budgets observed in nature was characterised by mild negative density dependence. Under these conditions, the model predicts a spatial redistribution of divers within the focal area that largely corresponds to expectations: densities were reduced within and in the immediate vicinity of OWFs, while higher densities emerged in the central German Bight and in the area between the northern OWFs in German waters and the southernmost OWFs in Danish waters. This redistribution pattern is consistent with expectations derived from the static grid values integrating bathymetry, avoidance behaviour, and vessel traffic, and it aligns well with findings from previous studies (HEINÄNEN ET AL. 2020; VILELA ET AL. 2021).

Unfortunately, our access to empirical data on diver distribution in Danish waters are limited (but see SCOTT-HAYWARD ET AL. 2024, 2025). Based on the restricted available information and the results from the habitat model (chapter 7), we would have expected lower densities in the north-western part of the focal area than those predicted by the IBM. At present, it is not possible to determine whether this discrepancy reflects insufficient sampling effort and limited empirical coverage, or whether the model lacks an important driver, such as additional spatial covariates (e.g. distance to

the Elbe estuary, proximity to frontal zones, or water temperature). Improved access to high-resolution density data from this region would therefore be highly valuable for further model validation.

Nevertheless, we additionally observed that with increasing negative density dependence the density of divers within OWFs increased. Most likely when foraging efficiency is reduced in unaffected areas individuals are more likely to get closer or even enter the OWFs to find sufficient food resources. Although we don´t know whether divers in nature follow movement rules analogous to those implemented by the Metropolis algorithm, this observation begs to further investigate possible habituation of divers towards OWFs as indicated in the habitat model (chapter 7) as well as in a recent study (BURGER ET AL. 2025), although in the latter study this pattern was mostly driven by reductions in vessel traffic.

Under natural conditions, an observed reduced avoidance rate might alternatively be explained by increased prey densities caused by a reef effect and the absence of fishing activity within the OWFs, but this was not implemented in the model. In such a case divers are technically not habituating to the presence of OWFs, they still might have the same neophobic tendency of the OWFs, but they are more willing to get closer because the reward in form of increased foraging efficiency is increasing (landscape of fear theory, see e.g. GAYNOR ET AL. 2019).

Such an increased foraging success close to or in OWFs can function as a positive reinforcer both on the individual level and evolutionary level.

Gaining more insight into the fitness of individuals with different avoidance rates would help to disentangle these mechanisms as this might have implications for mitigation measures.

10.4.2 Vessel traffic

Including vessel traffic in the focal area (i.e. scenario A and B) substantially improved the simulated spatial distribution of divers, resulting in a considerably better match with the tracking and aerial survey data. This improvement is largely attributable to vessel traffic occurring along the eastern and southeastern parts of the focal area (mostly fishing vessels) which appears to displace divers from that area, thereby influencing movement patterns and energy expenditure.

Results from the IBM indicate that, aside from differences in spatial distribution, overall differences between scenarios with and without vessel traffic in terms of time and behavioural budgets were small. As expected, in the absence of vessel traffic (scenario C), divers moved slightly less and expended little but significantly less time and energy on flying, and consequently exhibited a marginally but not significantly higher body mass at the end of the simulation in comparison to scenario B.

While both scenarios without OWFs showed a significant higher body mass in comparison to scenario A, the proportion of individuals remaining above a critical minimum mass (two-thirds of the initial body mass) tended to be higher (just not significant) in scenario C (excluding vessel traffic) but not in scenario B. This suggests that vessel traffic, next to shaping spatial distribution of divers, may also ultimately play an important role in population viability.

This finding is particularly noteworthy given that vessel traffic was implemented in the model as a static environmental variable. In natural systems, vessel traffic is likely to induce even greater movement and energetic costs due to flight responses to approaching vessels, which are commonly observed in divers (FLIESSBACH ET AL. 2019).

It is also important to note that completely omitting vessel traffic may have complex and potentially opposing effects on the behaviour of simulated individuals. On the one hand, excluding vessel traffic increases the extent of suitable habitat within the focal area, which could lead to increased movement. On the other hand, the expansion of suitable habitat relaxes negative density dependence, which, as shown by the model results, reduces movement and associated energetic costs. The relative strength of these opposing mechanisms, or whether they effectively balance each other, is difficult to determine. However, the comparison between scenarios B and C suggests that the magnitude of these effects is modest, providing confidence that the overall conclusions are robust.

Nonetheless, it would be valuable to investigate in greater detail how divers respond to vessel traffic in natural settings and how this influences spatial distribution and density-dependent processes. Especially the relative contribution of OWF-related vessel traffic to the overall effect needs further study, as previous analyses showed significant impacts of these vessels on displacement distances (BURGER ET AL. 2025). Likewise, implementing vessel traffic as a more realistic and dynamic environmental component within the IBM would be a worthwhile avenue for future work.

10.4.3 Conclusions

The performance of the individual-based model (IBM) depends on how accurately it represents the underlying biological mechanisms and environmental conditions. Although extensive empirical data—particularly tracking data from this study—were used to calibrate and constrain the parameter space and achieve close agreement with observed behavioural and spatial metrics, several key parameters could not be derived directly from field data. These include dive success rates, energetic content of prey, and digestion times, which were therefore estimated based on best-available knowledge, introducing uncertainty into the results.

Furthermore, the model is mechanistic and assumes specific processes underlying the observed behaviour. While these assumptions are biologically plausible at a coarse scale, for example, birds dive to capture fish, captured prey must be digested, and prey move through space, creating spatiotemporal variation in prey density - the exact mechanisms and parameter values are still not fully understood, leading to additional uncertainty. As with any modelling approach, the IBM simplifies natural complexity to focus on the dominant drivers of observed patterns. Nevertheless, comparison of model outputs with empirical data from this and previous studies provided a robust basis for validating the model's ability to reproduce key aspects of natural behaviour.

Despite some limitations, we are confident that the IBM produces realistic results, as its outputs closely match those from tracking studies, consistent with the pattern-oriented modelling approach applied here (GRIMM ET AL. 2005). Importantly, this agreement was not hard-wired into the model; rather, the observed patterns emerged from the underlying mechanistic processes implemented.

This enables the model not only to quantify effect sizes under different environmental conditions instead of simply assuming negative effects, but also let us elucidate the biological mechanisms driving these effects and their magnitude.

Nevertheless, improved empirical estimates of predator-prey interactions including dive efficiency, foraging success rates and energetic gain per successful dive would substantially enhance our understanding of diver behavioural and physiological budgets and, in turn, greatly improve the performance of mechanistic IBMs such as the one used in this study.

As it is, mechanistic IBMs are highly useful tools to investigate a multitude of aspects of the influences OWFs may have on divers on its own or in conjunction with other stressors. For example, how a potential reef effect of OWFs changes the distribution under different food constraints. Also, climate change might influence the energy budget: less energy might be needed for thermoregulation, but foraging efficiency might be decreased due to changes in prey composition. Further questions could be how much a reduction of vessel traffic in certain areas within the focal area would influence divers' movement and associated cost? How would a change in avoidance behaviour affect negative density dependence and thus energetic gain by divers?

11 IMPLICATIONS FOR SPATIAL PLANNING AND THE DEVELOPMENT OF MITIGATION MEASURES

11.1 Introduction

The red-throated diver is one of the most sensitive seabird species in relation to offshore wind farms (OWFs) in the German North Sea. At the same time, the species' wintering areas overlap with areas of wind energy production. For the German North Sea, the offshore area west of the island of Sylt is an important spring staging area for these birds, before they continue migration to the breeding grounds. The SPA "Eastern German Bight" was established there in 2004, in order to protect red-throated divers and other species. However, the larger area also hosts several OWF, with one OWF located within the SPA. Expansion of OWF developments is progressing rapidly, in the German North as well as the Baltic Sea, where also several diver hotspots are located (MENDEL ET AL. 2008; SKOV ET AL. 2011). There are concerns that the disturbance and loss of important foraging habitat might negatively impact divers and there is a high demand for measures to mitigate negative effects.

The main ways wind farms affect red-throated divers:

1. **Displacement / Habitat loss**: After construction, densities of red-throated divers were strongly reduced around OWFs, with displacement distances reaching up to around 15 km (MENDEL ET AL. 2019; HEINÄNEN ET AL. 2020; VILELA ET AL. 2021)

2. **Restricted foraging**: Avoidance of OWFs likely constrains where divers can feed, limiting their choice of foraging areas and thereby also reducing their foraging flexibility (GARTHE ET AL. 2023)

3. **Barrier effects**: OWFs may act as barriers in key movement corridors which could exclude birds from certain areas beyond the area of the OWF itself and force them to fly longer detours, which could potentially increase their energy expenditure.

4. **Disturbance** from OWF-related ship traffic (BURGER ET AL. 2025)

5. **Cumulative effects**: As many OWFs are built, the combined loss of habitat / displacement may have population-level consequences (GOODALE 2018; GARTHE ET AL. 2023)

11.2 Recap of important findings within the DiverLog project

Results from this project have given us very detailed insights into the movements and behaviours of these birds within their spring staging area. This allowed us to simulate the impacts of OWFs on the body condition of our model birds (chapter 10), a crucial factor when trying to estimate population effects.

In chapter 5, we analysed the foraging behaviour by analysing dives in detail. This revealed information on dive depth and durations, showing that birds mainly fed on pelagic prey, but also do benthic dives occasionally. Overall, birds spent relatively little time foraging, compared to other studies, and did not show an adjustment of their foraging behaviour (e.g. time spent diving or dive characteristics) with the distance to OWFs.

In chapter 6, time-energy budgets were analysed, showing that birds spend most of their time in the area resting/swimming with only few longer movements (flights). The energy expenditure per day showed a weak correlation with distance to OWFs, with birds spending more energy when staying closer to an OWF. This could mainly be explained by more flying activity closer to OWFs, possibly because of increased disturbance or because birds had to fly around this potential barrier. No changes in overall movement patterns (step length) relative to the distance to OWFs could be detected.

In chapter 7, a habitat model was used to model the distribution of birds within the area and identify important parameters affecting the distribution. Ship traffic (averages per day) was one of the most important predictors, indicating that birds avoid areas with high ship traffic, confirming previous findings. As in previous analyses, distance to OWFs as well as environmental parameters (bathymetry, salinity) also showed significant effects on the distribution of these birds.

In chapter 8, the direct effects of ship encounters on movements of divers were investigated. Ship presence affected relocation distances in a radius of 5 km, but encounters between birds and ships were few overall, indicating that divers consistently avoid areas with high ship traffic (similar to findings in chapter 7). Birds reacted on ships mainly during day, while at night bird movements were lower overall.

In chapter 9, previous results on the migratory routes and potential breeding areas could be confirmed, showing that most individuals are long-distance migrants breeding in north-east Russia, with smaller numbers migrating to Scandinavia, Svalbard and Greenland. In addition, some overlaps between GPS locations of overwintering divers and planned or existing OWFs were identified throughout the wintering range, albeit to a very limited extent overall.

The results of the individual-based model (IBM) in chapter 10 indicated that the presence of OWFs has a slight but significant negative effect on the mean body condition of staging divers when the model is parameterized such that time and behavioural budgets match those observed in nature. This negative effect becomes substantially stronger under scenarios of pronounced negative density dependence, which lead to reduced foraging efficiency. This suggests that potential further reductions in foraging efficiency within the focal area might amplify the negative effects of OWFs. Further analyses would be necessary to assess the extent to which the minor negative effects on body condition currently observed under the given parameterisation will have an impact in the long term.

Based on the results from these chapters, the previous DIVER project and other available literature, a number of possible mitigation measures can be derived that could help reduce negative impacts, especially habitat displacement, and some considerations for their feasibility are listed below. The focus will be on possible mitigation measures that can be applied within the focal area/North Sea.

Other compensatory measures that would need to be applied in other regions, for example enhancing the breeding habitat and therefore increasing reproductive output, are not considered here.

11.3 Spatial Planning and Mitigation Measures

11.3.1 Maritime Spatial Planning

1. Avoidance ("Strategic Siting")

Substantial environmental monitoring has been performed in German waters of the North and Baltic Sea during the last 25 years. This has resulted in good knowledge about the distribution of seabird species in the offshore area and their reactions towards OWFs. Furthermore, several research projects were conducted that used modelling of sea bird distribution over several years and seabird tracking. These studies have provided detailed knowledge on the effects of OWF development on seabird distribution and individual movement patterns (DORSCH ET AL. 2019; PESCHKO ET AL. 2020b; VILELA ET AL. 2022; GARTHE ET AL. 2023). From these studies it is possible to identify the most important areas for seabirds that should be considered in maritime spatial planning (e.g. PESCHKO ET AL. 2024). A high number of recent publications have shown negative impacts of OWF on red-throated divers and large-scale monitoring data has allowed to outline a main concentration area (BMU 2009) of this species in the German North Sea during spring. Based on this knowledge, the area of the OWF "Butendiek" has been excluded from further OWF development, according to the most recent site development plan for the German North Sea (BSH 2025). For sites N-4 and N-5, which are located (partly) within the main concentration area, no further development is planned until the decommissioning of the wind farms "Butendiek" and "DanTysk". For new OWF sites planned near the main concentration area, far-reaching disturbance effects are taken into account.

However, whether a static spatial approach is sufficient or whether changes in local distributions due to other factors like prey availability or climate change can be implemented in spatial planning is currently uncertain. Further, if birds might habituate to OWF after some years of exposure, an adjustment of displacement distances would be justified.

2. OWF configuration

One recent study suggests that OWF configuration, i.e. mainly the distance between turbines, might affect avoidance response of divers, with larger turbine distances leading to less avoidance (SCOTT-HAYWARD ET AL. 2024). Size (height) of wind turbines has been increasing rapidly over the last years and the size of new OWF developments largely exceed some of the first OWFs. This has led to a lower number of turbines per km² (but with increased height) and thus also larger distances between turbines. Whether it is a general pattern that divers show a weaker reaction towards these recent OWFs of different design and configuration than towards the ones built over the last two decades remains to be seen. Given that this could only be shown at one location so far, it could also be a site-specific effect. However, a synthesis on the effects of OWF configurations in fact showed stronger impacts when turbine density was lower, but some confounding factors were present

(LAMB ET AL. 2024). Further, more detailed studies into the effects of turbine height and OWF configuration on diver distribution and behaviour would be required to test for general patterns.

11.3.2 Mitigation and Compensatory Measures

In this section, compensatory and mitigation measures are suggested, that may be adopted to avoid or reduce negative effects of OWFs on divers in areas with already existing OWFs or when strategic siting is not an option. In this context, mitigation measures are those which reduce the impact itself (disturbance, displacement), while compensatory measures do not reduce the impact from the OWFs itself but provide ecological gains elsewhere or in a broader context to balance the loss. Also measures for monitoring and research as well as regulatory measures are included here, as these can provide a base for the development of effective mitigation measures.

Our study area (focal area) included two neighbouring Natura-2000 areas, one in German and one in Danish waters, with several OWFs located at the borders of these SPA and one OWF within the German SPA. The management plan for the Natura-2000 area "Sylt Outer Reef - Eastern German Bight" (BFN 2020) states already a number of measures that can be applied to improve conditions for the key species in this area, with red-throated diver being one of the focal species. Suggested measures include for example a reduction of fisheries impacts, restrictions for OWF-related ship traffic and reductions in emissions. Furthermore, monitoring of the effectiveness of such measures is suggested.

Based on a literature review, several measures that could be applied (or adapted) to specifically help mitigate or compensate impacts on red-throated divers are listed below.

1. Fishery management

Reduction of fisheries of potential diver prey species such as herring or in other areas sandeel can improve prey availability. In the UK, for example, a permanent closure of sandeel fisheries was ordered that is effective since March 2024 to protect a range of seabird species and other marine life that rely on sandeel for food (https://www.rspb.org.uk/whats-happening/news/a-huge-victory-for-seabirds-as-uk-and-scottish-closure-of-sandeel-fishing-stands).

2. Shipping management (re-routing, speed limits)

A promising mitigation measure for red-throated divers is the regulation of ship traffic in their main concentration areas. Divers react very sensitive to shipping (SCHWEMMER ET AL. 2011; FLIESSBACH ET AL. 2019). Previous and current work have shown responses up to 5 km distance to ships (BURGER ET AL. 2019; MENDEL ET AL. 2019). Especially high-speed crafts were identified as creating the strongest responses (BURGER ET AL. 2019). These high-speed crafts are frequently used for OWF-service operations.

One measure to reduce effects of OWFs could thus be to manage OWF related shipping traffic by speed limits and avoiding sensitive sites and times. The new site development plan for the German North Sea of 2025 demands the development of similar concepts for all OWF service traffic

traversing the SPA and the main diver concentration area (BSH 2025), including measures like speed reductions, the use of channelled routes and overall traffic reductions during sensitive time periods.

For the OWF "Butendiek", from 2021 the regulator already demanded adjustments to the OWF service traffic: during springtime, the number of transits had to be reduced, routes had to be channelled and adjusted so to avoid crossing the SPA as much as possible. In addition, a speed limit of 9 kn was imposed for all vessels within the SPA during this time period. A recent study showed that the displacement effect is reduced on days without ship traffic in the vicinity of the OWF (BURGER ET AL. 2025).

3. Demand-driven nighttime marking

It has been shown that divers avoid OWFs also during the night (DORSCH ET AL. 2019), although the visibility of the structures themselves as well as the rotor movements are then strongly reduced. It seems obvious that the birds react to the nighttime markings, especially the aviation markings on the nacelles, which, on clear nights, are visible at a large distance (personal observation during diver captures).

At onshore wind farms in Germany, demand-driven nighttime marking has been implemented in recent years in order to reduce bird collisions. In addition to reducing the collision risk of migrating birds, demand-driven nighttime lighting at OWFs could possibly also reduce the avoidance distances of divers to OWF at night.

4. Designation or extension of protected areas

The creation or extension of Marine Protected Areas (MPAs) or Special Protection Areas (SPAs) is an option to cover important diver sites. One example for this is the case of the OWF "Butendiek": As a compensation for the continued operation of the OWF located with the SPA, an extension of the protected area was implemented by the nature conservation authority, which consists of an area highly used by red-throated divers during spring and which did not have a protection status yet.

5. Monitoring and Research

- **Long-term telemetry / tracking**: Projects like DiverLog use GPS or data-loggers on red-throated divers to understand their movement, habitat use, and how they respond to OWFs. This can help to identify suitable mitigation strategies and inform maritime spatial planning.
- **Post-construction monitoring**: Conduct seabird surveys before, during, and after OWF construction to assess displacement, changes in density, and habituation. Several large-scale studies have been conducted during the last years (VILELA ET AL. 2022; GARTHE ET AL. 2023).
- **Adaptive management frameworks**: Use monitoring data to adjust mitigation / compensation over time. For example, if divers begin to habituate, mitigation strategies might evolve.

6. Regulatory / Policy Measures

- **Strategic compensation funds**: Use mechanisms like marine recovery funds, where wind developers contribute to a fund that supports compensatory actions (habitat, monitoring, research). For example, the UK has started consultations for a Marine Recovery Fund to deliver strategic compensatory measures (https://www.gov.uk/government/consultations/offshore-wind-setting-up-the-marine-recovery-fund/outcome/summary-of-responses-and-government-response).

- **Best-practice guidelines**: Adhere to guidance from bodies like OSPAR, which is developing best practices for mitigation and compensation for marine birds (https://www.ospar.org/work-areas/bdc/species-habitats/marine-birds/offshore-wind-mitigation-compensation-measures?).

- **International cooperation**: Since seabirds like divers cross many international boundaries, coordination of mitigation / compensation across countries via MSP and conservation frameworks is important.

11.4 Challenges & Considerations

- **Effectiveness uncertainty**: While many measures are promising, the actual effectiveness for divers (especially for non-breeding-season displacement) is only shown in one case: a significant reduction of the displacement effect on days with low ship traffic in the vicinity of an OWF (BURGER ET AL. 2025). In other cases, for instance compensation via fisheries closures, robust evidence is still lacking, as it is unknown whether food limitation is a key demographic bottleneck.

- **Cumulative impacts**: As more OWFs are built, cumulative (in-combination) effects may overwhelm local mitigation. Strategic planning and compensation must account for cumulative loss of habitat.

- **Trade-offs**: Some measures (e.g., very large exclusion zones) reduce OWF area or increase costs. Balancing climate goals and biodiversity goals is critical.

- **Monitoring costs and logistics**: Long-term tracking, shutdowns, adaptive management, etc., all require resources.

- **Regulatory alignment**: There needs to be alignment across maritime spatial planning, environmental permitting, and conservation policies so that mitigation is enforceable and meaningful.

11.5 Conclusions

Avoiding or reducing impacts of offshore wind expansion on sensitive seabirds like the red-throated diver wintering in offshore areas of the North and Baltic Sea will likely require a multi-pronged approach. Maritime spatial planning such as choosing development sites away from key areas of these species is the most important measure to avoid negative impacts of OWFs in the first place. However, balancing targets for the expansion of renewable energies and nature conservation can be challenging. In cases when (complete) avoidance of sensitive areas is not an option or when OWF were built before knowledge of their large-scale effects emerged, direct mitigation measures might be required. Presently, the only mitigation measure proven to successfully reduce negative effects of OWFs on red-throated divers is the regulation of OWF related shipping traffic. The combination of reduced OWF-service traffic during the sensitive time period, speed limits and channelled routes are likely to significantly reduce disturbance of divers and should be applied wherever possible.

However, based on scientific findings regarding the behaviour of red-throated divers and other seabird species, there are some additional measures that also sound promising, but would yet have to be tested. One example is the demand-driven nighttime marking which might be a promising way to reduce disturbance during the night. A case study testing this is currently lacking, as demand-driven nighttime marking is currently not operational for any OWFs, due to pending approval under aviation law. More research is also needed on the effects of OWF configuration and whether this can also help to reduce displacement effects.

Long-term monitoring of important areas allows potential changes in avoidance rates to be identified that can be attributed, for example, to habituation or other environmental changes, such as changes in prey abundance, which lead to changes in habitat suitability. Such monitoring, combined with targeted research, enables the adjustment of predicted responses and the investigation of the effectiveness of specific mitigation measures.

Finally, it is particularly important that wind farm developers, regulators, and conservationists collaborate to strategically plan new developments or mitigate already existing impacts.

12 LITERATURE

Anderson, S. C., E. J. Ward, P. A. English, L. A. K. Barnett & J. T. Thorson (2024) sdmTMB: An R Package for Fast, Flexible, and User-Friendly Generalized Linear Mixed Effects Models with Spatial and Spatiotemporal Random Fields.

Austin, M. (2007) Species distribution models and ecological theory: A critical assessment and some possible new approaches. Ecological Modelling (1, vol. 200), pp. 1–19.

Bailey, H., K. L. Brookes & P. M. Thompson (2014) Assessing environmental impacts of offshore wind farms: lessons learned and recommendations for the future. Aquatic Biosystems (1, vol. 10), p. 8.

Barrett, T., M. Dowle, A. Srinivasan, J. Gorecki, M. Chirico, T. Hocking, B. Schwendinger & I. Krylov (2006) data.table: Extension of `data.frame`. Institution: Comprehensive R Archive Network, p. 1.18.2.1.

Bellebaum, J. (2020) Biologische Maßstäbe für artenschutzrechtliche Tötungsverbot. Stand und Anwendungsmöglichkeiten. Natur und Landschaftsplanung (1, vol. 52), pp. 24–30.

Bellebaum, J., A. Diederichs, J. Kube, A. Schulz & G. Nehls (2006) Flucht- und Meidedistanzen überwinternder Seetaucher und Meeresenten gegenüber Schiffen auf See. Orn. Rundbrief Mecklenburg-Vorpommern (vol. 45, Sonderheft 1 (Tagungsband 5. deutsches See-und Küstenvogelkolloquium)), pp. 86-90.

Berndt, R. K. & D. Drenckhahn (eds.) (1990) Vogelwelt Schleswig-Holsteins. 1: Seetaucher bis Flamingo. ED. 2., korr. Aufl, publ. Karl-Wacholtz Verlag, pp. 240.

BfN (2020) Managementplan für das NSG „Sylter Außenriff – Östliche Deutsche Bucht“ (MPSyl). (auts. Krause, J., N. Schröder, A. Kreutle, C. Kuhmann, B. Wölfing & M. Sollich; ed. Bundesamt für Naturschutz). no. Az. MAR-34324-04.

BirdLife International (ed.) (2015) European Red List of Birds. publ. Office for Official Publications of the European Communities, pp. 67.

Birt-Friesen, V. L., W. A. Montevecchi, D. K. Cairns & S. A. Macko (1989) Activity-Specific Metabolic Rates of Free-Living Northern Gannets and Other Seabirds. Ecology (2, vol. 70), pp. 357–367.

BMU (2009) Positionspapier des Geschäftsbereichs des Bundesumweltministeriums zur kumulativen Bewertung des Seetaucherhabitatverlusts durch Offshore-Windparks in der deutschen AWZ der Nord- und Ostsee als Grundlage für eine Übereinkunft des BfN mit dem BSH. Einführung eines neuen fachlich begründeten Bewertungsverfahrens. (aut. BMU). p. 5.

Bradbury, G., M. Trinder, B. Furness, A. N. Banks, R. W. G. Caldow & D. Hume (2014) Mapping Seabird Sensitivity to Offshore Wind Farms. PLoS ONE (9, vol. 9), p. e106366.

Brooks, M., E., K. Kristensen, K. Benthem J. ,van, A. Magnusson, C. Berg W., A. Nielsen, H. Skaug J., M. Mächler & B. Bolker M. (2017) glmmTMB Balances Speed and Flexibility Among Packages for Zero-inflated Generalized Linear Mixed Modeling. The R Journal (2, vol. 9), pp. 378–400.

Brown, J. H., J. F. Gillooly, A. P. Allen, V. M. Savage & G. B. West (2004) Toward a metabolic theory of ecology. Ecology (7, vol. 85), pp. 1771–1789.

BSH (2025) Flächenentwicklungsplan 2025 für die deutsche Nordsee und Ostsee. no. BSH-Nummer 7608.

Buckingham, L., F. Daunt, M. I. Bogdanova, R. W. Furness, S. Bennett, J. Duckworth, R. E. Dunn, S. Wanless, M. P. Harris, D. C. Jardine, M. A. Newell, R. M. Ward, E. D. Weston & J. A. Green (2023) Energetic synchrony throughout the non-breeding season in common guillemots from four colonies. Journal of Avian Biology (1–2, vol. 2023), p. e03018.

Buckingham, L., E. A. Masden, K. Layton-Matthews, I. S. Bringsvor, V. S. Bråthen, N. Dehnhard, P. Fauchald, S. Lorentsen, T. K. Reiertsen, K. R. Searle, A. Tarroux & S. Christensen-Dalsgaard (2026) An individual-based model to quantify the non-breeding season impact of wind farms on seabirds. Ecological Solutions and Evidence (1, vol. 7), p. e70196.

Bundesamt für Justiz (2017) Verordnung über die Festsetzung des Naturschutzgebietes „Sylter Außenriff - Östliche Deutsche Bucht" (NSGSylV).

Burger, C., A. Diederichs, M. Stelter, R. Castillo, V. Kosarev & G. Nehls (2025) Gewöhnung oder wirksame Minderungsmaßnahme bei einem Offshore-Windpark? Eine Fallstudie zu Seetauchern in der Nordsee. MeeresumweltsymposiumHamburg.

Burger, C., A. Schubert, S. Heinänen, M. Dorsch, B. Kleinschmidt, R. Žydelis, J. Morkūnas, P. Quillfeldt & G. Nehls (2019) A novel approach for assessing effects on distributions and movements of seabirds in relation to shipping traffic. Journal of Environmental Management (vol. 251), p. 109511.

Calenge, C. (2006) The package “adehabitat” for the R software: A tool for the analysis of space and habitat use by animals. Ecological Modelling (3, vol. 197), pp. 516–519.

Calenge, C. (2019) Analysis of Animal Movements in R: the **adehabitatLT** Package.

Carboneras, C., D. A. Christie & E. F. J. Garcia (2020) Red-throated Loon (Gavia stellata). in Handbook of the Birds of the World Alive, publ. Lynx Ediciones.

Carlsen, A. A., S. H. Lorentsen, J. Mattisson & J. Wright (2023) Temporal non-independence of foraging dive and surface duration sequences in the European shag *Gulosus aristotelis*. Ethology.

Carlsen, A. A., S.-H. Lorentsen & J. Wright (2021) Recovery, body mass and buoyancy: a detailed analysis of foraging dive cycles in the European shag. Animal Behaviour (vol. 178), pp. 247–265.

Ceia, F. R. & J. A. Ramos (2015) Individual specialization in the foraging and feeding strategies of seabirds: a review. Marine Biology (10, vol. 162), pp. 1923–1938.

Chamberlain, S. (2025) rerddap: General Purpose Client for "ERDDAP™" Servers.

Chivers, L. S., M. H. Lundy, K. Colhoun, S. F. Newton, J. D. R. Houghton & N. Reid (2012) Foraging trip time-activity budgets and reproductive success in the black-legged kittiwake. Marine Ecology Progress Series (vol. 456), pp. 269–277.

Chung, H., J. Lee & W. Y. Lee (2021) A Review: Marine Bio-logging of Animal Behaviour and Ocean Environments. Ocean Science Journal (2, vol. 56), pp. 117–131.

Codling, E. A., M. J. Plank & S. Benhamou (2008) Random walk models in biology. Journal of The Royal Society Interface (25, vol. 5), pp. 813–834.

Collins, P. M., L. G. Halsey, J. P. Y. Arnould, P. J. A. Shaw, S. Dodd & J. A. Green (2016) Energetic consequences of time-activity budgets for a breeding seabird. Journal of Zoology (3, vol. 300), pp. 153–162.

Cramp, S. & K. E. L. Simmons (1977) The Birds of the Western Palearctic. ED. Vol. 1, publ. Oxford University Press.

Croxall, J. P., S. H. Butchart, B. Lascelles, A. J. Stattersfield, B. Sullivan, A. Symes & P. Taylor (2012) Seabird conservation status, threats and priority actions: a global assessment. Bird Conservation International (1, vol. 22), pp. 1–34.

Daub, B. C. (1989) Behavior of Common Loons in Winter. Journal of Field Ornithology (3, vol. 60), pp. 305–311.

Daunt, F., T. E. Reed, M. Newell, S. Burthe, R. A. Phillips, S. Lewis & S. Wanless (2014) Longitudinal bio-logging reveals interplay between extrinsic and intrinsic carry-over effects in a long-lived vertebrate. Ecology (8, vol. 95), pp. 2077–2083.

Dias, M. P., R. Martin, E. J. Pearmain, I. J. Burfield, C. Small, R. A. Phillips, O. Yates, B. Lascelles, P. G. Borboroglu & J. P. Croxall (2019) Threats to seabirds: A global assessment. Biological Conservation (vol. 237), pp. 525–537.

Dierschke, V., R. W. Furness & S. Garthe (2016) Seabirds and offshore wind farms in European waters: Avoidance and attraction. Biological Conservation (vol. 202), pp. 59–68.

Dormann, C. F., J. Elith, S. Bacher, C. Buchmann, G. Carl, G. Carré, J. R. G. Marquéz, B. Gruber, B. Lafourcade, P. J. Leitão, T. Münkemüller, C. McClean, P. E. Osborne, B. Reineking, B. Schröder, A. K. Skidmore, D. Zurell & S. Lautenbach (2013) Collinearity: a review of methods to deal with it and a simulation study evaluating their performance. Ecography (1, vol. 36), pp. 27–46.

Dorsch, M., C. Burger, S. Heinänen, B. Kleinschmidt, J. Morkūnas, G. Nehls, P. Quillfeldt, A. Schubert & R. Žydelis (2019) DIVER – German tracking study of seabirds in areas of planned Offshore Wind Farms at the example of divers. (eds. BioConsult SH, Justus Liebig University

of Gießen (JLU), DHI & Ornitela). no. FKZ 0325747A/B, Final report on the joint project DIVER, funded by the Federal Ministry of Economics and Energy (BMWi) on the basis of a decision by the German Bundestag; https://www.bioconsult-sh.de/fileadmin/user_upload/Publikationen/2019/BMWi-Fkz0325747A_B_final_150dpi.pdf.

Drewitt, A. L. & R. H. W. Langston (2006) Assessing the impacts of wind farms on birds. IBIS (vol. 148), pp. 29–42.

Duckworth, J. A. (2023) Using behavioural and energetic insights to assess the impacts of displacement from offshore wind farms on red-throated divers (*Gavia stellata*). PhD Thesis, University of Liverpool, pp. 220.

Duckworth, J., S. O'Brien, R. E. Dunn, I. K. Petersen, A. Petersen, G. Benediktsson, L. Johnson, P. Lehikoinen, D. J. Okill, R. Väisänen, J. Williams, S. Williams, F. Daunt & J. A. Green (2024) Linking Foraging Behaviour and Habitat Preferences During Moult Across Multiple Populations of Red-Throated Diver. Ecology and Evolution (12, vol. 14), p. e70733.

Duckworth, J., S. O'Brien, I. K. Petersen, G. Benediktsson, L. Johnson, P. Lehikoinen, D. Okill, R. Väisänen, J. Williams, S. Williams, F. Daunt & J. A. Green (2021) Spatial and temporal variation in foraging of breeding red-throated divers. Journal of Avian Biology (12).

Duckworth, J., S. O'Brien, I. K. Petersen, A. Petersen, G. Benediktsson, L. Johnson, P. Lehikoinen, D. Okill, R. Väisänen, J. Williams, S. Williams, F. Daunt & J. A. Green (2022) Winter locations of red-throated divers from geolocation and feather isotope signatures. Ecology and Evolution (8, vol. 12).

Duckworth, J., S. O'Brien, R. Väisänen, P. Lehikoinen, I. K. Petersen, F. Daunt & J. A. Green (2020) First biologging record of a foraging Red-Throated Loon *Gavia stellata* shows shallow and efficient diving in freshwater environments. Marine Ornithology (vol. 48), pp. 17–22.

Dunn, R. E., J. Duckworth & J. A. Green (2023) A framework to unlock marine bird energetics. Journal of Experimental Biology (24, vol. 226), p. jeb246754.

Dunn, R. E., J. Duckworth, S. O'Brien, R. W. Furness, L. Buckingham, F. Daunt, M. Bogdanova & J. A. Green (2024) Temporal and spatial variability in availability bias has consequences for marine bird abundance estimates during the non-breeding season. Ecology.

Dunn, R. E., J. A. Green, S. Wanless, M. P. Harris, M. A. Newell, M. I. Bogdanova, C. Horswill, F. Daunt & J. Matthiopoulos (2022) Modelling and mapping how common guillemots balance their energy budgets over a full annual cycle. Functional Ecology.

Dunn, R. E., S. Wanless, F. Daunt, M. P. Harris & J. A. Green (2020) A year in the life of a North Atlantic seabird: behavioural and energetic adjustments during the annual cycle. Scientific Reports (5993, vol. 10).

Durinck, J., H. Skov & P. Andell (1993) Seabird distribution and numbers selected offshore parts of the Baltic Sea, winter 1992. Ornis Svecica (vol. 3), pp. 11–26.

Durinck, J., H. Skov, F. P. Jensen & S. Pihl (1994) Important Marine Areas for Wintering Birds in the Baltic Sea. Report to the European Commission, EU DG XI research contract no. 2242/90-09-01, p. 104.

Elliott, K. H. (2025) Seabirds: Energy efficiency and foraging on the high seas. Current Biology (4, vol. 35), pp. R156–R158.

Elliott, K. H. & A. J. Gaston (2015) Diel vertical migration of prey and light availability constrain foraging in an Arctic seabird. Marine Biology (9, vol. 162), pp. 1739–1748.

Elliott, K. H., R. E. Ricklefs, A. J. Gaston, S. A. Hatch, J. R. Speakman & G. K. Davoren (2013) High flight costs, but low dive costs, in auks support the biomechanical hypothesis for flightlessness in penguins. Proceedings of the National Academy of Sciences (23, vol. 110), pp. 9380–9384.

Elliott, K. H., K. Woo, A. J. Gaston, S. Benvenuti, L. Dall´Antonia & G. K. Davoren (2008) Seabird foraging behaviour indicates prey type. Marine Ecology Progress Series (vol. 354), pp. 289–303.

Ellis, H. I. & G. W. Gabrielsen (2002) Energetics of free-ranging seabirds. (eds. Schreiber, B. A. & J. Burger). in Biology of Marine Birds, publ. CRC Press, pp. 359–407.

Eriksson, M. O. G. (2010) Storlommen och smålommen i Sverige – populationsstatus, hotbild och förvaltning. in Projekt LOM.

Eriksson, M. O. G. (2015) Reduced survival of Black-throated Diver *Gavia arctica* chicks – an effect of changes in the abundance of fish, light conditions or exposure to mercury in the breeding lakes? Ornis Svecica (vol. 25), pp. 131–152.

European Union (ed.) (2010) Directive 2009/147/EC of the European Parliament and of the Council of 30 November 2009 on the conservation of wild birds (codified version).

Everaert, J. & E. W. Stienen (2007) Impact of wind turbines on birds in Zeebrugge (Belgium). Significant effect on breeding tern colony due to collisions. Biodiversity and Conservation (12, vol. 16), pp. 3345–3359.

Exo, K.-M., O. Hüppop & S. Garthe (2003) Birds and offshore wind farm: a hot topic in marine ecology. Wader Study Group Bulletin (vol. 100), pp. 50–53.

Fauchald, P. (2009) Spatial interaction between seabirds and prey: review and synthesis. Marine Ecology Progress Series (vol. 391), pp. 139–151.

Fayet, A. L., R. Freeman, T. Anker-Nilssen, A. Diamond, K. E. Erikstad, D. Fifield, M. G. Fitzsimmons, E. S. Hansen, M. P. Harris, M. Jessopp, A.-L. Kouwenberg, S. Kress, S. Mowat, C. M. Perrins, A. Petersen, I. K. Petersen, T. K. Reiertsen, G. J. Robertson, P. Shannon, I. A. Sigurðsson, A. Shoji, S. Wanless & T. Guilford (2017) Ocean-wide Drivers of Migration Strategies and Their Influence on Population Breeding Performance in a Declining Seabird. Current Biology (24, vol. 27), pp. 3871-3878.e3.

Fayet, A. L., R. Freeman, A. Shoji, H. L. Kirk, O. Padget, C. M. Perrins & T. Guilford (2016) Carry-over effects on the annual cycle of a migratory seabird: an experimental study. Journal of Animal Ecology (6, vol. 85), pp. 1516–1527.

Fetting, C. (2020) "The European Green Deal." ESDN Report.

Finney, S. K., S. Wanless & M. P. Harris (1999) The Effect of Weather Conditions on the Feeding Behaviour of a Diving Bird, the Common Guillemot *Uria aalge*. Journal of Avian Biology (1, vol. 30), p. 23.

Fliessbach, K. L., K. Borkenhagen, N. Guse, N. Markones, P. Schwemmer & S. Garthe (2019) A ship traffic disturbance vulnerability index for northwest european seabirds as a tool for marine Spatial planning. Frontiers in Marine Science (vol. 6), p. 192.

Florko, K. R. N., R. R. Togunov, R. Gryba, E. Sidrow, S. H. Ferguson, D. J. Yurkowski & M. Auger-Méthé (2025) An introduction to statistical models used to characterize species-habitat associations with animal movement data. Movement Ecology (1, vol. 13), p. 27.

Ford, T. B. & J. A. Gieg (1995) Winter Behavior of the Common Loon. Journal of Field Ornithology (1, vol. 66), pp. 22–29.

Fort, J., W. P. Porter & D. Grémillet (2011) Energetic modelling: A comparison of the different approaches used in seabirds. Comparative Biochemistry and Physiology Part A: Molecular & Integrative Physiology (3, vol. 158), pp. 358–365.

Frankish, C. K., A. M. Von Benda-Beckmann, J. Teilmann, J. Tougaard, R. Dietz, S. Sveegaard, B. Binnerts, C. A. F. De Jong & J. Nabe-Nielsen (2023) Ship noise causes tagged harbour porpoises to change direction or dive deeper. Marine Pollution Bulletin (vol. 197), p. 115755.

Furness, R. W., H. M. Wade & E. A. Masden (2013) Assessing vulnerability of marine bird populations to offshore wind farms. Journal of Environmental Management (vol. 119), pp. 56–66.

Garthe, S., N. Guse, W. A. Montevecchi, J.-F. Rail & F. Grégoire (2014) The daily catch: Flight altitude and diving behavior of northern gannets feeding on Atlantic mackerel. Journal of Sea Research (vol. 85), pp. 456–462.

Garthe, S. & O. Hüppop (2004) Scaling possible adverse effects of marine wind farms on seabirds: developing and applying a vulnerability index. Journal of Applied Ecology (4, vol. 41), pp. 724–734.

Garthe, S., H. Schwemmer, N. Markones, S. Müller & P. Schwemmer (2015) Verbreitung, Jahresdynamik und Bestandsentwicklung der Seetaucher *Gavia* spec. in der Deutschen Bucht (Nordsee). Vogelwarte (vol. 53), pp. 121–138.

Garthe, S., H. Schwemmer, M. Mercker, V. Dierschke, N. Markones, V. Peschko, P. Schwemmer & J. C. Krause (2025) Wind farms in proximity to marine protected areas put conservation targets at risk. Journal for Nature Conservation (126805, vol. 84).

Garthe, S., H. Schwemmer, V. Peschko, N. Markones, S. Müller, P. Schwemmer & M. Mercker (2023) Large-scale effects of offshore wind farms on seabirds of high conservation concern. Scientific Reports (4779, vol. 13).

Garthe, Stefan, Schwemmer, Henriette, Markones; Nele, Müller, Sabine & Schwemmer, Philipp (2015) Verbreitung, Jahresdynamik und Bestandsentwicklung der Seetaucher *Gavia* spec. in der Deutschen Bucht (Nordsee). Vogelwarte (vol. 53), pp. 121–138.

Gaynor, K. M., J. S. Brown, A. D. Middleton, M. E. Power & J. S. Brashares (2019) Landscapes of Fear: Spatial Patterns of Risk Perception and Response. Trends in Ecology & Evolution (4, vol. 34), pp. 355–368.

Gill, J. A., K. Norris & W. J. Sutherland (2001) Why behavioural responses may not reflect the population consequences of human disturbance. Biological Conservation (2, vol. 97), pp. 265–268.

Glutz von Blotzheim, U. N. & K. M. Bauer (1987) Handbuch der Vögel Mitteleuropas. Band 1 - Gaviformes - Phoenicopteriformes. Seetaucher, Lappentaucher, Sturmvögel, Ruderfüßler, Schreitvögel, Flamingos. (ed. Glutz von Blotzheim, U. N.). ED. 2., durchgesehene Auflage, publ. AULA-Verlag, pp. 483.

Goodale, M. (2018) Cumulative adverse effects of offshore wind energy development on wildlife. Dissertation, University of Massachusetts Amherst, pp. 142.

Grémillet, D., D. Chevallier & C. Guinet (2022) Big data approaches to the spatial ecology and conservation of marine megafauna. ICES Journal of Marine Science (4, vol. 79), pp. 975–986.

Grémillet, D. & S. Descamps (2023) Ecological impacts of climate change on Arctic marine megafauna. Trends in Ecology & Evolution (8, vol. 38), pp. 773–783.

Grimm, V., E. Revilla, U. Fricke, F. Jeltsch, W. M. Mooij, S. F. Railsback, H.-H. Thulke, J. Weiner, T. Wiegand & D. L. DeAngelis (2005) Pattern-Oriented Modeling of Agent-Based Complex Systems: Lessons from Ecology. Science (5750, vol. 310), pp. 987–991.

Grolemund, G. & H. Wickham (2011) Dates and Times Made Easy with lubridate. Journal of Statistical Software (3, vol. 40).

Grunst, M. L., A. S. Grunst, J. Fort & J. K. Grace (2025) Editorial: Bioenergetic and behavioral effects of rapid anthropogenic change and eco-evolutionary implications. Frontiers in Bird Science (vol. 4), p. 1654140.

Guse, N., S. Garthe & B. Schirmeister (2009) Diet of red-throated divers *Gavia stellata* reflects the seasonal availability of Atlantic herring *Clupea harengus* in the southwestern Baltic Sea. Journal of Sea Research (4, vol. 62), pp. 268–275.

Halsey, L. G., C.-A. Bost & Y. Handrich (2007) A thorough and quantified method for classifying seabird diving behaviour. Polar Biology (8, vol. 30), pp. 991–1004.

Hedd, A., P. M. Regular, W. A. Montevecchi, A. D. Buren, C. M. Burke & D. A. Fifield (2009) Going deep: common murres dive into frigid water for aggregated, persistent and slow-moving capelin. Marine Biology (4, vol. 156), pp. 741–751.

Heinänen, S., R. Žydelis, M. Dorsch, G. Nehls & H. Skov (2017) High-resolution sea duck distribution modeling: Relating aerial and ship survey data to food resources, anthropogenic pressures, and topographic variables. The Condor (2, vol. 119), pp. 175–190.

Heinänen, S., R. Žydelis, B. Kleinschmidt, M. Dorsch, C. Burger, J. Morkūnas, P. Quillfeldt & G. Nehls (2020) Satellite telemetry and digital aerial surveys show strong displacement of red-throated divers (*Gavia stellata*) from offshore wind farms. Marine Environmental Research (104989, vol. 160).

HELCOM (2013) HELCOM Red List Bird Expert Group 2013 www.helcom.fi > Baltic Sea trends > Biodiversity > Red List of species.

Hemmer, J. (2020) Red-throated diver: Gavia stellata. publ. Books on Demand.

Hemmingsson, E. & M. O. G. Eriksson (2002) Ringing of Red-throated Diver *Gavia stellata* Black-throated Diver *Gavia arctica* in Sweden. Wetlands International Diver/Loon Specialist Group Newsletter (4), pp. 8–13.

Hüppop, O., J. Dierschke, K. M. Exo, E. Fredrich & R. Hill (2006) Bird migration studies and potential collision risk with offshore wind turbines. Ibis (vol. 148), pp. 90–109.

Iannarilli, F., B. D. Gerber, J. Erb & J. R. Fieberg (2025) A 'how-to' guide for estimating animal diel activity using hierarchical models. Journal of Animal Ecology (2, vol. 94), pp. 182–194.

IPCC (2014) Climate Change 2014: Synthesis Report. Contribution of Working Groups I, II and III to the Fifth Assessment Report of the Intergovernmental Panel on Climate Change. (aut. IPCC; eds. Core Writing Team, R. K. Pachauri & L. A. Meyer). p. 151.

Jarrett, D., J. Calladine, A. Cotton, M. W. Wilson & E. Humphreys (2020) Behavioural responses of non-breeding waterbirds to drone approach are associated with flock size and habitat. Bird Study (2, vol. 67), pp. 190–196.

Jeltsch, F., M. Roeleke, A. Abdelfattah, R. Arlinghaus, G. Berg, N. Blaum, L. D. Meester, E. Dittmann, J. A. Eccard, B. Fournier, U. Gaedke, C. Gallagher, L. Govaert, M. Hauber, J. M. Jeschke, S. Kramer-Schadt, A. Linstädter, U. Lucke, V. Mazza, R. Metzler, C. Nendel, V. Radchuk, M. C. Rillig, M. Ryo, K. Scheiter, R. Tiedemann, B. Tietjen, C. C. Voigt, G. Weithoff, J. Wolinska & D. Zurell (2025) The need for an individual-based global change ecology. Individual-based Ecology (vol. 1), p. e148200.

Johnston, A., A. S. C. P. Cook, L. J. Wright, E. M. Humphreys & N. H. K. Burton (2014) Modelling flight heights of marine birds to more accurately assess collision risk with offshore wind turbines. Journal of Applied Ecology (1, vol. 51), pp. 31–41.

Kenow, K., L. Fara, S. Houdek, B. Gray, D. Heard, M. Meyer, T. Fox, R. Kratt & C. Henderson (2023) Dive characteristics of Common Loons wintering in the Gulf of Mexico and off the southern U.S. Atlantic coast. Journal of Field Ornithology (1, vol. 94), p. art1.

Kleinschmidt, B., C. Burger, P. Bustamante, M. Dorsch, S. Heinänen, J. Morkūnas, R. Žydelis, G. Nehls & P. Quillfeldt (2022) Annual movements of a migratory seabird—the NW European red-throated diver (*Gavia stellata*)—reveals high individual repeatability but low migratory connectivity. Marine Biology (114, vol. 169).

Kleinschmidt, B., C. Burger, M. Dorsch, G. Nehls, S. Heinänen, J. Morkūnas, R. Žydelis, R. J. Moorhouse-Gann, H. Hipperson, W. O. C. Symondson & P. Quillfeldt (2019) The diet of red-throated divers (*Gavia stellata*) overwintering in the German Bight (North Sea) analysed using molecular diagnostics. Marine Biology (6, vol. 166), p. 77.

Van der Kolk, H., B. J. Ens, K. Oosterbeek, E. Jongejans & M. Van de Pol (2021) The hidden cost of disturbance: Eurasian Oystercatchers (*Haematopus ostralegus*) avoid a disturbed roost site during the tourist season. Ibis.

Van Kooten, T., F. Soudijn, I. Tulp, C. Chen, D. Benden & M. Leopold (2019) The consequences of seabird habitat loss from offshore wind turbines, version 2. Displacement and population level effects in 5 selected species. no. Wageningen Marine Research report C063/19, p. 116.

Korschgen, C. E., K. P. Kenow, A. Gendron-Fitzpatrick, W. L. Green & F. J. Dein (1996) Implanting Intra-Abdominal Radiotransmitters with External Whip Antennas in Ducks. The Journal of Wildlife Management (1, vol. 60), pp. 132–137.

Lamb, J., J. Gulka, E. Adams, A. Cook & K. A. Williams (2024) A synthetic analysis of post-construction displacement and attraction of marine birds at offshore wind energy installations. Environmental Impact Assessment Review (107611, vol. 108).

Langley, L. P., S. D. J. Lang, L. Ozsanlav-Harris & A. M. Trevail (2024) ExMove : An open-source toolkit for processing and exploring animal-tracking data in R. Journal of Animal Ecology (7, vol. 93), pp. 784–795.

Langton, R., I. M. Davies & B. E. Scott (2014) A simulation model coupling the behaviour and energetics of a breeding central place forager to assess the impact of environmental changes. Ecological Modelling (vol. 273), pp. 31–43.

Lovvorn, J. R. (2001) Upstroke Thrust, Drag Effects, and Stroke-glide Cycles in Wing-propelled Swimming by Birds. American Zoologist (2, vol. 41), pp. 154–165.

Luque, S. P. (2007) Diving Behaviour Analysis in R. R news, Institution: Comprehensive R Archive Network, p. 1.6.4.

Masden, E. (2015) Developing an avian collision risk model to incorporate variability and uncertainty. p. 26.

Masden, E. A., D. T. Haydon, A. D. Fox & R. W. Furness (2010) Barriers to movement: modelling energetic costs of avoiding marine wind farms amongst breeding seabirds. Marine Pollution Bulletin (7, vol. 60), pp. 1085–1091.

Mendel, B., P. Schwemmer, V. Peschko, S. Müller, H. Schwemmer, M. Mercker & S. Garthe (2019) Operational offshore wind farms and associated ship traffic cause profound changes in distribution patterns of Loons (*Gavia spp.*). Journal of Environmental Management (vol. 231), pp. 429–438.

Mendel, B., N. Sonntag, J. Wahl, P. Schwemmer, H. Dries, N. Guse, S. Müller & S. Garthe (2008) Artensteckbriefe von See- und Wasservögeln der deutschen Nord- und Ostsee: Verbreitung, Ökologie und Empfindlichkeiten gegenüber Eingriffen in ihren marinen Lebensraum. (ed. Bundesamt für Naturschutz). in Naturschutz und biologische Vielfalt / no. 59, pp. 437.

Metropolis, N., A. W. Rosenbluth, M. N. Rosenbluth, A. H. Teller & E. Teller (1953) Equation of State Calculations by Fast Computing Machines. The Journal of Chemical Physics (6, vol. 21), pp. 1087–1092.

Monaghan, P., P. Walton, S. Wanless, J. D. Uttley & M. D. Bljrns (1994) Effects of prey abundance on the foraging behaviour, diving efficiency and time allocation of breeding Guillemots *Uria aalge*. Ibis (2, vol. 136), pp. 214–222.

Monier, S. A. (2024) Social interactions and information use by foraging seabirds. Biological Reviews (5, vol. 99), pp. 1717–1735.

Morris, M. D. (1991) Factorial Sampling Plans for Preliminary Computational Experiments. Technometrics (2, vol. 33), pp. 161–174.

Mulcahy, D. M. & D. N. Esler (1999) Surgical and immediate postrelease mortality of harlequin ducks (*Histrionicus histrionicus*) implanted with abdominal radio transmitters with percutaneous antennae. Journal of Zoo and Wildlife Medicine (3, vol. 30), p. 397401.

Müller, K. (2017) here: A Simpler Way to Find Your Files. Institution: Comprehensive R Archive Network, p. 1.0.2.

Norberg, R. Å. & U. M. Norberg (1971) Take-Off, Landing, and Flight Speed during Fishing Flights of *Gavia stellata* (Pont.). Ornis Scandinavica (1, vol. 2), p. 55.

Norris, D. R. & C. M. Taylor (2006) Predicting the consequences of carry-over effects for migratory populations. Biology Letters (1, vol. 2), pp. 148–151.

Okill, J. D. (1992) Natal dispersal and breeding site fidelity of red-throated Divers *Gavia stellata* in Shetland. Ringing & Migration (1, vol. 13), pp. 57–58.

Oliver, T. H. & D. B. Roy (2015) The pitfalls of ecological forecasting. Biological Journal of the Linnean Society (3, vol. 115), pp. 767–778.

Pebesma, E. (2018) Simple Features for R: Standardized Support for Spatial Vector Data. The R Journal (1, vol. 10), pp. 439–446.

performance (2021) performance: An R Package for Assessment, Comparison and Testing of Statistical Models. (auts. Lüdecke, D., M. Ben-Shachar, I. Patil, P. Waggoner & D. Makowski). Journal of Open Source Software (60, vol. 6), p. 3139.

Peschko, V., B. Mendel, S. Müller, N. Markones, M. Mercker & S. Garthe (2020a) Effects of offshore windfarms on seabird abundance: Strong effects in spring and in the breeding season. Marine Environmental Research (vol. 162), p. 105157.

Peschko, V., M. Mercker & S. Garthe (2020b) Telemetry reveals strong effects of offshore wind farms on behaviour and habitat use of common guillemots (*Uria aalge*) during the breeding season. Marine Biology (118, vol. 167).

Peschko, V., H. Schwemmer, M. Mercker, N. Markones, K. Borkenhagen & S. Garthe (2024) Cumulative effects of offshore wind farms on common guillemots (*Uria aalge*) in the southern North Sea - climate versus biodiversity? Biodiversity and Conservation.

Petersen, I. K. & A. D. Fox (2007) Changes in bird habitat utilisation around the Horns Rev 1 offshore wind farm, with particular emphasis on Common Scoter. Report request, Commissioned by Vattenfall A/S, p. 36.

Petersen, I. K., A. D. Fox & J. Kahlert (2008) Waterbird distribution in and around the Nysted offshore wind farm, 2007. p. 42.

Phillips, R. A., J. Fort & M. P. Dias (2023) Conservation status and overview of threats to seabirds. in Conservation of Marine Birds, publ. Elsevier, pp. 33–56.

Phillips, R. A., S. Lewis, J. González-Solís & F. Daunt (2017) Causes and consequences of individual variability and specialization in foraging and migration strategies of seabirds. Marine Ecology Progress Series (vol. 578), pp. 117–150.

Pigeault, R., A. Ruser, N. C. Ramírez-Martínez, S. C. V. Geelhoed, J. Haelters, D. A. Nachtsheim, T. Schaffeld, S. Sveegaard, U. Siebert & A. Gilles (2024) Maritime traffic alters distribution of the harbour porpoise in the North Sea. Marine Pollution Bulletin (116925, vol. 208).

Piper, W. H., M. R. Glines & K. C. Rose (2024) Climate change-associated declines in water clarity impair feeding by common loons. Ecology (5, vol. 105), p. e4291.

Van de Pol, M. & J. Wright (2009) A simple method for distinguishing within- versus between-subject effects using mixed models. Animal Behaviour (3, vol. 77), pp. 753–758.

R Core Team (2022) R: A language and environment for statistical computing, R version 4.2.2.

Regular, P. M., G. K. Davoren, A. A. Hedd & W. A. Montevecchi (2010) Crepuscular foraging by a pursuit-diving seabird: tactics of common murres in response to the diel vertical migration of capelin. Marine Ecology Progress Series (vol. 415), pp. 295–304.

Regular, P. M., A. Hedd & W. A. Montevecchi (2011) Fishing in the Dark: A Pursuit-Diving Seabird Modifies Foraging Behaviour in Response to Nocturnal Light Levels. PLoS ONE (10, vol. 6), p. e26763.

Ricker, M. & E. V. Stanev (2020) Circulation of the European northwest shelf: a Lagrangian perspective. Ocean Science (3, vol. 16), pp. 637–655.

Sandvik, H., K. E. Erikstad, P. Fauchald & T. Tveraa (2008) High survival of immatures in a long-lived seabird: insights from a long-term study of the atlantic puffin (*Fratercula arctica*). The Auk (3, vol. 125), pp. 723–730.

Santon, M., F. Korner-Nievergelt, N. K. Michiels & N. Anthes (2023) A versatile workflow for linear modelling in R. Frontiers in Ecology and Evolution (vol. 11), p. 1065273.

Scheffer, M., J. M. Baveco, D. L. DeAngelis, K. A. Rose & E. H. Van Nes (1995) Super-individuals a simple solution for modelling large populations on an individual basis. Ecological Modelling (2, vol. 80), pp. 161–170.

Schielzeth, H. (2010) Simple means to improve the interpretability of regression coefficients. Methods in Ecology and Evolution (2, vol. 1), pp. 103–113.

Schuster, E., L. Bulling & J. Köppel (2015) Consolidating the State of Knowledge: A Synoptical Review of Wind Energy's Wildlife Effects. Environmental Management (2, vol. 56), pp. 300–331.

Schwemmer, H., N. Markones, S. Müller, K. Borkenhagen, M. Mercker & S. Garthe (2019) Aktuelle Bestandsgröße und -entwicklung des Sterntauchers (*Gavia stellata*) in der deutschen Nordsee. Berichtfür das Bundesamt für Seeschifffahrt und Hydrographie und das Bundesamt für Naturschutz.

Schwemmer, P., B. Mendel, N. Sonntag, V. Dierschke & S. Garthe (2011) Effects of ship traffic on seabirds in offshore waters: implications for marine conservation and spatial planning. Ecological Applications (5, vol. 21), pp. 1851–1860.

Scott, I., P. I. Mitchell & P. R. Evans (1994) Seasonal changes in body mass, body composition and food requirements in wild migratory birds. Proceedings of the Nutrition Society (3, vol. 53), pp. 521–531.

Scott-Hayward, L., I. Krag Petersen, M. MacKenzie, C. L. Pedersen, S. Isojunno, R. Due Nilson, J. Sterup, H. M. Thomsen & R. S. Neergaard (2025) Bird distribution responses to wind farms, Horns Rev. (ed. Energinet Eltransmission A/S). in Changes in the distribution and abundance of common scoter and diver species in the Horns Rev I, II and III offshore windfarm areas, Denmark, 2025.

Scott-Hayward, L., I. K. Petersen, M. MacKenzie, C. L. Pedersen, S. Isojunno, R. D. Nielsen, J. Sterup, H. M. Thomsen & R. S. Neergaard (2024) Changes in the distribution and abundance of common scoter and diver species in the Horns Rev I, II and III offshore windfarm areas, Denmark.

Searle, K. R., D. C. Mobbs, A. Butler, R. W. Furness, M. N. Trinder & F. Daunt (2018) Finding out the Fate of Displaced Birds (FCR/2015/19): Scottish Marine and Freshwater Science Vol 9 No 8.

Shoji, A., K. Elliott, A. Fayet, D. Boyle, C. Perrins & T. Guilford (2015) Foraging behaviour of sympatric razorbills and puffins. Marine Ecology Progress Series (vol. 520), pp. 257–267.

Skov, H., J. Durinck, M. F. Leopold & M. L. Tasker (1995) Important bird areas for seabirds in the North Sea. publ. BirdLife International.

Skov, H., S. Heinänen, R. Žydelis, J. Bellebaum, S. Bzoma, M. Dagys, J. Durinck, S. Garthe, G. Grishanov, M. Hario, J. J. Kieckbusch, J. Kube, A. Kuresoo, K. Larsson, L. Luigujoe, W. Meissner, H. W. Nehls, L. Nilsson, I. K. Petersen, M. M. Roos, S. Pihl, N. Sonntag, A. Stock, A. Stipniece & J. Wahl (2011) Waterbird populations and pressures in the Baltic Sea. in TemaNord, publ. Nordic Council of Ministers, pp. 201.

Skov, H. & E. Prins (2001) Impact of estuarine fronts on the dispersal of piscivorous birds in the German Bight. Marine Ecology Progress Series (vol. 214), pp. 279–287.

Sobol', I. M. (2001) Global sensitivity indices for nonlinear mathematical models and their Monte Carlo estimates. Mathematics and Computers in Simulation (1–3, vol. 55), pp. 271–280.

Spiegel, C. S., A. M. Berlin, A. T. Gilbert, C. O. Gray, W. A. Montevecchi, I. J. Stenhouse, S. L. Ford, G. H. Olsen, J. L. Fiely, L. Savoy, M. W. Goodale & C. M. Burke (2017) Determining fine-scale use and movement patterns of diving bird species in federal waters of the Mid-Atlantic United States using satellite telemetry. no. OCS Study BOEM 2017-069, Technical Report, Prepared under BOEM Intra-agency Agreement #M12PG00005, p. 204.

Stanev, E. V., B. Jacob & J. Pein (2019) German Bight estuaries: An inter-comparison on the basis of numerical modeling. Continental Shelf Research (vol. 174), pp. 48–65.

Stenberg, C., J. G. Støttrup, M. Van Van Deurs, C. W. Berg, G. E. Dinesen, H. Mosegaard, T. M. Grome & S. B. Leonhard (2015) Long-term effects of an offshore wind farm in the North Sea on fish communities. Marine Ecology Progress Series (vol. 528), pp. 257–265.

Stillman, R. A. (2008) MORPH—an individual-based model to predict the effect of environmental change on foraging animal populations. Ecological modelling (3–4, vol. 216), pp. 265–276.

Sutherland, W. J. (1997) From Individual Behaviour to Population Ecology. vol. 66 out of, publ. Oxford University Press, pp. 224.

The ODD protocol (2010) The ODD protocol: A review and first update. (auts. Grimm, V., U. Berger, D. L. DeAngelis, J. G. Polhill, J. Giske & S. F. Railsback). Ecological Modelling (23, vol. 221), pp. 2760–2768.

Thieurmel, B. & A. El Marhraoui (2022) suncalc: Compute Sun Position, Sunlight Phases, Moon Position and Lunar Phase.

Thompson, S. A. & J. J. Price (2006) Water Clarity and Diving Behavior in Wintering Common Loons. Waterbirds (2, vol. 29), pp. 169–175.

Tomlinson, S., S. G. Arnall, A. Munn, S. D. Bradshaw, S. K. Maloney, K. W. Dixon & R. K. Didham (2014) Applications and implications of ecological energetics. Trends in Ecology & Evolution (5, vol. 29), pp. 280–290.

Topping, C. & I. K. Petersen (2011) Report on a red-throated diver agent-based model to assess the cumulative impact from offshore wind farms. Reprot comissioned by the Environmental Group, p. 44.

UNEP/AEWA Secretariat (2022) Agreement on the Conservation of African-Eurasian Migratory Waterbirds (AEWA). Agreement Text and Annexes - As amended at the 8th Session of the Meeting of the Parties to AEWA 26 - 30 September 2022, Budapest, Hungary. pp. 61.

Vilela, R., C. Burger, A. Diederichs, F. E. Bachl, L. Szostek, A. Freund, A. Braasch, J. Bellebaum, B. Beckers, W. Piper & G. Nehls (2021) Use of an INLA latent gaussian modeling approach to assess bird population changes due to the development of offshore wind farms. Frontiers in Marine Science (701332, vol. 8).

Vilela, R., C. Burger, A. Diederichs, F. Bachl, L. Szostek, A. Freund, A. Braasch, B. Beckers, W. Piper & G. Nehls (2022) Divers (Gavia spp.) in the German North Sea: Recent Changes in Abundance and Effects of Offshore Wind Farms. (eds. BioConsult SH, IBL Umweltplanung & IfAÖ). Final Report, p. 59.

Vilela, R., C. Burger, A. Diederichs, G. Nehls, F. Bachl, L. Szostek, A. Freund, A. Braasch, J. Bellebaum, B. Beckers & W. Piper (2020) Divers (*Gavia spp.*) in the German North Sea: Changes in abundance and effects of Offshore Wind Farms. A study into diver abundance and distribution based on aerial survey data in the German North Sea. Prepared for Bundesverband der Windparkbetreiber Offshore e.V.

Vindenes, H., K. A. Orvik, H. Søiland & H. Wehde (2018) Analysis of tidal currents in the North Sea from shipboard acoustic Doppler current profiler data. Continental Shelf Research (vol. 162), pp. 1–12.

Warwick-Evans, V., P. W. Atkinson, I. Walkington & J. A. Green (2018) Predicting the impacts of wind farms on seabirds: An individual-based model. Journal of Applied Ecology (2, vol. 55), pp. 503–515.

Webster, M. M. & C. Rutz (2020) How STRANGE are your study animals? Nature (7812, vol. 582), pp. 337–340.

Whitworth, D. L., J. Y. Takekawa, H. R. Carter & W. R. McIver (1997) A Night-Lighting Technique for At-Sea Capture of Xantus' Murrelets. Colonial Waterbirds (3, vol. 20), pp. 525–531.

Wickham, H., M. Averick, J. Bryan, W. Chang, L. McGowan, R. François, G. Grolemund, A. Hayes, L. Henry, J. Hester, M. Kuhn, T. Pedersen, E. Miller, S. Bache, K. Müller, J. Ooms, D. Robinson, D. Seidel, V. Spinu, K. Takahashi, D. Vaughan, C. Wilke, K. Woo & H. Yutani (2019) Welcome to the Tidyverse. Journal of Open Source Software (43, vol. 4), p. 1686.

Yates, K. L., P. J. Bouchet, M. J. Caley, K. Mengersen, C. F. Randin, S. Parnell, A. H. Fielding, A. J. Bamford, S. Ban, A. M. Barbosa, C. F. Dormann, J. Elith, C. B. Embling, G. N. Ervin, R. Fisher, S. Gould, R. F. Graf, E. J. Gregr, P. N. Halpin, R. K. Heikkinen, S. Heinänen, A. R. Jones, P. K. Krishnakumar, V. Lauria, H. Lozano-Montes, L. Mannocci, C. Mellin, M. B. Mesgaran, E. Moreno-Amat, S. Mormede, E. Novaczek, S. Oppel, G. Ortuño Crespo, A. T. Peterson, G. Rapacciuolo, J. J. Roberts, R. E. Ross, K. L. Scales, D. Schoeman, P. Snelgrove, G. Sundblad, W. Thuiller, L. G. Torres, H. Verbruggen, L. Wang, S. Wenger, M. J. Whittingham, Y. Zharikov, D. Zurell & A. M. M. Sequeira (2018) Outstanding Challenges in the Transferability of Ecological Models. Trends in Ecology & Evolution (10, vol. 33), pp. 790–802.

A APPENDIX

A.1 Chapter 5: Foraging patterns of red-throated divers in the German Bight and the effect of offshore wind farms

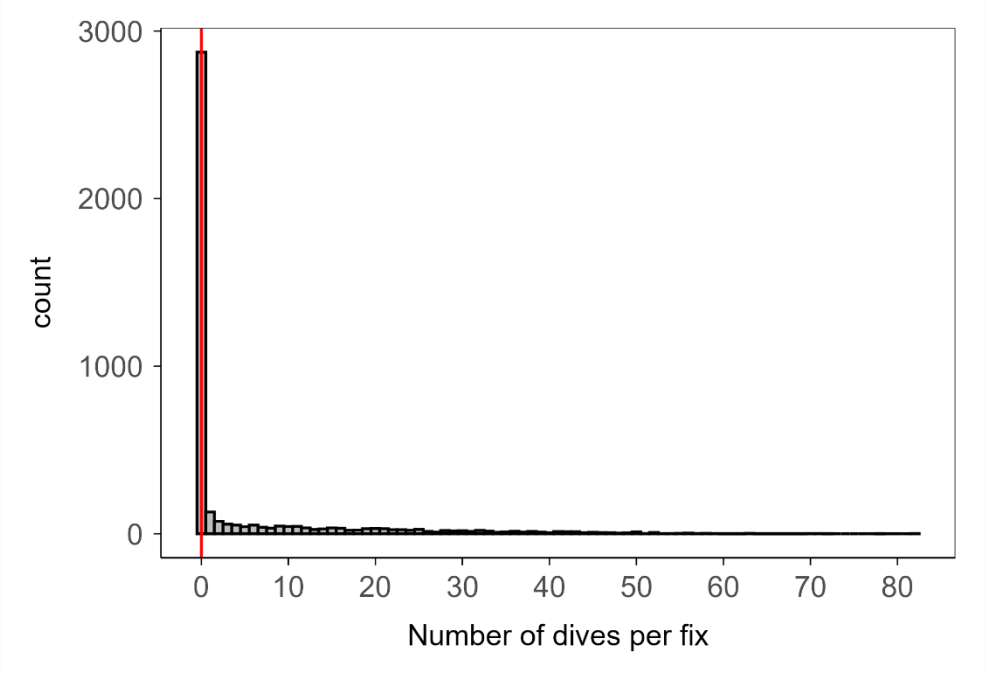

Fig. A 1 *Distribution of the number of dives occurring per GPS fix, when considering locations with and without dives. Note the large zero inflation due to the large number of fixes which showed no diving behaviour.*

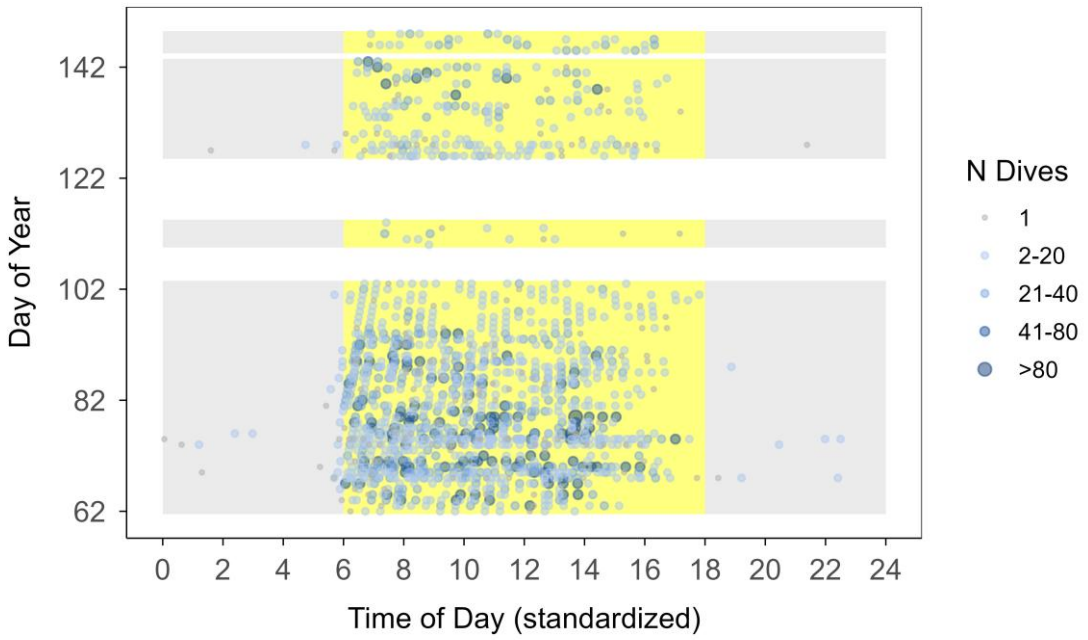

Fig. A 2 *Figure showing the intensity of dive behaviour (number of dives at a location) over the time of day across days of the year with time standardized. Darker blue shades and larger points indicate more dives at a location.*

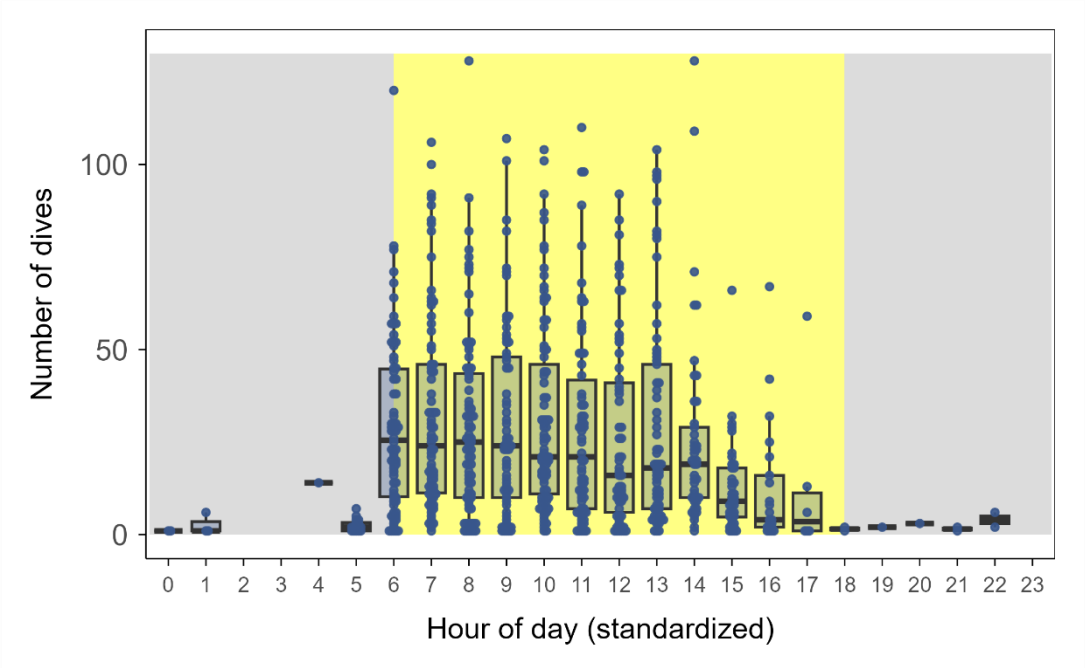

Fig. A 3 *The distribution of the number of dives per hour over the hours of a day across all days of monitoring with time standardized relative to dawn and dusk times. Boxplots used to indicate the distribution of number of dives per hour.*

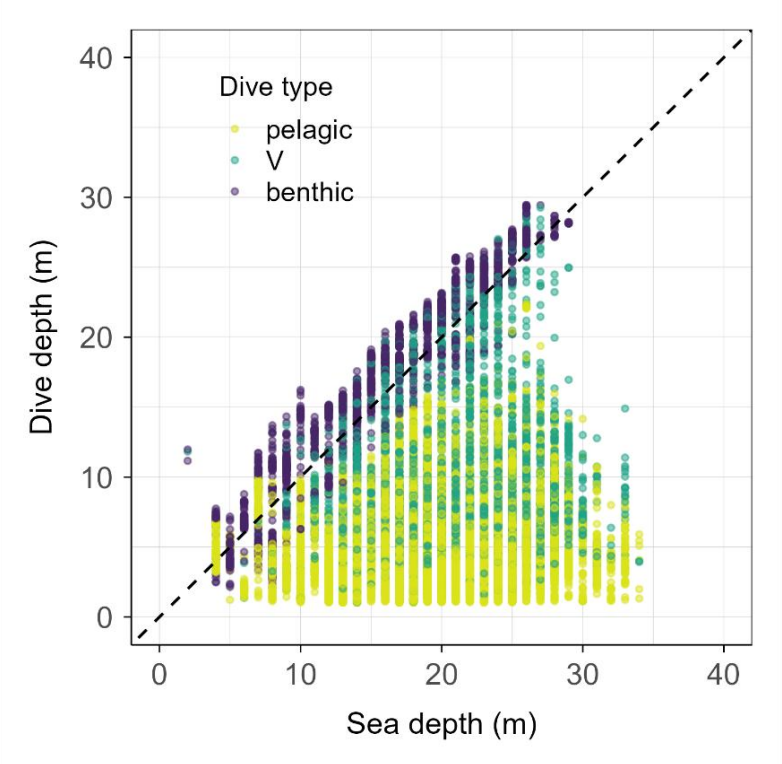

Fig. A 4 *The dive depth of each dive plotted against the sea depth at the location of the dive. Indicated using colour are the three different types of dives as classified in this study (see Methods).*

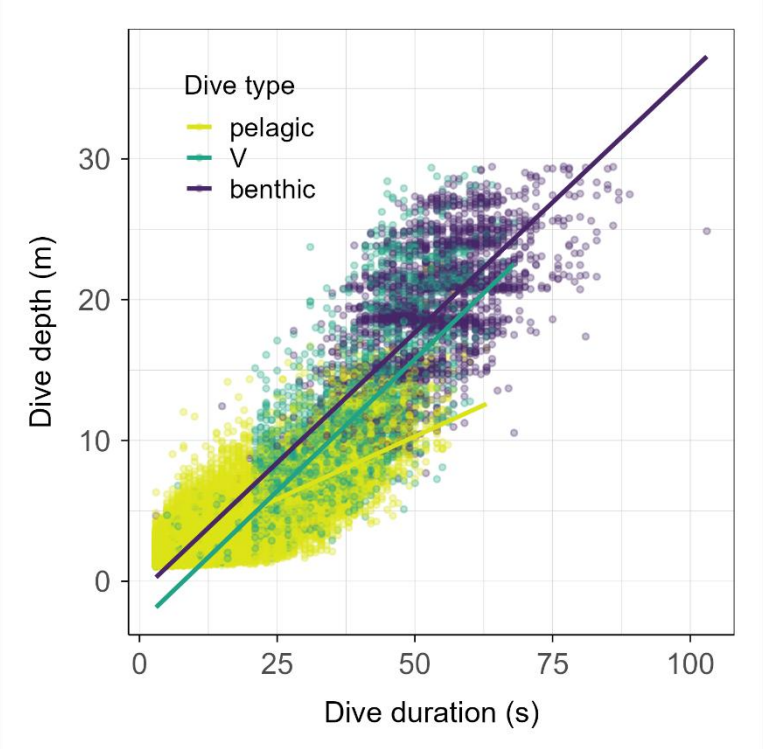

Fig. A 5 *The dive depth of each dive plotted against the dive duration of each dive. Indicated using colour are the three different types of dives as classified in this study (see Methods). Shown additionally are the dive-type-specific regression lines.*

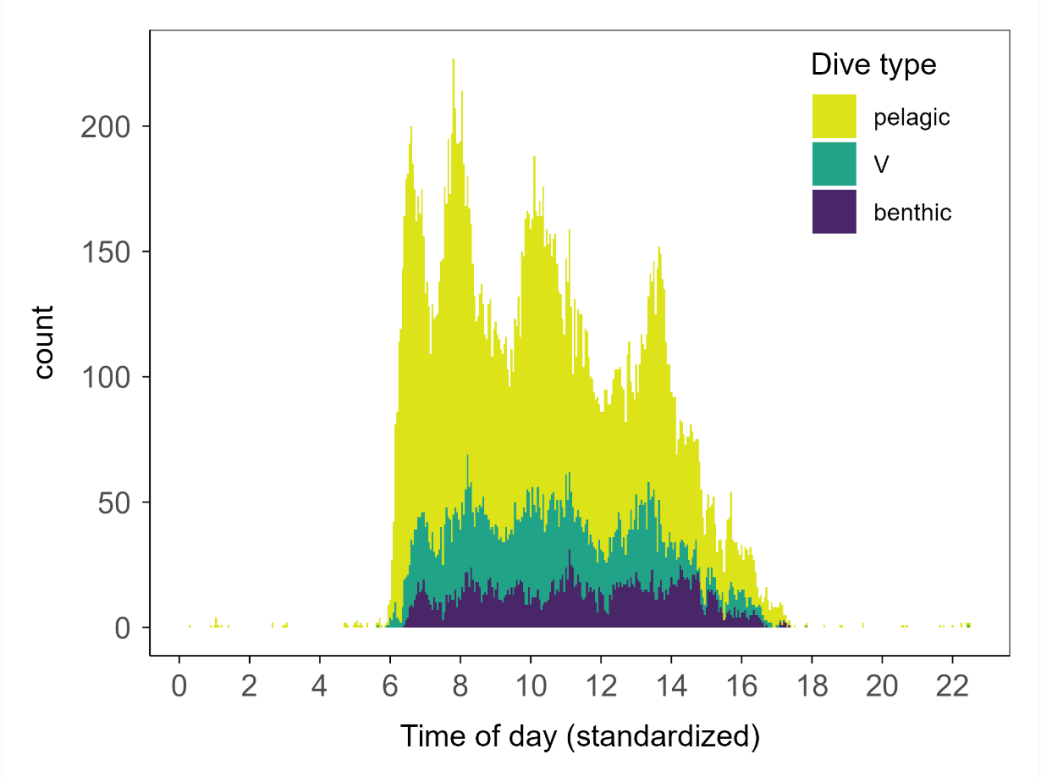

Fig. A 6 *A distribution showing the number of dives of each dive type (pelagic, V-dive and benthic) occurring over the day, after standardizing time of day to dawn (06:00) and dusk (18:00).*

A.2 Chapter 6: Time-Energy Budgets and Movement Patterns

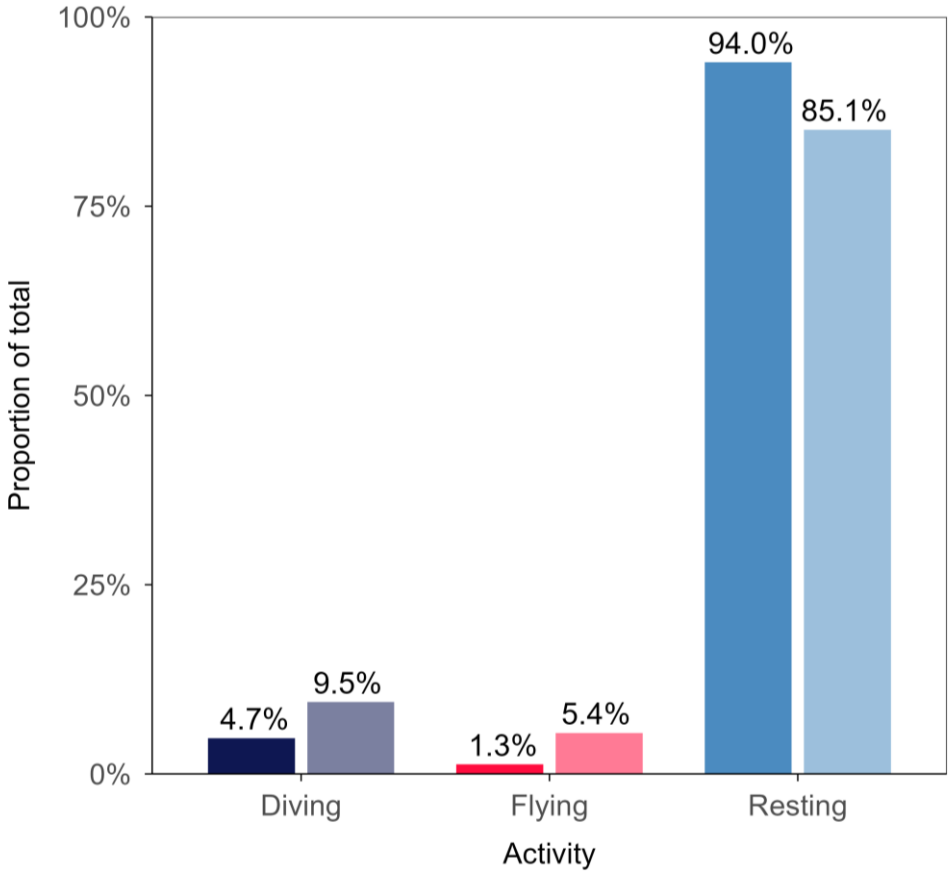

Fig. A 7 *A comparison of the percentage of time versus energy spent in different activities within the focal area across all individuals. Solid colours indicate time, while faded colours indicate energy.*

A.3 Chapter 7: Habitat model

Below, the statistical output of all 10 sub-models is given.

```
> model_sub1
Spatial model fit by ML ['sdmTMB']
Formula: ID ~ s(depth, k = 5) + s(sal, k = 5) + AIShotspot + owf + (1 |
 Formula:     tag_id)
Mesh: mesh (isotropic covariance)
Data: occurrence1
Family: binomial(link = 'logit')

              coef.est coef.se
(Intercept)      -3.57    0.93
AIShotspot       -0.04    0.02
owf2(0-5km)       1.33    0.58
owf3(5-10km)      1.24    0.62
owf4(10-15km)     1.66    0.66
owf5(>15km)       1.65    0.69
sdepth           -1.01    0.60
ssal              0.10    0.16

Smooth terms:
           Std. Dev.
sds(depth)      3.11
sds(sal)        7.29

Random intercepts:
       Std. Dev.
tag_id      0.25

Matérn range: 47.46
Spatial SD: 1.71
ML criterion at convergence: 2148.957
```

```
> model_sub2
Spatial model fit by ML ['sdmTMB']
Formula: ID ~ s(depth, k = 5) + s(sal, k = 5) + AIShotspot + owf + (1 |
 Formula:     tag_id)
Mesh: mesh2 (isotropic covariance)
Data: occurrence2
Family: binomial(link = 'logit')

              coef.est coef.se
(Intercept)      -3.86    1.00
AIShotspot       -0.05    0.02
owf2(0-5km)       1.48    0.53
owf3(5-10km)      1.53    0.56
owf4(10-15km)     1.85    0.60
owf5(>15km)       1.99    0.64
sdepth           -0.61    0.43
ssal              0.18    0.16

Smooth terms:
           Std. Dev.
sds(depth)      2.19
sds(sal)        8.73

Random intercepts:
       Std. Dev.
tag_id      0.26

Matérn range: 56.15
Spatial SD: 1.75
ML criterion at convergence: 2167.260

See ?tidy.sdmTMB to extract these values as a data frame.
```

```
> model_sub3
Spatial model fit by ML ['sdmTMB']
Formula: ID ~ s(depth, k = 5) + s(sal, k = 5) + AIShotspot + owf + (1 |
 Formula:     tag_id)
Mesh: mesh3 (isotropic covariance)
Data: occurrence3
Family: binomial(link = 'logit')

              coef.est coef.se
(Intercept)      -3.16    0.93
AIShotspot       -0.05    0.02
owf2(0-5km)       0.81    0.48
owf3(5-10km)      0.82    0.52
owf4(10-15km)     1.46    0.56
owf5(>15km)       1.51    0.59
sdepth            1.93    0.69
ssal             -0.09    0.17

Smooth terms:
           Std. Dev.
sds(depth)      8.44
sds(sal)        9.34

Random intercepts:
       Std. Dev.
tag_id      0.24

Matérn range: 53.54
Spatial SD: 1.73
ML criterion at convergence: 2157.113

> model_sub4
Spatial model fit by ML ['sdmTMB']
Formula: ID ~ s(depth, k = 5) + s(sal, k = 5) + AIShotspot + owf + (1 |
 Formula:     tag_id)
Mesh: mesh4 (isotropic covariance)
Data: occurrence4
Family: binomial(link = 'logit')

              coef.est coef.se
(Intercept)      -3.05    0.76
AIShotspot       -0.06    0.02
owf2(0-5km)       0.83    0.56
owf3(5-10km)      0.80    0.61
owf4(10-15km)     1.05    0.66
owf5(>15km)       1.26    0.70
sdepth           -2.11    0.74
ssal              0.30    0.16

Smooth terms:
           Std. Dev.
sds(depth)      8.42
sds(sal)        5.91

Random intercepts:
       Std. Dev.
tag_id      0.14

Matérn range: 28.17
Spatial SD: 1.69
ML criterion at convergence: 2149.504
```

```
> model_sub5
Spatial model fit by ML ['sdmTMB']
Formula: ID ~ s(depth, k = 5) + s(sal, k = 5) + AIShotspot + owf + (1 |
 Formula:     tag_id)
Mesh: mesh5 (isotropic covariance)
Data: occurrence5
Family: binomial(link = 'logit')

              coef.est coef.se
(Intercept)      -4.23    1.04
AIShotspot       -0.07    0.02
owf2(0-5km)       1.62    0.56
owf3(5-10km)      1.89    0.59
owf4(10-15km)     2.26    0.62
owf5(>15km)       2.42    0.65
sdepth            0.85    0.59
ssal              0.33    0.15

Smooth terms:
           Std. Dev.
sds(depth)      4.61
sds(sal)        4.93

Random intercepts:
       Std. Dev.
tag_id      0.19

Matérn range: 58.53
Spatial SD: 1.75
ML criterion at convergence: 2144.038

> model_sub6
Spatial model fit by ML ['sdmTMB']
Formula: ID ~ s(depth, k = 5) + s(sal, k = 5) + AIShotspot + owf + (1 |
 Formula:     tag_id)
Mesh: mesh6 (isotropic covariance)
Data: occurrence6
Family: binomial(link = 'logit')

              coef.est coef.se
(Intercept)      -3.96    0.99
AIShotspot       -0.03    0.02
owf2(0-5km)       1.68    0.66
owf3(5-10km)      1.86    0.69
owf4(10-15km)     1.97    0.72
owf5(>15km)       2.13    0.75
sdepth           -0.87    0.48
ssal             -0.09    0.17

Smooth terms:
           Std. Dev.
sds(depth)      2.18
sds(sal)        8.78

Random intercepts:
       Std. Dev.
tag_id      0.27

Matérn range: 50.24
Spatial SD: 1.65
ML criterion at convergence: 2162.162
```

```
> model_sub7
Spatial model fit by ML ['sdmTMB']
Formula: ID ~ s(depth, k = 5) + s(sal, k = 5) + AIShotspot + owf + (1 |
 Formula:     tag_id)
Mesh: mesh7 (isotropic covariance)
Data: occurrence7
Family: binomial(link = 'logit')

              coef.est coef.se
(Intercept)      -4.97    1.53
AIShotspot       -0.06    0.02
owf2(0-5km)       1.84    0.57
owf3(5-10km)      2.12    0.61
owf4(10-15km)     2.62    0.64
owf5(>15km)       2.85    0.67
sdepth            0.17    0.21
ssal              0.16    0.17

Smooth terms:
           Std. Dev.
sds(depth)      0.00
sds(sal)       11.48

Random intercepts:
       Std. Dev.
tag_id      0.28

Matérn range: 79.05
Spatial SD: 2.28
ML criterion at convergence: 2127.427

See ?tidy.sdmTMB to extract these values as a data frame.

> model_sub8
Spatial model fit by ML ['sdmTMB']
Formula: ID ~ s(depth, k = 5) + s(sal, k = 5) + AIShotspot + owf + (1 |
 Formula:     tag_id)
Mesh: mesh8 (isotropic covariance)
Data: occurrence8
Family: binomial(link = 'logit')

              coef.est coef.se
(Intercept)      -3.34    1.64
AIShotspot       -0.07    0.02
owf2(0-5km)       0.89    0.47
owf3(5-10km)      1.01    0.51
owf4(10-15km)     1.09    0.56
owf5(>15km)       1.08    0.60
sdepth           -0.01    0.62
ssal             -0.01    0.16

Smooth terms:
           Std. Dev.
sds(depth)      0.85
sds(sal)        8.15

Random intercepts:
       Std. Dev.
tag_id      0.29

Matérn range: 76.84
Spatial SD: 2.54
ML criterion at convergence: 2165.699
```

```
> model_sub9
Spatial model fit by ML ['sdmTMB']
Formula: ID ~ s(depth, k = 5) + s(sal, k = 5) + AIShotspot + owf + (1 |
 Formula:     tag_id)
Mesh: mesh9 (isotropic covariance)
Data: occurrence9
Family: binomial(link = 'logit')

              coef.est coef.se
(Intercept)      -2.84    0.70
AIShotspot       -0.05    0.02
owf2(0-5km)       0.51    0.45
owf3(5-10km)      0.71    0.49
owf4(10-15km)     1.01    0.53
owf5(>15km)       1.12    0.57
sdepth            1.12    0.47
ssal              0.20    0.16

Smooth terms:
           Std. Dev.
sds(depth)      2.91
sds(sal)        6.18

Random intercepts:
       Std. Dev.
tag_id      0.24

Matérn range: 38.74
Spatial SD: 1.41
ML criterion at convergence: 2192.269
```

```
> model_sub10
Spatial model fit by ML ['sdmTMB']
Formula: ID ~ s(depth, k = 5) + s(sal, k = 5) + AIShotspot + owf + (1 |
 Formula:     tag_id)
Mesh: mesh10 (isotropic covariance)
Data: occurrence10
Family: binomial(link = 'logit')

              coef.est coef.se
(Intercept)      -3.67    0.89
AIShotspot       -0.06    0.02
owf2(0-5km)       1.17    0.59
owf3(5-10km)      1.25    0.63
owf4(10-15km)     1.63    0.67
owf5(>15km)       1.86    0.70
sdepth           -2.26    0.88
ssal             -0.06    0.17

Smooth terms:
           Std. Dev.
sds(depth)      6.56
sds(sal)        9.90

Random intercepts:
       Std. Dev.
tag_id      0.37

Matérn range: 42.71
Spatial SD: 1.67
ML criterion at convergence: 2148.875
```

A.4 Chapter 9: Migratory Patterns of tagged Divers

A.4.1 Maps of individual birds

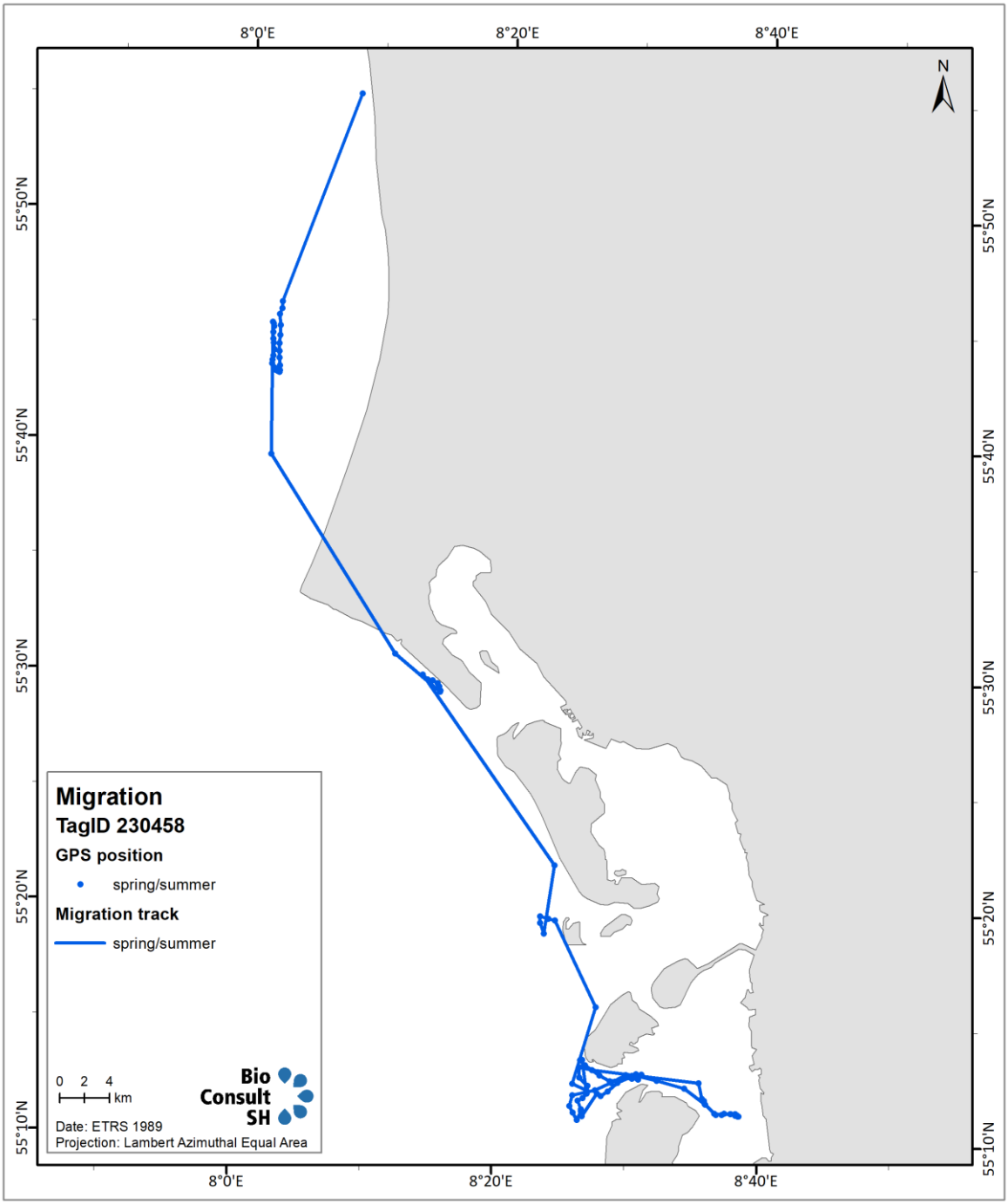
8°0'E
8°20'E
8°40'E
N
55°50'N
55°40'N
55°30'N
55°20'N
55°10'N
Migration
TagID 230458
GPS position
spring/summer
Migration track
spring/summer
0 2 4
km
Bio Consult SH
Date: ETRS 1989
Projection: Lambert Azimuthal Equal Area

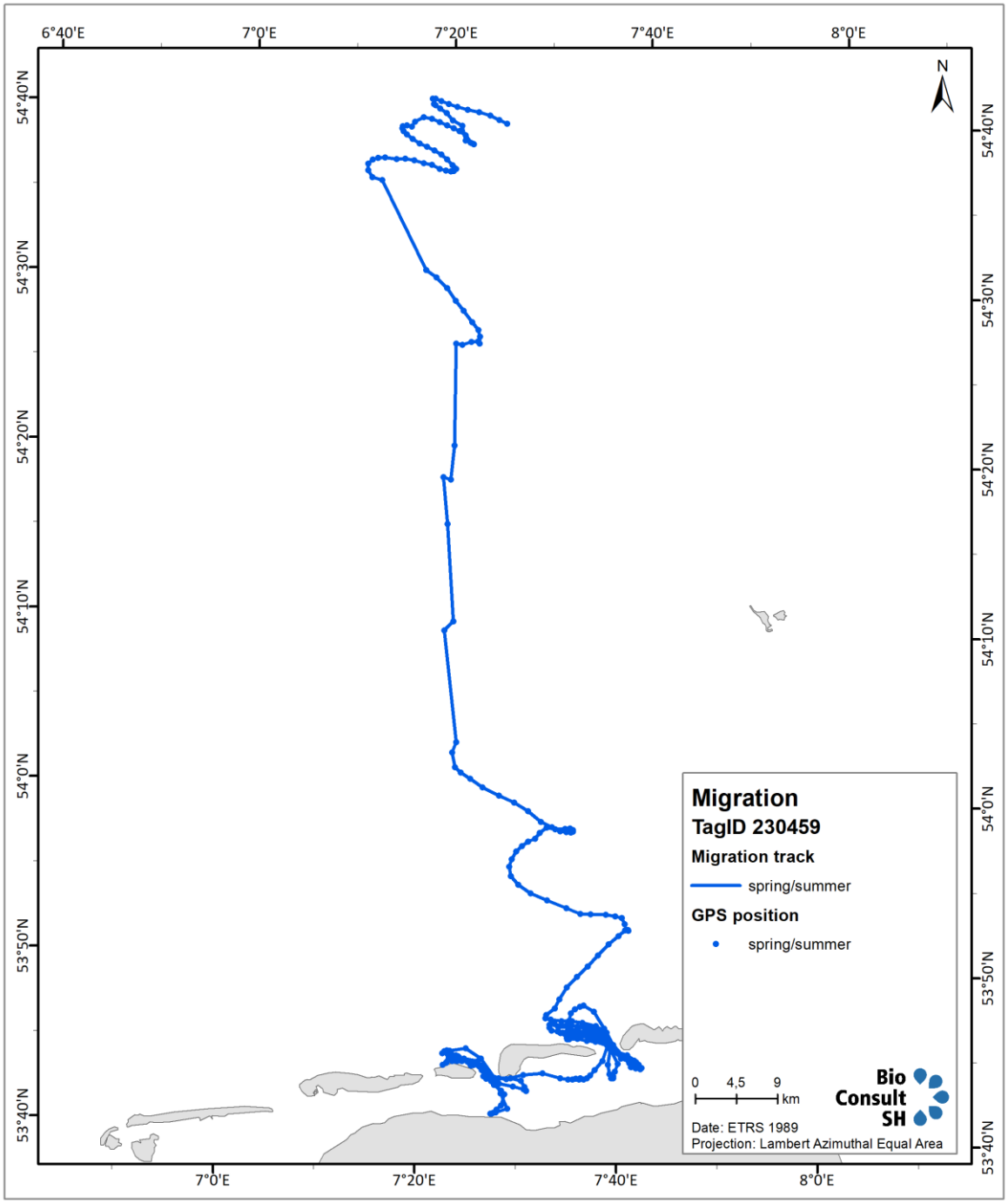
6°40'E
7°0'E
7°20'E
7°40'E
8°0'E
54°40'N
54°30'N
54°20'N
54°10'N
54°0'N
53°50'N
53°40'N
N
Migration
TagID 230459
Migration track
spring/summer
GPS position
spring/summer
0 4,5 9
km
Bio Consult SH
Date: ETRS 1989
Projection: Lambert Azimuthal Equal Area

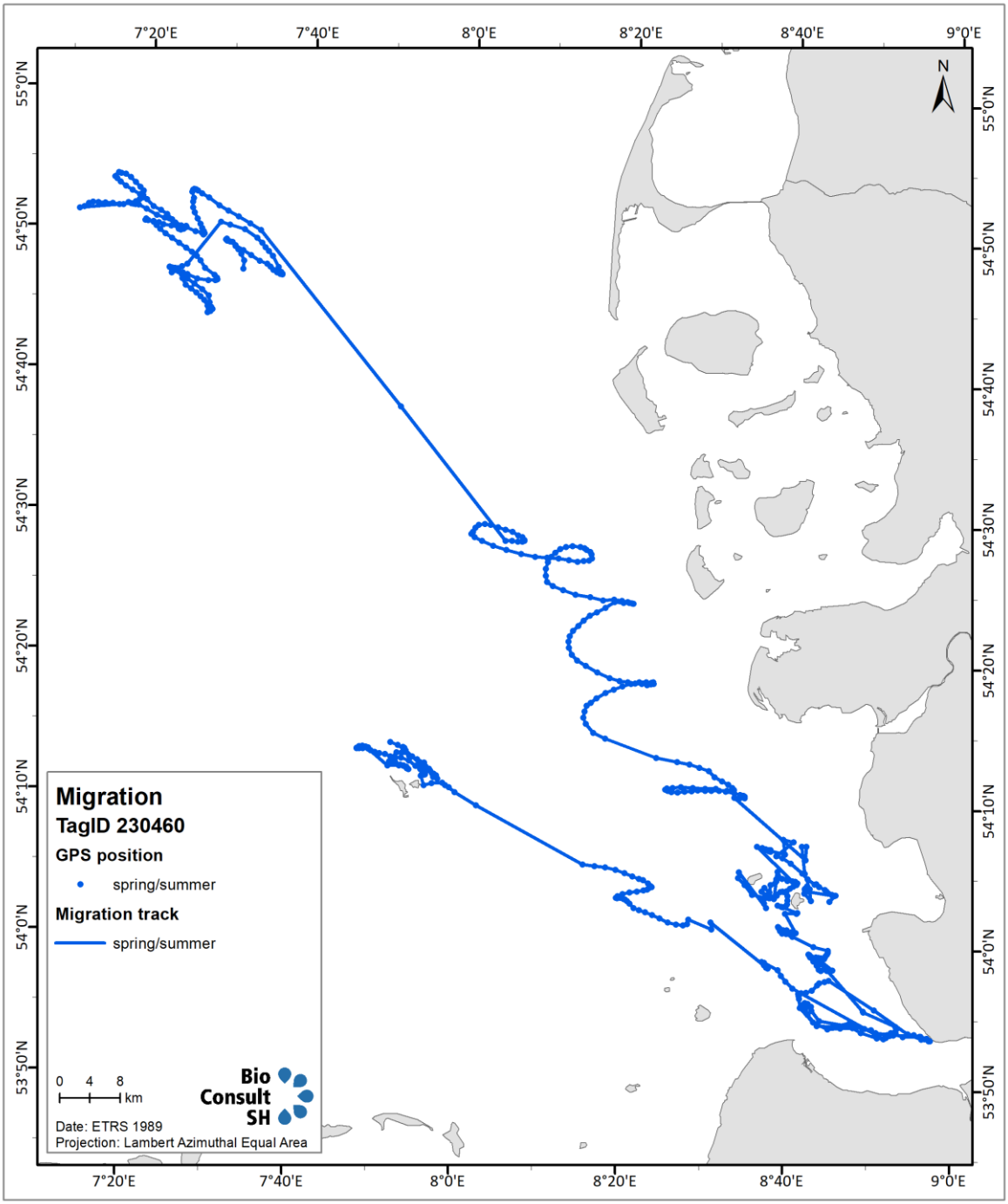
7°20'E
7°40'E
8°0'E
8°20'E
8°40'E
9°0'E
55°0'N
54°50'N
54°40'N
54°30'N
54°20'N
54°10'N
54°0'N
53°50'N
N
Migration
TagID 230460
GPS position
spring/summer
Migration track
spring/summer
0 4 8
km
Bio Consult SH
Date: ETRS 1989
Projection: Lambert Azimuthal Equal Area

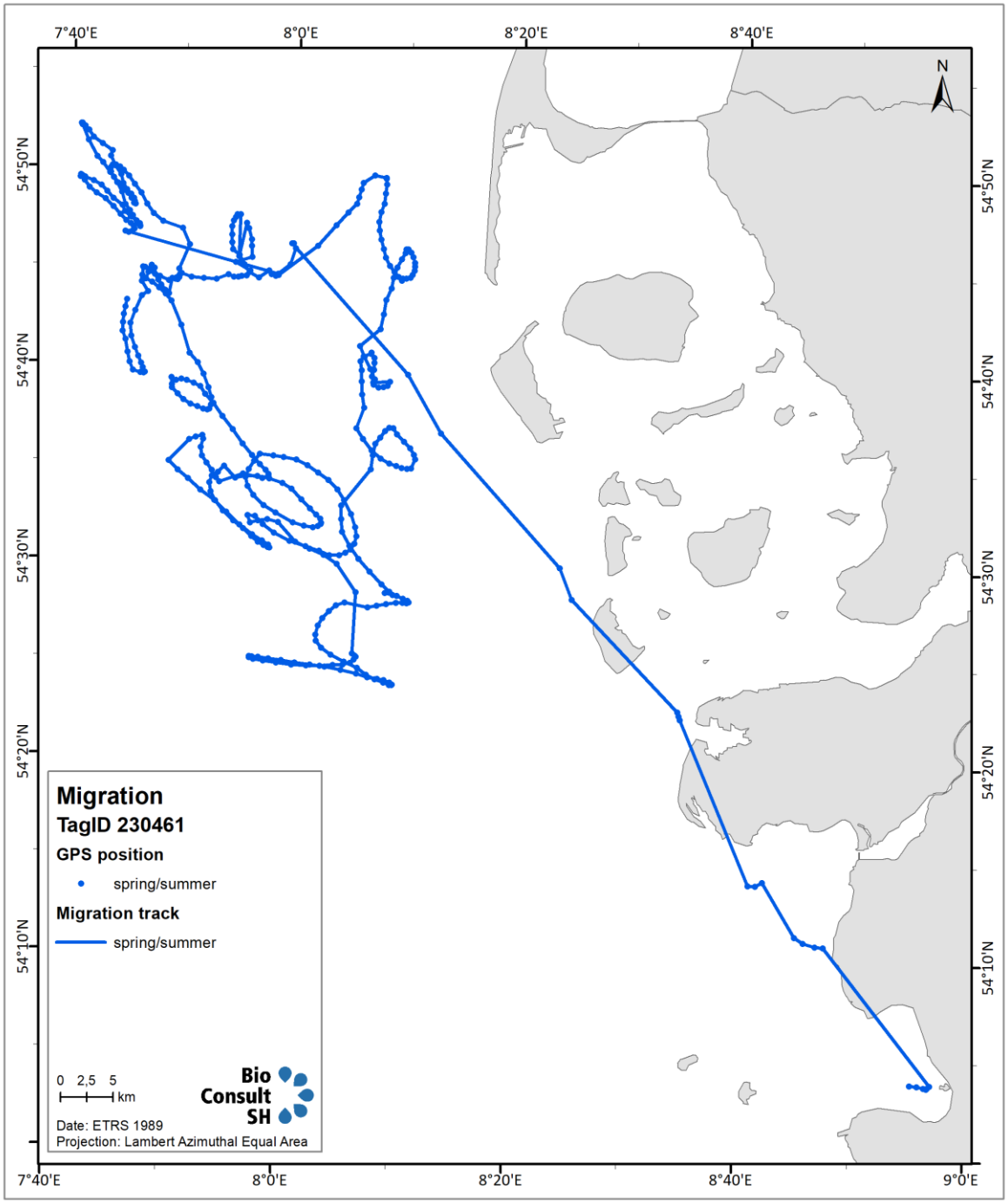
7°40'E
8°0'E
8°20'E
8°40'E
9°0'E
54°50'N
54°40'N
54°30'N
54°20'N
54°10'N
N
Migration
TagID 230461
GPS position
spring/summer
Migration track
spring/summer
0 2,5 5
km
Bio Consult SH
Date: ETRS 1989
Projection: Lambert Azimuthal Equal Area

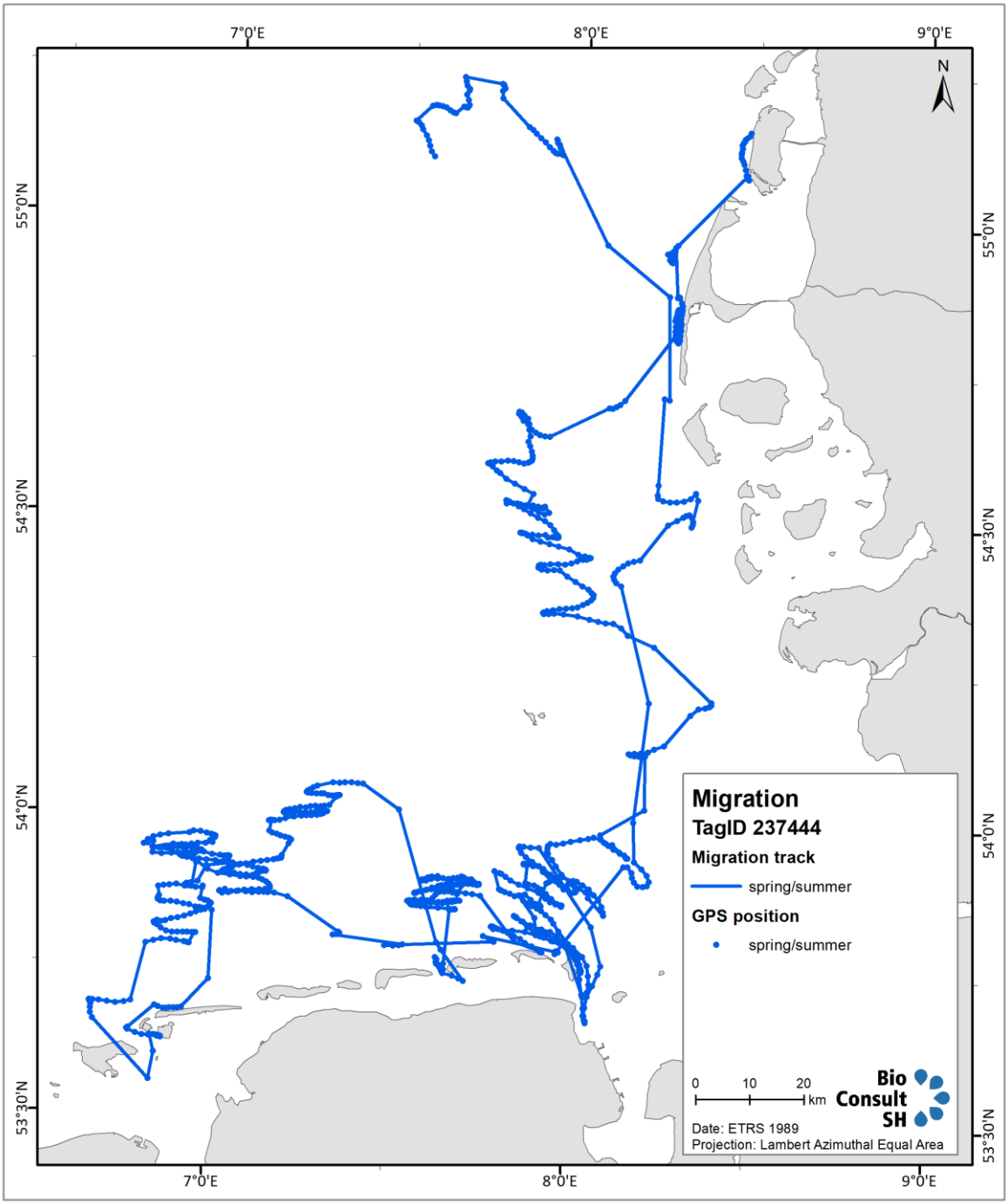
7°0'E
8°0'E
9°0'E
55°0'N
54°30'N
54°0'N
53°30'N
N
Migration
TagID 237444
Migration track
spring/summer
GPS position
spring/summer
0
10
20
km
Bio Consult SH
Date: ETRS 1989
Projection: Lambert Azimuthal Equal Area

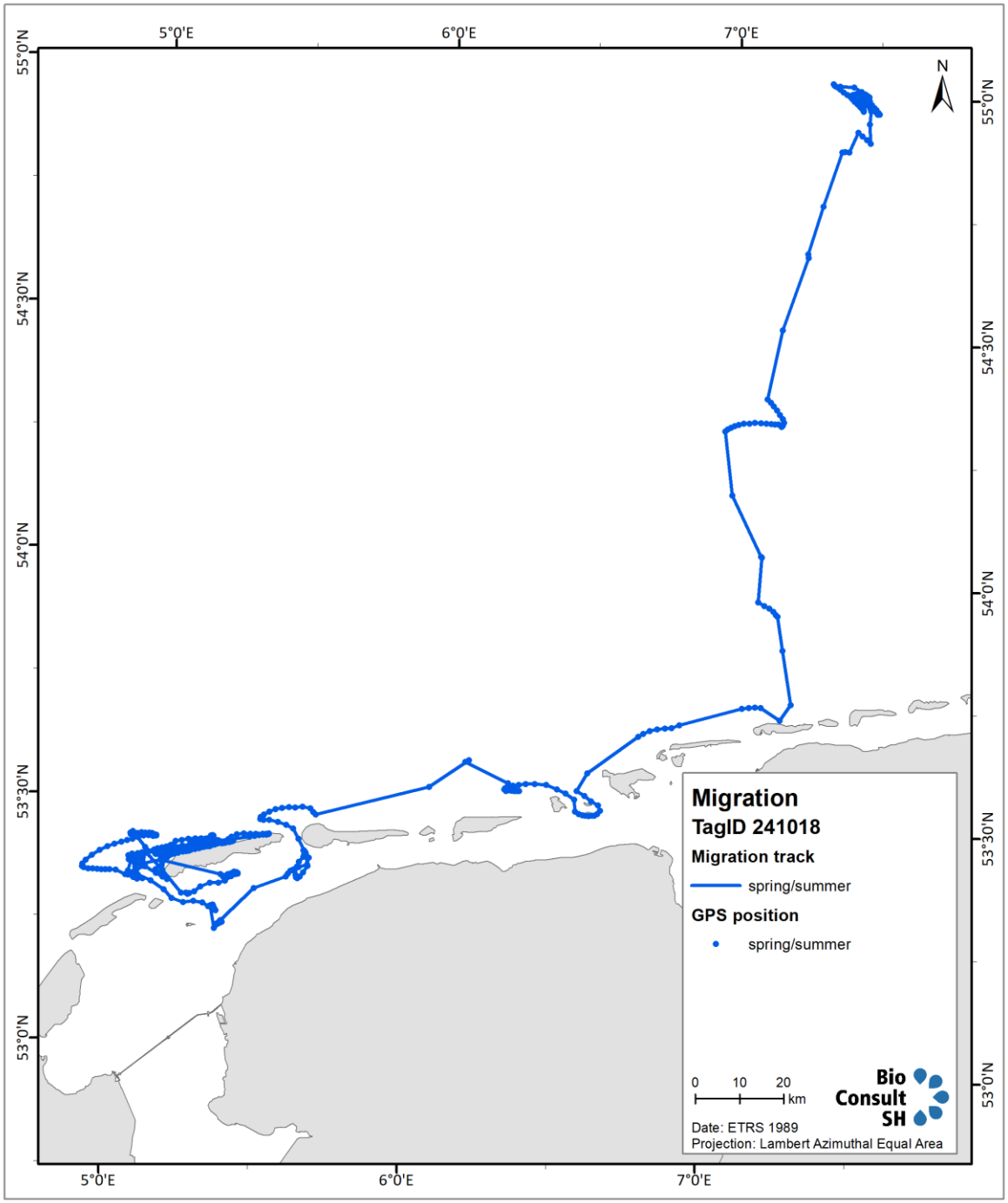
5°0'E
6°0'E
7°0'E
55°0'N
54°30'N
54°0'N
53°30'N
53°0'N
N
Migration
TagID 241018
Migration track
spring/summer
GPS position
spring/summer
0 10 20
km
Bio Consult SH
Date: ETRS 1989
Projection: Lambert Azimuthal Equal Area

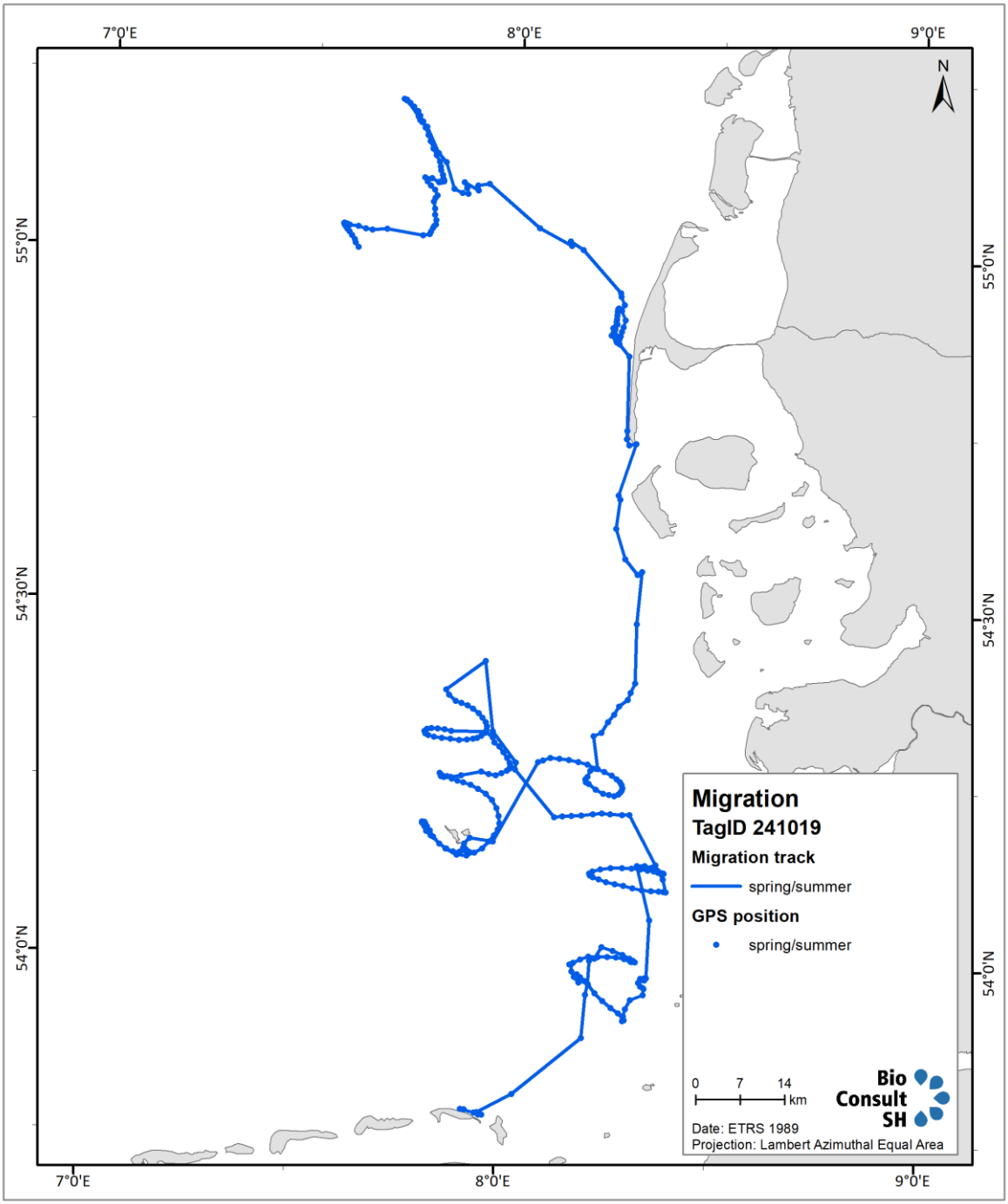
7°0'E
8°0'E
9°0'E
N
55°0'N
54°30'N
54°0'N
Migration
TagID 241019
Migration track
spring/summer
GPS position
spring/summer
0 7 14
km
Bio Consult SH
Date: ETRS 1989
Projection: Lambert Azimuthal Equal Area

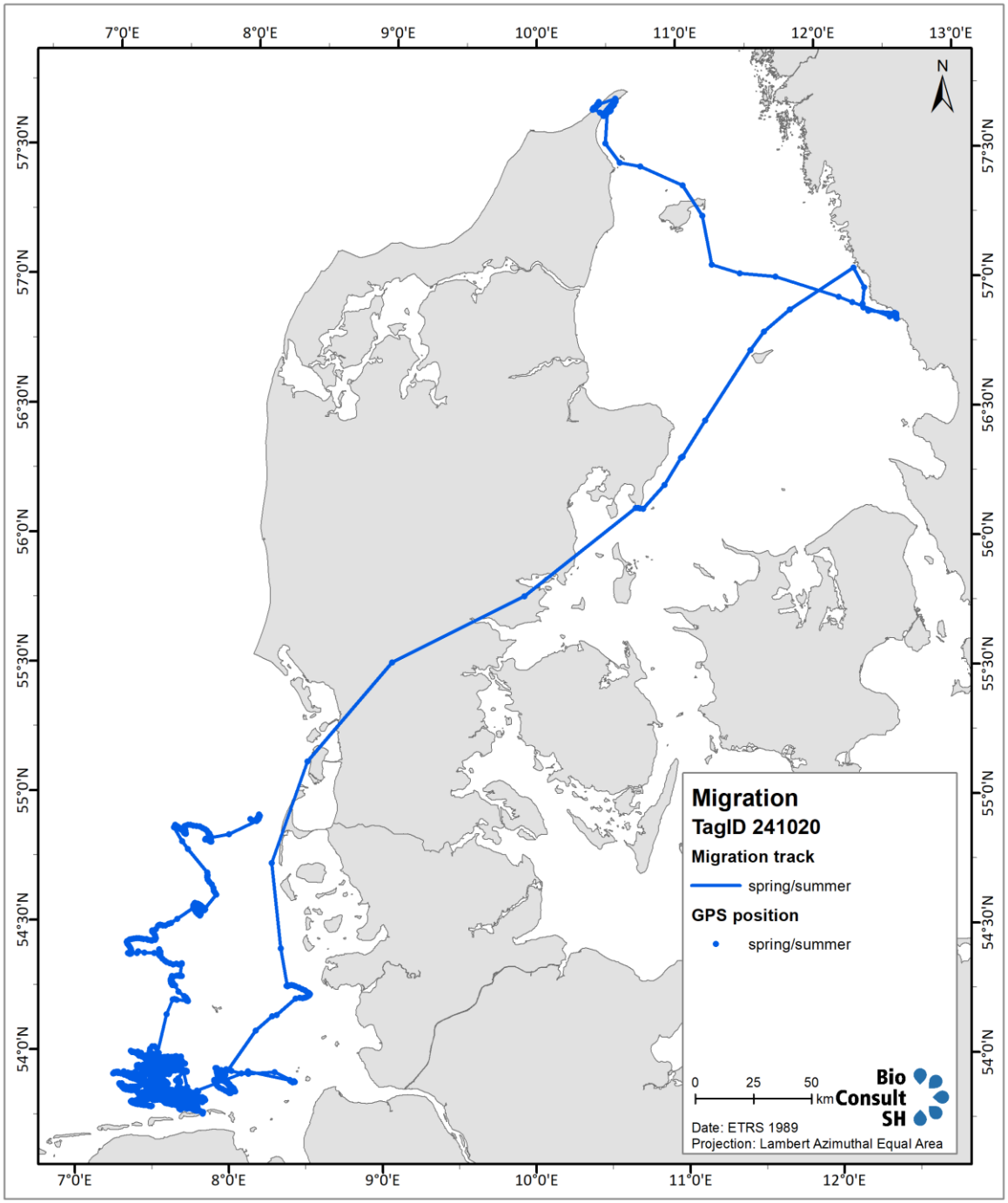
7°0'E
8°0'E
9°0'E
10°0'E
11°0'E
12°0'E
13°0'E
57°30'N
57°0'N
56°30'N
56°0'N
55°30'N
55°0'N
54°30'N
54°0'N
N
Migration
TagID 241020
Migration track
spring/summer
GPS position
spring/summer
0
25
50
km
Bio Consult SH
Date: ETRS 1989
Projection: Lambert Azimuthal Equal Area

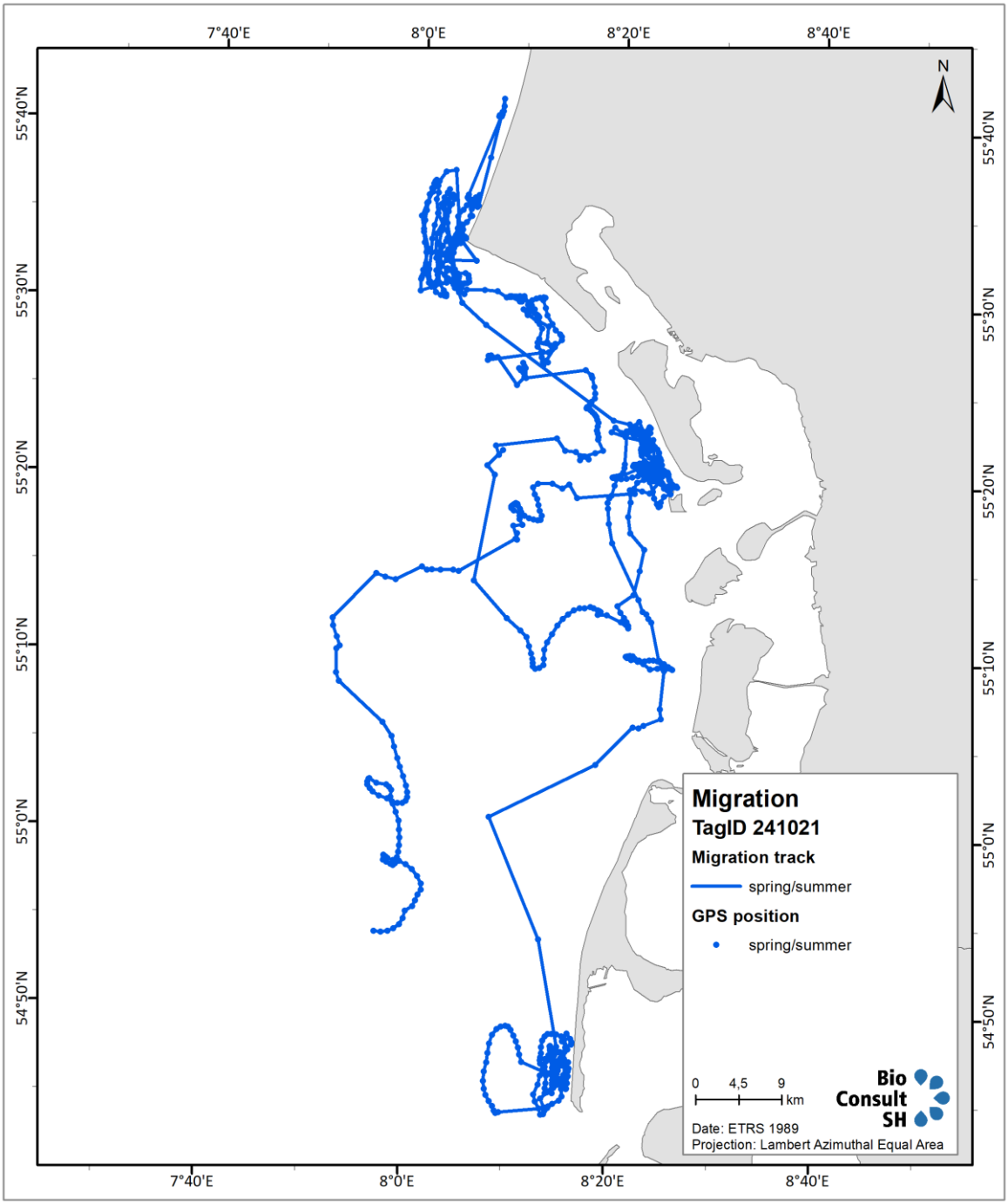
7°40'E
8°0'E
8°20'E
8°40'E
55°40'N
55°30'N
55°20'N
55°10'N
55°0'N
54°50'N
N
Migration
TagID 241021
Migration track
spring/summer
GPS position
spring/summer
0 4,5 9
km
Bio Consult SH
Date: ETRS 1989
Projection: Lambert Azimuthal Equal Area

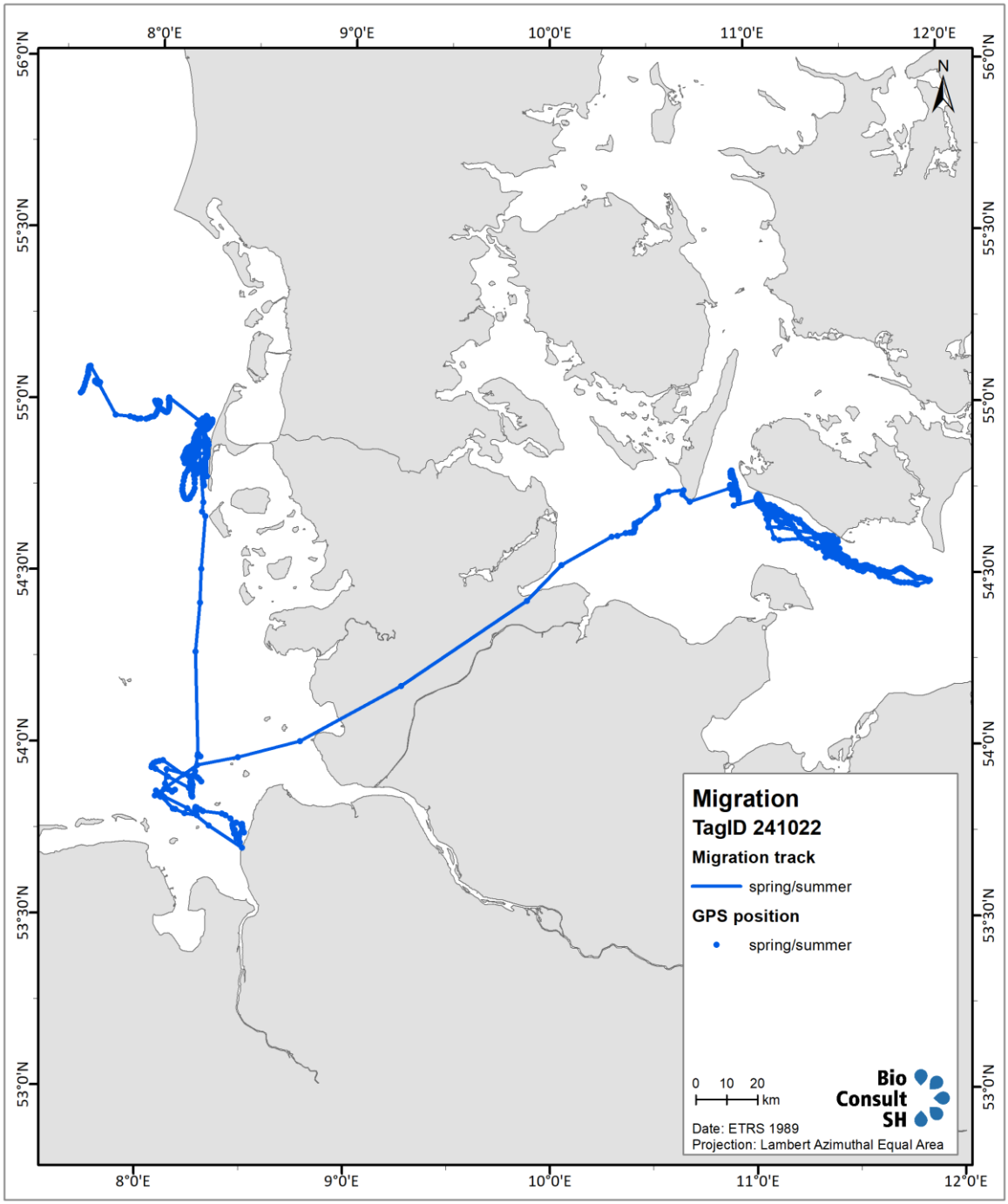
8°0'E
9°0'E
10°0'E
11°0'E
12°0'E
56°0'N
55°30'N
55°0'N
54°30'N
54°0'N
53°30'N
53°0'N
N
Migration
TagID 241022
Migration track
spring/summer
GPS position
spring/summer
0 10 20
km
Bio Consult SH
Date: ETRS 1989
Projection: Lambert Azimuthal Equal Area

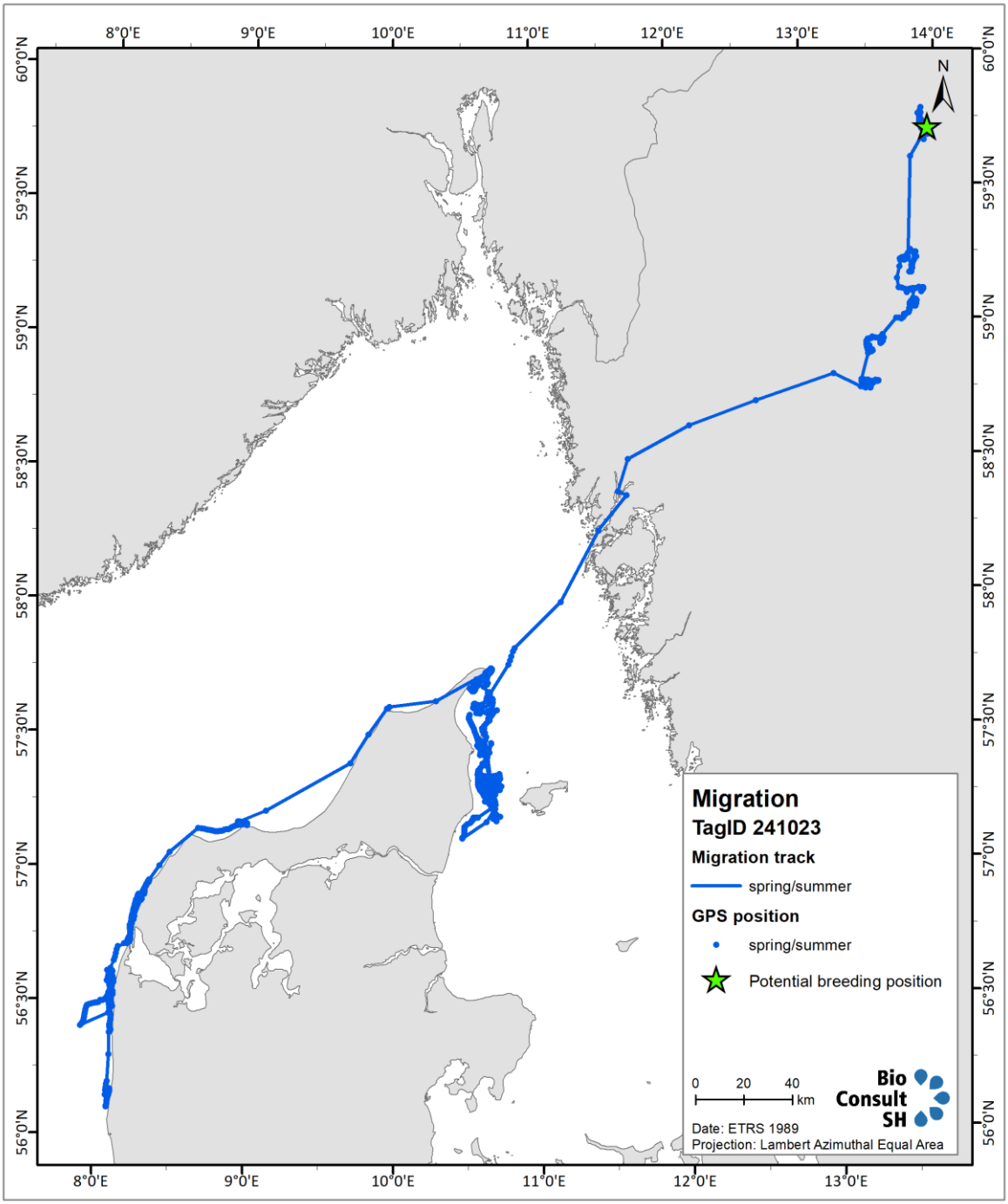
8°0'E
9°0'E
10°0'E
11°0'E
12°0'E
13°0'E
14°0'E
60°0'N
59°30'N
59°0'N
58°30'N
58°0'N
57°30'N
57°0'N
56°30'N
56°0'N
N
Migration
TagID 241023
Migration track
spring/summer
GPS position
spring/summer
Potential breeding position
0 20 40 km
Bio Consult SH
Date: ETRS 1989
Projection: Lambert Azimuthal Equal Area

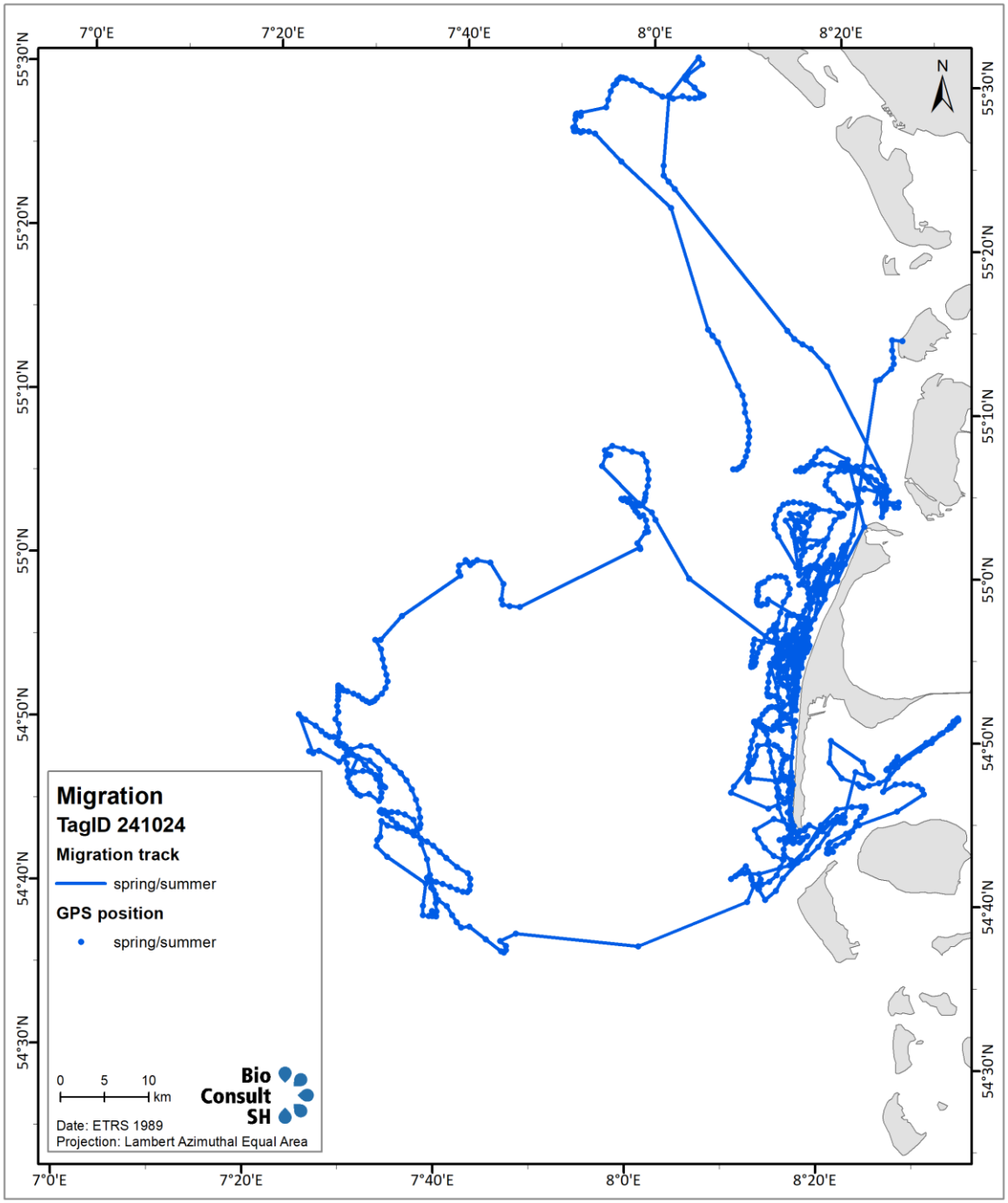
7°0'E
7°20'E
7°40'E
8°0'E
8°20'E
55°30'N
55°20'N
55°10'N
55°0'N
54°50'N
54°40'N
54°30'N
N
Migration
TagID 241024
Migration track
spring/summer
GPS position
spring/summer
0 5 10
km
Bio Consult SH
Date: ETRS 1989
Projection: Lambert Azimuthal Equal Area

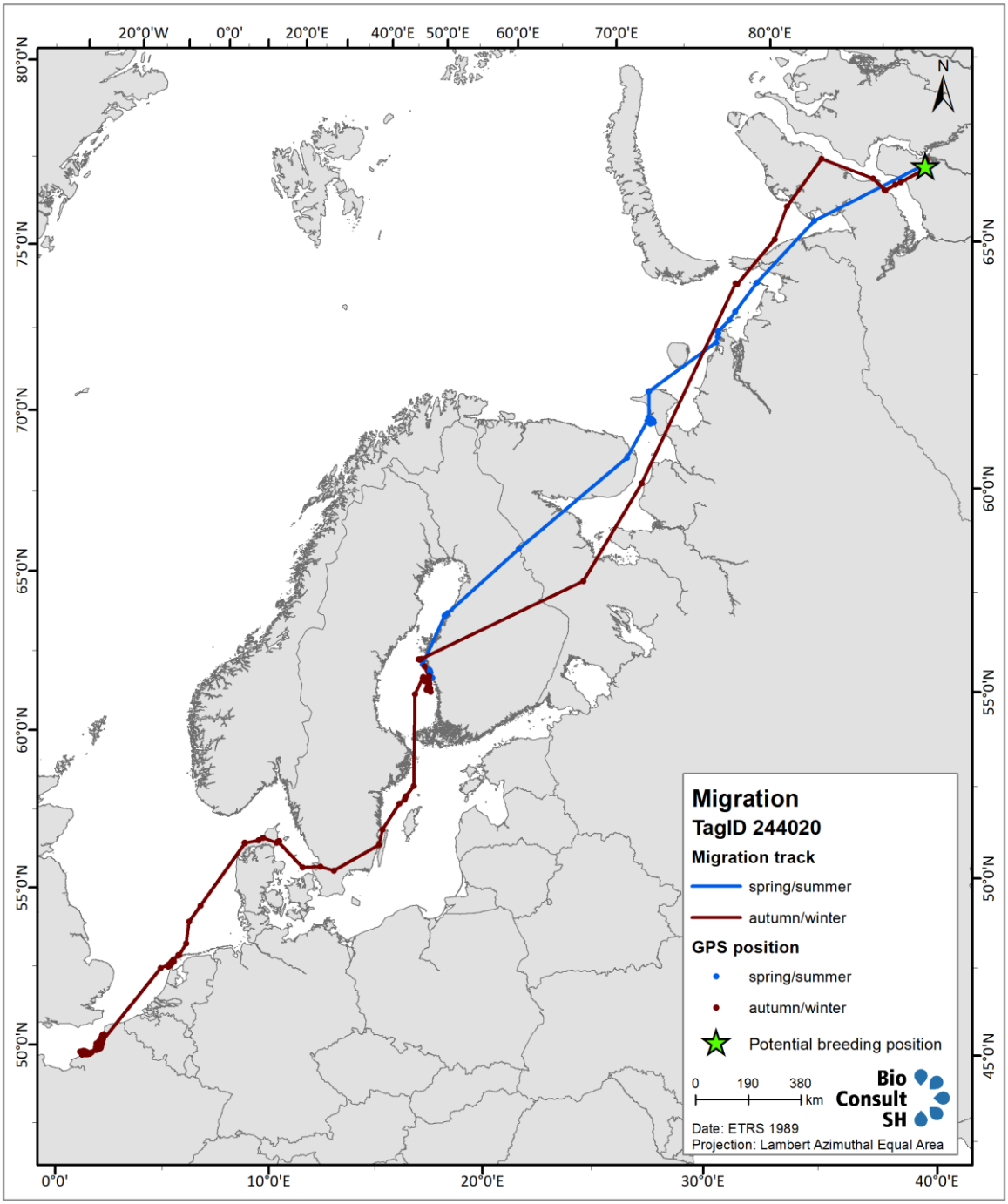
20°0'W
0°0'
20°0'E
40°0'E
50°0'E
60°0'E
70°0'E
80°0'E
80°0'N
75°0'N
70°0'N
65°0'N
60°0'N
55°0'N
50°0'N
45°0'N
N
Migration
TagID 244020
Migration track
spring/summer
autumn/winter
GPS position
spring/summer
autumn/winter
Potential breeding position
0
190
380
km
Bio Consult SH
Date: ETRS 1989
Projection: Lambert Azimuthal Equal Area
0°0'
10°0'E
20°0'E
30°0'E
40°0'E

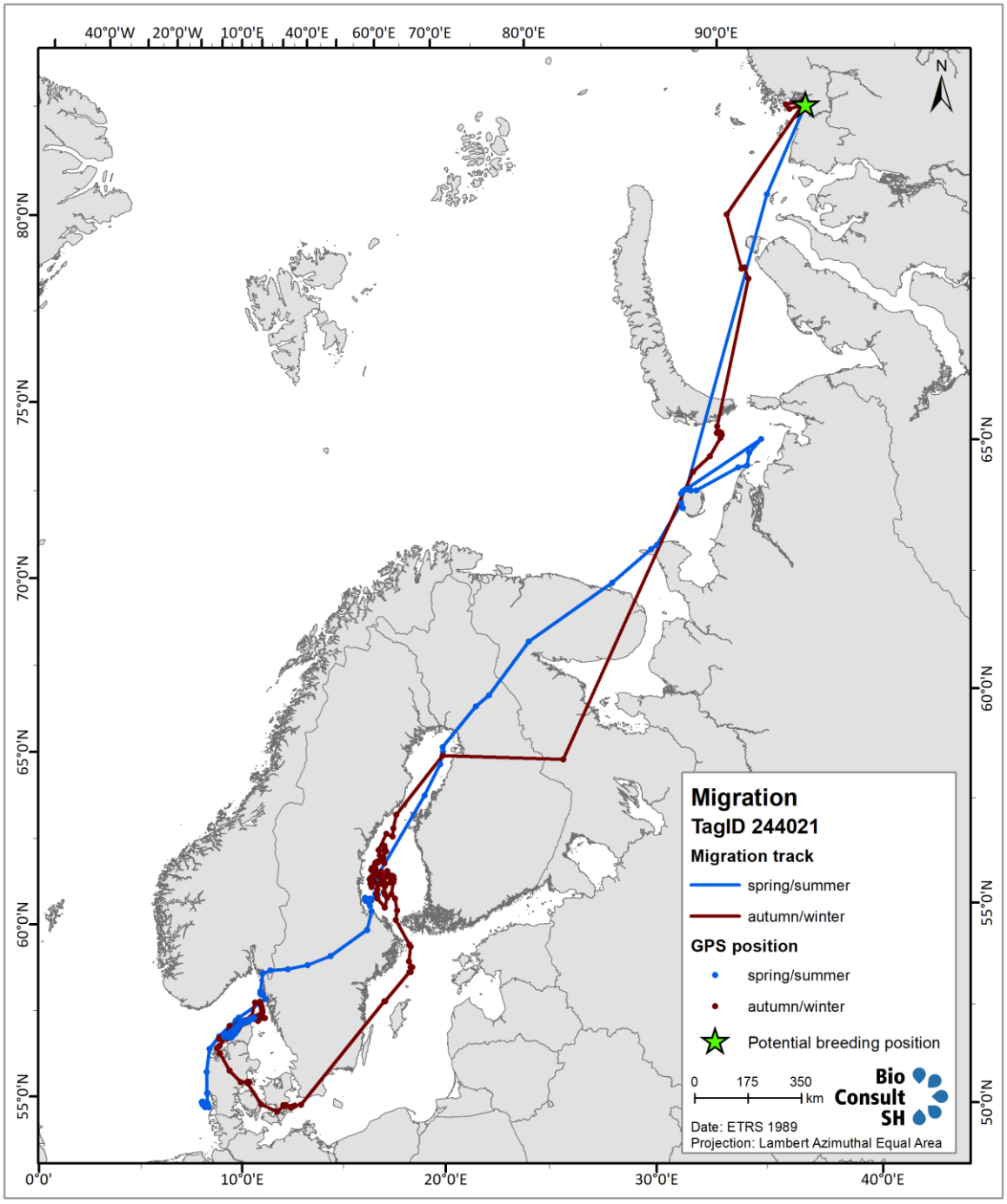
40°0'W
20°0'W
10°0'E
40°0'E
60°0'E
70°0'E
80°0'E
90°0'E
N
80°0'N
75°0'N
70°0'N
65°0'N
60°0'N
55°0'N
65°0'N
60°0'N
55°0'N
50°0'N
0°0'
10°0'E
20°0'E
30°0'E
40°0'E
Migration
TagID 244021
Migration track
spring/summer
autumn/winter
GPS position
spring/summer
autumn/winter
Potential breeding position
0
175
350
km
Bio Consult SH
Date: ETRS 1989
Projection: Lambert Azimuthal Equal Area

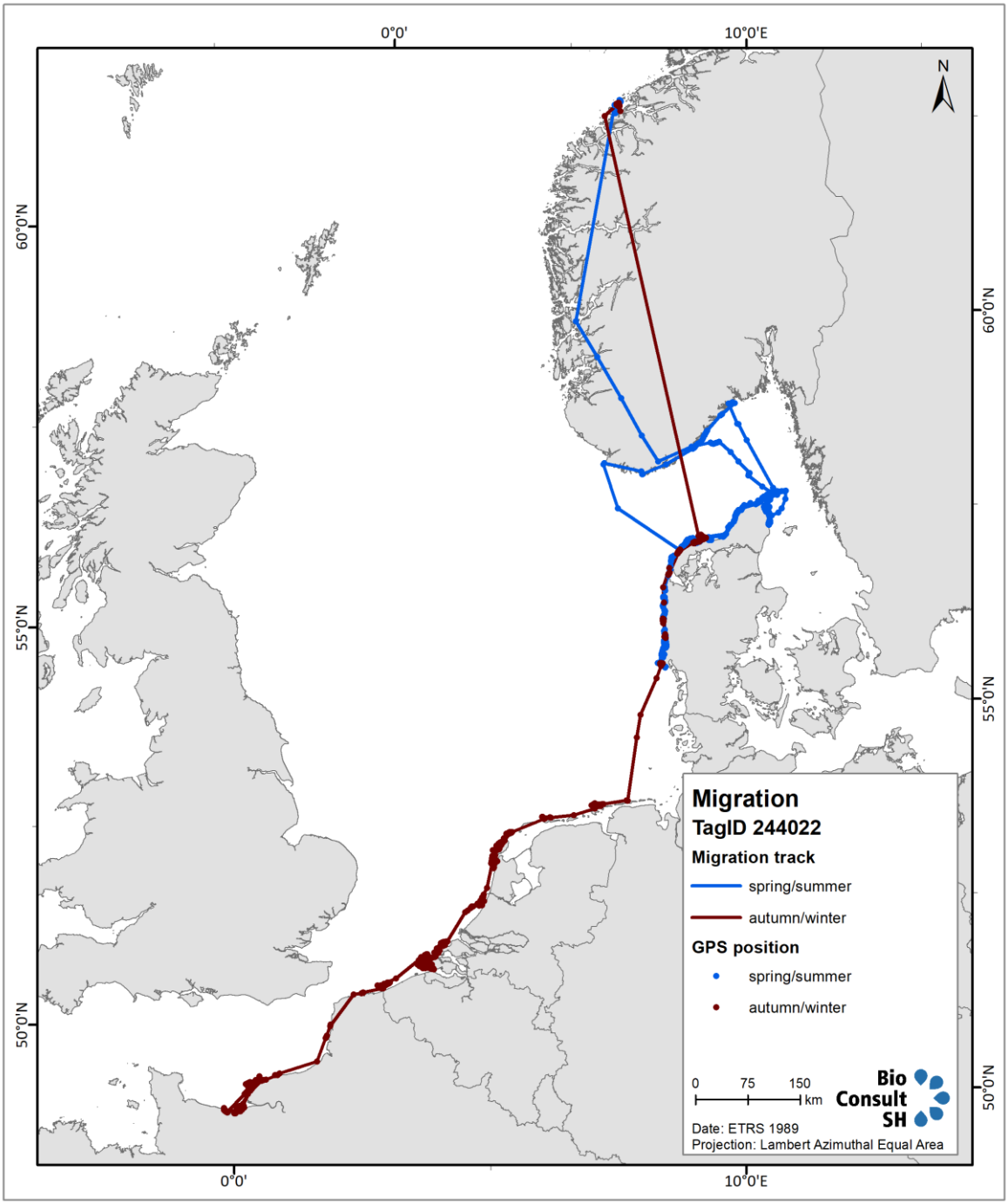
0°0'
10°0'E
N
60°0'N
55°0'N
50°0'N
Migration
TagID 244022
Migration track
spring/summer
autumn/winter
GPS position
spring/summer
autumn/winter
0 75 150
km
Bio Consult SH
Date: ETRS 1989
Projection: Lambert Azimuthal Equal Area

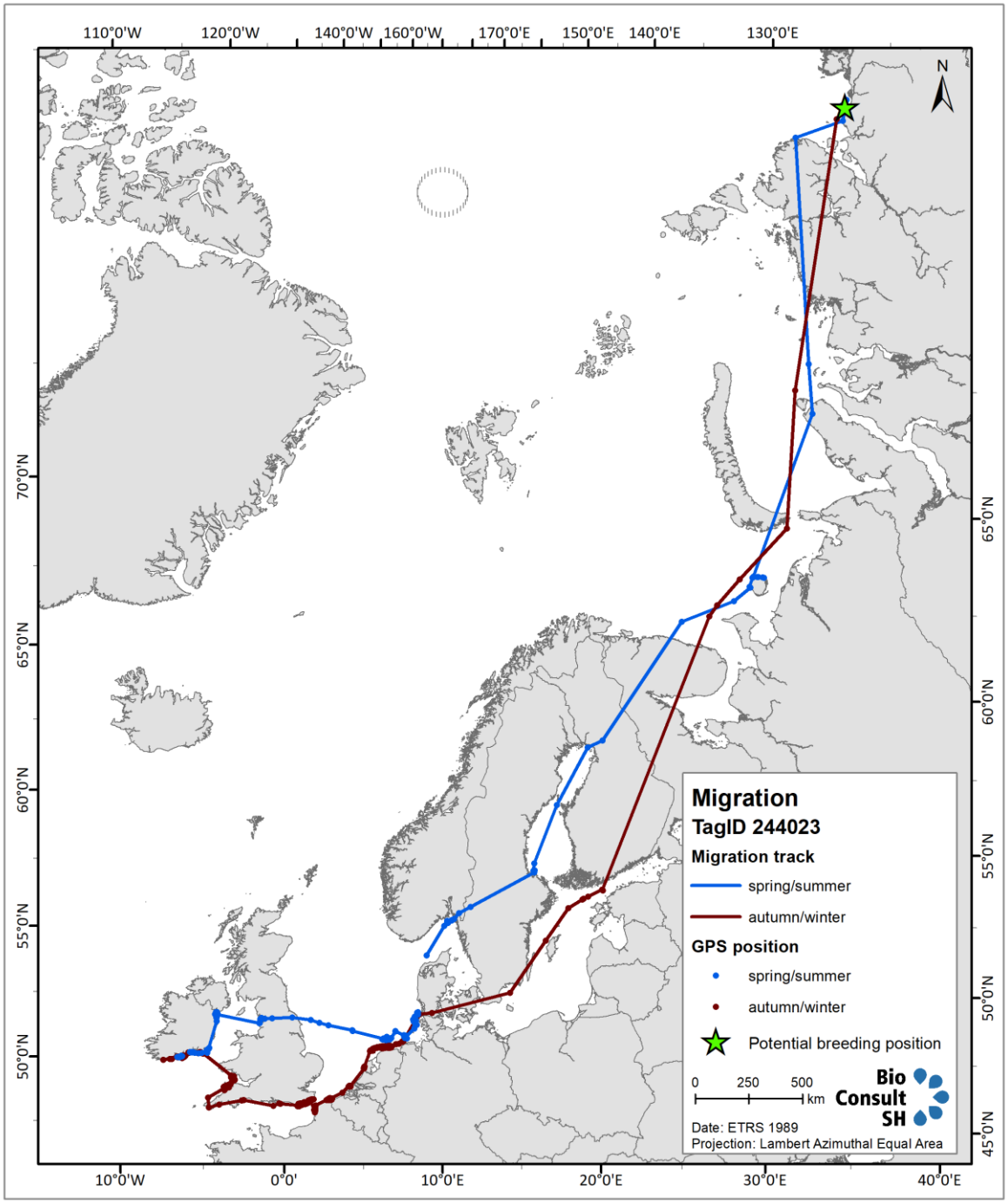
110°0'W
120°0'W
140°0'W
160°0'W
170°0'E
150°0'E
140°0'E
130°0'E
70°0'N
65°0'N
60°0'N
55°0'N
50°0'N
10°0'W
0°0'
10°0'E
20°0'E
30°0'E
40°0'E
65°0'N
60°0'N
55°0'N
50°0'N
45°0'N
N
Migration
TagID 244023
Migration track
spring/summer
autumn/winter
GPS position
spring/summer
autumn/winter
Potential breeding position
0
250
500
km
Bio Consult SH
Date: ETRS 1989
Projection: Lambert Azimuthal Equal Area

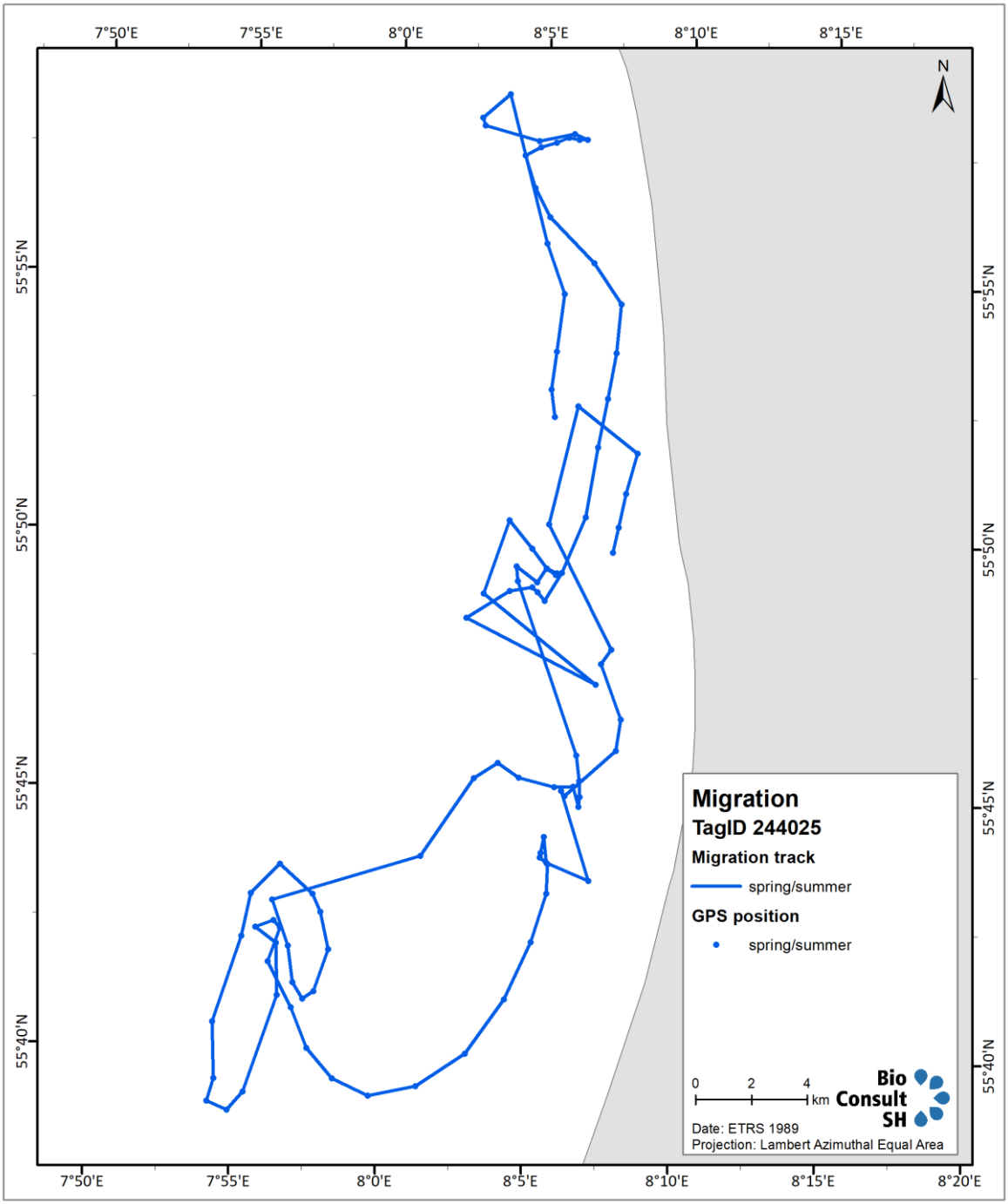
7°50'E
7°55'E
8°0'E
8°5'E
8°10'E
8°15'E
8°20'E
55°55'N
55°50'N
55°45'N
55°40'N
N
Migration
TagID 244025
Migration track
spring/summer
GPS position
spring/summer
0
2
4
km
Bio Consult SH
Date: ETRS 1989
Projection: Lambert Azimuthal Equal Area

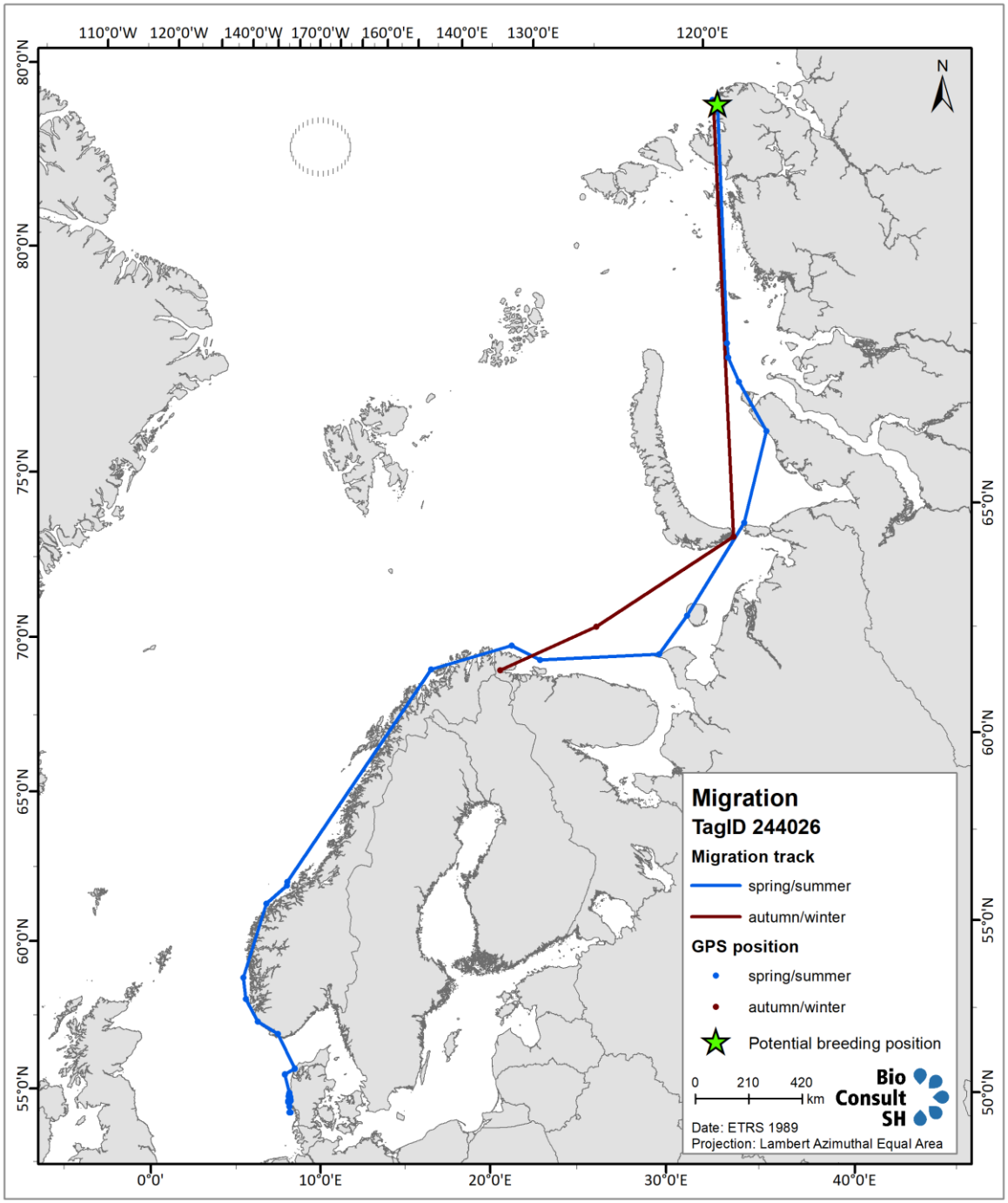
110°0'W
120°0'W
140°0'W
170°0'W
160°0'E
140°0'E
130°0'E
120°0'E
80°0'N
75°0'N
70°0'N
65°0'N
60°0'N
55°0'N
65°0'N
60°0'N
55°0'N
50°0'N
0°0'
10°0'E
20°0'E
30°0'E
40°0'E
N
Migration
TagID 244026
Migration track
spring/summer
autumn/winter
GPS position
spring/summer
autumn/winter
Potential breeding position
0
210
420
km
Bio Consult SH
Date: ETRS 1989
Projection: Lambert Azimuthal Equal Area

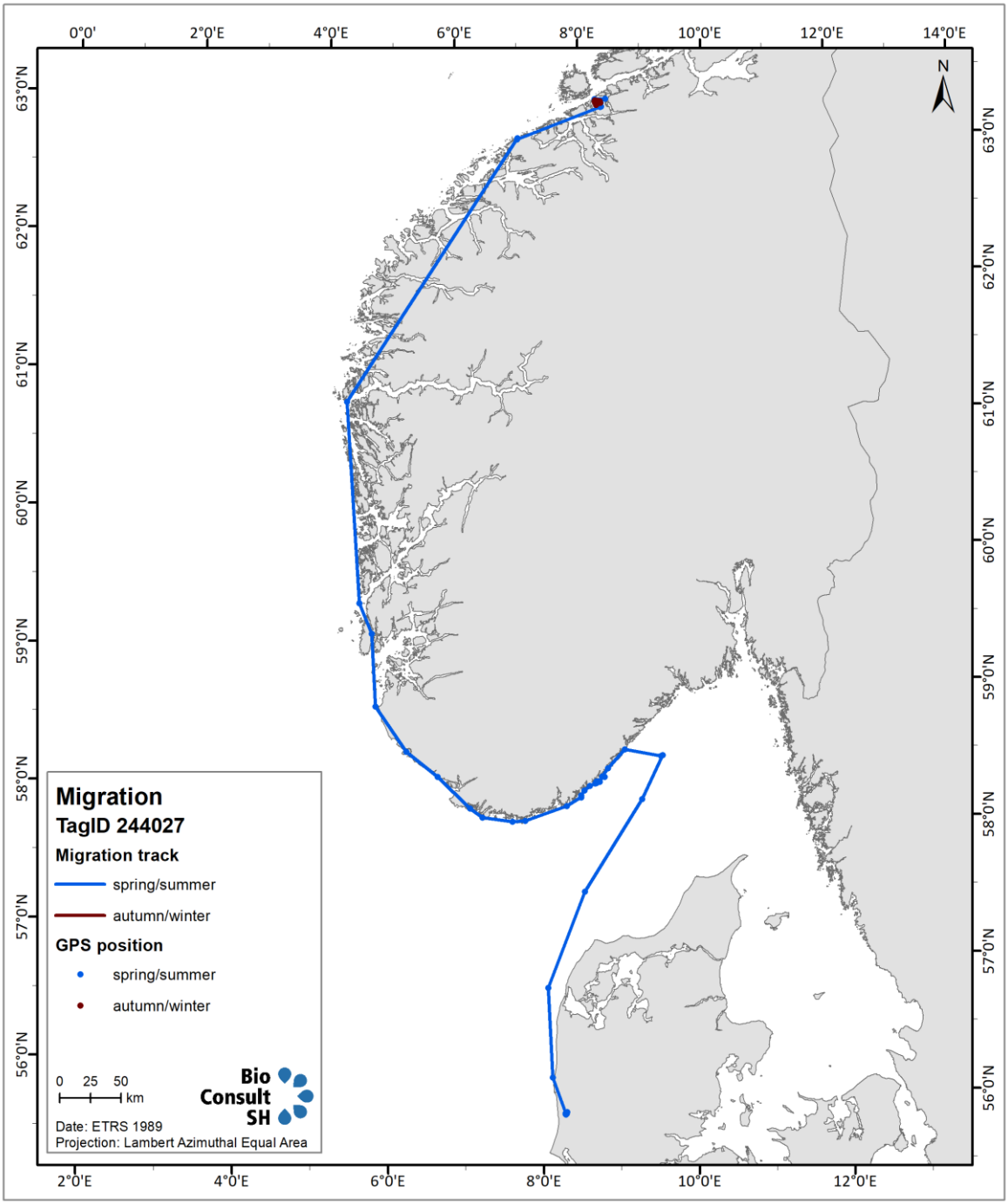
0°0'
2°0'E
4°0'E
6°0'E
8°0'E
10°0'E
12°0'E
14°0'E
63°0'N
62°0'N
61°0'N
60°0'N
59°0'N
58°0'N
57°0'N
56°0'N
N
Migration
TagID 244027
Migration track
spring/summer
autumn/winter
GPS position
spring/summer
autumn/winter
0 25 50
km
Bio Consult SH
Date: ETRS 1989
Projection: Lambert Azimuthal Equal Area

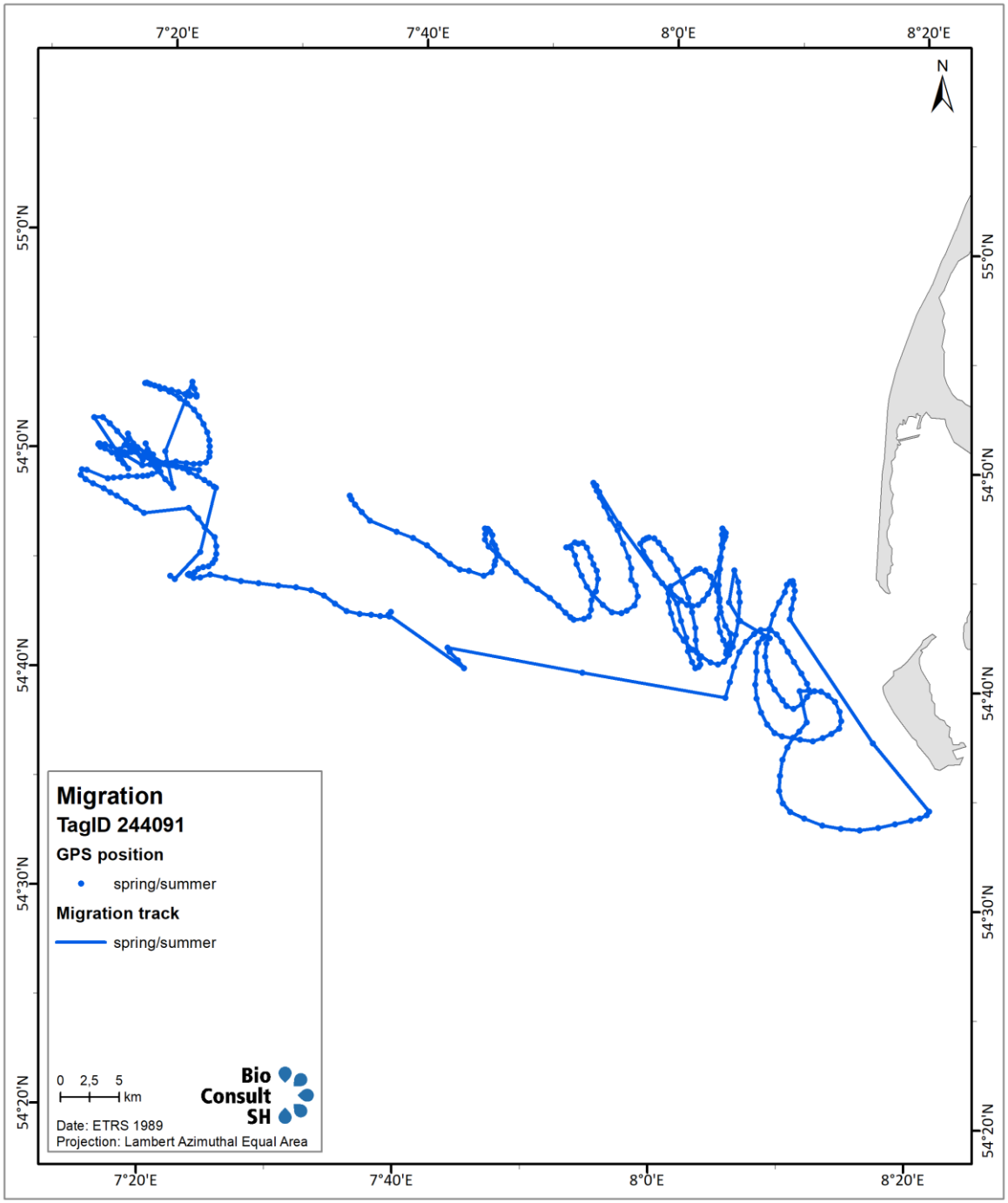
7°20'E
7°40'E
8°0'E
8°20'E
N
55°0'N
54°50'N
54°40'N
54°30'N
54°20'N
Migration
TagID 244091
GPS position
spring/summer
Migration track
spring/summer
0 2,5 5
km
Bio Consult SH
Date: ETRS 1989
Projection: Lambert Azimuthal Equal Area

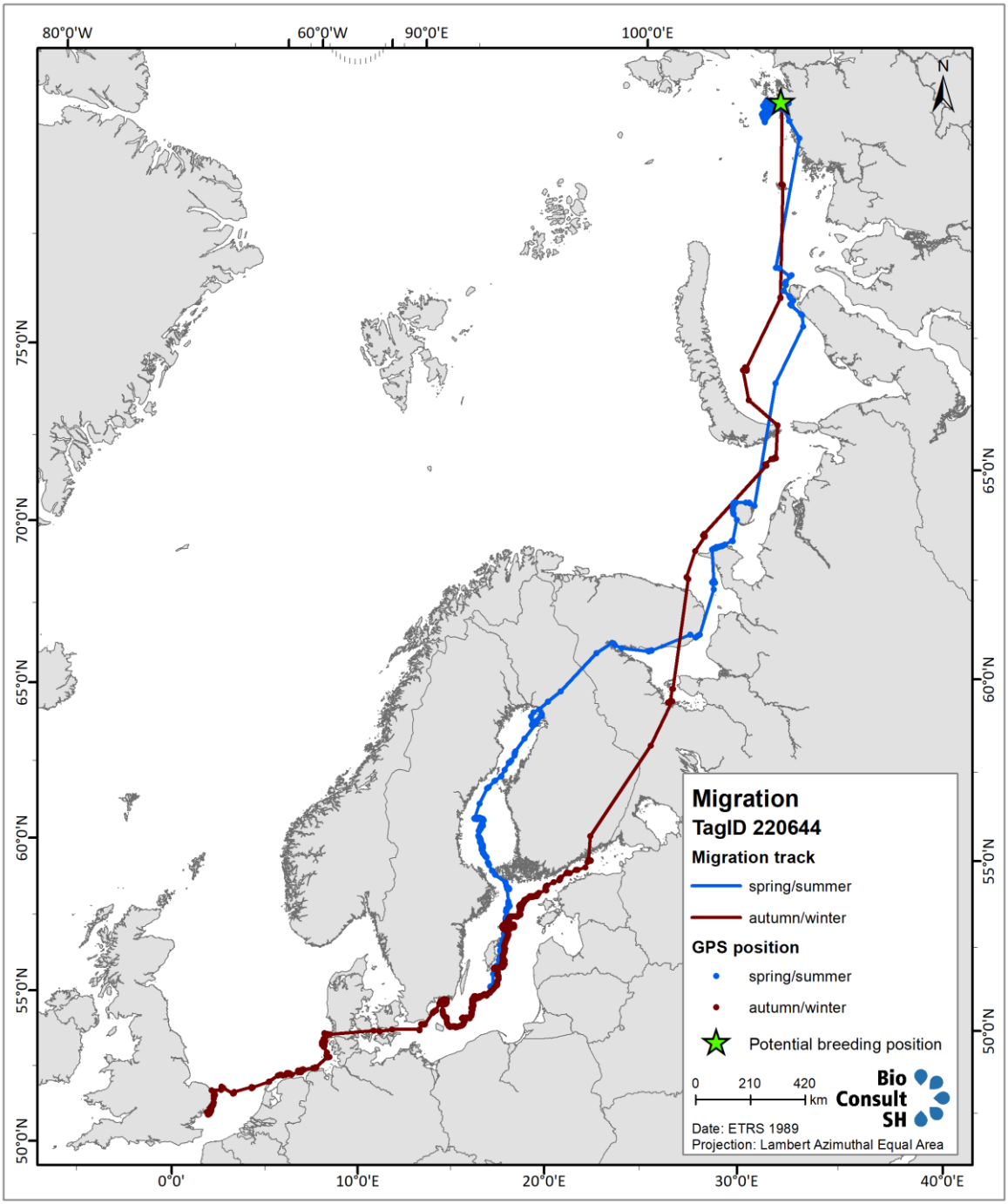
80°0'W
60°0'W
90°0'E
100°0'E
N
75°0'N
70°0'N
65°0'N
60°0'N
55°0'N
50°0'N
0°0'
10°0'E
20°0'E
30°0'E
40°0'E
Migration
TagID 220644
Migration track
spring/summer
autumn/winter
GPS position
spring/summer
autumn/winter
Potential breeding position
0
210
420
km
Bio Consult SH
Date: ETRS 1989
Projection: Lambert Azimuthal Equal Area

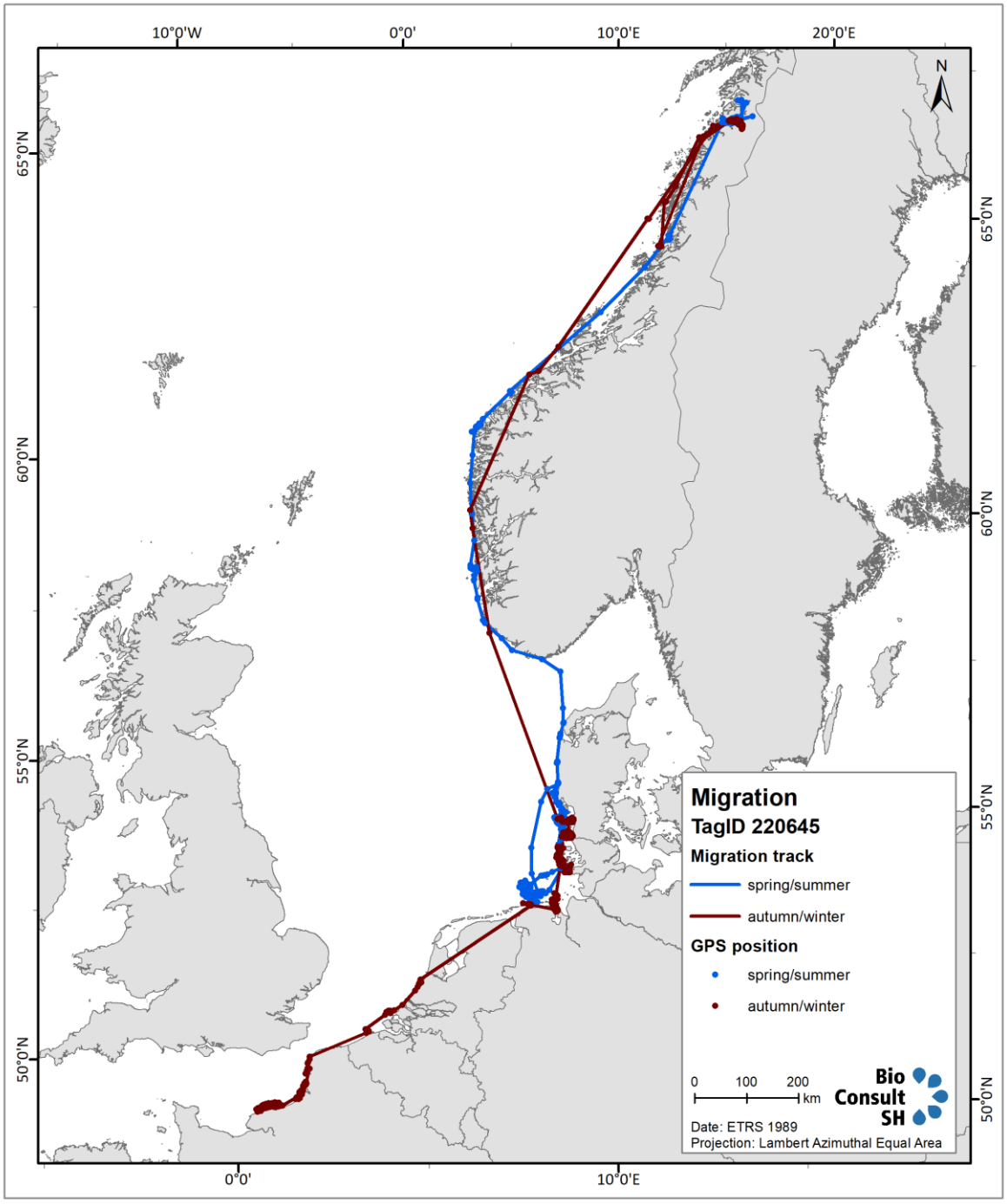
10°0'W
0°0'
10°0'E
20°0'E
65°0'N
60°0'N
55°0'N
50°0'N
N
Migration
TagID 220645
Migration track
spring/summer
autumn/winter
GPS position
spring/summer
autumn/winter
0
100
200
km
Bio Consult SH
Date: ETRS 1989
Projection: Lambert Azimuthal Equal Area

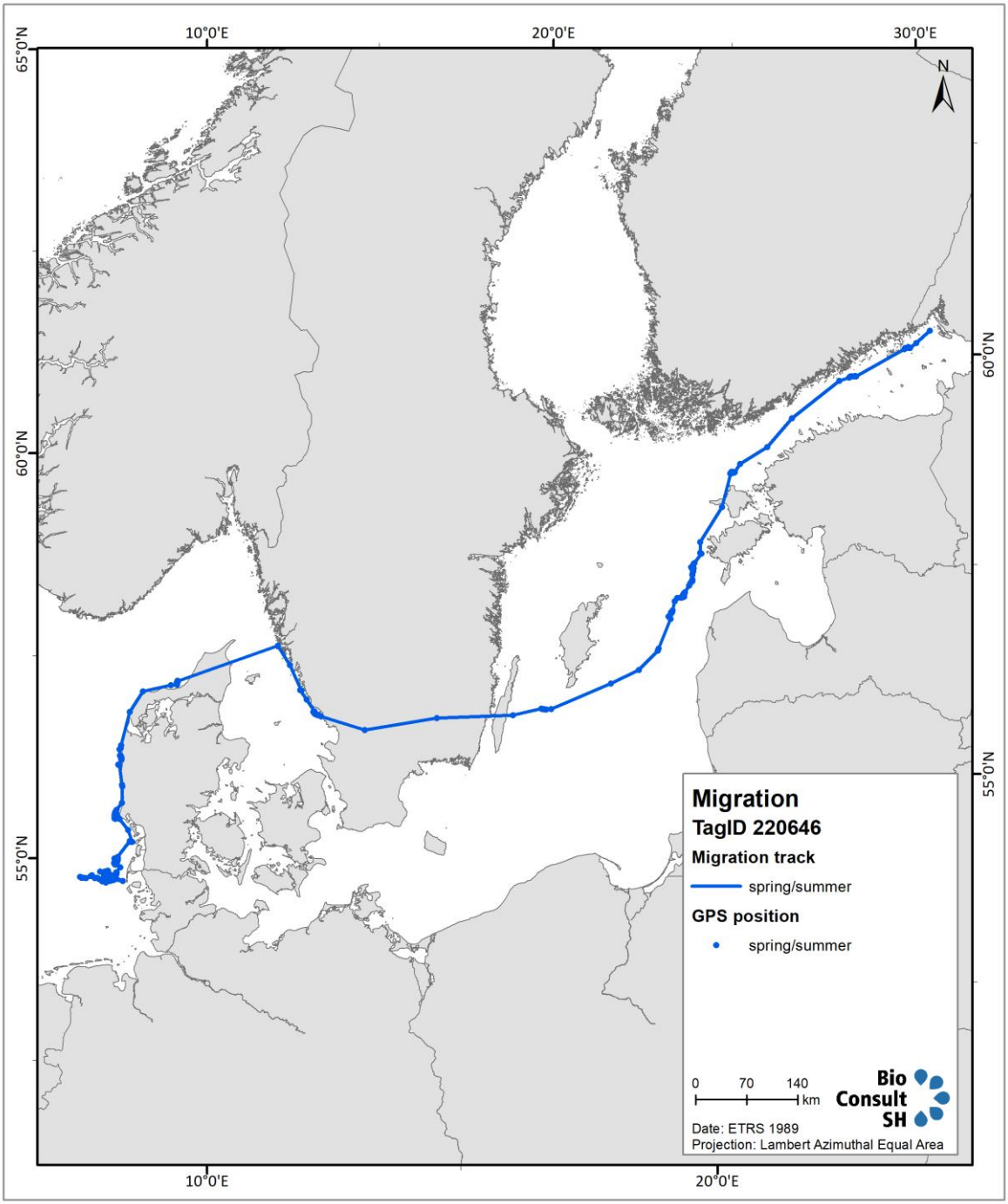
10°0'E
20°0'E
30°0'E
65°0'N
60°0'N
55°0'N
N
Migration
TagID 220646
Migration track
spring/summer
GPS position
spring/summer
0
70
140
km
Bio Consult SH
Date: ETRS 1989
Projection: Lambert Azimuthal Equal Area

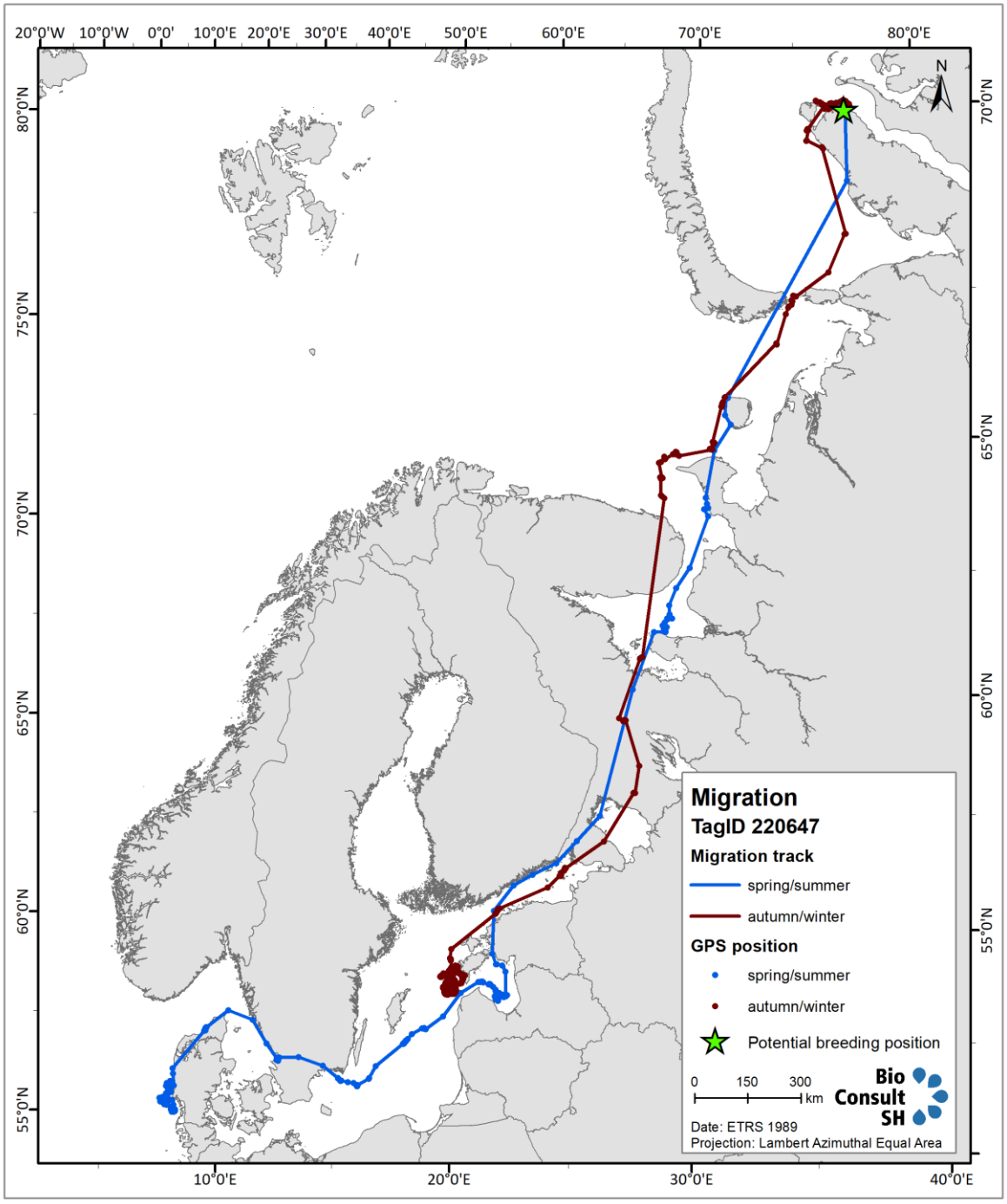
20°0'W
10°0'W
0°0'
10°0'E
20°0'E
30°0'E
40°0'E
50°0'E
60°0'E
70°0'E
80°0'E
80°0'N
75°0'N
70°0'N
65°0'N
60°0'N
55°0'N
N
Migration
TagID 220647
Migration track
spring/summer
autumn/winter
GPS position
spring/summer
autumn/winter
Potential breeding position
0
150
300
km
Bio Consult SH
Date: ETRS 1989
Projection: Lambert Azimuthal Equal Area

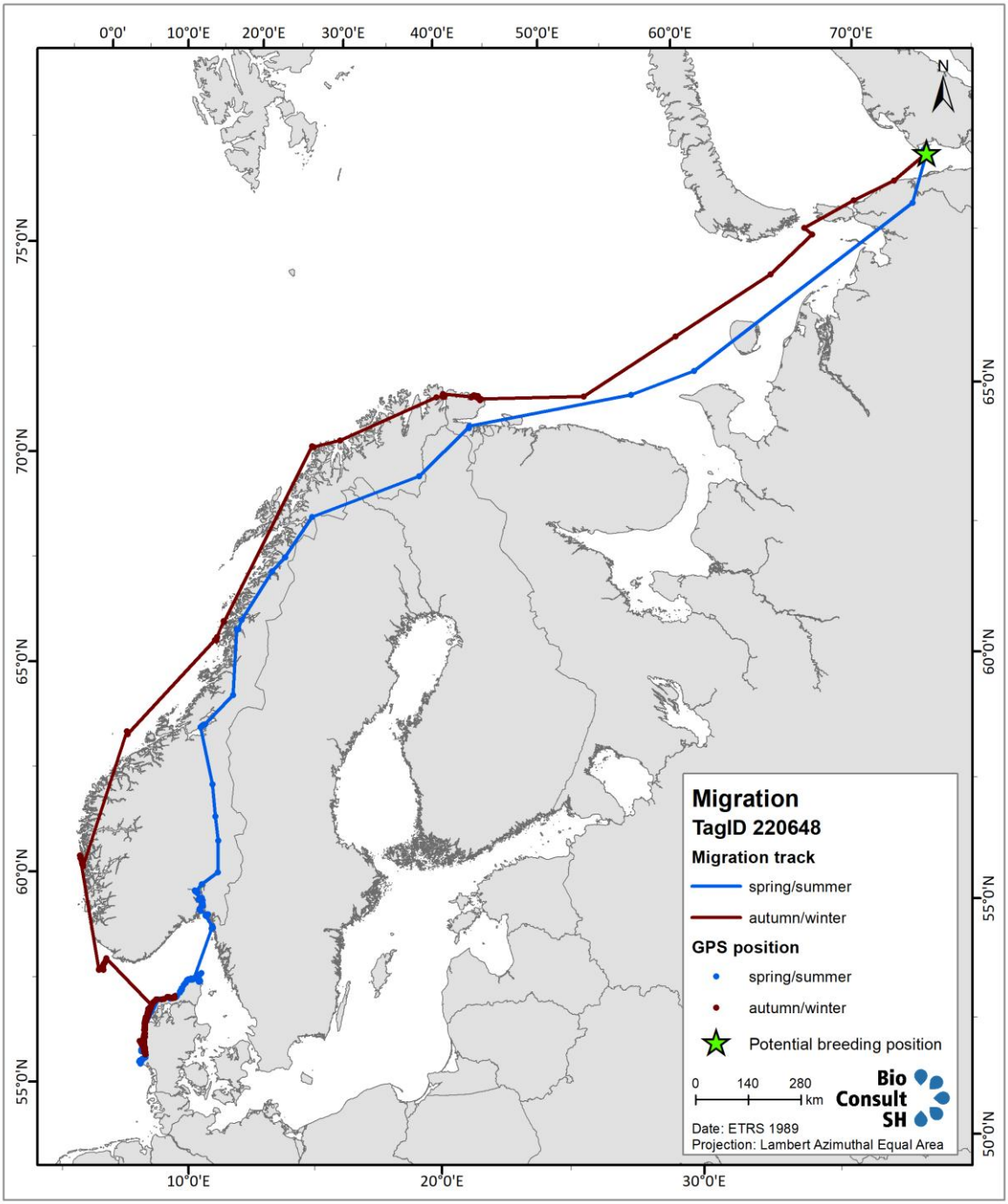
0°0'
10°0'E
20°0'E
30°0'E
40°0'E
50°0'E
60°0'E
70°0'E
75°0'N
70°0'N
65°0'N
60°0'N
55°0'N
50°0'N
N
Migration
TagID 220648
Migration track
spring/summer
autumn/winter
GPS position
spring/summer
autumn/winter
Potential breeding position
0
140
280
km
Bio Consult SH
Date: ETRS 1989
Projection: Lambert Azimuthal Equal Area

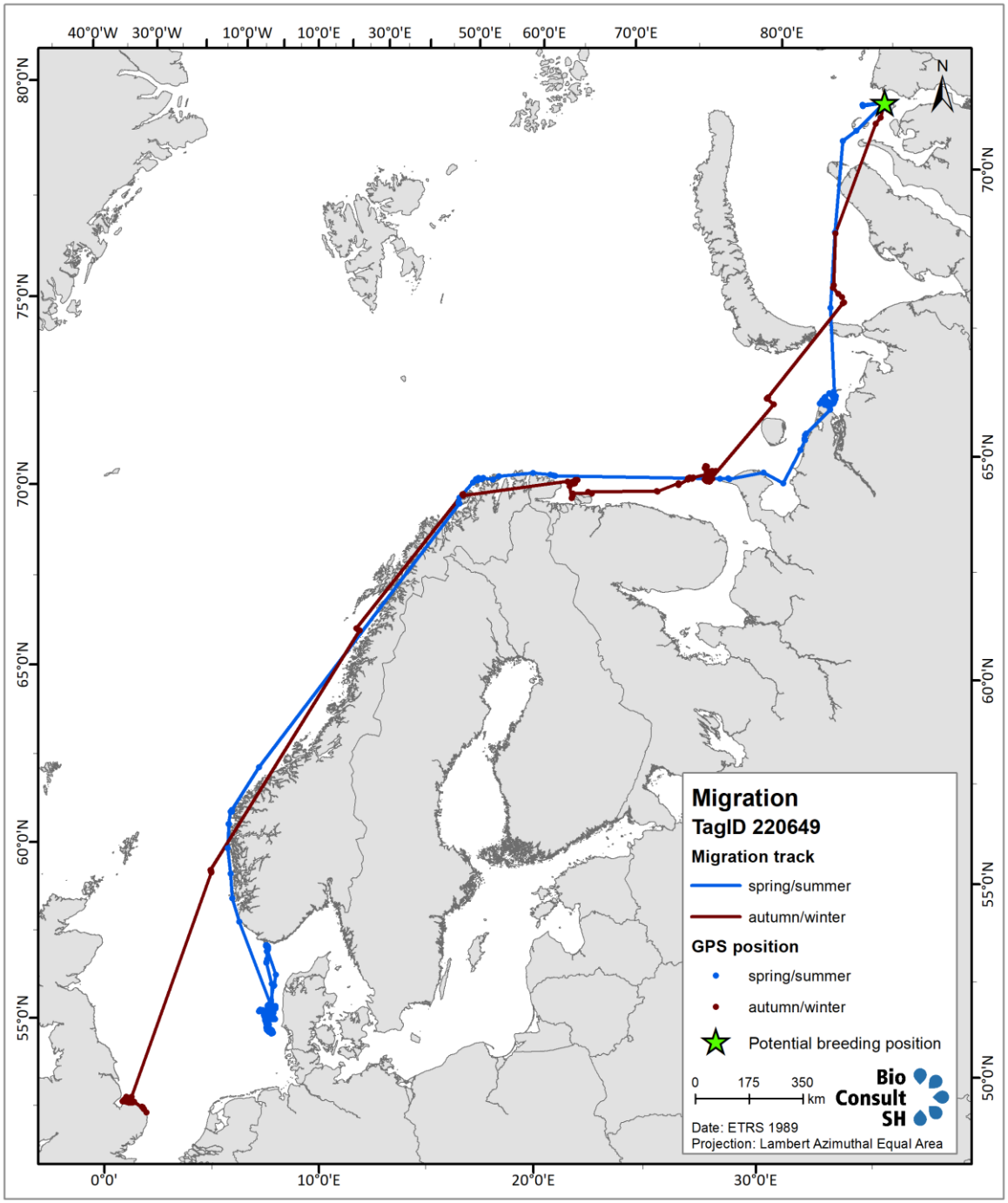
40°0'W
30°0'W
10°0'W
10°0'E
30°0'E
50°0'E
60°0'E
70°0'E
80°0'E
80°0'N
75°0'N
70°0'N
65°0'N
60°0'N
55°0'N
50°0'N
N
0°0'
10°0'E
20°0'E
30°0'E
Migration
TagID 220649
Migration track
spring/summer
autumn/winter
GPS position
spring/summer
autumn/winter
Potential breeding position
0
175
350
km
Bio Consult SH
Date: ETRS 1989
Projection: Lambert Azimuthal Equal Area

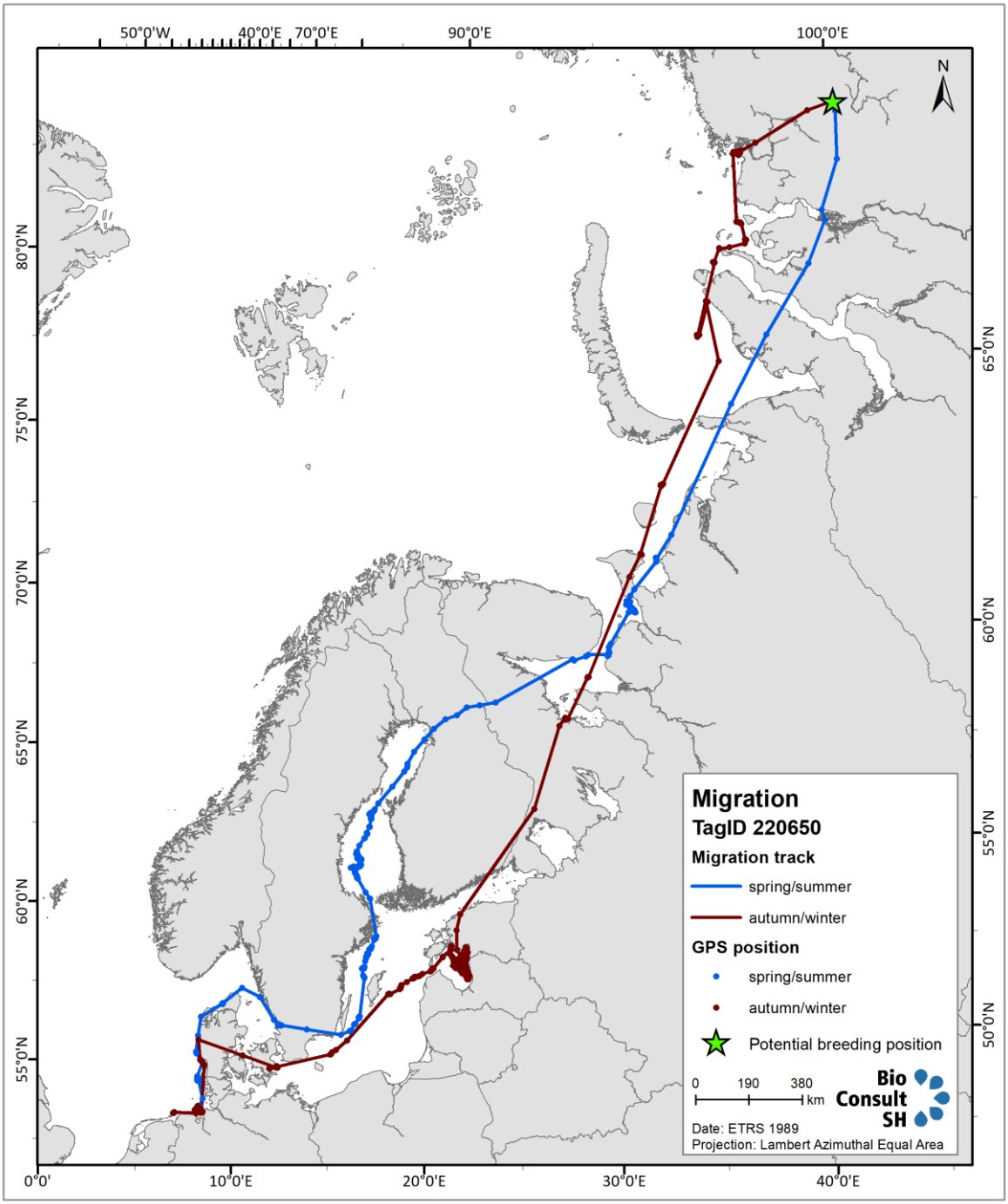
50°0'W
40°0'E
70°0'E
90°0'E
100°0'E
N
80°0'N
75°0'N
70°0'N
65°0'N
60°0'N
55°0'N
50°0'N
0°0'
10°0'E
20°0'E
30°0'E
40°0'E
Migration
TagID 220650
Migration track
spring/summer
autumn/winter
GPS position
spring/summer
autumn/winter
Potential breeding position
0
190
380
km
Bio Consult SH
Date: ETRS 1989
Projection: Lambert Azimuthal Equal Area

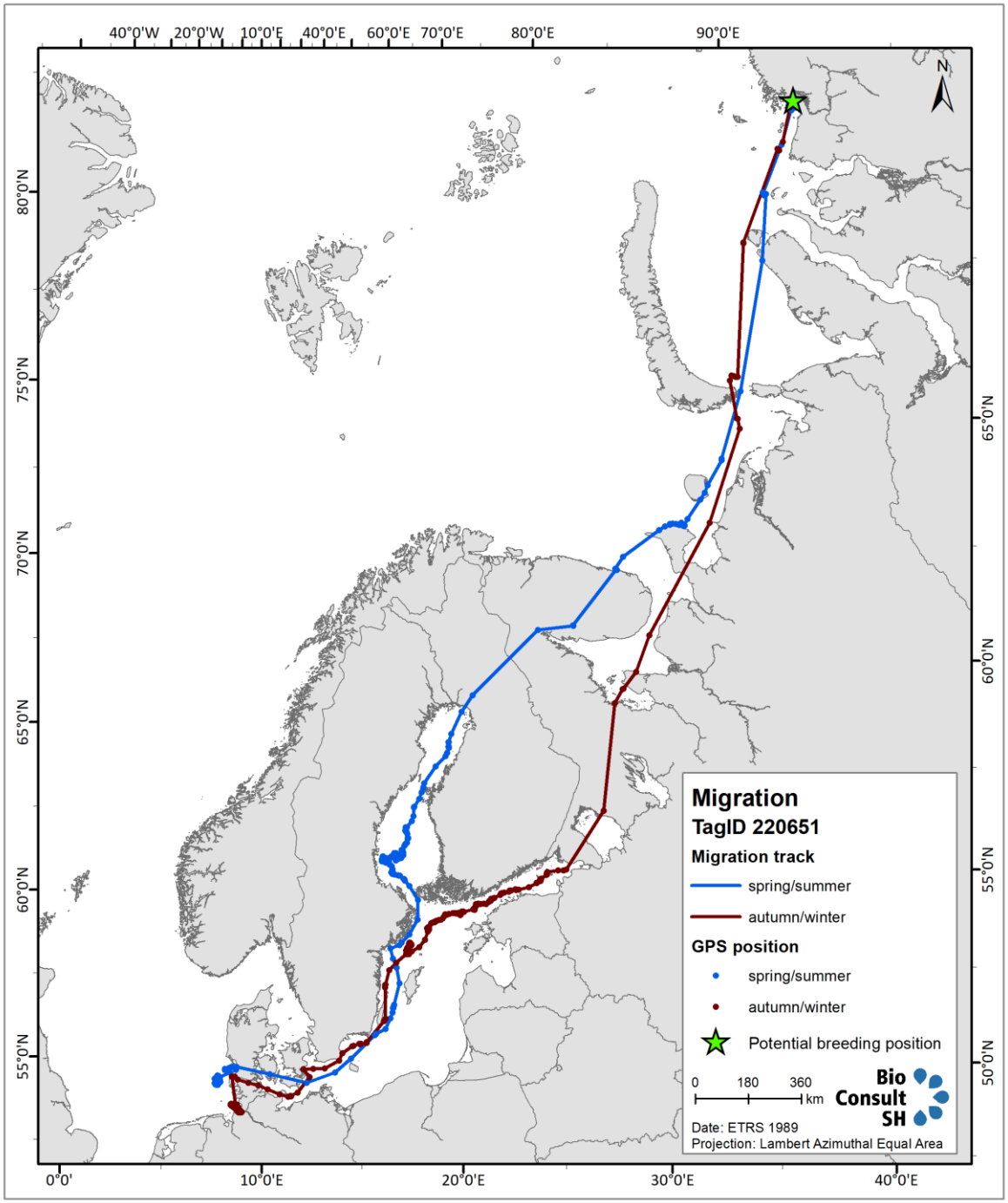
40°0'W
20°0'W
10°0'E
40°0'E
60°0'E
70°0'E
80°0'E
90°0'E
80°0'N
75°0'N
70°0'N
65°0'N
60°0'N
55°0'N
65°0'N
60°0'N
55°0'N
50°0'N
0°0'
10°0'E
20°0'E
30°0'E
40°0'E
N
Migration
TagID 220651
Migration track
spring/summer
autumn/winter
GPS position
spring/summer
autumn/winter
Potential breeding position
0
180
360
km
Bio Consult SH
Date: ETRS 1989
Projection: Lambert Azimuthal Equal Area

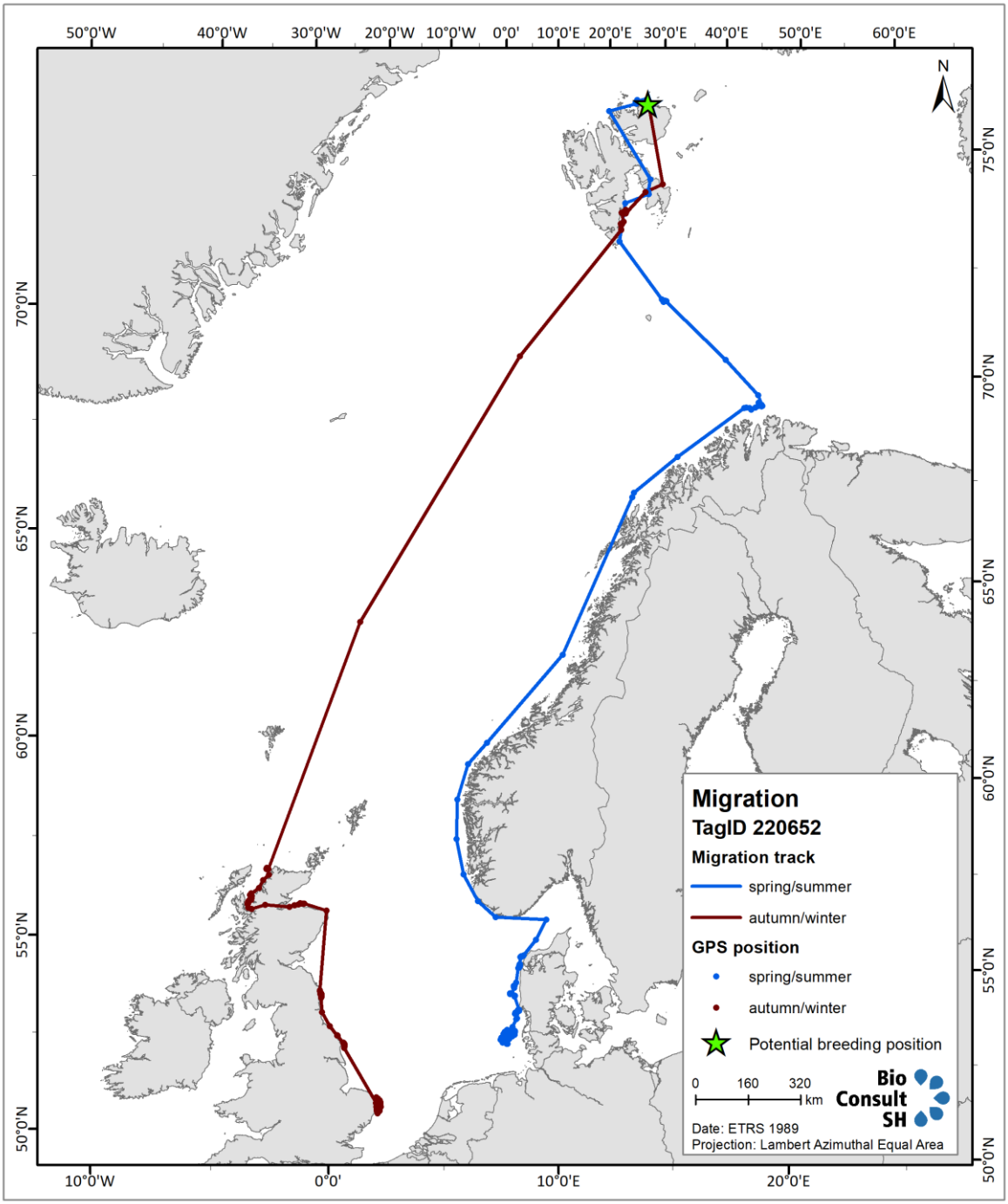
50°0'W
40°0'W
30°0'W
20°0'W
10°0'W
0°0'
10°0'E
20°0'E
30°0'E
40°0'E
50°0'E
60°0'E
N
75°0'N
70°0'N
65°0'N
60°0'N
55°0'N
50°0'N
10°0'W
0°0'
10°0'E
20°0'E
Migration
TagID 220652
Migration track
spring/summer
autumn/winter
GPS position
spring/summer
autumn/winter
Potential breeding position
0
160
320
km
Bio Consult SH
Date: ETRS 1989
Projection: Lambert Azimuthal Equal Area

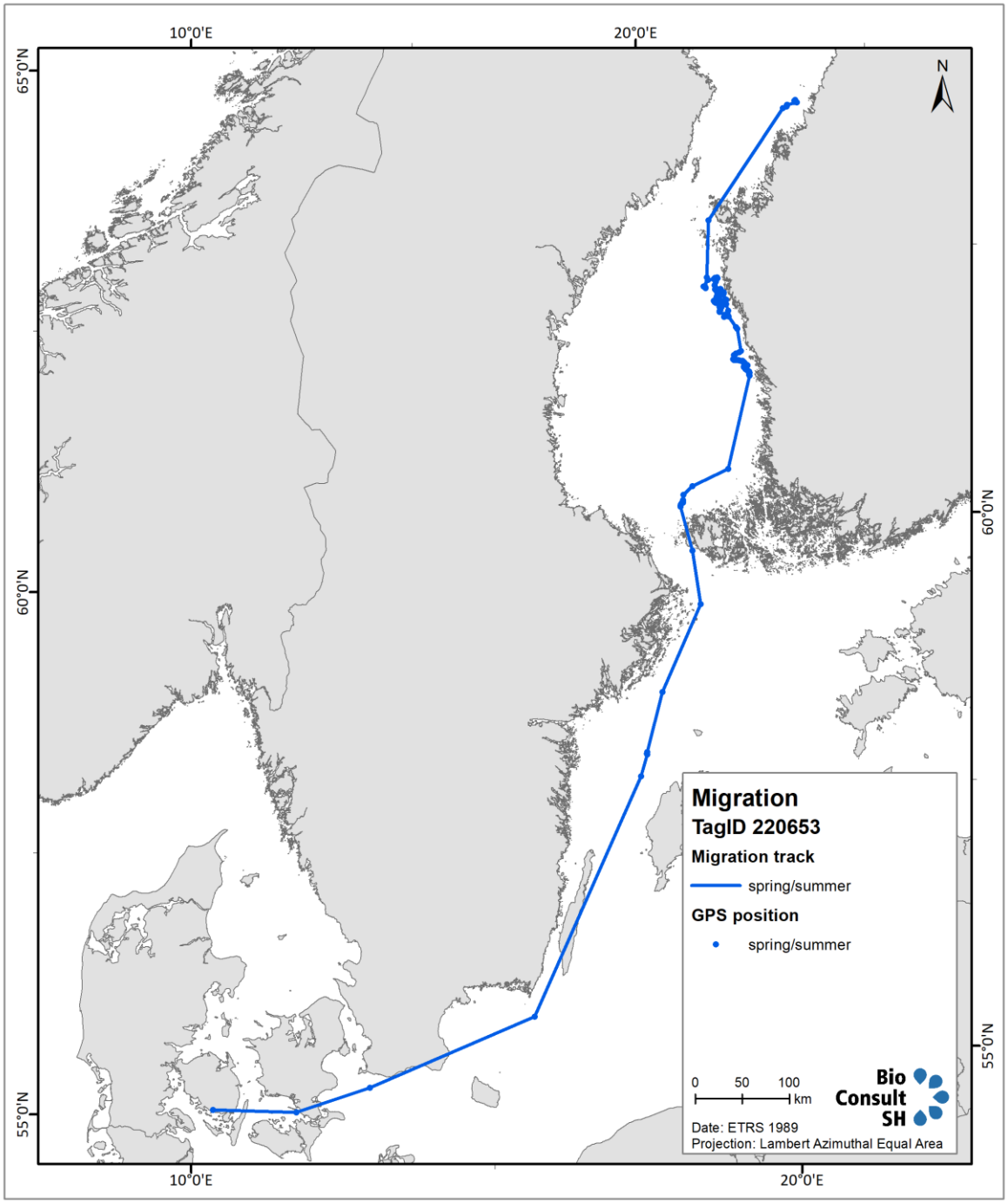
10°0'E
20°0'E
65°0'N
60°0'N
55°0'N
N
Migration
TagID 220653
Migration track
spring/summer
GPS position
spring/summer
0 50 100
km
Bio Consult SH
Date: ETRS 1989
Projection: Lambert Azimuthal Equal Area

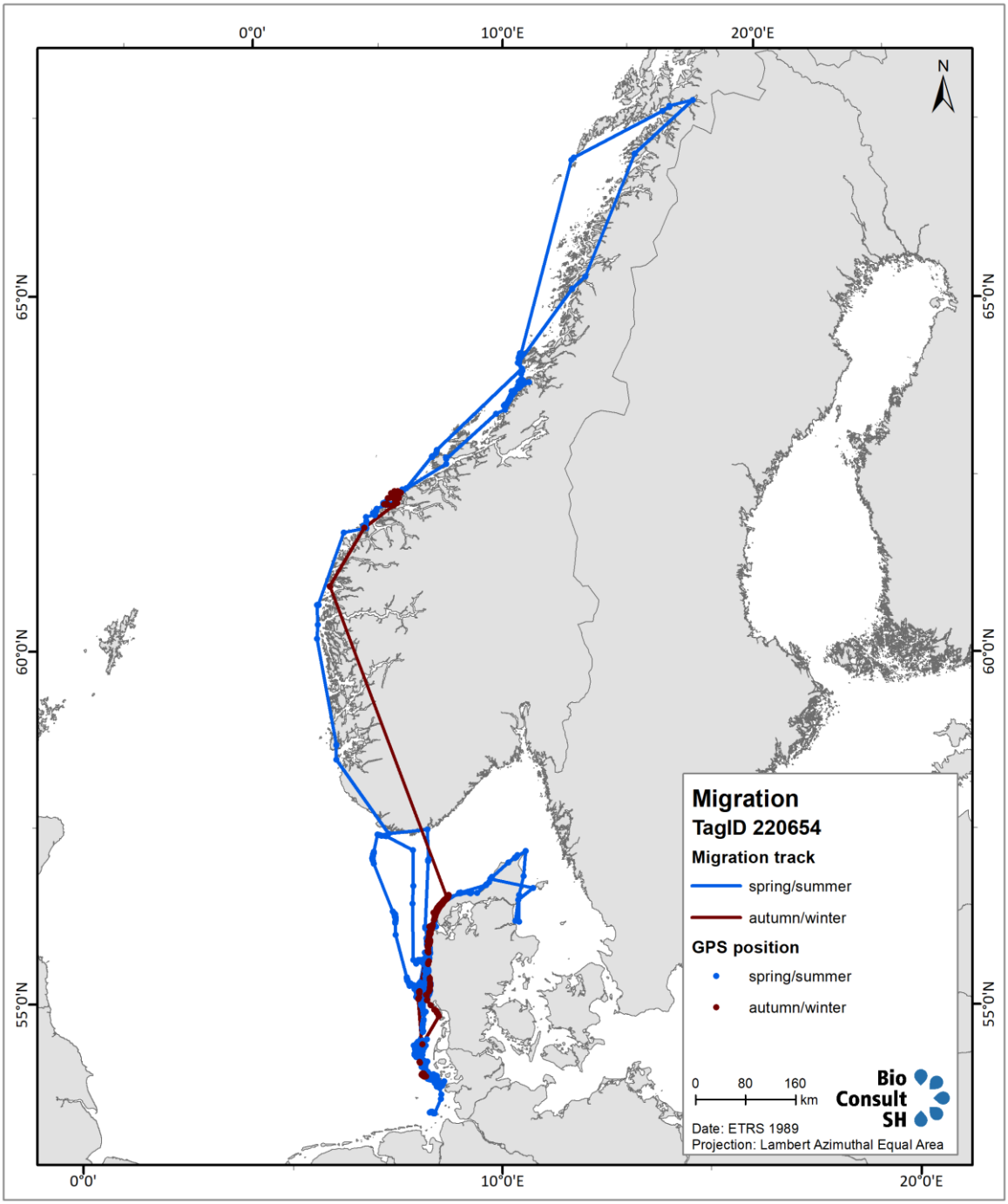
0°0'
10°0'E
20°0'E
N
65°0'N
60°0'N
55°0'N
Migration
TagID 220654
Migration track
spring/summer
autumn/winter
GPS position
spring/summer
autumn/winter
0
80
160
km
Bio Consult SH
Date: ETRS 1989
Projection: Lambert Azimuthal Equal Area

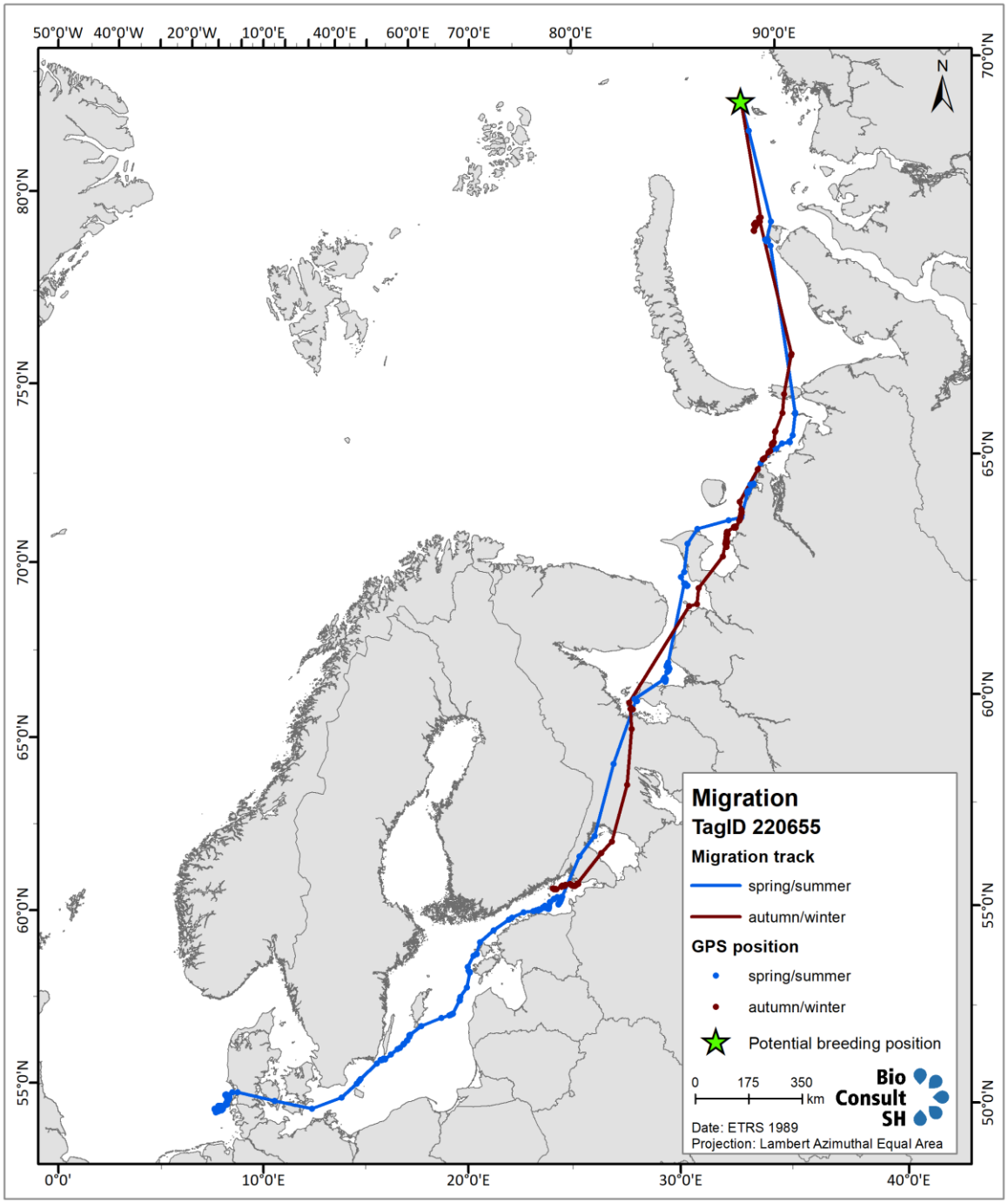
50°0'W
40°0'W
20°0'W
10°0'E
40°0'E
60°0'E
70°0'E
80°0'E
90°0'E
70°0'N
80°0'N
75°0'N
65°0'N
70°0'N
60°0'N
65°0'N
55°0'N
60°0'N
50°0'N
0°0'
10°0'E
20°0'E
30°0'E
40°0'E
N
Migration
TagID 220655
Migration track
spring/summer
autumn/winter
GPS position
spring/summer
autumn/winter
Potential breeding position
0
175
350
km
Bio Consult SH
Date: ETRS 1989
Projection: Lambert Azimuthal Equal Area

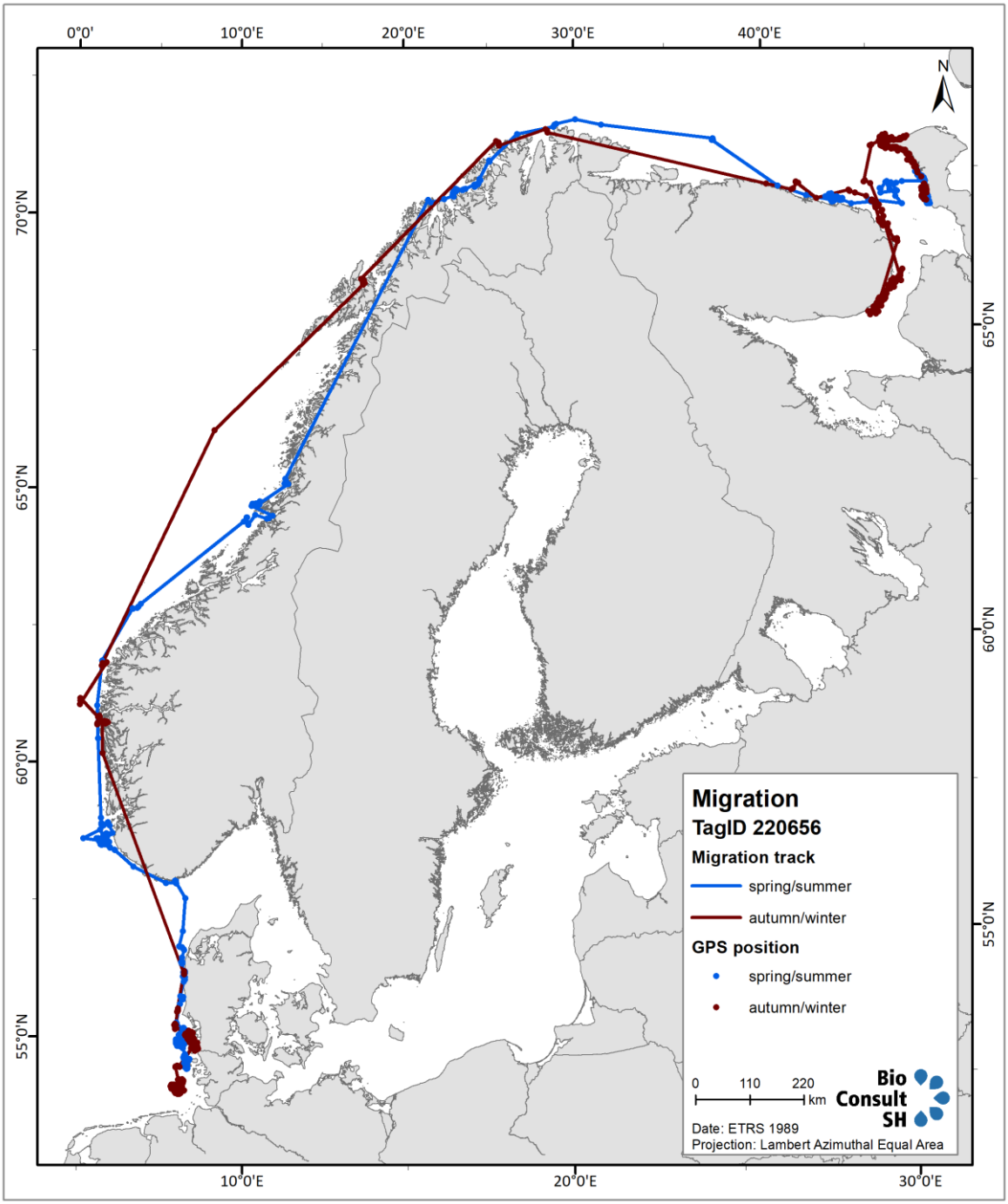
0°0'
10°0'E
20°0'E
30°0'E
40°0'E
70°0'N
65°0'N
60°0'N
55°0'N
N
Migration
TagID 220656
Migration track
spring/summer
autumn/winter
GPS position
spring/summer
autumn/winter
0
110
220
km
Bio Consult SH
Date: ETRS 1989
Projection: Lambert Azimuthal Equal Area

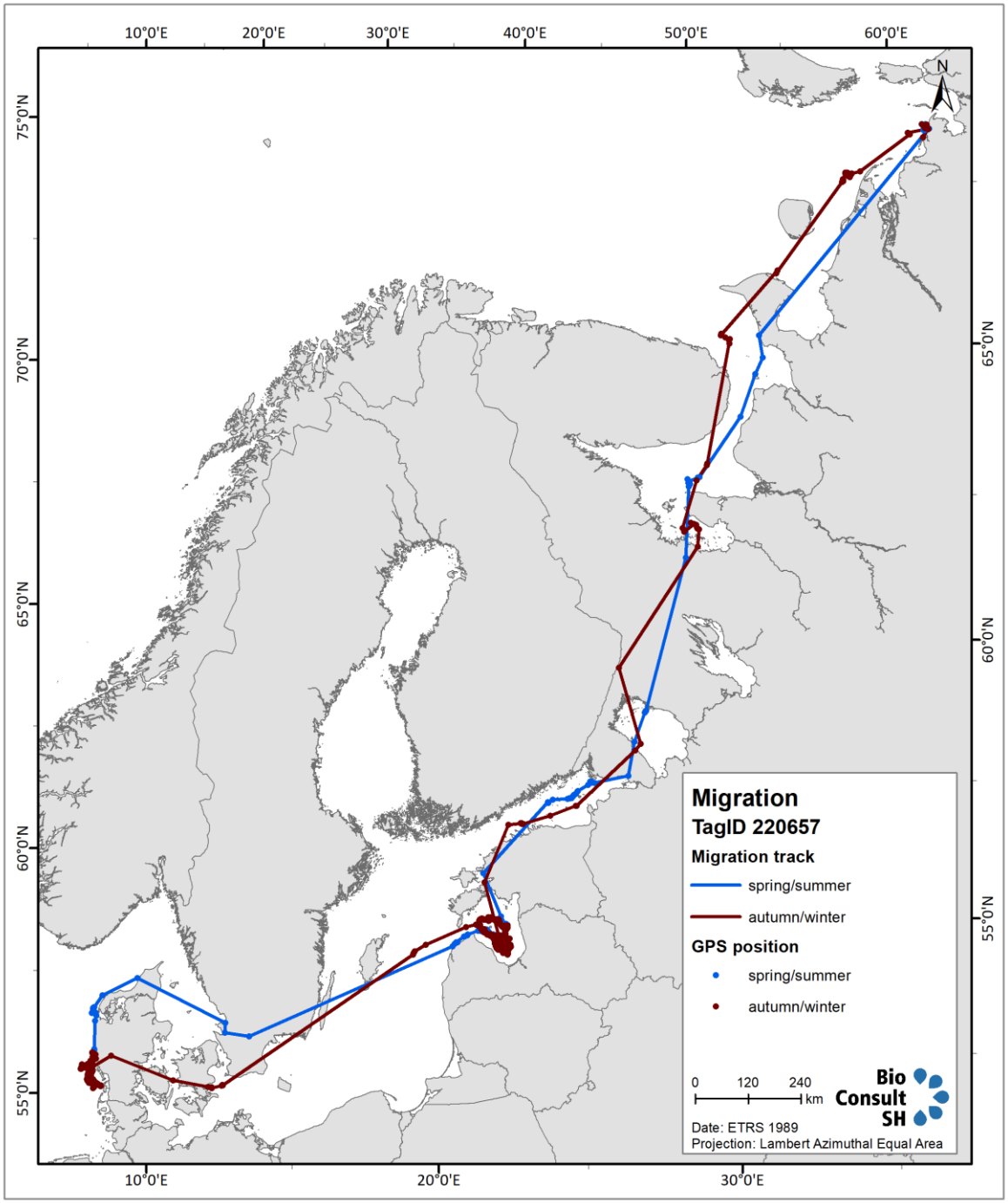
10°0'E
20°0'E
30°0'E
40°0'E
50°0'E
60°0'E
75°0'N
70°0'N
65°0'N
60°0'N
55°0'N
N
Migration
TagID 220657
Migration track
spring/summer
autumn/winter
GPS position
spring/summer
autumn/winter
0
120
240
km
Bio Consult SH
Date: ETRS 1989
Projection: Lambert Azimuthal Equal Area

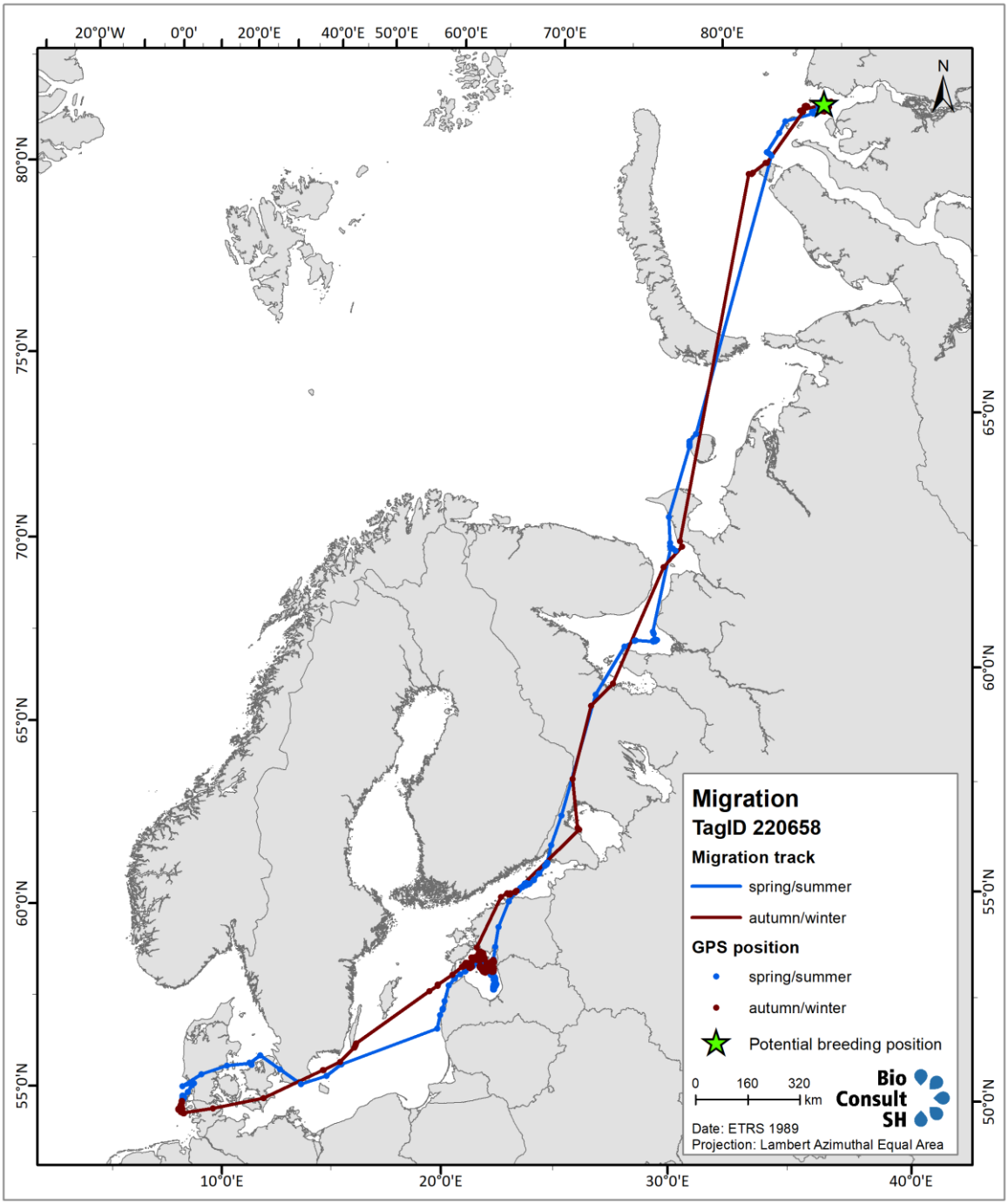
20°0'W
0°0'
20°0'E
40°0'E
50°0'E
60°0'E
70°0'E
80°0'E
80°0'N
75°0'N
70°0'N
65°0'N
60°0'N
55°0'N
65°0'N
60°0'N
55°0'N
50°0'N
10°0'E
20°0'E
30°0'E
40°0'E
N
Migration
TagID 220658
Migration track
spring/summer
autumn/winter
GPS position
spring/summer
autumn/winter
Potential breeding position
0
160
320
km
Bio Consult SH
Date: ETRS 1989
Projection: Lambert Azimuthal Equal Area

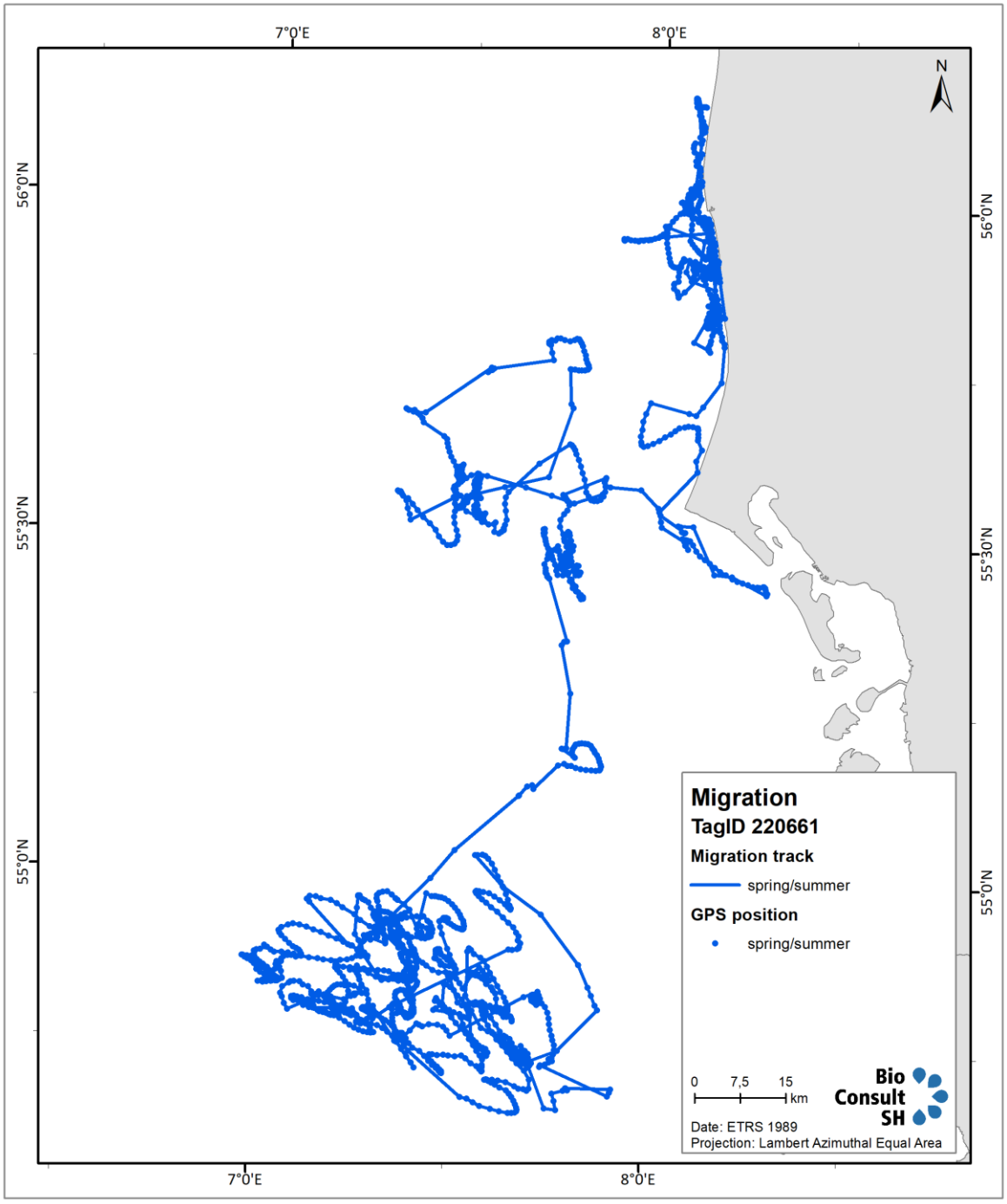
7°0'E
8°0'E
56°0'N
55°30'N
55°0'N
N
Migration
TagID 220661
Migration track
spring/summer
GPS position
spring/summer
0 7,5 15
km
Bio Consult SH
Date: ETRS 1989
Projection: Lambert Azimuthal Equal Area

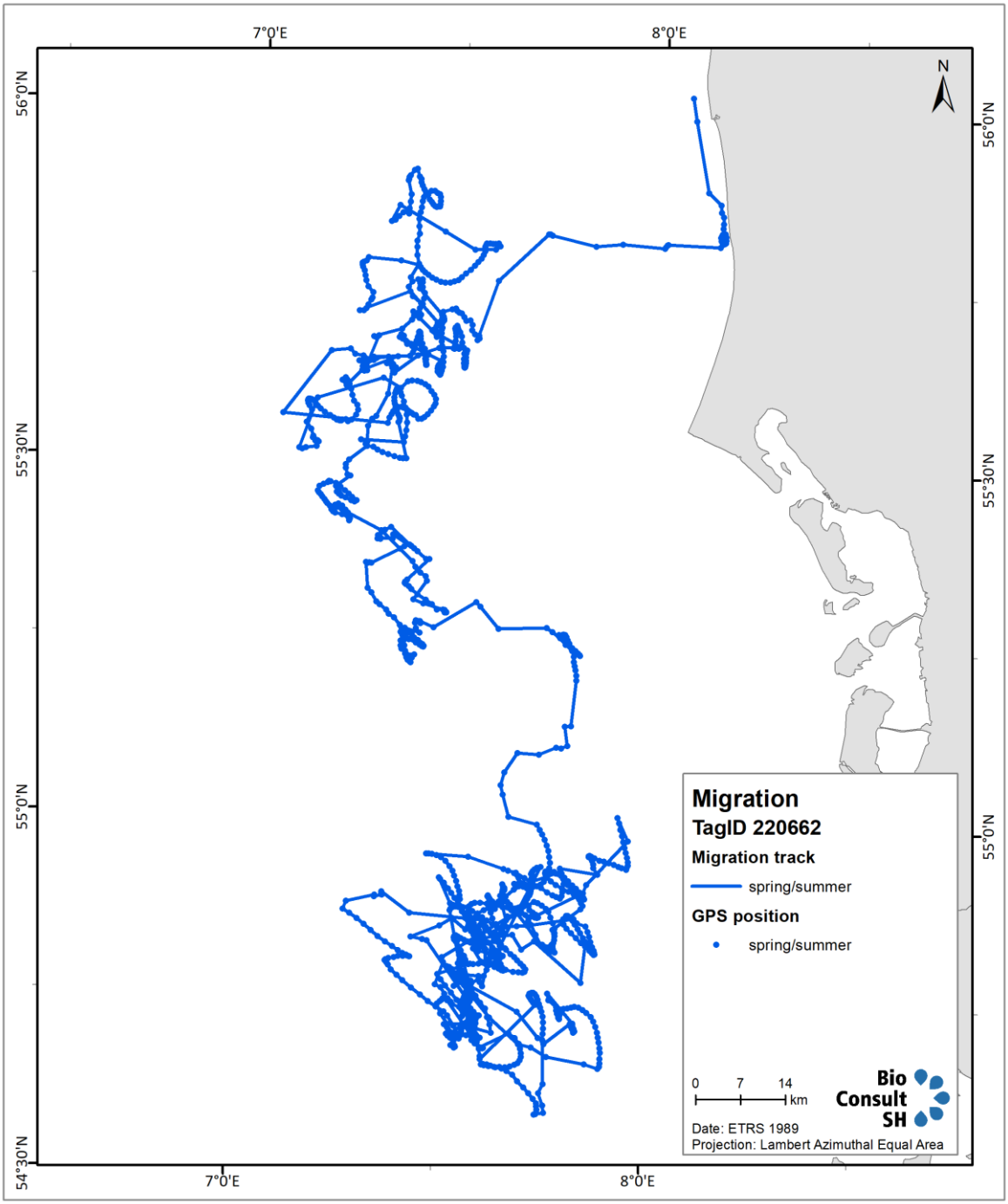
7°0'E
8°0'E
56°0'N
55°30'N
55°0'N
54°30'N
N
Migration
TagID 220662
Migration track
spring/summer
GPS position
spring/summer
0 7 14
km
Bio Consult SH
Date: ETRS 1989
Projection: Lambert Azimuthal Equal Area

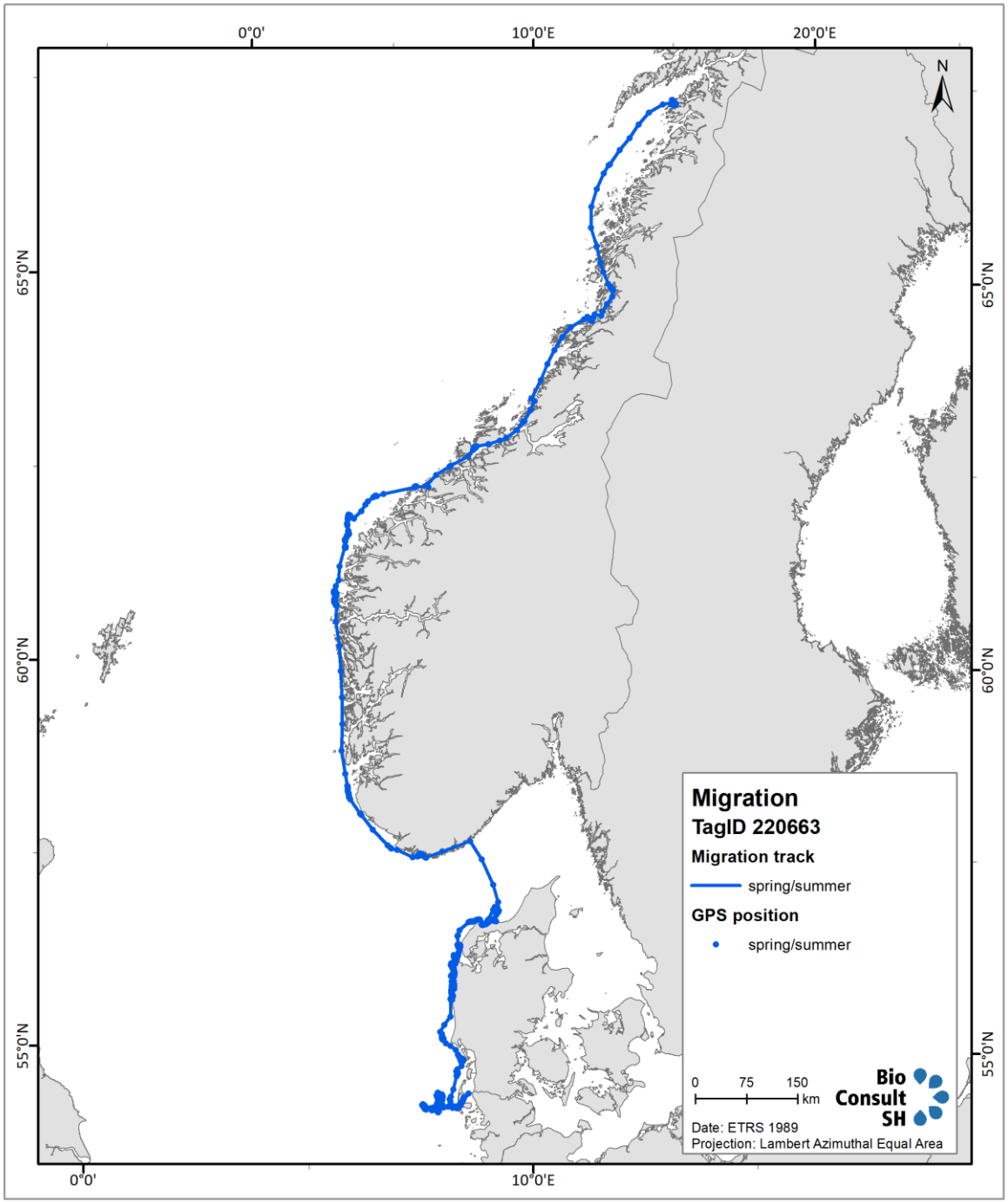
0°0'
10°0'E
20°0'E
N
65°0'N
60°0'N
55°0'N
Migration
TagID 220663
Migration track
spring/summer
GPS position
spring/summer
0
75
150
km
Bio Consult SH
Date: ETRS 1989
Projection: Lambert Azimuthal Equal Area

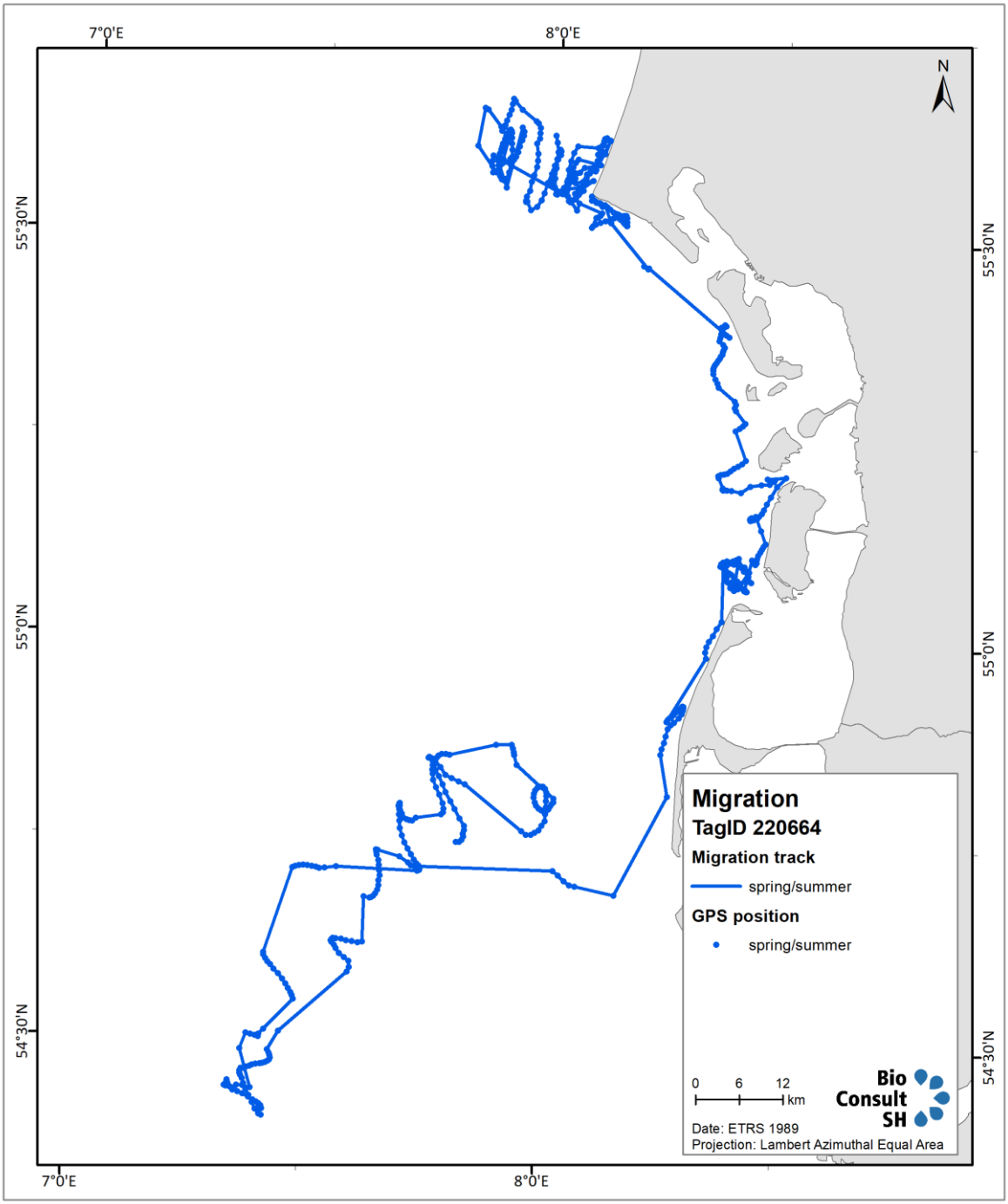
7°0'E
8°0'E
N
55°30'N
55°0'N
54°30'N
Migration
TagID 220664
Migration track
spring/summer
GPS position
spring/summer
0 6 12
km
Bio Consult SH
Date: ETRS 1989
Projection: Lambert Azimuthal Equal Area

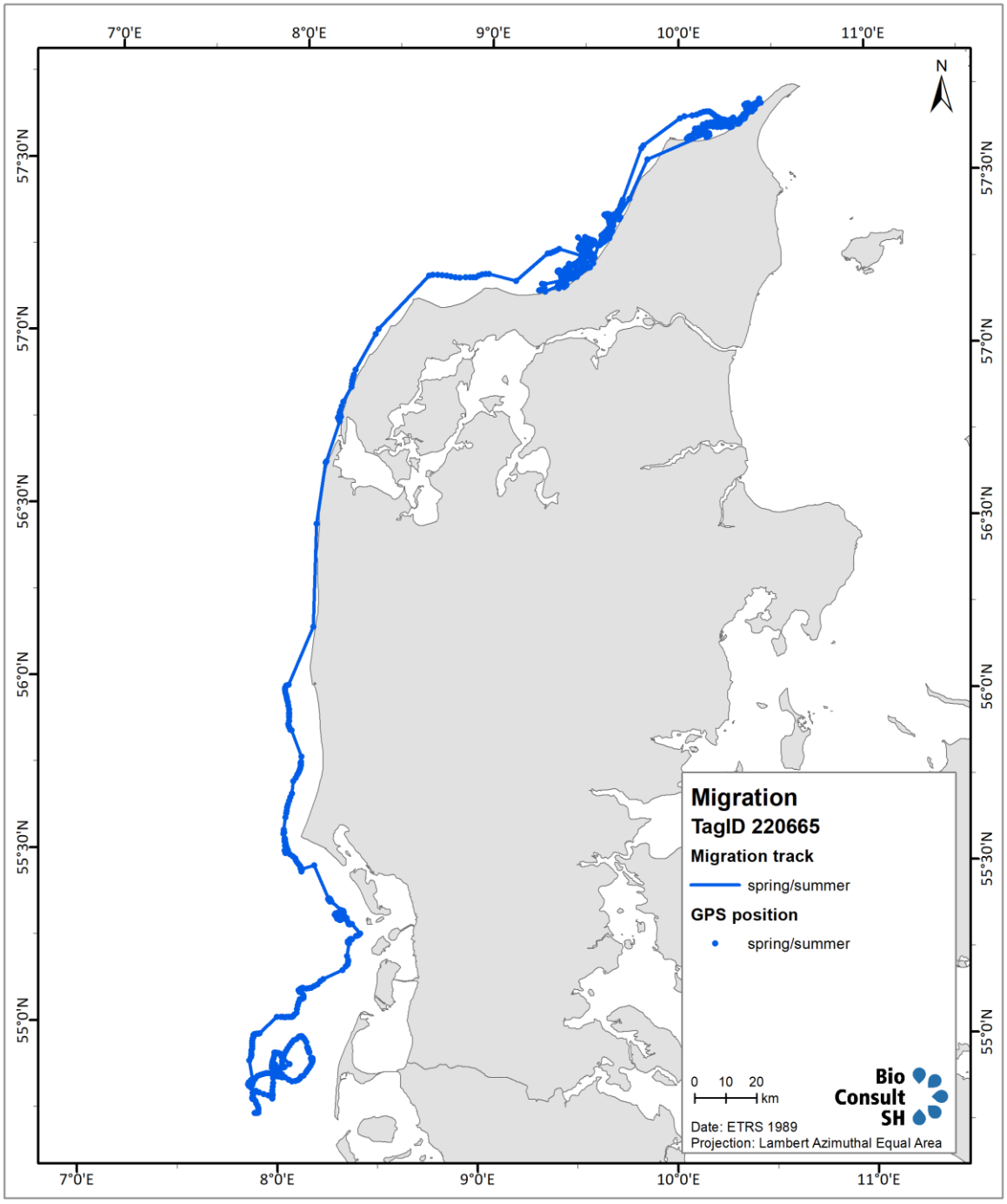
7°0'E
8°0'E
9°0'E
10°0'E
11°0'E
57°30'N
57°0'N
56°30'N
56°0'N
55°30'N
55°0'N
N
Migration
TagID 220665
Migration track
spring/summer
GPS position
spring/summer
0 10 20
km
Bio Consult SH
Date: ETRS 1989
Projection: Lambert Azimuthal Equal Area

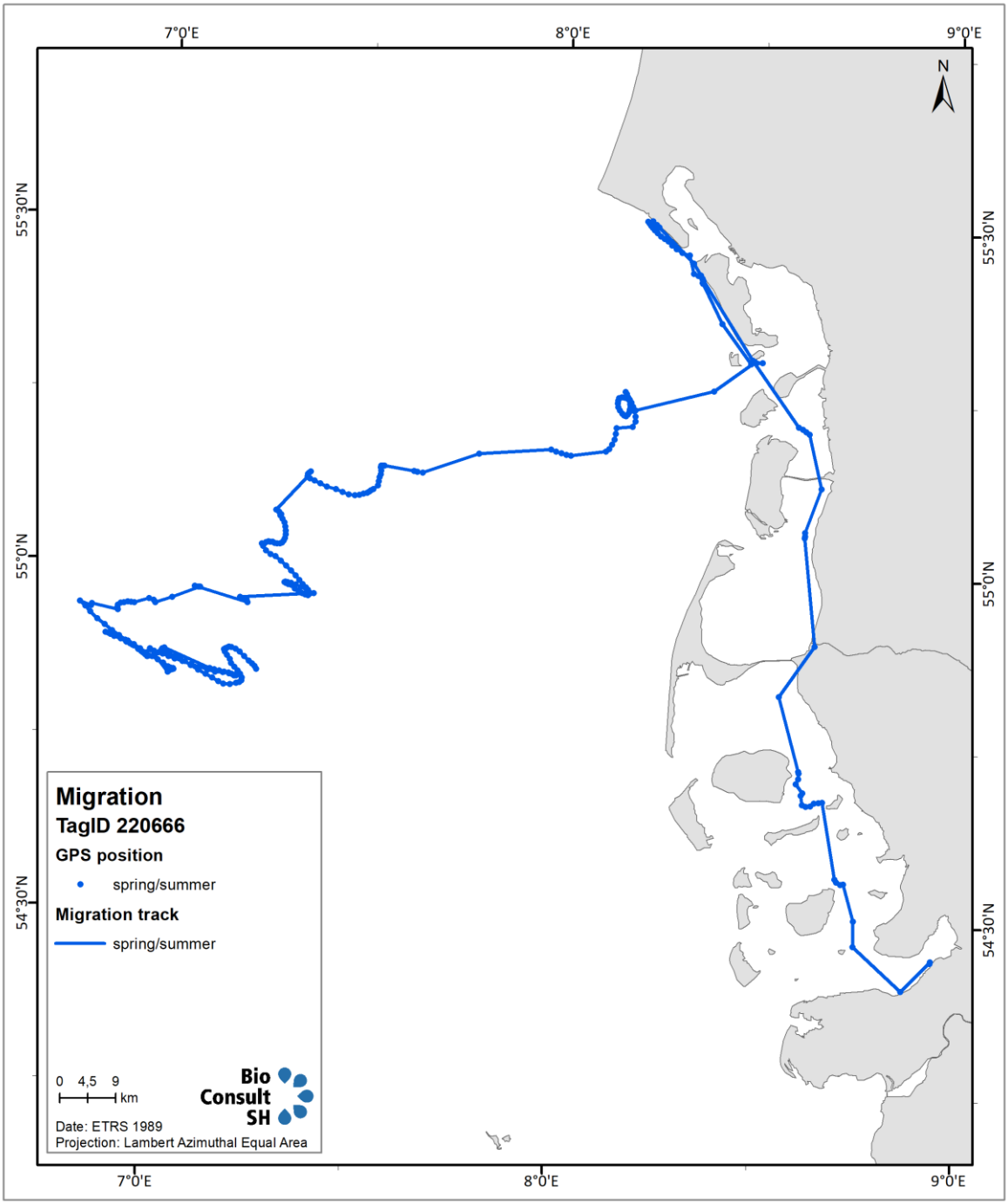
7°0'E
8°0'E
9°0'E
55°30'N
55°0'N
54°30'N
N
Migration
TagID 220666
GPS position
spring/summer
Migration track
spring/summer
0 4,5 9
km
Bio Consult SH
Date: ETRS 1989
Projection: Lambert Azimuthal Equal Area

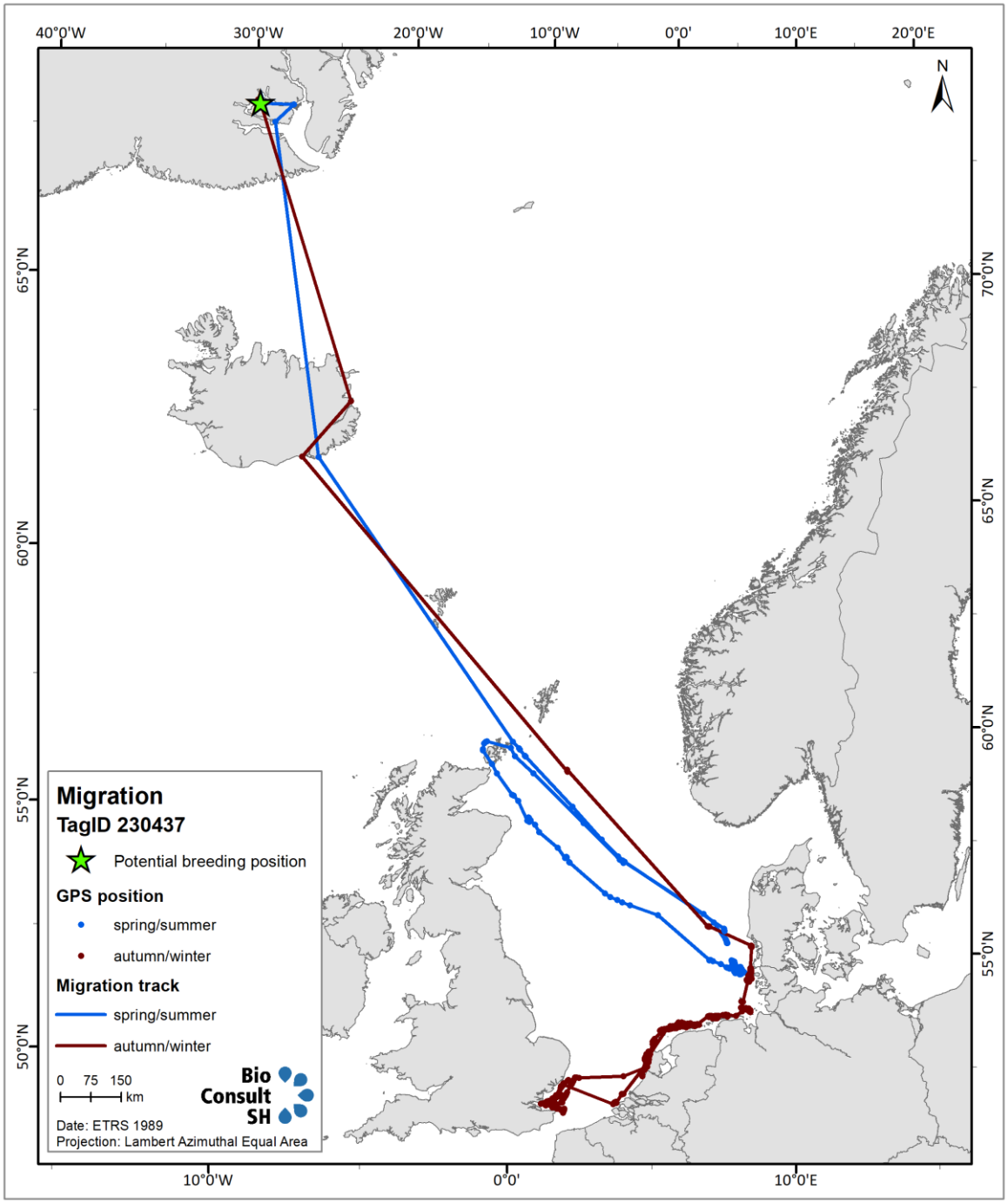
40°0'W
30°0'W
20°0'W
10°0'W
0°0'
10°0'E
20°0'E
N
65°0'N
60°0'N
55°0'N
50°0'N
70°0'N
65°0'N
60°0'N
55°0'N
10°0'W
0°0'
10°0'E
Migration
TagID 230437
Potential breeding position
GPS position
spring/summer
autumn/winter
Migration track
spring/summer
autumn/winter
0 75 150
km
Bio Consult SH
Date: ETRS 1989
Projection: Lambert Azimuthal Equal Area

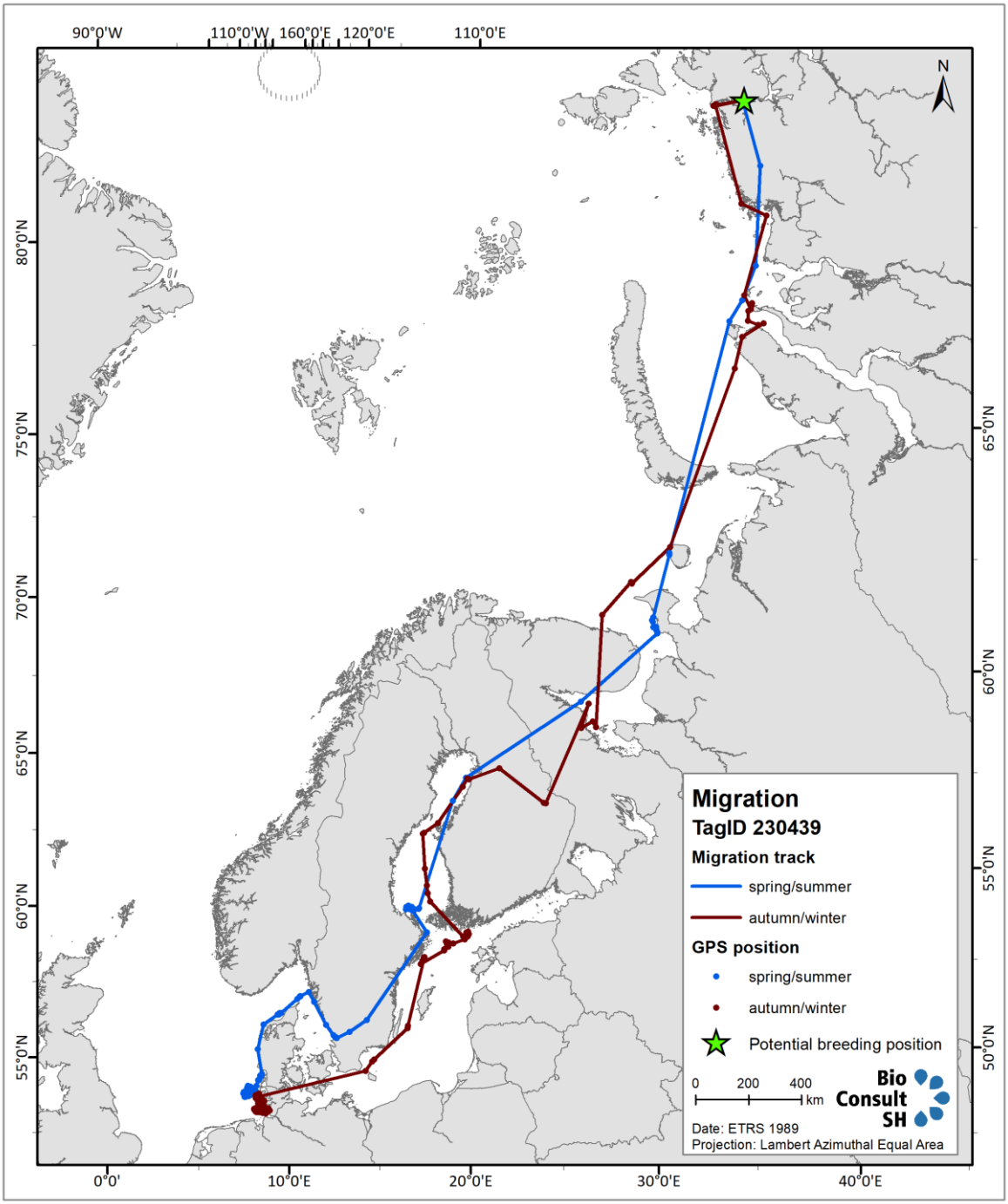
90°0'W
110°0'W
160°0'E
120°0'E
110°0'E
N
80°0'N
75°0'N
70°0'N
65°0'N
60°0'N
55°0'N
65°0'N
60°0'N
55°0'N
50°0'N
0°0'
10°0'E
20°0'E
30°0'E
40°0'E
Migration
TagID 230439
Migration track
spring/summer
autumn/winter
GPS position
spring/summer
autumn/winter
Potential breeding position
0
200
400
km
Bio Consult SH
Date: ETRS 1989
Projection: Lambert Azimuthal Equal Area

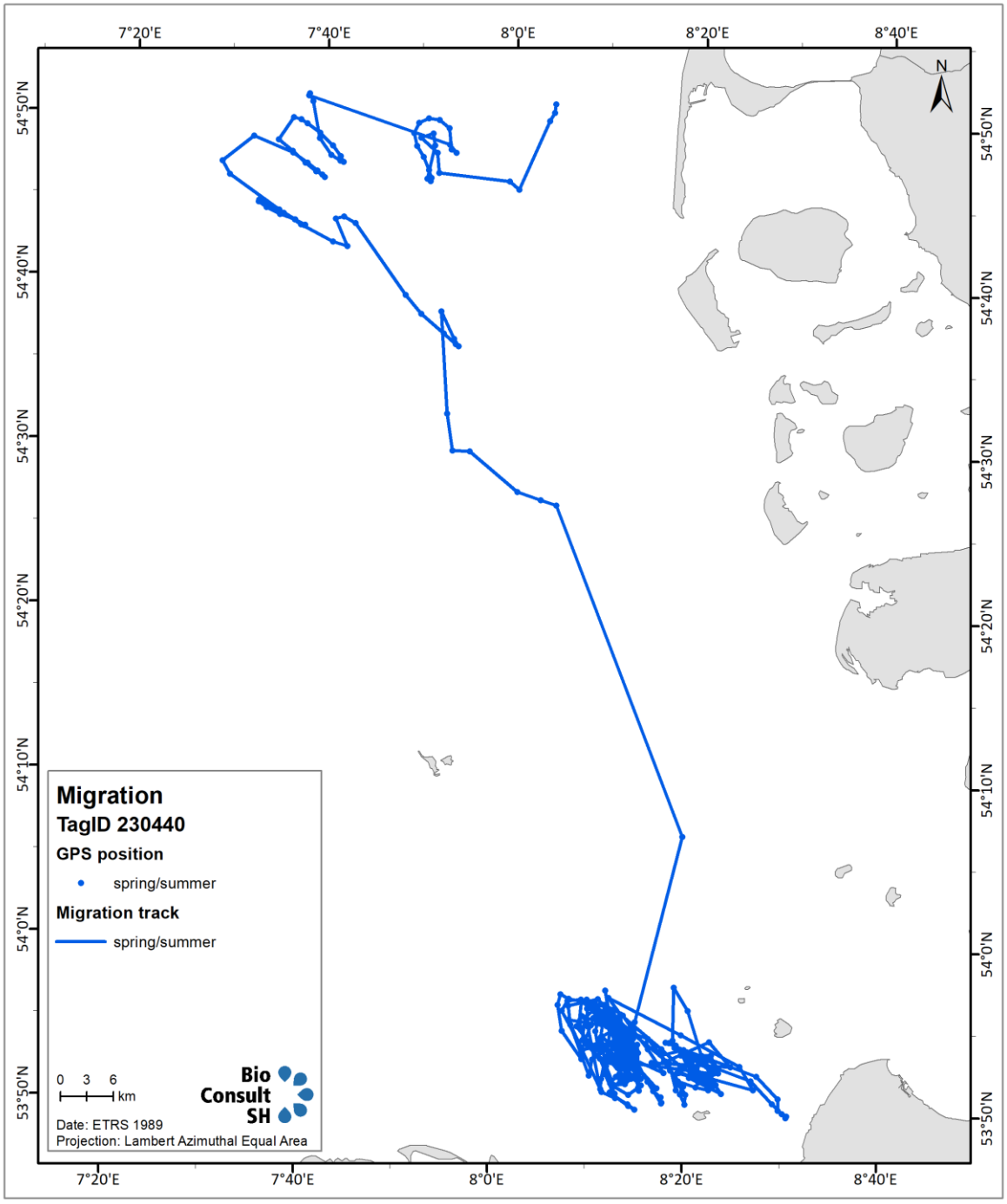
7°20'E
7°40'E
8°0'E
8°20'E
8°40'E
54°50'N
54°40'N
54°30'N
54°20'N
54°10'N
54°0'N
53°50'N
N
Migration
TagID 230440
GPS position
spring/summer
Migration track
spring/summer
0 3 6
km
Bio Consult SH
Date: ETRS 1989
Projection: Lambert Azimuthal Equal Area

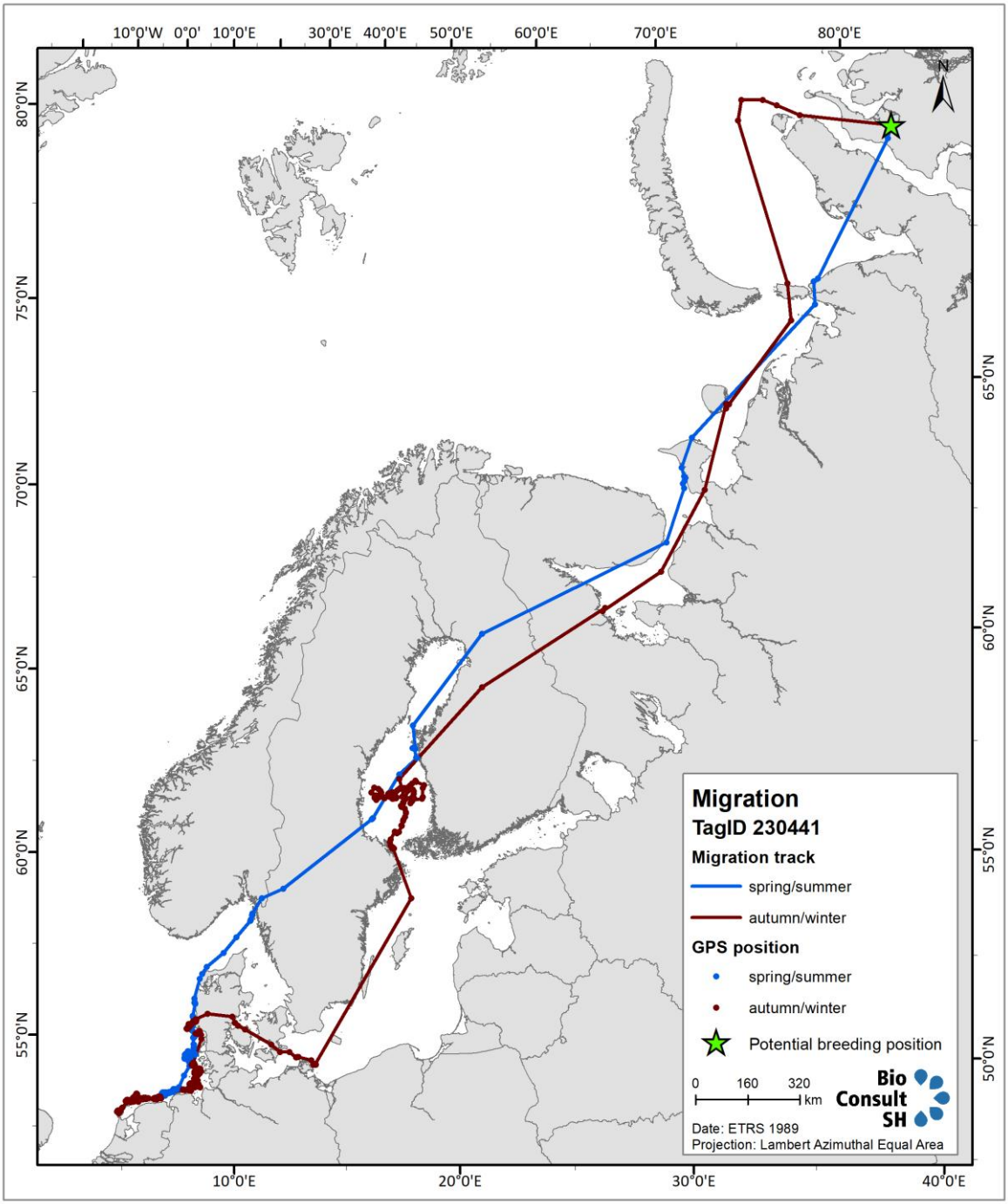
10°0'W
0°0'
10°0'E
30°0'E
40°0'E
50°0'E
60°0'E
70°0'E
80°0'E
80°0'N
75°0'N
70°0'N
65°0'N
60°0'N
55°0'N
50°0'N
N
Migration
TagID 230441
Migration track
spring/summer
autumn/winter
GPS position
spring/summer
autumn/winter
Potential breeding position
0
160
320
km
Bio Consult SH
Date: ETRS 1989
Projection: Lambert Azimuthal Equal Area

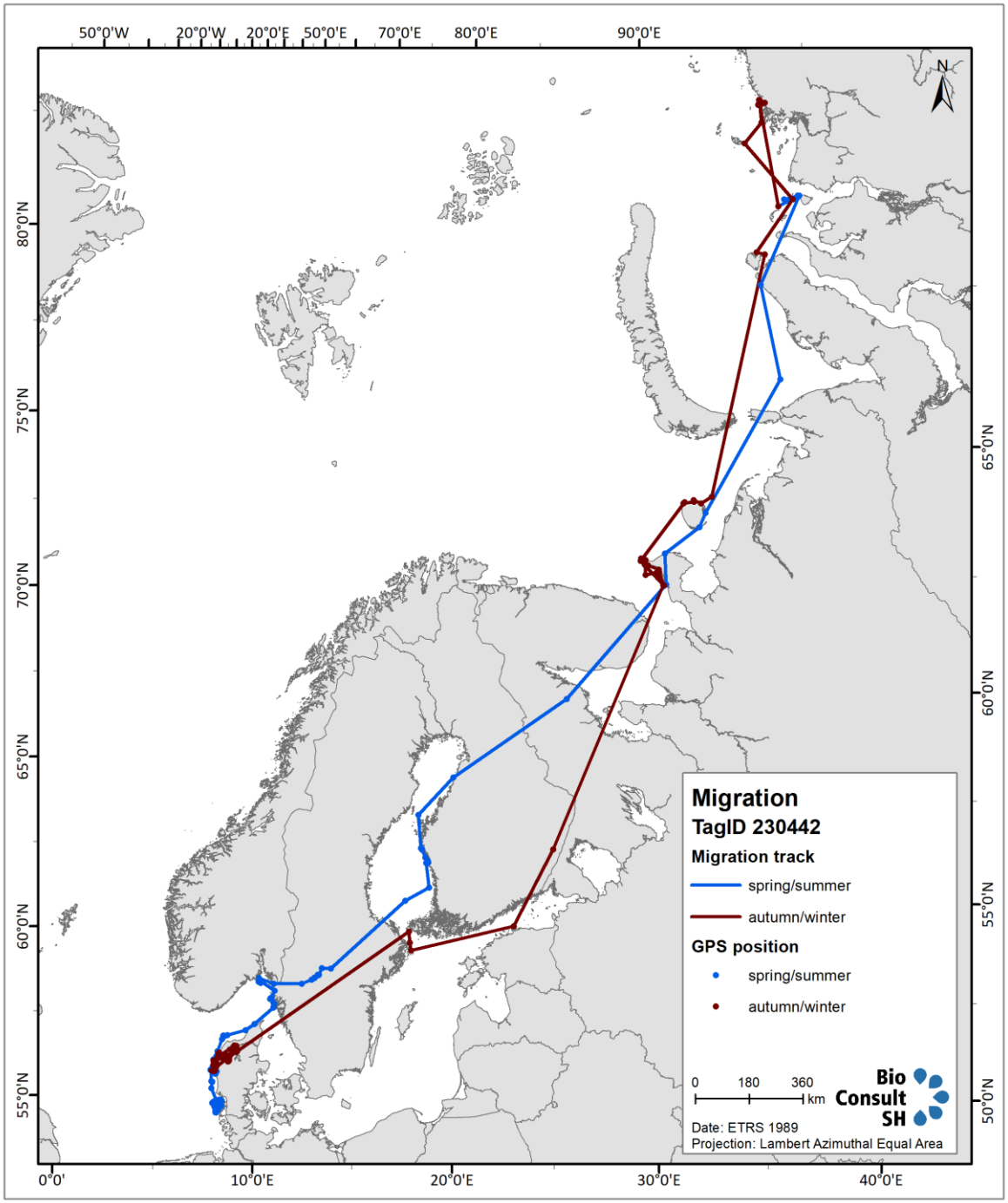
50°0'W
20°0'W
20°0'E
50°0'E
70°0'E
80°0'E
90°0'E
N
80°0'N
75°0'N
70°0'N
65°0'N
60°0'N
55°0'N
65°0'N
60°0'N
55°0'N
50°0'N
0°0'
10°0'E
20°0'E
30°0'E
40°0'E
Migration
TagID 230442
Migration track
spring/summer
autumn/winter
GPS position
spring/summer
autumn/winter
0
180
360
km
Bio Consult SH
Date: ETRS 1989
Projection: Lambert Azimuthal Equal Area

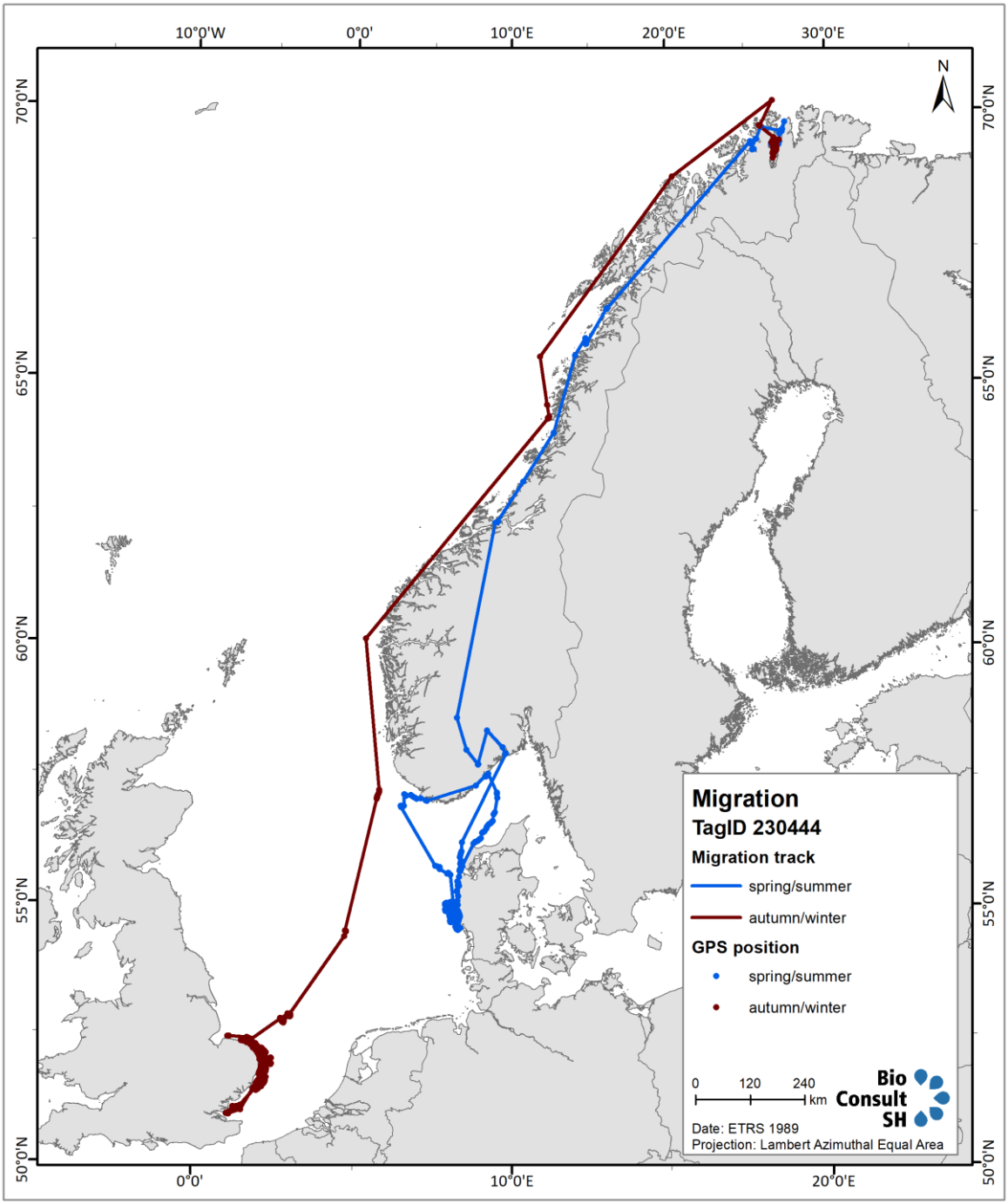
10°0'W
0°0'
10°0'E
20°0'E
30°0'E
70°0'N
65°0'N
60°0'N
55°0'N
50°0'N
N
Migration
TagID 230444
Migration track
spring/summer
autumn/winter
GPS position
spring/summer
autumn/winter
0
120
240
km
Bio Consult SH
Date: ETRS 1989
Projection: Lambert Azimuthal Equal Area

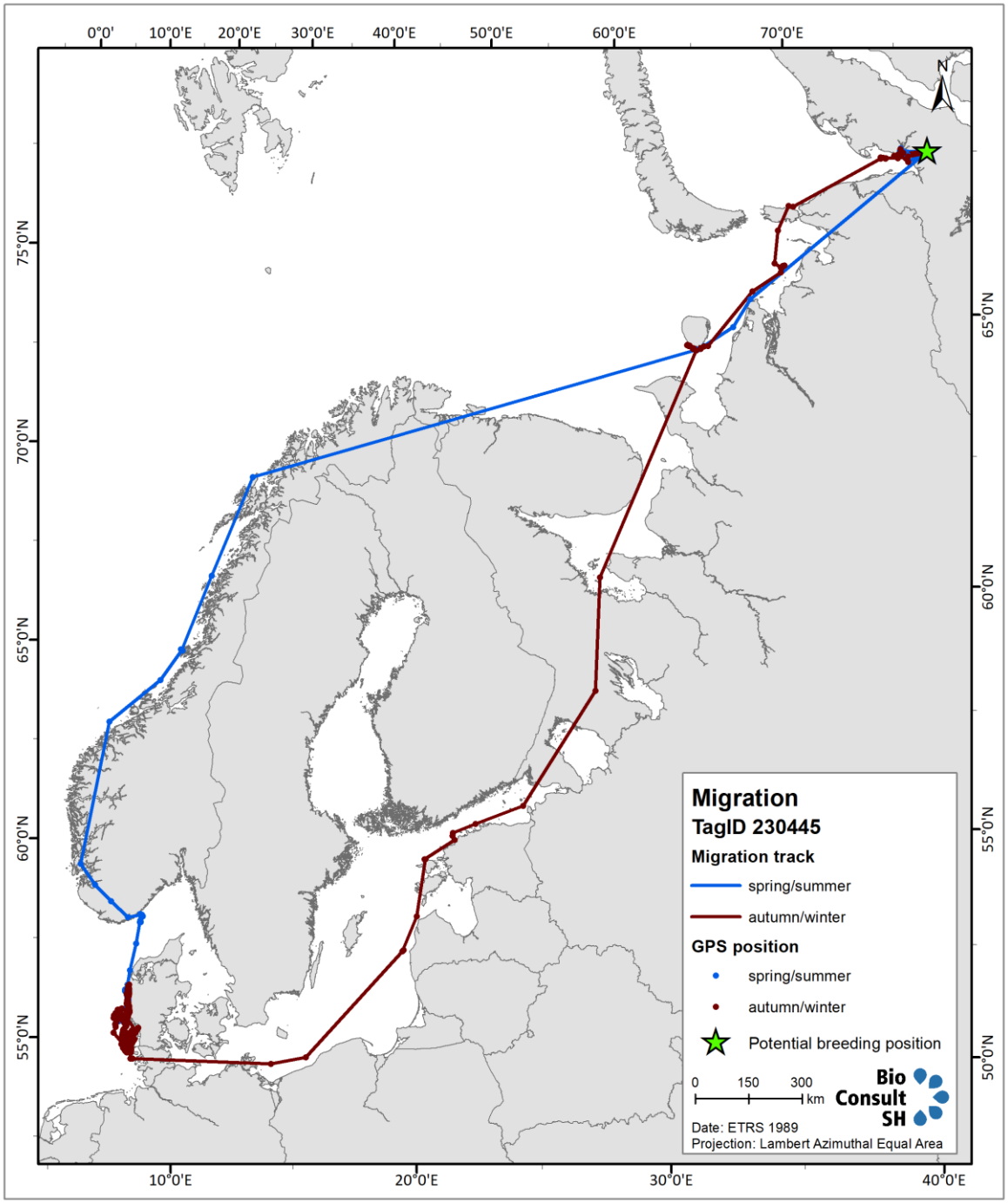
0°0'
10°0'E
20°0'E
30°0'E
40°0'E
50°0'E
60°0'E
70°0'E
75°0'N
70°0'N
65°0'N
60°0'N
55°0'N
50°0'N
N
Migration
TagID 230445
Migration track
spring/summer
autumn/winter
GPS position
spring/summer
autumn/winter
Potential breeding position
0
150
300
km
Bio Consult SH
Date: ETRS 1989
Projection: Lambert Azimuthal Equal Area

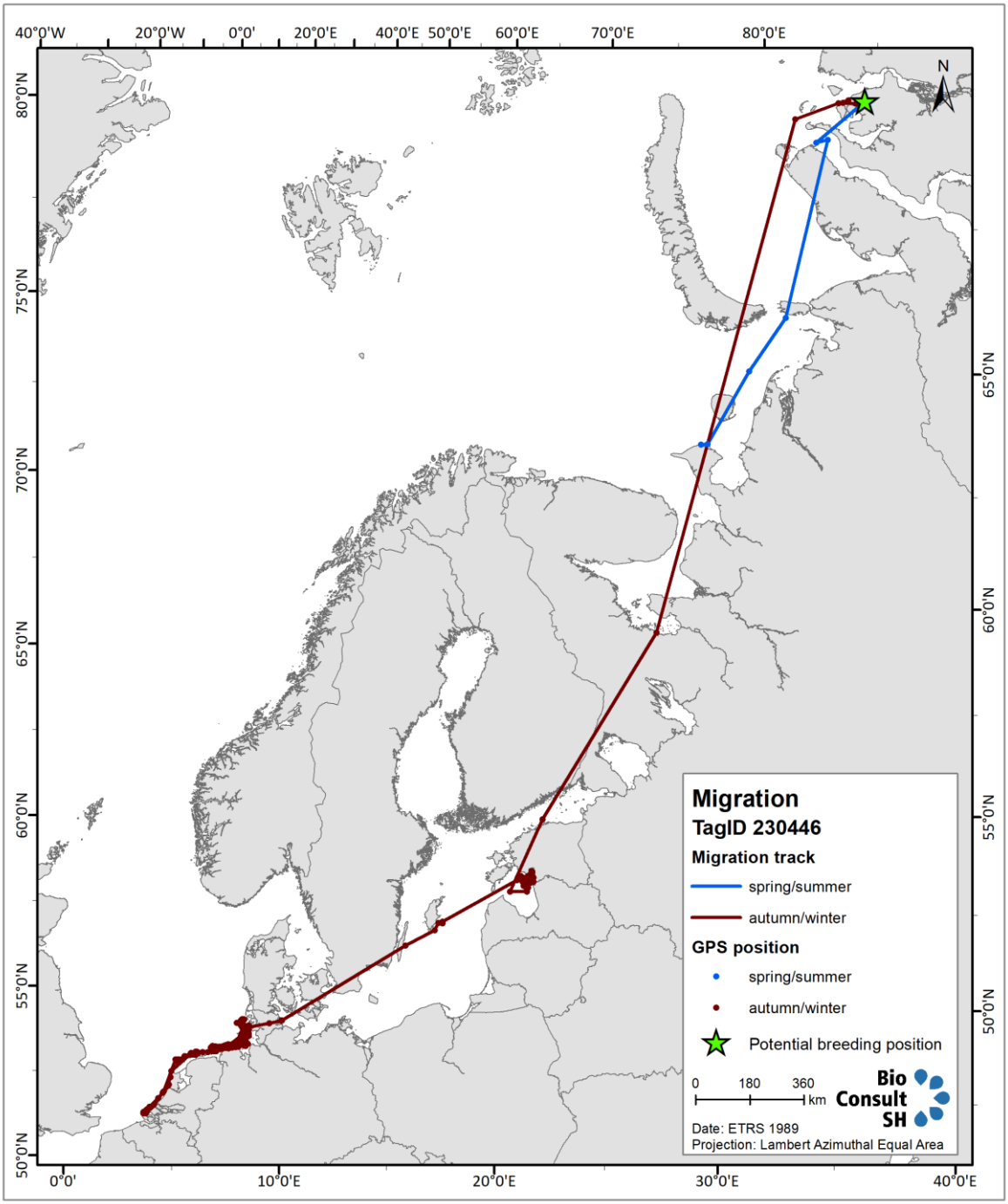
40°0'W
20°0'W
0°0'
20°0'E
40°0'E
50°0'E
60°0'E
70°0'E
80°0'E
80°0'N
75°0'N
70°0'N
65°0'N
60°0'N
55°0'N
50°0'N
N
Migration
TagID 230446
Migration track
spring/summer
autumn/winter
GPS position
spring/summer
autumn/winter
Potential breeding position
0
180
360
km
Bio Consult SH
Date: ETRS 1989
Projection: Lambert Azimuthal Equal Area
0°0'
10°0'E
20°0'E
30°0'E
40°0'E

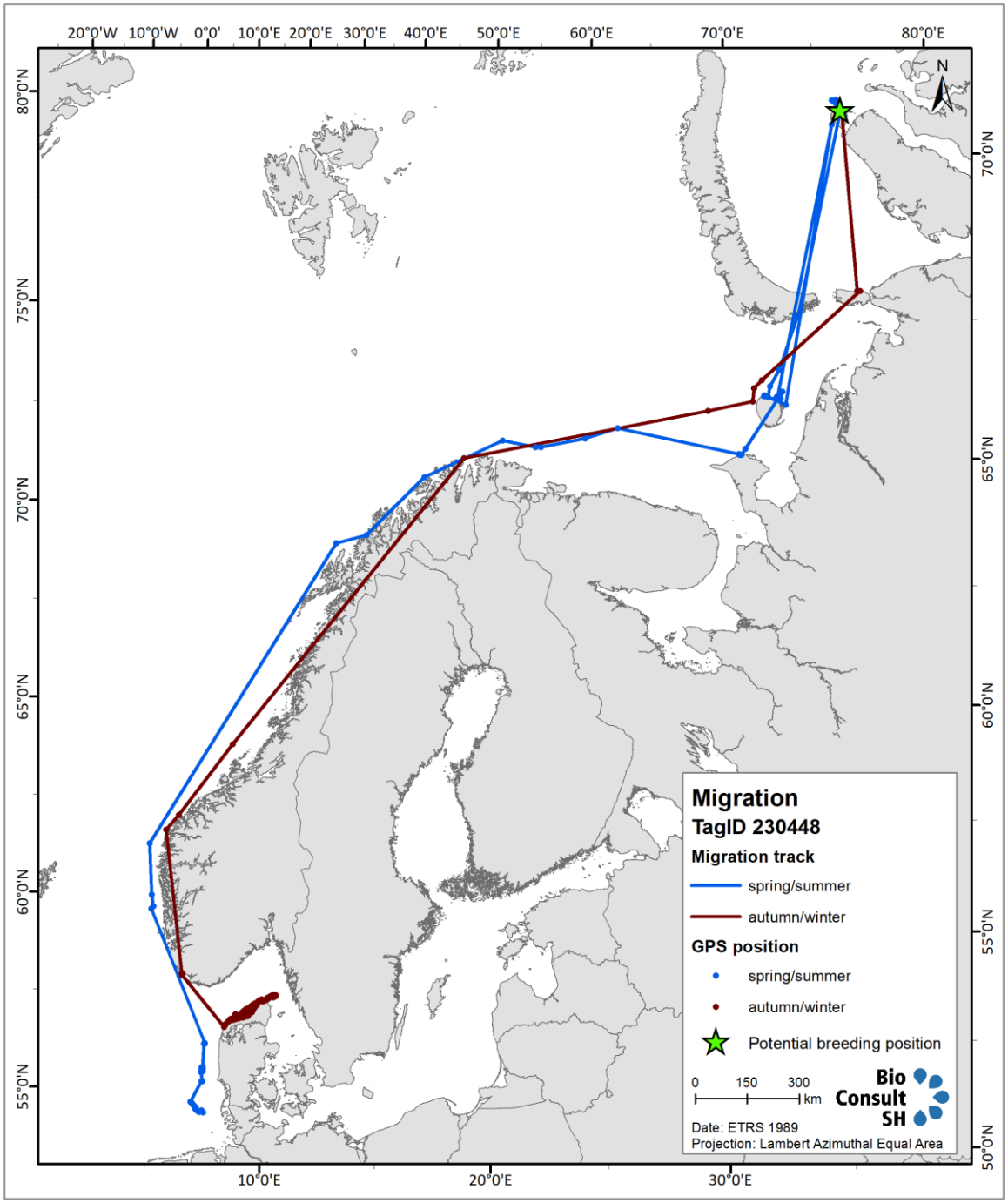
20°0'W
10°0'W
0°0'
10°0'E
20°0'E
30°0'E
40°0'E
50°0'E
60°0'E
70°0'E
80°0'E
80°0'N
75°0'N
70°0'N
65°0'N
60°0'N
55°0'N
50°0'N
N
Migration
TagID 230448
Migration track
spring/summer
autumn/winter
GPS position
spring/summer
autumn/winter
Potential breeding position
0
150
300
km
Bio Consult SH
Date: ETRS 1989
Projection: Lambert Azimuthal Equal Area

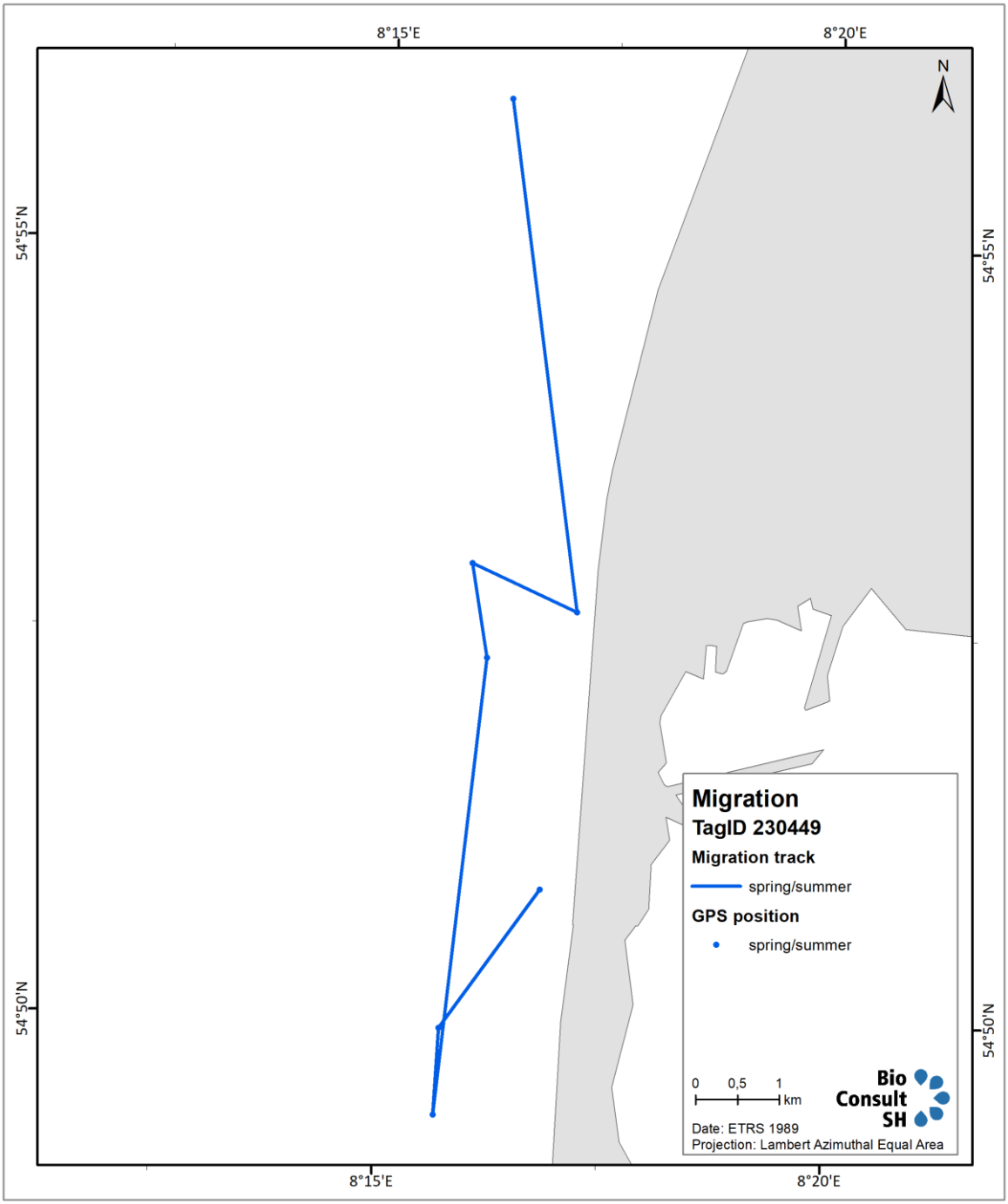
8°15'E
8°20'E
N
54°55'N
54°50'N
Migration
TagID 230449
Migration track
spring/summer
GPS position
spring/summer
0 0,5 1 km
Bio Consult SH
Date: ETRS 1989
Projection: Lambert Azimuthal Equal Area

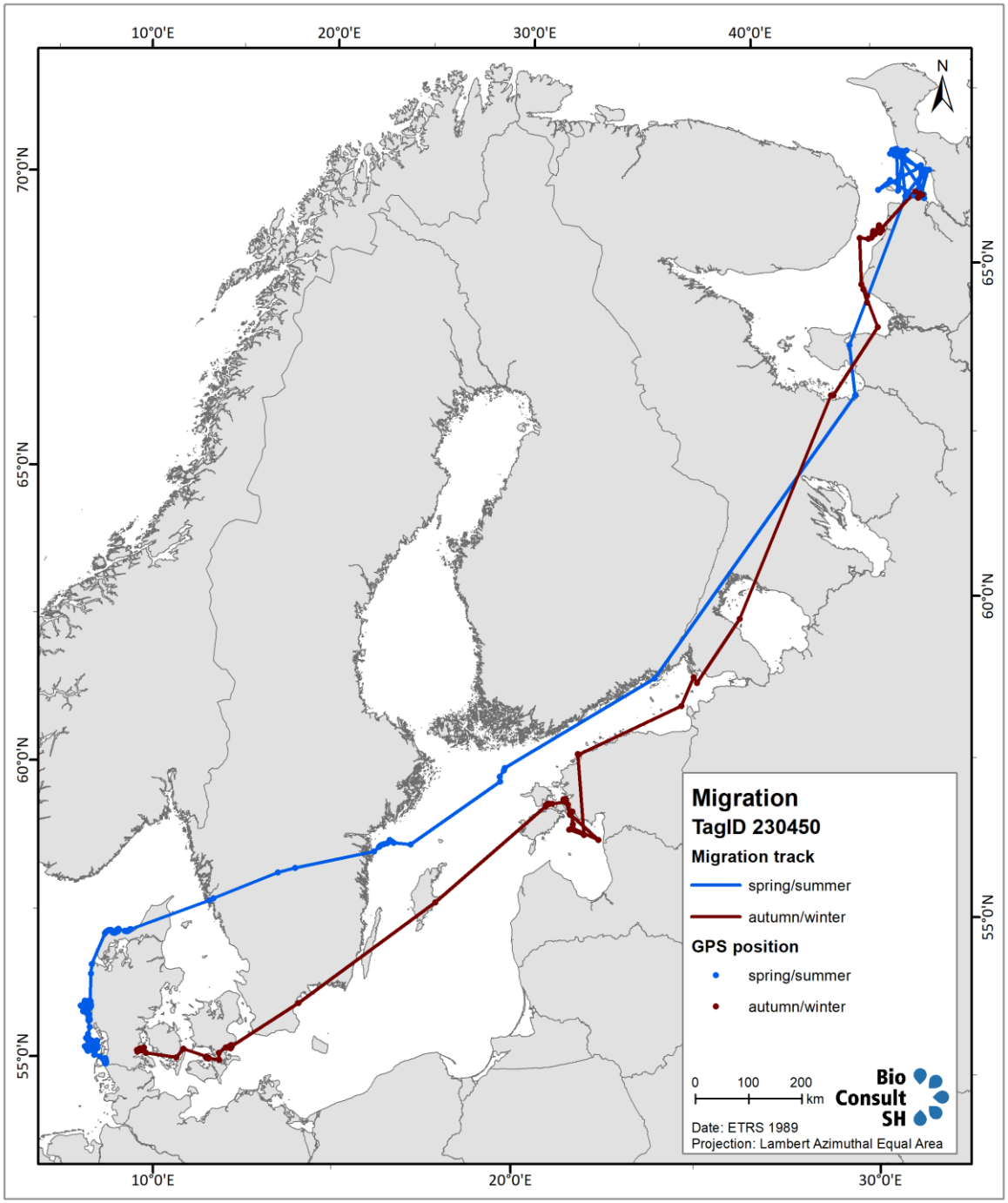
10°0'E
20°0'E
30°0'E
40°0'E
70°0'N
65°0'N
60°0'N
55°0'N
N
Migration
TagID 230450
Migration track
spring/summer
autumn/winter
GPS position
spring/summer
autumn/winter
0
100
200
km
Bio Consult SH
Date: ETRS 1989
Projection: Lambert Azimuthal Equal Area

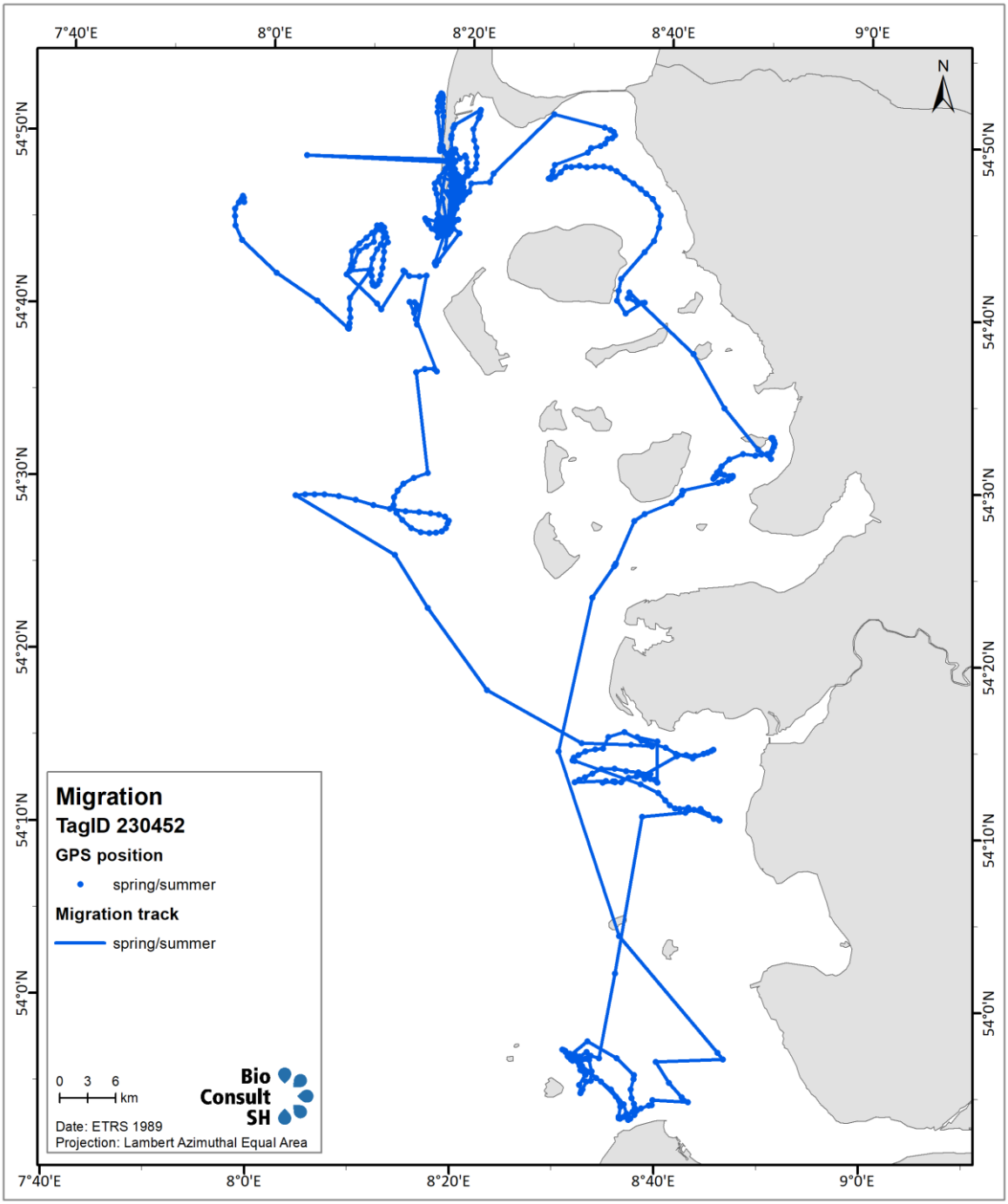
7°40'E
8°0'E
8°20'E
8°40'E
9°0'E
54°50'N
54°40'N
54°30'N
54°20'N
54°10'N
54°0'N
N
Migration
TagID 230452
GPS position
spring/summer
Migration track
spring/summer
0 3 6
km
Bio Consult SH
Date: ETRS 1989
Projection: Lambert Azimuthal Equal Area

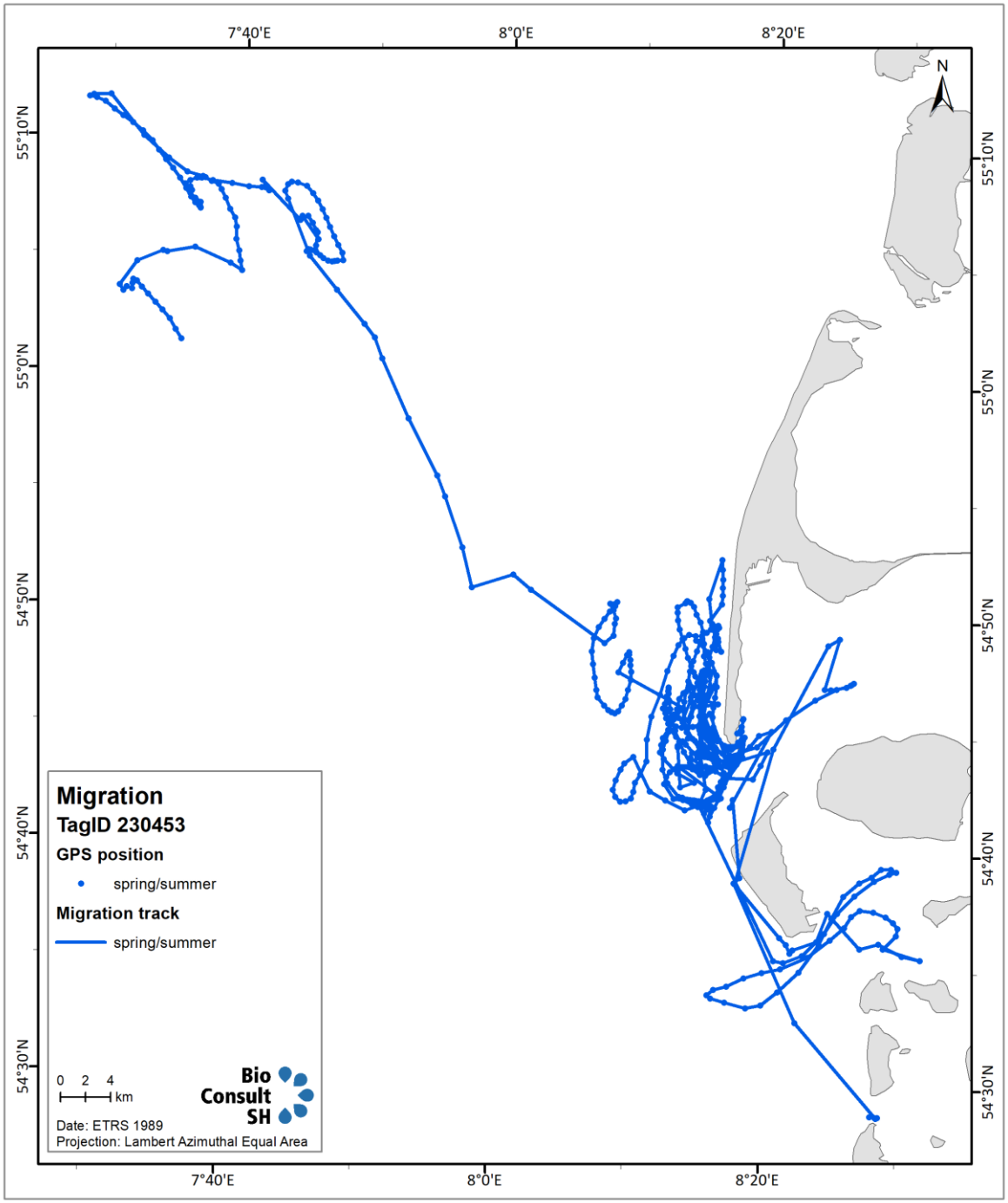
7°40'E
8°0'E
8°20'E
55°10'N
55°0'N
54°50'N
54°40'N
54°30'N
N
Migration
TagID 230453
GPS position
spring/summer
Migration track
spring/summer
0 2 4
km
Bio Consult SH
Date: ETRS 1989
Projection: Lambert Azimuthal Equal Area

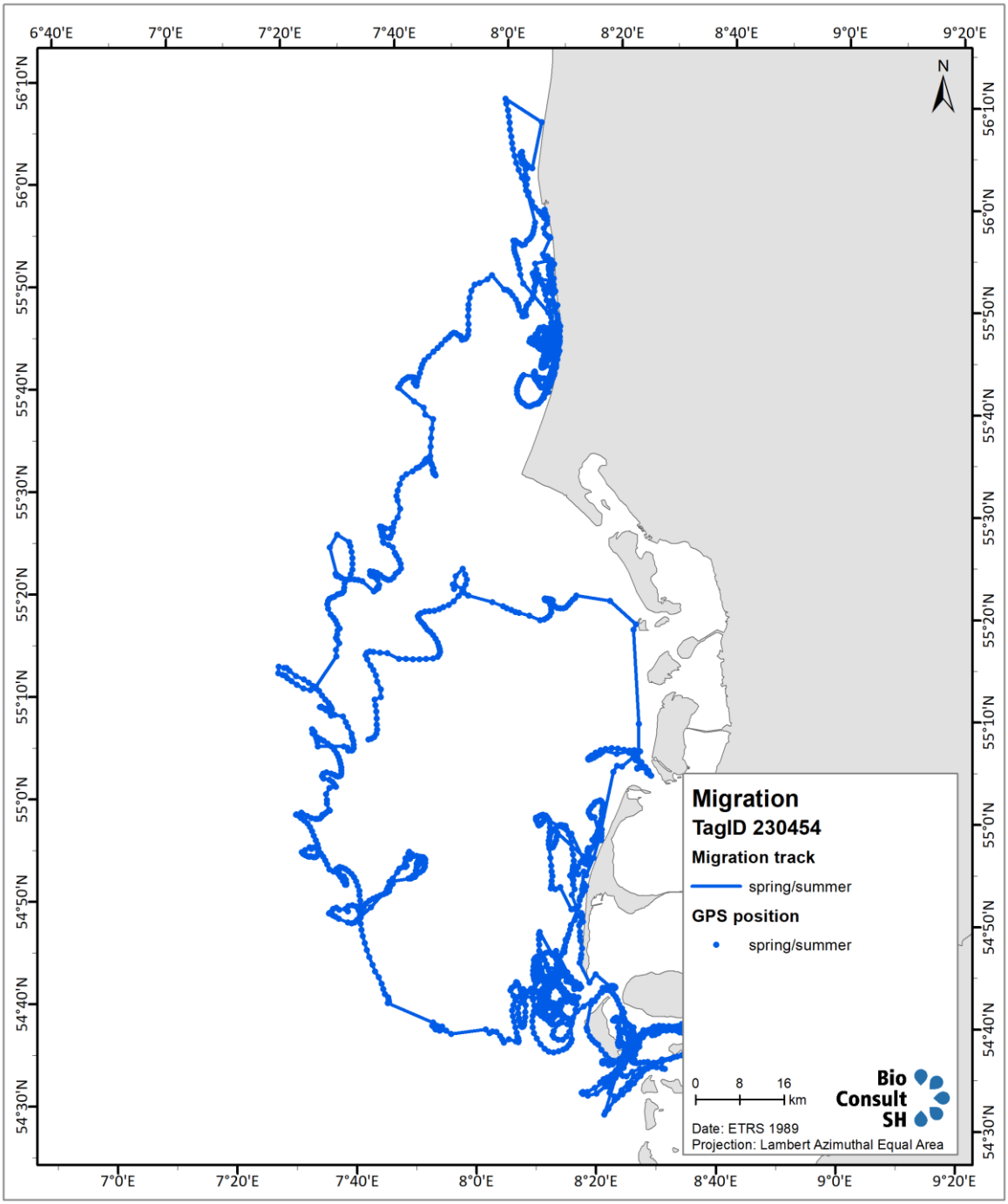
6°40'E
7°0'E
7°20'E
7°40'E
8°0'E
8°20'E
8°40'E
9°0'E
9°20'E
56°10'N
56°0'N
55°50'N
55°40'N
55°30'N
55°20'N
55°10'N
55°0'N
54°50'N
54°40'N
54°30'N
N
Migration
TagID 230454
Migration track
spring/summer
GPS position
spring/summer
0 8 16
km
Bio Consult SH
Date: ETRS 1989
Projection: Lambert Azimuthal Equal Area

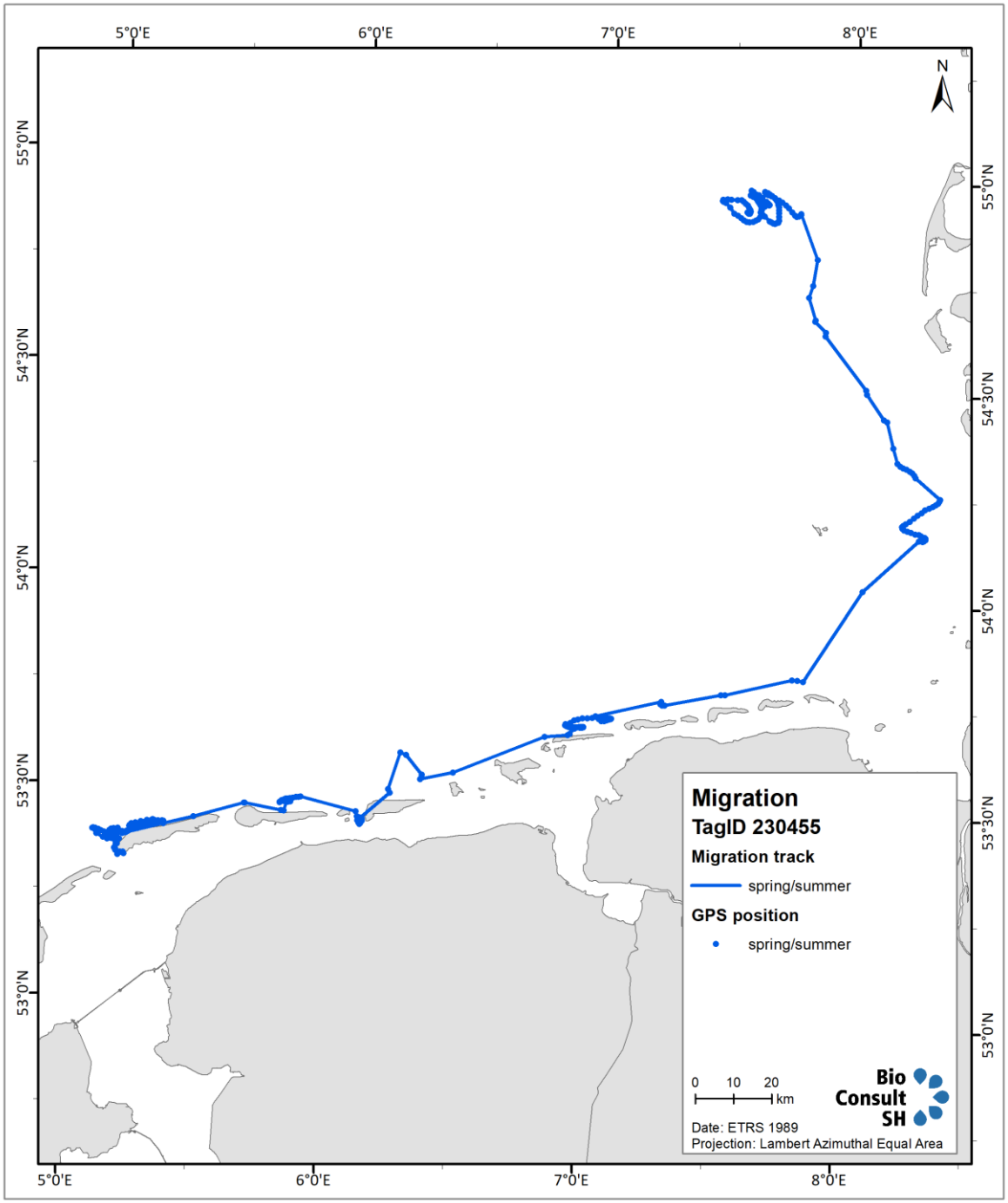
5°0'E
6°0'E
7°0'E
8°0'E
N
55°0'N
54°30'N
54°0'N
53°30'N
53°0'N
Migration
TagID 230455
Migration track
spring/summer
GPS position
spring/summer
0 10 20
km
Bio Consult SH
Date: ETRS 1989
Projection: Lambert Azimuthal Equal Area

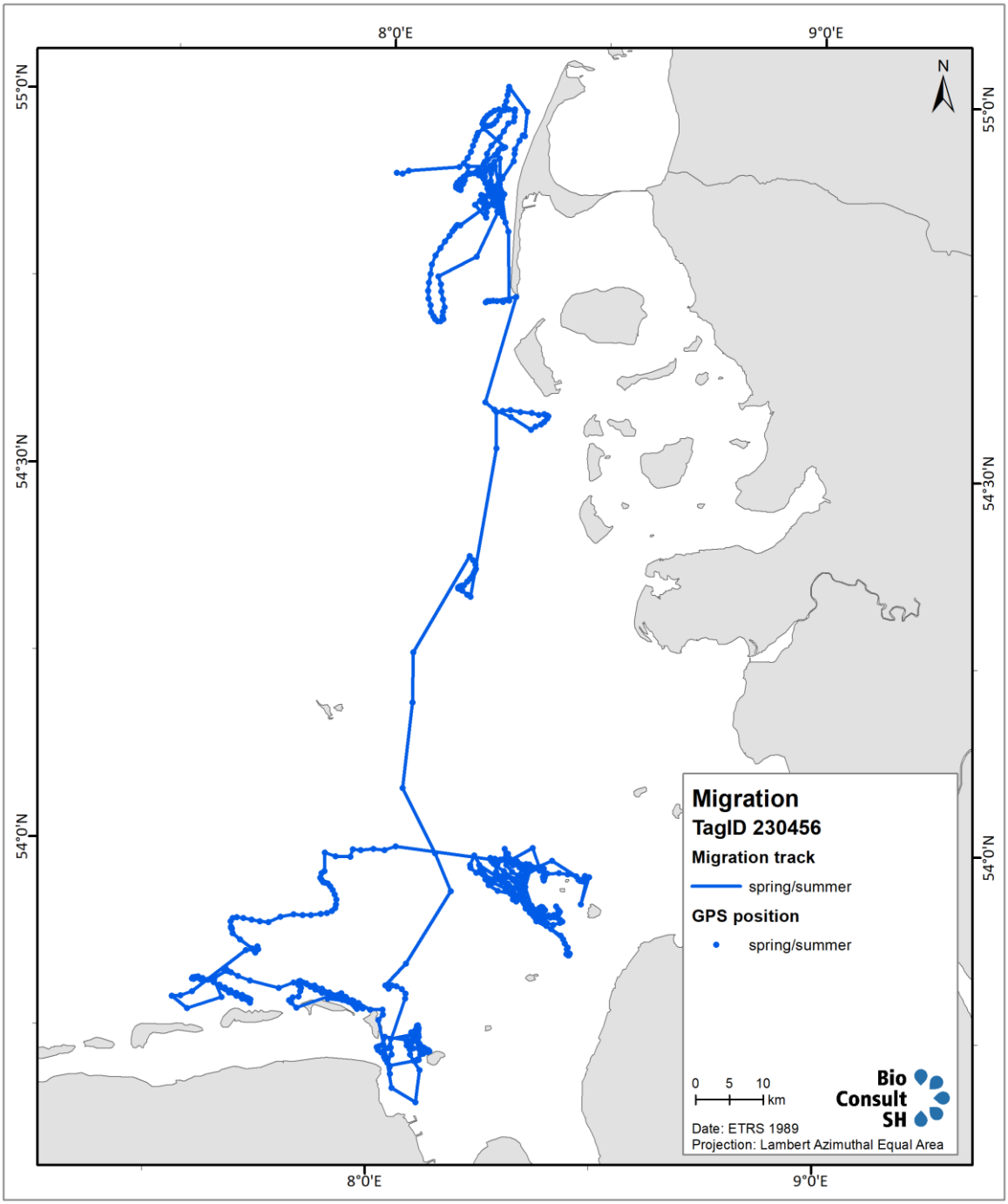
8°0'E
9°0'E
55°0'N
54°30'N
54°0'N
N
Migration
TagID 230456
Migration track
spring/summer
GPS position
spring/summer
0 5 10
km
Bio Consult SH
Date: ETRS 1989
Projection: Lambert Azimuthal Equal Area

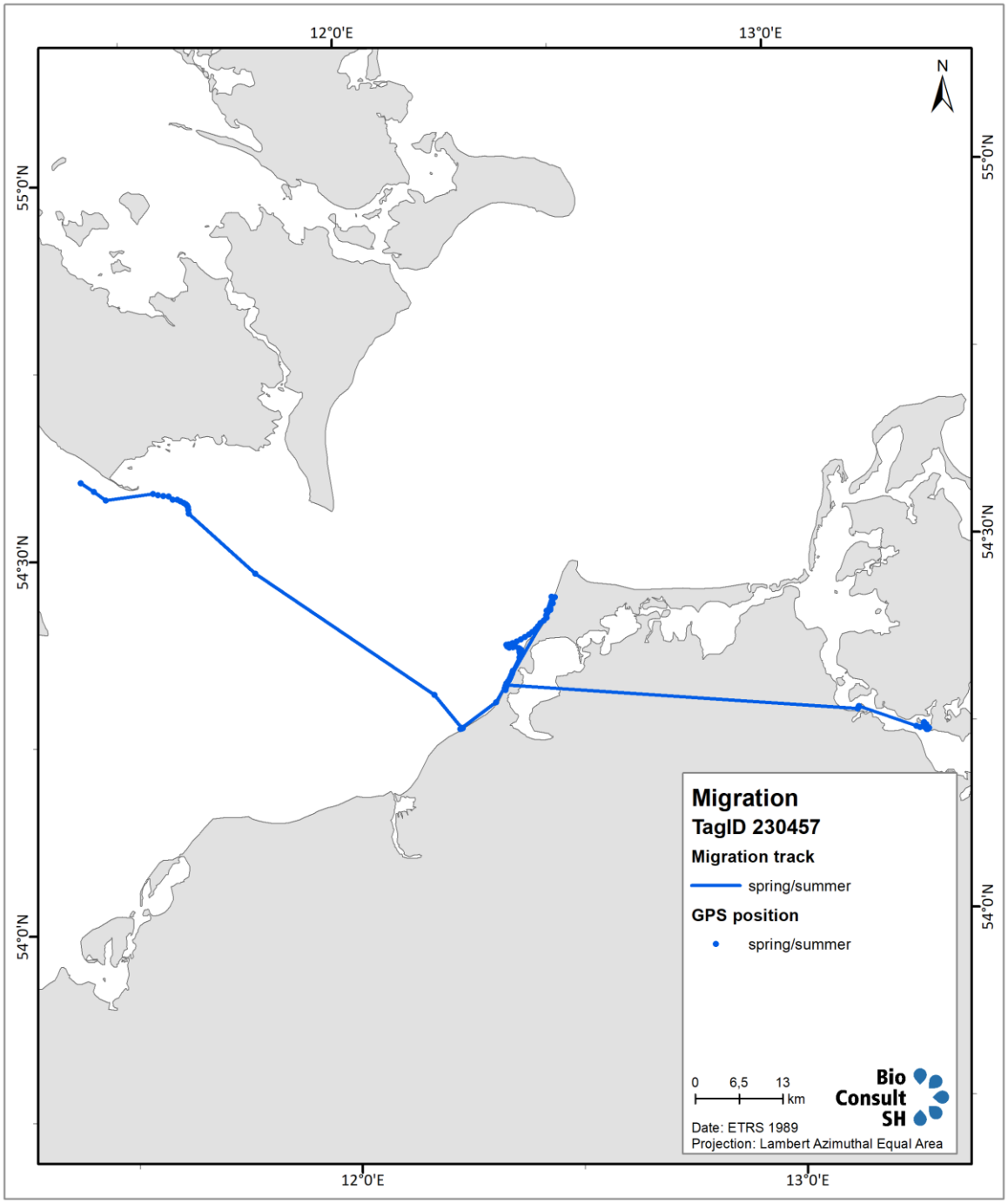
12°0'E
13°0'E
N
55°0'N
54°30'N
54°0'N
Migration
TagID 230457
Migration track
spring/summer
GPS position
spring/summer
0 6,5 13
km
Bio Consult SH
Date: ETRS 1989
Projection: Lambert Azimuthal Equal Area

A.5 Chapter 10: IBM

Tab. A 1 *Percentage of daytime spent diving (population mean and CIs) as a function of the parameter ppt, which modulates prey responsiveness to predators. Higher ppt values correspond to reduced negative density dependence in divers. Results are shown in **bold** when the 95% confidence intervals (CIs) of scenario B or C do not overlap with those of scenario A, and in italics when the CIs of scenarios B and C do not overlap with each other. Results for ppt = 5, which best matched the tracking data, are highlighted in light blue.*

Percent of daytime spent diving									
ppt	Scenario A a = 1; v=1			Scenario B a = 0; v = 1			Scenario C a = 0; v =0		
value	mean	lower CI	upper CI	mean	lower CI	upper CI	mean	lower CI	upper CI
2	**37.84**	**37.81**	**37.87**	**38.65**	**38.62**	**38.69**	**38.84**	**38.82**	**38.86**
3	**40.12**	**40.05**	**40.19**	**40.96**	**40.87**	**41.04**	**40.86**	**40.72**	**40.99**
4	**35.92**	**35.68**	**36.15**	**34.43**	**33.85**	**35.02**	**34.09**	**33.70**	**34.47**
5	**15.88**	**15.75**	**16.01**	**15.29**	**15.23**	**15.36**	**15.17**	**15.05**	**15.29**
6	**14.94**	**14.80**	**15.08**	**14.42**	**14.32**	**14.51**	**14.38**	**14.30**	**14.45**
7	**13.44**	**13.39**	**13.49**	**13.11**	**13.05**	**13.16**	**13.08**	**13.02**	**13.14**
8	**13.18**	**13.14**	**13.22**	**12.90**	**12.82**	**12.97**	**12.86**	**12.80**	**12.92**
9	**12.73**	**12.67**	**12.79**	**12.54**	**12.50**	**12.59**	**12.51**	**12.47**	**12.55**
10	**12.63**	**12.57**	**12.70**	**12.48**	**12.44**	**12.51**	**12.44**	**12.37**	**12.51**
11	**12.55**	**12.48**	**12.62**	**12.31**	**12.25**	**12.37**	**12.25**	**12.20**	**12.31**
12	**12.41**	**12.36**	**12.45**	**12.25**	**12.20**	**12.30**	**12.22**	**12.18**	**12.25**
13	**12.40**	**12.34**	**12.46**	**12.23**	**12.19**	**12.28**	**12.19**	**12.12**	**12.26**
14	**12.35**	**12.29**	**12.41**	**12.16**	**12.10**	**12.21**	**12.16**	**12.10**	**12.22**

Tab. A 2 *Percentage of daytime spent flying (population mean and CIs) as a function of the parameter ppt, which modulates prey responsiveness to predators. Higher ppt values correspond to reduced negative density dependence in divers. Results are shown in **bold** when the 95% confidence intervals (CIs) of scenario B or C do not overlap with those of scenario A, and in italics when the CIs of scenarios B and C do not overlap with each other. Results for ppt = 5, which best matched the tracking data, are highlighted in light blue.*

Percent of daytime spent flying									
ppt	Scenario A a = 1; v = 1			Scenario B a = 0; v = 1			Scenario C a = 0; v = 0		
value	mean	lower CI	upper CI	mean	lower CI	upper CI	mean	lower CI	upper CI
2	**14.85**	**14.82**	**14.87**	**14.77**	**14.75**	**14.79**	**14.73**	**14.72**	**14.75**
3	**13.00**	**12.96**	**13.04**	**12.84**	**12.80**	**12.88**	***12.71***	***12.66***	***12.77***
4	**10.49**	**10.39**	**10.60**	**9.52**	**9.28**	**9.75**	**9.31**	**9.15**	**9.46**

Percent of daytime spent flying									
5	**2.08**	**2.03**	**2.13**	**1.72**	**1.69**	**1.75**	***1.64***	***1.59***	***1.68***
6	**1.72**	**1.67**	**1.77**	**1.38**	**1.35**	**1.41**	***1.33***	***1.31***	***1.36***
7	**1.12**	**1.09**	**1.14**	**0.89**	**0.87**	**0.90**	**0.85**	**0.84**	**0.87**
8	**1.01**	**1.00**	**1.03**	**0.83**	**0.80**	**0.85**	**0.78**	**0.76**	**0.80**
9	**0.87**	**0.86**	**0.89**	**0.71**	**0.70**	**0.72**	**0.68**	**0.66**	**0.70**
10	**0.84**	**0.82**	**0.87**	**0.69**	**0.68**	**0.70**	**0.66**	**0.64**	**0.68**
11	**0.81**	**0.79**	**0.84**	**0.65**	**0.63**	**0.66**	***0.61***	***0.59***	***0.62***
12	**0.77**	**0.76**	**0.78**	**0.63**	**0.62**	**0.64**	***0.59***	***0.58***	***0.60***
13	**0.76**	**0.75**	**0.78**	**0.62**	**0.61**	**0.64**	***0.58***	***0.56***	***0.60***
14	**0.75**	**0.74**	**0.77**	**0.61**	**0.59**	**0.62**	**0.58**	**0.56**	**0.59**

Tab. A 3 *Population mean of distances moved (in km) per date including, active and passive swimming and flight as a function of the parameter ppt, which modulates prey responsiveness to predators. Higher ppt values correspond to reduced negative density dependence in divers. Results are shown in **bold** when the 95% confidence intervals (CIs) of scenario B or C do not overlap with those of scenario A, and in italics when the CIs of scenarios B and C do not overlap with each other. Results for ppt = 5, which best matched the tracking data, are highlighted in light blue.*

Distance moved per date									
ppt	Scenario A a = 1; v = 1			Scenario B a = 0; v = 1			Scenario C a = 0; v = 0		
value	mean	lower CI	upper CI	mean	lower CI	upper CI	mean	lower CI	upper CI
2	**179.95**	**179.82**	**180.07**	**183.11**	**183.00**	**183.23**	***184.05***	***183.98***	***184.12***
3	**164.22**	**163.83**	**164.61**	**166.32**	**165.92**	**166.72**	**165.73**	**165.08**	**166.39**
4	**135.72**	**134.44**	**137.00**	**126.39**	**123.49**	**129.28**	**124.74**	**122.82**	**126.65**
5	**39.77**	**39.28**	**40.25**	**36.56**	**36.29**	**36.82**	**35.98**	**35.49**	**36.47**
6	**36.02**	**35.49**	**36.55**	**33.01**	**32.64**	**33.37**	**32.84**	**32.57**	**33.12**
7	**29.81**	**29.64**	**29.99**	**27.67**	**27.51**	**27.83**	**27.60**	**27.38**	**27.82**
8	**28.74**	**28.66**	**28.82**	**26.98**	**26.74**	**27.22**	**26.78**	**26.57**	**27.0**
9	**27.11**	**26.92**	**27.31**	**25.60**	**25.45**	**25.75**	**25.51**	**25.37**	**25.65**
10	**26.77**	**26.50**	**27.04**	**25.39**	**25.27**	**25.50**	**25.26**	**25.04**	**25.48**
11	**26.41**	**26.15**	**26.68**	**24.82**	**24.63**	**25.01**	**24.61**	**24.38**	**24.83**
12	**25.92**	**25.76**	**26.08**	**24.59**	**24.46**	**24.72**	**24.46**	**24.37**	**24.54**
13	**25.82**	**25.62**	**26.02**	**24.48**	**24.33**	**24.63**	**24.29**	**24.06**	**24.53**
14	**25.64**	**25.48**	**25.81**	**24.28**	**24.12**	**24.43**	**24.24**	**24.06**	**24.42**

Tab. A 4 *Population mean of body mass (body mass in gram) as a function of the parameter ppt, which modulates prey responsiveness to predators. Higher ppt values correspond to reduced negative density dependence in divers. Results are shown in **bold** when the 95% confidence intervals (CIs) of scenario B or C do not overlap with those of scenario A, and in italics when the CIs of scenarios B and C do not overlap with each other. Results for ppt = 5, which best matched the tracking data, are highlighted in light blue.*

Mean body mass in g (population mean)									
ppt	Scenario A a = 1; v = 1			Scenario B a = 0; v = 1			Scenario C a = 0; v = 0		
value	mean	lower CI	upper CI	mean	lower CI	upper CI	mean	lower CI	upper CI
2	−243.62	−252.04	−235.19	−234.86	−240.80	−228.91	−237.86	−243.45	−232.27
3	**191.05**	**184.93**	**197.16**	**209.91**	**200.97**	**218.84**	**215.5**	**206.78**	**224.21**
4	**510.46**	**496.52**	**524.40**	**604.08**	**583.47**	**624.69**	**638.16**	**620.08**	**656.25**
5	**1689.70**	**1683.84**	**1695.56**	**1720.67**	**1713.24**	**1728.10**	**1725.71**	**1716.42**	**1735.0**
6	**1721.39**	**1715.48**	**1727.29**	**1745.90**	**1736.85**	**1754.95**	**1743.8**	**1736.77**	**1750.82**
7	1774.06	1767.67	1780.45	1784.65	1778.12	1791.18	**1792.49**	**1785.2**	**1799.79**
8	1784.20	1776.33	1792.07	1791.06	1784.47	1797.65	1789.96	1779.49	1800.43
9	**1789.69**	**1783.62**	**1795.76**	**1801.36**	**1796.74**	**1805.98**	1801.18	1792.52	1809.84
10	**1791.15**	**1784.03**	**1798.28**	**1804.16**	**1799.18**	**1809.15**	**1804.99**	**1799.2**	**1810.77**
11	**1788.46**	**1781.99**	**1794.93**	**1800.37**	**1795.06**	**1805.68**	**1807.52**	**1799.65**	**1815.39**
12	1801.98	1793.79	1810.18	1804.34	1795.61	1813.07	1806.66	1800.72	1812.6
13	1795.15	1787.96	1802.33	1804.10	1799.14	1809.07	1805.54	1799.29	1811.83
14	1797.04	1792.06	1802.01	1806.39	1801.40	1811.37	1808.73	1799.8	1817.65

Tab. A 5 *Percent of population staying above lower threshold of body mass as a function of the parameter ppt, which modulates prey responsiveness to predators. Higher ppt values correspond to reduced negative density dependence in divers. Results are shown in **bold** when the 95% confidence intervals (CIs) of scenario B or C do not overlap with those of scenario A, and in italics when the CIs of scenarios B and C do not overlap with each other. Results for ppt = 5, which best matched the tracking data, are highlighted in light blue.*

Percent of individuals above lower body mass									
ppt	Scenario A a = 1; v = 1			Scenario B a = 0; v = 1			Scenario C a = 0; v = 0		
value	mean	lower CI	upper CI	mean	lower CI	upper CI	mean	lower CI	upper CI
2	0.000	0.000	0.000	0.000	0.000	0.000	0.000	0.000	0.000
3	0.040	0.000	0.100	0.000	0.000	0.000	0.000	0.000	0.000
4	**0.780**	**0.453**	**1.107**	**2.620**	**2.008**	**3.232**	***4.540***	***3.733***	***5.347***
5	98.900	98.596	99.204	99.180	98.796	99.564	99.400	99.198	99.602
6	99.220	98.923	99.517	99.500	99.254	99.746	99.620	99.449	99.791
7	99.720	99.515	99.925	99.760	99.528	99.992	99.720	99.566	99.874
8	99.660	99.508	99.812	99.720	99.599	99.841	99.760	99.670	99.850

Percent of individuals above lower body mass									
9	99.700	99.506	99.894	99.880	99.780	99.980	99.880	99.780	99.980
10	99.840	99.709	99.971	99.920	99.846	99.994	99.840	99.727	99.953
11	99.740	99.574	99.906	99.740	99.574	99.906	99.880	99.759	100.000
12	99.820	99.695	99.945	99.900	99.778	100.000	99.860	99.708	100.000
13	99.900	99.799	100.000	99.700	99.474	99.926	99.780	99.524	100.000
14	99.900	99.825	99.975	99.840	99.727	99.953	99.820	99.678	99.962

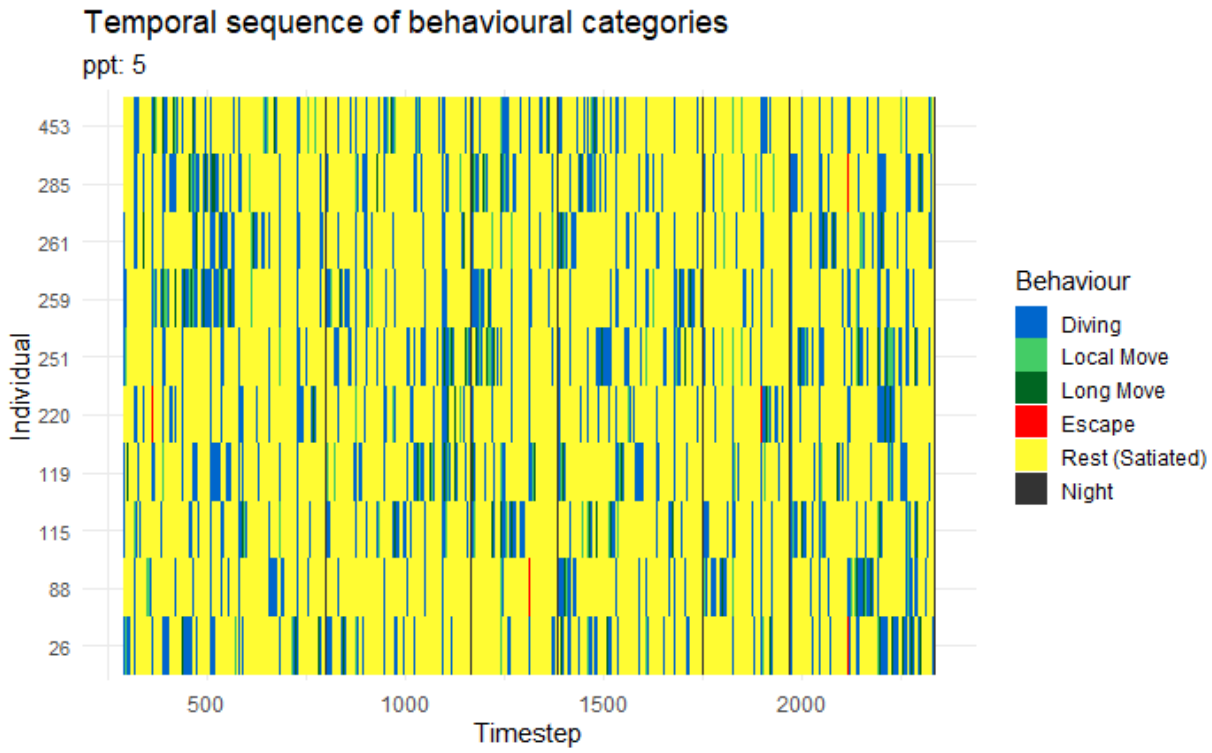

Fig. A 8 *Temporal sequence of behavioural categories for 10 randomly selected individuals over 28 simulated days. Colours indicate behaviour type (see legend); night was represented as a single time step in the simulation and therefore appears as thin black lines.*